H. Wanner
M. Grosjean
R. Röthlisberger
E. Xoplaki
Editors

Climate Variability, Predictability and Climate Risks

A European Perspective

NCCR CLIMATE
Swiss Climate Research

Springer

CLIMATE VARIABILITY, PREDICTABILITY AND CLIMATE RISKS

A European Perspective

CLIMATE VARIABILITY, PREDICTABILITY AND CLIMATE RISKS

A European Perspective

Edited by
Heinz Wanner
Martin Grosjean
Regine Röthlisberger
Elena Xoplaki
NCCR Climate Management Center,
University of Bern, Switzerland

NCCR CLIMATE
Swiss Climate Research

The National Centres of Competence in Research (NCCR) are a
research instrument of the Swiss National Science Foundation

SWISS NATIONAL SCIENCE FOUNDATION

Springer

cover picture – copyright keystone

Printed on acid-free paper

Contents

Climate variability, predictability and climate risks: a European perspective

**Heinz Wanner · Martin Grosjean ·
Regine Röthlisberger · Elena Xoplaki**

The aim of climate research is to increase our knowledge about the nature of climate and the causes of climate variability and change. Increasing our understanding of the physical processes on various spatial and temporal scales will ultimately reduce uncertainty and improve our capabilities to predict climate on monthly to seasonal timescales and allow us to separate the anthropogenic and natural causes of long term climate change.

Current estimates of past and future climate change, projections of future greenhouse gas (GHG) emissions and their effects are subject to various uncertainties. Climate policy-making faces a wide range of significant scientific and socio-economic uncertainties pointing to the question of whether scientific understanding is sufficient to justify particular types of technical and political actions (Lempert et al. 2004; Manning et al. 2004).

The public and policy-makers need current and accurate estimates of climate change projections, uncertainty in future costs, benefits and impacts of potential choices, design of greenhouse gas mitigation, preparation for adaptation, and the funding level of research across many related disciplines. (Webster 2003; Webster et al. 2003). Without this information, policy discussion is unavoidably divided in two opposing parties, those who support calls for immediate action, i.e., reduction of human-caused greenhouse gases emissions, and those who wish not to take action because they are waiting for more information (e.g., Reilly et al. 2001). In addition, due to the potential social disruptions and high economic costs of emissions reductions, a vigorous debate has developed concerning the magnitude and the nature of the projected climate changes and whether they will actually lead to serious impacts (e.g., Mahlman 1997). Thus, climate-change policy formulation constitutes a great challenge since it introduces the problem of decision-making under uncertainty (Webster et al. 2003 and references therein).

The uncertainty analysis seems at first rather "uncomplicated", in reality however many empirical, methodological, institutional and philosophical challenges arise. Additionally, the optimal decisions of today do not only depend on the current uncertainties but also on the change in the uncertainties and our past and future responses. Policy decisions are therefore

H. Wanner · M. Grosjean · R. Röthlisberger · E. Xoplaki (✉)
NCCR Climate, University of Bern, Erlachstrasse 9a, 3012 Bern, Switzerland
e-mail: xoplaki@giub.unibe.ch

better modeled as sequential decisions under uncertainty (Hammitt et al. 1992; Manne and Richels 1995; Webster 2002). The sequential decision process adapts to new knowledge and responds to new information and events. This flexible decision process requires a careful adhesion to the uncertainties' change whilst continuously integrating new knowledge on climate system processes and socio-economic consequences and reactions (Webster 2003; Webster et al. 2003).

The quantification of uncertainty requires a model describing the fundamental and well known multi-sectoral (scientific as well as socio-economic) processes that contribute to the results. Furthermore, the use of consistent and well-documented methods to develop uncertainty estimates will allow the changes in our understanding to be tracked through time. In this case, a useful proportion of the uncertainties could be captured, although the parameters and assumptions of the model will still include some uncertainty (Webster 2003). Hence, a significant part of our uncertainty about past and future climate change will be unavoidable (Webster et al. 2003).

The importance of adequately quantifying and communicating uncertainty has been recently accepted in the climate research community. The authors for the Third Assessment Report (TAR) of the Intergovernmental Panel on Climate Change (IPCC) were encouraged to quantify uncertainty as much as possible (Moss and Schneider 2000).

However, various limitations characterise these attempts to quantify uncertainty: (a) Climate observations were not used to constrain the uncertainty in climate model parameters (Wigley and Raper 2001). (b) By using only one Atmosphere-Ocean General Circulation Model (AOGCM), uncertainties in climate model response are reduced to uncertainty in a single scaling factor for optimizing the model's agreement with observations (Stott and Kettleborough 2002). (c) The IPCC emissions scenarios have been used as of equal likelihood (Wigley and Raper 2001). (d) Some studies analysed the uncertainty only in the climate system response without characterizing the economic uncertainty except through individual IPCC emissions scenarios, by estimating uncertainty in future climate change only applied to specific IPCC emissions scenarios (Allen et al. 2000; Knutti et al. 2002; Stott and Kettleborough 2002). (e) The uncertainty analysis was in no case done under a policy scenario leading to stabilisation of GHG concentrations. (f) Uncertainty estimates for reconstructions of past climate (e.g., Mann et al. 1999; Luterbacher et al. 2004; Xoplaki et al. 2005) usually do not take into account dating uncertainty of the climate proxies (natural and documentary), loss of signal confidence within the twentieth century calibration period, uncertainties in the instrumental data (e.g. Brohan et al. 2006 and references therein), assumptions about signal stationarity, proxies exhibiting an unquantified degradation in reliability, reduction of sample replication, etc. (Esper et al. 2005).

Across all areas of climate change, it is found that uncertainty tends to increase when moving from global to regional scales. Regional information is clearly highly relevant to policy, but generally is much less precise and can be ambiguous and confusing. Thus, a careful balance is needed when considering the scale at which policy relevant information can be provided (Manning et al. 2004). The assessment of potential regional impacts of climate change has, up to now, relied on data from coarse resolution AOGCMs, which do not resolve spatial scales of less than ~300 km (Mearns et al. 2001).

According to Dessai and Hulme (2004) there are two different sources of uncertainty, the "epistemic" and the "stochastic". Epistemic uncertainty originates from incomplete knowledge of processes that influence events. These sources of uncertainty can be reduced by further studying the climate system, improving the state of knowledge, etc. Stochastic sources of uncertainty are those that are considered "unknowable" knowledge – items such as variability in the system, the chaotic nature of the climate system, and the indeterminacy of human systems
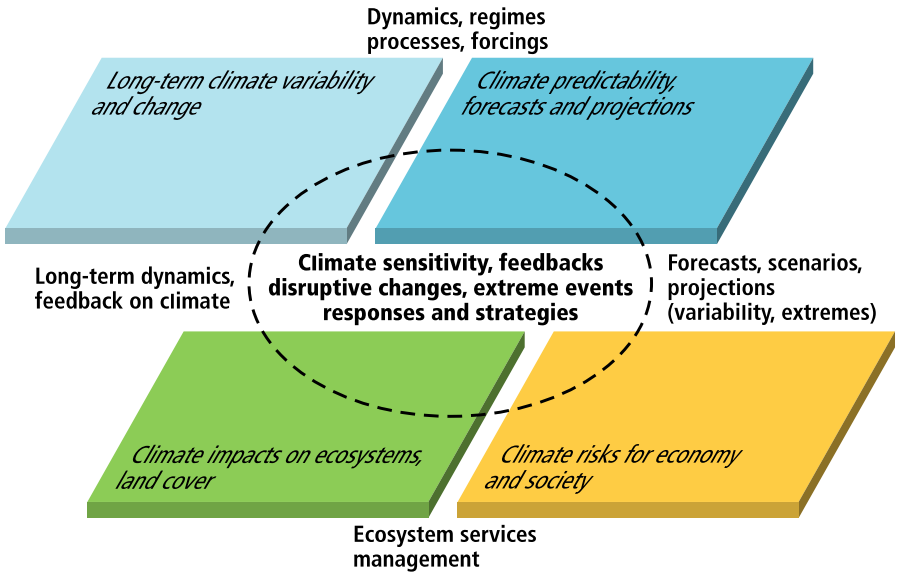
Fig. 1 Structure of NCCR Climate and major fields of inter-Work-Package (in different colours) collaboration and interaction

(Dessai and Hulme 2004). Further, the likelihood of various scenarios will likely change as soon as a prediction is made, because society begins to react (and adapt) and therefore change the outcome in ways that were not incorporated into the prediction (Sarewitz et al. 2003).

The sources of uncertainty in climate forecasting that have to be taken into consideration, as suggested at the IPCC Workshop on Communicating Uncertainty and Risk (Manning et al. 2004), are: (a) Uncertainty in anthropogenic forcing due to different emission paths ("scenario uncertainty"). (b) Uncertainty due to natural variability, encompassing internal chaotic climate variability and externally driven (e.g., solar, volcanic) natural climate change ("natural variability"). (c) Uncertainty in the climate system's response to external forcing due to incomplete knowledge of feedbacks and timescales in the system ("response uncertainty") (Allen et al. 2004).

The National Centre of Excellence in Research on Climate (NCCR Climate), which is based in Bern, Switzerland, aims at increasing our knowledge of the climate system by carrying out interdisciplinary research on its variability and future change, climate impacts and their financial evaluation, and climate policies (Figure 1). It is a scientific network bringing together 130 researchers from 13 Swiss partner institutions (http://www.nccr-climate.unibe.ch/). The NCCR Climate is a long-term research programme that started in 2001.[1]

The core theme of NCCR Climate is: "Climate variability, predictability, and climate risks". It builds on three interlinked research fields that frame the research activities:

---
[1] The NCCR Climate in its second phase (2005–2009) is building on the scientific and institutional achievements of the first phase and focuses on: (1) European past climate variability covering the last 1000 years; (2) Climate predictability, global to regional climate processes, and projections on seasonal to interannual scales and more accurate predictions and extreme events; (3) Ecosystem impacts and adaptation, assessing implications for ecosystems and evaluating strategies for the management of forests and agriculture; (4) Climate risks addressing questions on the potential perspectives for regional and global post-Kyoto climate policies and the vulnerability and adaptation costs of regional and global economies to global climate change.

1. What is the nature of past, current and future climate? What is the sensitivity of the climate system (including the internal variations and extremes) to anthropogenic and natural perturbations? What are the feedbacks between the atmosphere, the ocean, the cryosphere, land surfaces and the anthroposphere?
2. What are the forced climate impacts on ecosystems, economy and society? What is the likelihood of rapid transitions and changes with disruptive impacts? What is the role of extreme climate events on ecosystems, the economy and society?
3. What are the options and strategies for the management of ecosystems, economic systems and societal systems to respond to such climate changes and to reduce vulnerability?

Within the structure of the NCCR climate research, there are three geographical scales (Switzerland including the greater Alpine area, Europe and global) and three temporal scales (the last 500 years, the present and the 21st century).

The issues targeted in NCCR Climate require work at a wide range of spatial and temporal scales as well as the combination and integration of results from observational, experimental and modelling studies. Developing methodologies and providing an environment to work across the boundaries of different scales and methods is a priority area in climate research. It is intellectually and technically challenging, but a prerequisite to address the complex nature of the research issues in an adequate manner.

This book (special issue) compiles seven consecutive and integrative chapters, which (i) address some of the aforementioned common scientific challenges in current climate and climate impact research and (ii) synthesize the interdisciplinary research across the large thematic umbrella of the NCCR Climate. The scientific voyage starts with two selected problems of atmospheric and climate research, that address (i) different scales in time from the past to the future with different types of data availability (Raible et al. 2006), and (ii) reducing uncertainty of climate predictions and projections (Schwierz et al. 2006). We then move on to the topic of future climate change impacts on natural and managed ecosystems. The main challenge of climate impacts research is to consolidate the large scale projections to regional or local scales of climate variability and change, which can then be integrated into more specialised climate impact models (Calanca et al. 2006). Impacts are not limited to ecosystems but encompass the entire social, technological and economic systems (Fuhrer et al. 2006). Thus, building a modelling framework where the climate system and the energy-economy-environment systems communicate interactively with each other (Bahn et al. 2006) is fundamental in order to assess future development paths, strategies and options for climate change mitigation policies (Viguier et al. 2006). Finally, it is the society, at different hierarchical levels with different organizational forms and institutions, which makes the decisions and assesses the future failure or success of any climate change policy (Bürgenmeier et al. 2006).

Raible et al. (2006) assessed the natural climate variability on interannual to decadal timescales by using AOGCMs, state-of-the-art regional circulation models in combination with multiproxy climate reconstructions from regional to continental scales. The reconstructions reveal pronounced interdecadal variations, which seem to "lock" the atmospheric circulation in quasi-steady long-term patterns over multi-decadal periods, which partly control the continental alpine temperature and precipitation variability. In contrast, the climate model simulations indicate some substantial differences to the observations, indicating that the teleconnectivity between modeled climate variables is weaker than in observations however, in the future these teleconnections seem to be more stable. This partial disagreement between the reconstructions and the model simulations implies the need for better instrumental and more numerous natural/documentary proxy data sets, further improvement in reconstruction

methods and multi-model ensemble approaches (combination of regional and global models) (e.g., Yoshimori et al. 2005; Goosse et al. 2005, 2006; Raible et al. 2006).

Today's climate models capture the essence of the large-scale aspects of the current climate and its considerable natural variability reasonably well on time scales ranging from one day to decades. Despite this significant achievement, the models show weaknesses that add uncertainty to the very best model projections of human-induced climate changes.

Schwierz et al. (2006) present an overview of the uncertainties in climate model projections that arise from various sources. They identified uncertainties stemming from the complexity and non-linearity of the climate system, its irregular evolution and the changing climate sensitivity, the emission scenarios selection and their implications for the radiative forcing, and the inevitably incomplete and inadequate representation of the climate system in a weather or climate model. The latter uncertainty can be separated into that which is connected with the model equations representing the climate system interactions, the limited representation of physical processes due to the low resolution of the models and the limited knowledge of some physical processes including the non-linear interactions between the climate components. Schwierz et al. (2006) report that a hierarchy of models is a powerful approach to estimate and assess uncertainty, while the combination of different kinds of models of different complexity with an overlap between the model evaluations can contribute to the quantification and reduction of uncertainties from future climate model projections.

Calanca et al. (2006) combined simulations with a state-of-the-art Global Circulation Model (GCM) complemented by an experiment with a high-resolution spatially distributed hydrological model in order to quantify the impact of climate change and to reveal regional differences in the response, both across the alpine region as well as within individual river basins in Switzerland. They found that GCMs alone cannot capture the detailed regional scale results, demonstrating the danger of a simple extrapolation of GCM results and underlining the importance of a highly resolved hydrological model for the quantitative assessment of the regional impacts of climate change. Current spatial resolution of GCMs is too coarse to adequately represent areas of complex topography and land use change (Calanca et al. 2006).

Fuhrer et al. (2006) assessed climate risks on ecosystems using simulations for present climate with a 50-km Regional Climate Model (RCM) with boundary conditions from a GCM control experiment and compared the model output with observations. Climate risks arise from complex interactions between climate, environment, social and economic systems. They represent combinations of the likelihood of climate events and their consequences for society and the environment. The assessment of climate risks depends on both the ability to simulate extreme events in various scales and the understanding of the responses of the target system. The projections of climate risks are dependant on the quality of the link between larger-scale climate simulations and small-scale effects. Extreme climate events are often related to large-scale synoptic conditions, but the scales at which impacts occur can vary from local to regional (Fuhrer et al. 2006).

In order to obtain an integrated assessment of climate policies, Bahn et al. (2006) established a two-way coupling between the economic module of a well-established integrated assessment model and an intermediate complexity "3-D" climate model. The coupling is achieved through the implementation of an advanced "oracle based optimisation technique" which permits the integration of information coming from the climate model during the search for the optimal economic growth path. They showed that further applications of this method could include the coupling of an economic model and an advanced climate model that could describe the carbon cycle. Additionally, the spatial resolution of the climate model allows the construction of regional damage functions or in other words, the ability to link climate feedbacks with economic activity (e.g. agriculture). A further step is the coupling of

a macro-economic growth module with a detailed techno-economic model, in addition to the coupling with a moderate complexity climate model (Bahn et al. 2006).

Viguier et al. (2006) used an optimal economic growth model, a multi-region bottom-up process model and a multi-region computable general economic equilibrium (CGE) model for the assessment of climate change policies. Their assessment reveals the important effect of endogenising technological learning by early investments in research and development (R&D) activities and demonstration and deployment (D&D) programs. These programs could support the development and diffusion of cleaner technologies in the long term, and influence the strategic behaviour of climate policy makers and ultimately the success of international climate-policy. The strategic behaviour of the different countries towards the Kyoto protocol is related with the connected costs and the ability of the governments to afford these costs.

Bürgenmeier et al. (2006) explore the reasons behind the reluctant application of economic instruments of climate change. They stress the need for interdisciplinary research linking economic theory and empirical testing to deliberative political procedures. They found that the promotion of economic policies of climate change has to be completed by social policies to capture the ethical aspects. Additionally, the problem of the social acceptance of economic instruments of climate change can be overcome by using a) Conventional models that consider the environment, either through public goods theory or through property rights theory and b) More global models featuring relationships between economics, the biosphere and social aspects in order to come closer to the concept of sustainable development.

The understanding of the likelihood of future climate requires further and repeated analysis of the up-to-date combined knowledge on the climate and socio-economic systems (Webster et al. 2003).

References

Allen MR, Booth BBB, Frame DJ, Gregory JM, Kettleborough JA, Smith LA, Stainforth DA, Stott PA (2004) Observational constraints on future climate: distinguishing robust from model-dependent statements of uncertainty in climate forecasting. In: Manning et al. (eds) Describing scientific uncertainties in climate change to support analysis of risk and of options May 2004 IPCC workshop report. IPCC Working Group I Technical Support Unit, Boulder, Colorado, USA, pp 53–57(Available at: http://www.ipcc.ch/)

Allen MR, Stott PA, Mitchell JFB, Schnur R, Delworth TL (2000) Quantifying the uncertainty in forecasts of anthropogenic climate change. Nature 407:617–620

Bahn O, Drouet L, Edwards NR, Haurie A, Knutti R, Kypreos S, Stocker TF, Vial JP (2006) The coupling of optimal economic growth and climate dynamics. Clim Change, DOI: 10.1007/s10584-006-9108-4 (this issue)

Brohan P, Kennedy JJ, Harris I, Tett SFB, Jones PD (2006) Uncertainty estimates in regional and global observed temperature changes: a new dataset from 1850. J Geophys Res DOI: 10.1029/2005JD00654

Bürgenmeier B, Baranzini A, Ferrier C, Germond-Duret C, Ingold K, Perret S, Rafaj P, Kypreos S, Wokaun A (2006) Economics of climate policy and collective decision making. Clim Change, DOI: 10.1007/s10584-006-9147-x (this issue)

Calanca P, Roesch A, Jasper K, Wild M (2006) Global warming and the summertime evapotranspiration regime of the alpine region. Clim Change, DOI: 10.1007/s10584-006-9103-9 (this issue)

Dessai S, Hulme M (2004) Does climate adaptation policy need probabilities? Climate Policy 4:107–128

Esper J, Wilson RJS, Frank DC, Moberg A, Wanner H, Luterbacher J (2005) Climate: past ranges and future changes. Quat Sci Rev 24:2164–2166

Fuhrer J, Beniston M, Fischlin A, Frei C, Goyette S, Jasper K, Pfister C (2006) Climate risks and their impact on agriculture and forests in switzerland. Clim Change, DOI: 10.1007/s10584-006-9106-6 (this issue)

Goosse H, Renssen H, Timmermann A, Bradley RS (2005) Natural and forced climate variability during the last millennium: A model-data comparison using ensemble simulations Quat Sci Rev 24:1345–1360

Goosse H, Renssen H, Timmermann A, Bradley RS, Mann ME (2006) Using paleoclimate proxy-data to select and optimal realisation in an ensemble of simulations of the climate of the past millennium Clim Dynam.. DOI: 10.1007/s00382-006-0128-6, 27:165–184

Hammit JK, Lempert RJ, Schlesinger ME (1992) A sequential-decision strategy for abating climate change. Nature 357:315–318

Knutti R, Stocker TF, Joos F, Plattner GK (2002) Constraints on radiative forcing and future climate change from observations and climate model ensembles. Nature 416:719–723

Lempert R, Nakicenovic N, Sarewitz D, Schlesinger ME (2004) Characterizing climate-change uncertainties for decision-makers. Clim Change 65:1–9

Luterbacher J, Dietrich D, Xoplaki E, Grosjean M, Wanner H (2004) European seasonal and annual temperature variability, trends, and extremes since 1500. Science 303:1499–1503

Mahlman JD (1997) Uncertainties in projections of human-caused climate warming. Science 278:1416–1417

Mann ME, Bradley RS, Hughes MK (1999) Northern hemisphere temperatures during the past millennium: inferences, uncertainties, and limitations. Geophys Res Lett 26:759–762

Manne AS, Richels RG (1995) The greenhouse debate: economic efficiency, burden sharing and hedging strategies. Energy J 16:1–37

Manning et al. (eds.) (2004) Describing scientific uncertainties in climate change to support analysis of risk and of options, may 2004 ipcc workshop report. IPCC Working Group I Technical Support Unit, Boulder, Colorado, USA, pp 138. (Available at: http://www.ipcc.ch/)

Mearns LO, Hulme M, Carter TR, Leemans R, Lal M, Whetton PH (2001) Climate scenario development. Chapter 13 In: Houghton J, et al. (eds), Clim Change 2001: The Scientific Basis, Intergovernmental Panel on Climate Change, Cambridge University Press, pp 739–768

Moss RH, Schneider SH (2000) In: Pachauri R, Taniguchi T, Tanaka K (eds), Guidance papers on the cross cutting issues of the third assessment report. World Meteorological Organization, Geneva, pp 33–57

Raible CC, Casty C, Luterbacher J, Pauling A, Esper J, Frank DC, Büntgen U, Roesch AC, Tschuck P, Wild M, Vidale PL, Schär C, Wanner H (2006) Climate variability – observations, reconstructions, and model simulations for the atlantic-european and alpine region from 1500–2100 AD. Clim Change, DOI: 10.1007/s10584-006-9061-2 (this issue)

Reilly J, Stone PH, Forest CE, Webster MD, Jacoby HD, Prinn RG (2001) Climate change: uncertainty and climate change assessments. Science 293:430–433

Sarewitz D, Pielke RA Jr., Keykhah M (2003) Vulnerability and risk: some thoughts from a political and policy perspective. Risk Analysis 23:805–810

Schwierz C, Appenzeller C, Davies HC, Liniger MA, Müller W, Stocker TF, Yoshimori M (2006) Challenges posed by and approaches to the study of seasonal-to-decadal climate variability. Clim Change, DOI: 10.1007/s10584-006-9076-8 (this issue)

Stott P, Kettleborough JA (2002) Origins and estimates of uncertainty in predictions of twenty-first century temperature rise. Nature 416:723–726

Viguier L, Barreto L, Haurie A, Kypreos S, Rafaj P (2006) Modeling endogenous learning and imperfect competition effects in climate change economics. Clim Change, DOI: 10.1007/s10584-006-9070-1 (this issue)

Webster M (2002) The curious role of learning in climate policy: should we wait for more data? Energy J 23:97–119

Webster M (2003) Communicating climate change uncertainty to policy-makers and the public. Clim Change 61:1–8

Webster M, Forest C, Reilly J, Babiker M, Kicklighter D, Mayer M, Prinn R, Sarofim M, Sokolov A, Stone P, Wang C (2003) Uncertainty analysis of climate change and policy response. Clim Change 61:295–320

Wigley TML, Raper SCB (2001) Interpretations of high projections for global-mean warming. Science 293:451–454

Xoplaki E, Luterbacher J, Paeth H, Dietrich D, Steiner N, Grosjean M, Wanner H (2005) European spring and autumn land temperatures, variability and change of extremes over the last half millennium. Geophys Res Lett 32:L15713

Yoshimori M, Stocker TF, Raible CC, Renold M (2005) Externally-forced and internal variability in ensemble climate simulations of the Maunder Minimum. J Climate 18:4253–4270

Climate variability – observations, reconstructions, and model simulations for the Atlantic-European and Alpine region from 1500–2100 AD

**Christoph C. Raible · Carlo Casty · Jürg Luterbacher ·
Andreas Pauling · Jan Esper · David C. Frank ·
Ulf Büntgen · Andreas C. Roesch · Peter Tschuck ·
Martin Wild · Pier-Luigi Vidale · Christoph Schär ·
Heinz Wanner**

Abstract A detailed analysis is undertaken of the Atlantic-European climate using data from 500-year-long proxy-based climate reconstructions, a long climate simulation with perpetual 1990 forcing, as well as two global and one regional climate change scenarios. The observed and simulated interannual variability and teleconnectivity are compared and interpreted in order to improve the understanding of natural climate variability on interannual to decadal time scales for the late Holocene. The focus is set on the Atlantic-European and Alpine regions during the winter and summer seasons, using temperature, precipitation, and 500 hPa geopotential height fields. The climate reconstruction shows pronounced interdecadal variations that appear to "lock" the atmospheric circulation in quasi-steady long-term patterns over multi-decadal periods controlling at least part of the temperature and precipitation variability. Different circulation patterns are persistent over several decades for the period 1500 to 1900. The 500-year-long simulation with perpetual 1990 forcing shows some substantial differences, with a more unsteady teleconnectivity behaviour. Two global scenario simulations indicate a transition towards more stable teleconnectivity for the next 100 years. Time series of reconstructed and simulated temperature and precipitation over the Alpine region show comparatively small changes in interannual variability within the time frame considered, with the exception of the summer season, where a substantial increase in interannual variability is simulated by regional climate models.

C. C. Raible
Climate and Environmental Physics, Physics Institute, University of Bern, Sidlerstrasse 5, CH-3012 Bern, Switzerland

C. Casty · J. Luterbacher · A. Pauling · H. Wanner
Institute of Geography, University of Bern, Hallerstrasse 12, CH-3012 Bern, Switzerland

J. Esper · D. C. Frank · U. Büntgen
Swiss Federal Research Institute WSL, Zürcherstrasse 111, CH-8903 Birmensdorf, Switzerland

A. C. Roesch · P. Tschuck · M. Wild · P.-L. Vidale · C. Schär
Institute for Atmospheric and Climate Science ETH, Winterthurerstrasse 190, CH-8057 Zürich, Switzerland

1 Introduction

Observations and reconstructions for the late Holocene show that the warming since the 1960s is likely unprecedented over the last millennium (Jones and Mann 2004). Modelling studies give some evidence that the temperature change of at least the second half of the 20th century can only be explained by including anthropogenic forcing (Rind et al. 1999; Crowley 2000; IPCC 2001; Meehl et al. 2003; Bauer et al. 2003). Nevertheless, to assess future climate change for key regions, like the Atlantic-European area, with confidence, a thorough understanding of the underlying mechanisms of natural climate variability on different spatio-temporal scales for the late Holocene is necessary (Jones and Mann 2004).

One possibility to address the understanding of natural climate variability of the Atlantic-European region is to investigate general circulation models (GCMs). Modelling results show that for the mid-latitudes the coupling between atmosphere and ocean plays a major role on decadal variability (Grötzner et al. 1998; Raible et al. 2001; Marshall et al. 2001, and references therein). This coupling has implications for the low-frequency (decadal) behaviour of the North Atlantic Oscillation (NAO), with its well-known linkage to temperature and precipitation on the interannual time scale (Hurrell 1995; Hurrell and Loon 1997; Wanner et al. 2001; Hurrell et al. 2003). Even baroclinic high-frequency variations characterised by stationary and transient wave activity should be incorporated to understand enhanced low-frequency variability of the NAO (Raible et al. 2004). Additionally, future projections integrated with coupled atmosphere-ocean (AO-) GCMs show a systematic northeastward shift of the northern center of action of the NAO (Ulbrich and Christoph 1999), indicating that at least the modelled position of the pressure centers is not stable in time. Recently, a strong connection between sea surface temperature (SST) and the North Atlantic Thermohaline Circulation has been presented in unforced control AO-GCM simulations (Latif et al. 2004; Cheng et al. 2004). These SST anomalies, containing strong multi-decadal variability, may mask anthropogenic signals in the North Atlantic region. Another potential mechanism of generating low-frequency NAO variability is the stratosphere, where stratospheric processes can be influenced by changes in the external solar and volcanic forcing (Shindell et al. 2001, 2003). Another problem present in this region is illustrated by an ensemble modelling study for the Maunder Minimum from 1640 to 1715 (Yoshimori et al. 2005), showing that forcing signals, e.g., solar forcing, are difficult to detect due to the strong internal variability induced by the NAO.

Another approach to improve our understanding of natural climate variability is to extend the existing climate records for temperature, precipitation, and atmospheric circulation patterns back in time. One first step was to reconstruct temperature on hemispheric to global scales over the past centuries to millennia based on empirical proxy data (Bradley and Jones 1993; Overpeck et al. 1997; Jones et al. 1998; Mann et al. 1998; Briffa et al. 2001; Esper et al. 2002a; Cook et al. 2004; Jones and Mann 2004; Esper et al. 2004; Moberg et al. 2005). However, hemispheric-scale reconstructions provide little information about regional scale climate variability. Therefore, studies focusing on reconstruction of specific regions, e.g., Atlantic-Europe or high Asia, utilising documentary (Luterbacher et al. 2004; Xoplaki et al. 2005; Guiot et al. 2005) and tree-ring data (Esper 2000; Esper et al. 2002b, 2003; Büntgen et al. 2005) are also valuable.

Jones et al. (2003) found amongst others changes in the annual cycle of Northern Hemisphere temperatures indicating that, compared with earlier times, winters have warmed more relative to summers over the past 200 years.

A third research focus is on atmospheric circulation variability. Besides traditional reconstructions of the NAO index (Appenzeller et al. 1998; Luterbacher et al. 2002a; Cook

et al. 2002; Vinther et al. 2003), atmospheric circulation modes (Jacobeit et al. 2003) for each month in the year were derived from sea-level pressure field reconstructions (Luterbacher et al. 1999, 2002b). Utilising reconstructions of the 500 hPa geopotential height fields for the Atlantic-European region, Casty et al. (2005a) found that climate regimes, defined by the joint probability density function of the first two leading Empirical Orthogonal Functions, are not stable in time.

With a steadily growing data base, it is now possible to reconstruct climate variations from small regions like the European Alps (Casty et al. 2005b; Frank and Esper 2005; Büntgen et al. 2005). This could help to place extreme events, e.g., the hot European summer of 2003 (with its maximum deviation from the mean in central Europe and the Alps), in a longer-term context (Luterbacher et al. 2004). Recently, regional modelling studies (Schär et al. 2004) showed that in a scenario with increased atmospheric greenhouse-gas concentrations, future European temperature variability may increase by up to 100%, with maximum changes in central and eastern Europe. Such a change in variability would have a strong impact on not only the environment, but also on the society and the economy in these regions.

The National Center of Competence in Research on Climate (NCCR Climate) in Switzerland provides a substantial variety of different spatio-temporal highly-resolved climate information, ranging from natural and documentary proxy reconstructions, to high-quality instrumental measurements, to modeled data from state-of-the-art general circulation and regional models for both present day climate conditions (fixed to 1990 AD) as well as future scenarios. The aim of this study is to combine the two major types of information in the archive – the observations and reconstructions on the one hand, and the simulations for present day climate conditions and future scenarios on the other hand. This set of data and simulations will form the basis for the investigation of the atmospheric circulation and its links to the behaviour of temperature and precipitation in the Atlantic-European and the Alpine regions on interannual to decadal time scales. Additionally, changes in the annual cycle from 1500–2100 AD are discussed.

The outline of this paper is as follows: In Section 2 the reconstructed and modeled data, as well as some analysis techniques and definitions, are introduced. Subsequent analysis concentrates on the Atlantic-European (Section 3) and Alpine (Section 4) regions, illustrating the relationship between large-scale flow regimes and temperature and precipitation. The results are summarised and interpreted, in the context of published evidence, in Section 5.

2 Reconstructions, models, and analysis techniques

The study is based on a set of reconstructed and modeled data, which is introduced as follows. We focus on winter (December to February, DJF) and summer (June to August, JJA) of the Atlantic-European and the Alpine regions, respectively.

2.1 Reconstructions and models

Reconstructions of past pressure, temperature, and precipitation are performed through multivariate statistical climate fields reconstruction (CFR) approaches. CFR seeks to reconstruct a large-scale field by regressing a spatial network of proxy indicators (e.g., early instrumental, tree-ring data, and historical evidences) against instrumental field information (Jones and Mann 2004). During periods when both proxy and instrumental field information (reanalyses) are available, regression models are developed and fed with proxy data to reconstruct past climate variables.

For the Atlantic-European region reconstructions of seasonally resolved land surface air temperature (Luterbacher et al. 2004, 25°W–40°E and 35°N–70°N), precipitation (Pauling et al. 2006, 10°W–40°E and 35°N–70°N), and 500 hPa geopotential height fields (Luterbacher et al. 2002b, 30°W–40°E and 30°N–70°N) are available back to 1500. Independent reconstructions, i.e., sharing no common predictors, have been developed for seasonal land surface air temperatures and precipitation fields for the European Alps since 1500 (Casty et al. 2005b, 4°E–16°E and 43°N–48°N). These CFRs are multi-proxy based. The period from 1500 to the late 17th century comprises entirely documentary and natural proxies; the period from 1659 to around 1750 includes a mix of documentary, natural proxies as well as a few early instrumental data. The reconstructions for the last 250 years are entirely based on instrumental time series, the number of those increasing steadily over time. A compilation of all proxies and instrumental data used for those 500 year climate reconstructions is given in Luterbacher et al. (2004), Casty et al. (2005b), and Pauling et al. (2006). The spatial resolution for the temperature and precipitation reconstructions is 0.5° (∼60 km × 60 km) similar to the instrumental field information for the 1901–2000 period: Instrumental data from New et al. (2000) were used by Luterbacher et al. (2004); data from Mitchell et al. (2004) were used by Casty et al. (2005b) and Pauling et al. (2006). The 500 hPa fields are resolved on a 2.5° grid similar to the NCEP Reanalysis data (Kalnay et al. 1996; Kistler et al. 2001). For further details about reconstruction methods, proxy information, verification, and uncertainty estimates, the reader is referred to Luterbacher et al. (2002b, 2004), Casty et al. (2005b), and Pauling et al. (2006).

A new millennial-long tree-ring reconstruction utilising 1527 ring width measurement series from living and relict larch and pine samples from the Swiss and Austrian Alps (46.5°N–47°N and 7.5°N–11.5°E) is applied for further comparison and validation (Büntgen et al. 2005). This record was detrended using the Regional Curve Standardisation (RCS) method (Briffa et al. 1992), and calibrated and verified against high elevation station temperature data (Böhm et al. 2001) over the 1864–2002 period. Note that this reconstruction is independent from Casty et al. (2005b).

Two different ocean-atmosphere general circulation models (OA-GCMs) are used in this study. The first model is the Max Planck Institute for Meteorology global coupled model, ECHAM5/MPI-OM. The resolution of the atmospheric component, ECHAM5 (Roeckner et al. 2003, version 5.0), is 19 levels in the vertical dimension and T42 in spectral space, which corresponds to a horizontal resolution of about $2.8° \times 2.8°$. The oceanic component, MPI-OM (Marsland et al. 2003), is based on a Arakawa C-grid (Arakawa and Lamb 1981) version of the HOPE ocean model (Wolff et al. 1997). It is run on a curvilinear grid with equatorial refinement and includes 20 vertical levels. A dynamic/thermodynamic sea ice model (Marsland et al. 2003) and a hydrological discharge model (Hagemann and Duemenil-Gates 2001) are included. The atmospheric and oceanic components are connected with the OASIS coupler (Terray et al. 1998). The model does not employ flux adjustment or any other corrections. Initial ocean conditions are taken from a 500-yr control integration. The model is forced from stable conditions with a 1% CO_2 increase per year from 1990 (348 ppm) to 2100 (1039 ppm). Hereafter, this experiment is denoted as ECHAM5 1% CO_2. This forcing is a commonly used scenario to intercompare the sensitivity of different coupled climate models to increased greenhouse gases.

The second setup is the Climate Community System Model (CCSM), version 2.0.1,[1] developed by the National Center for Atmospheric Research (NCAR) (Kiehl et al. 1998;

Blackmon et al. 2001). The atmospheric part of this coupled model has a horizontal resolution of T31 ($\sim$3.75° $\times$ 3.75°) with 26 vertical levels; the ocean component has $\sim$3.6° $\times$ 1.8° resolution with 25 levels. The CCSM also runs without any flux corrections. Two simulations were carried out: a 550-yr simulation for constant present day climate conditions fixed to 1990 AD (denoted as CCSM 1990) and a 1% CO_2 simulation (denoted as CCSM 1% CO_2) starting from the stable state of the CCSM 1990 (Raible et al. 2005). Note that for the CCSM 1990, the first 50 years are ignored until the model adjusts to its stable climate state. The CCSM is integrated on two different computer platforms, an IBM SP4 and a Linux cluster (Renold et al. 2004). Note that the different computer platforms have no influence on the mean behaviour of the simulations.

Regionally, we use the Climate High Resolution Model (CHRM) which is driven by the Hadley Center HadAM3 atmospheric GCM at the lateral boundary (Pope et al. 2000). The CHRM regional model covers Europe and a fraction of the North Atlantic on a 81 by 91 grid point domain with a resolution of approximately 56 km and a time step of 300 s (see Vidale et al., 2003 for model set-up). The CHRM has been validated regarding its ability to represent natural interannual variations (Vidale et al. 2003) and the precipitation distribution in the Alpine region (Frei et al. 2003) using a simulation that is driven by the ECMWF reanalysis ERA-15 (Gibson et al. 1999). Two time-slice simulations are performed: For the control simulation from 1961–1990 the HadAM3 and the nested CHRM uses observed SSTs and observed greenhouse gas concentrations. The second experiment for the time-slice 2071–2100 uses the forcing of an IPCC A2 scenario (IPCC 2001). To assure that changes in variability between the two simulations are not associated to SST changes, but are due to the atmospheric models and their interaction with the land surface, the so-called delta change approach is applied to the experimental setup (Jones et al. 2001). Both GCM HadAM3 simulations, delivering the boundary conditions for the CHRM regional model, use the same SST variations (taken from the 1960–1990 observations), but a mean SST warming is added to the A2 scenario simulations by using the warming signal from the coupled HadCM simulation. Both simulations have a one year spin-up phase: 1960 and 2070, respectively.

2.2 Analysis techniques

The analysis presented in this paper is restricted to the Atlantic-European and the Alpine region. Time series are defined for both regions. The temperature time series is the mean over 25°W–40°E and 35°N–70°N for the European land area and over 4–16°E and 43–48°N for the Alpine region. For the precipitation time series the Atlantic-European region was reduced to 10°W–30°E and 35°N–70°N due to the smaller area available from the reconstructions (Pauling et al. 2006). To emphasise and extract low-frequency variability, a 31-yr triangular filter was applied. The first and the last 15 years of the time series are not analysed to avoid edge effect problems.

To merge the time series from climate simulations and reconstructions, and to account for biases of the model simulations, anomalies with respect to the overlapping 1990–2000 and 1961–1990 periods were used for the Atlantic-European and the Alpine area, respectively. Biases between the model output and the reconstructions are amongst others due to the coarse model resolution (horizontally and vertically) and the inclusion of sea areas which are not considered in the reconstructions. Moreover, due to the different horizontal resolution the size of the area slightly varies from the reconstructions. Other reasons for biases could also be the uncertainties of the proxy input data of the reconstruction method as well as systematic model errors, e.g., model drifts and underestimation of subgrid scale variability. Filtering
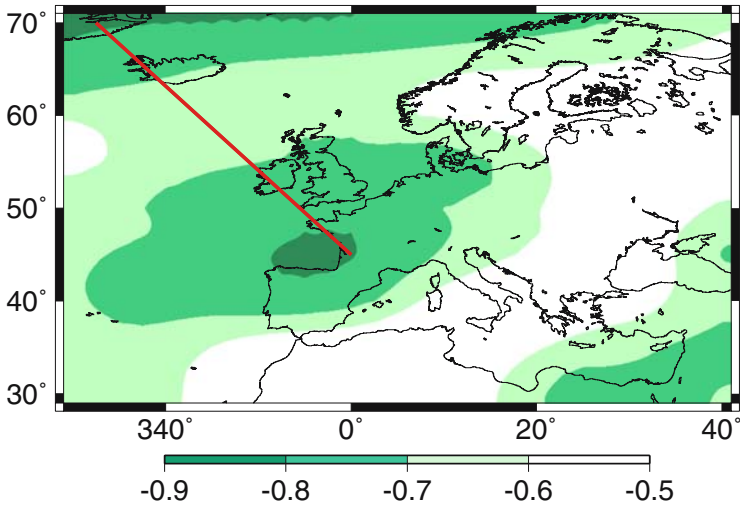
Fig. 1 An example of a 30-yr window (1973–2002), where the teleconnectivity of the 500 hPa geopotential height (DJF, shaded) and the corresponding axis of teleconnectivity (red line) is denoted

was applied to each time series separately in order to avoid mixing model and reconstruction data. However, this results in gaps in the filtered time series.

The spatio-temporal behaviour of the circulation of the free atmosphere can be characterised by the teleconnectivity of the 500 hPa geopotential height. According to Wallace and Gutzler (1981) the teleconnectivity is defined as the strongest negative correlation of one base point with all grid points assigned at the base point. As base point, all grid points are iteratively chosen. Only strong negative correlations which cluster together in a large area are considered as "centers of action". Thus, anticorrelated centers of action, e.g., the NAO with its poles near Iceland and the Azores, are easily identified. To find the center that is anticorrelated with another one, a search algorithm is applied to the teleconnectivity map. In a $20° \times 10°$ longitude/latitude neighbourhood the strongest negative correlation coefficient is identified. Provided that the region is large enough to capture one center of action, the size of search area is not a critical factor in this procedure. Then, this grid point is again correlated with all others in the 500 hPa geopotential height providing the position of the grid point which has the strongest negative correlation. These positions are connected with lines denoting the axis of the opposing centers of action. In order to illustrate this method, Figure 1 shows the teleconnectivity of the reconstructed 500 hPa geopotential height (shadings) in winter (DJF) and the axis of the anticorrelated centers of action (red line) for the 1973 to 2002 period. The two centers of action are easily identified. Perpendicular to the axis, the atmospheric flow is strengthened or weakened, depending on the sign of the centers of action. For example, if the northern center is negative and the southern is positive, the westerly atmospheric flow is stronger than average, and vice versa.

The technique was applied to the 500 hPa geopotential height data for a 30-yr running window, where only the axes of the conversing centers of action are displayed. This results in a three-dimensional Hovmöller diagram (e.g., Figure 5) which shows the spatio-temporal behaviour of atmospheric circulation patterns. The window size was chosen to fit to the filter applied to the time series and also to correspond to the window regularly used for time-slice experiments with highly resolved climate models in the climate change community (Wild

et al. 2003). Another reason for setting the size to 30 years is that the World Meteorological Organisation defines climatological mean to be a 30-yr mean. Nevertheless, tests with moderate changes of the window size, e.g., 40 years, confirm the results in the following sections.

3 Climate variability in the Atlantic-European area

To investigate climate variability in the Atlantic-European region we first focus on the reconstructed time series. The interannual variation of the temperature reconstruction (Luterbacher et al. 2004, Figure 2a,b) shows larger variability in winter (standard deviation of 1.1 °C) than in summer (standard deviation of 0.44 °C). This is in contrast to the three simulations, showing a standard deviation of about 0.65 °C in winter and 0.4 °C in summer, and illustrating a model deficiency in winter and/or the difference calculating the averages for different resolution. Comparing the CCSM 1990 simulation with the two scenario simulations, the variability on this time scale is nearly equal. Note that other simulations, especially regional simulations, show this variability change from winter to summer and therefore a better agreement with the observations and the reconstructions (IPCC 2001).

The reconstructed and simulated precipitation time series (Pauling et al. 2006, Figure 2c,d) show a slightly smaller interannual variability than in the observed period 1900–2000. Before 1800 the variability of the seasonally reconstructed precipitation (Figure 2c) decreases. For the first 300 years only a few natural proxies in combination with documentary precipitation information, unevenly distributed over Europe, are available. These scattered data obviously cannot fully resolve the variance at continental scale, thus the statistical method tends to calibrate more towards the long-term 20th century mean (climatology), and due

Fig. 2 Unfiltered time series of European temperature and precipitation for (a,c) DJF and (b,d) JJA. The time series are adjusted to the period 1990-2000. The multi-proxy reconstructions are based on Luterbacher et al. (2004) for temperature and Pauling et al. (2006) for precipitation (unit: mm per 3 months). Note also that the CCSM 1990 simulation is for perpetual 1990 conditions, thus the top blue x-axis shows model years

to the low number of degrees of freedom "extremes" are not well reconstructed. Over the last 200 years, when widespread instrumental precipitation data become available, the uncertainties in terms of unresolved variance within the 20th century calibration period, decrease and more accurate reconstructions are obtained. The interannual variability is further reduced in the scenario simulations (ECHAM5 and CCSM 1%CO_2) compared with the CCSM 1990 particularly in summer despite the fact that each model has its own climate sensitivity.

Switching to low-frequency variability, emphasised by a 31-yr triangular filter, the temperature reconstructions show several distinct cold phases, namely during the late 16th, late 17th and late 19th centuries (Figure 3a). Interestingly, the cold winter conditions during the last decades of the 17th century correspond to a period of low solar activity known as the Maunder Minimum. Comparing the CCSM 1990 with the reconstructed temperature, the low-frequency variability diverges, showing colder temperatures for the reconstructions in both seasons. This is not surprising since the radiative forcing of the simulation is set to fixed 1990 conditions (solar and greenhouse gas concentrations), whereas the observed mean radiative forcing over the past 500 years is lower than the 1990 value. However, the range of decadal variations is similar for the CCSM 1990 and the reconstruction from 1500–1900 leading to a signal detection problem as mentioned by Yoshimori et al. (2005). They showed in a modelling study of the Maunder Minimum that temperature variation on a hemispheric scale could be partly traced back to changes in the external forcing. On a regional scale this is more difficult, particularly in areas where the internal variability is high, e.g., the exit regions of the midlatitude storm tracks (Alaska, Atlantic-European area). As expected, the scenario simulations show for both seasons a strong temperature increase towards 2100. This increase
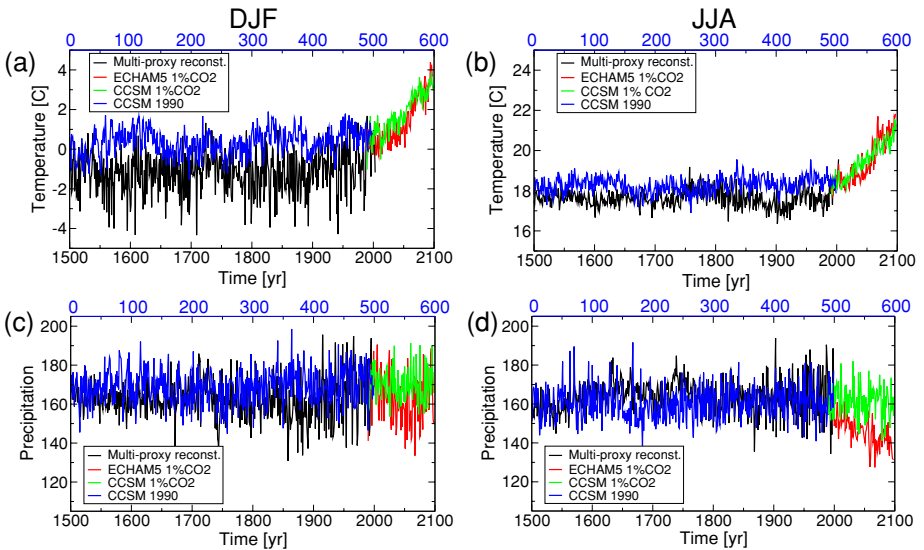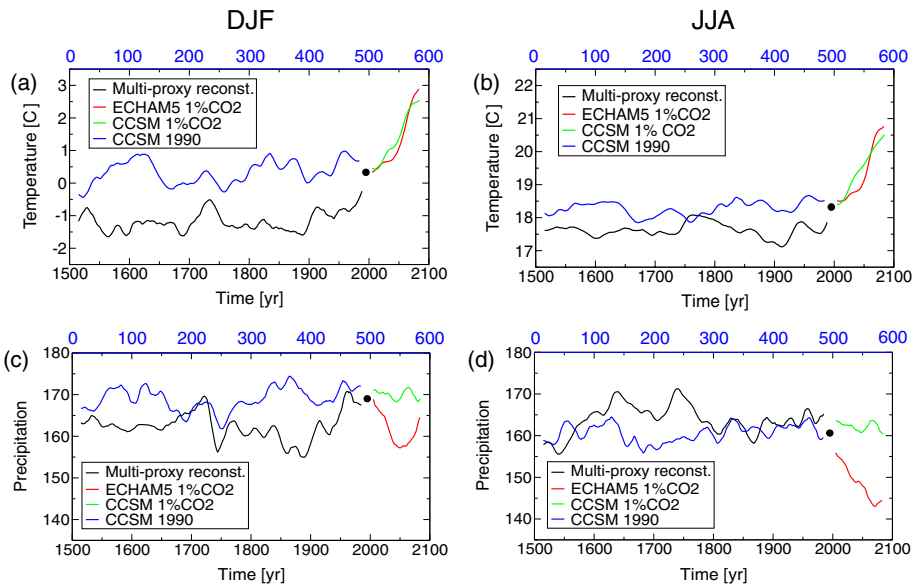

Fig. 3 Filtered time series of European temperature and precipitation for (a,c) DJF, (b,d) JJA. The time series are adjusted to the period 1990–2000 (denoted by the black dot). A 31-yr triangular filter is used emphasising the low-frequency variability in the time series. The multi-proxy reconstructions are based on Luterbacher et al. (2004) for temperature and Pauling et al. (2006) for precipitation (unit: mm per 3 months). Note also that the CCSM 1990 simulation is for perpetual 1990 conditions, thus the top blue *x*-axis shows model years

is unprecedented compared with increases in the CCSM 1990 or the reconstruction prior to 1900.

The low-frequency behaviour of precipitation (Figure 3c,d) also shows remarkable variations in the last centuries, but is reduced in the CCSM 1990 simulation compared with the reconstruction. The standard deviation of the filtered time series is reduced from 3.4 to 2.7 mm per three months in winter and from 3.5 to 2.1 mm per three months in summer, respectively. The scenario simulations show a decrease of precipitation mainly in summer.

To investigate seasonality in more detail, the difference between JJA and DJF is compared for temperature and precipitation (Figure 4) as suggested by Jones et al. (2003). However, a part of this difference may be due to the lack of variability in volcanic and solar forcing in the simulation (Hansen et al. 1992). Clearly the range of variation of the temperature difference (Figure 4a) is stronger in the reconstructions than in the model simulations resembling the results of Jones et al. (2003). Moreover, a negative trend from the 19th century to the 20th century is evident in the reconstructions. This decrease of summer to winter temperatures may also continue in the future as the CCSM 1% CO_2 in comparison to the CCSM 1990 suggests. Again, one has to be cautious as the other scenario does not show such a decrease.

For the precipitation difference, the range of variation is again stronger in the reconstructions than in the model simulations (Figure 4b). One scenario simulation (ECHAM5 1% CO_2) shows a decrease in precipitation seasonality. Notable is an increased seasonality in precipitation after the Late Maunder Minimum (∼1720) which goes along with a strong decrease of temperature difference. However, due to increased uncertainties prior to the 18th century the seasonality changes of the reconstruction have to be interpreted with caution.

The low-frequency changes of temperature and precipitation as well as their changes in seasonality may be related to low-frequency changes of the atmospheric flow-regime. Therefore, the temporal teleconnection behaviour illustrated by the teleconnectivity of the 500 hPa geopotential height is shown for the reconstructions (Luterbacher et al. 2002b; Casty et al. 2005a, Figure 5). In winter two direction axes are frequently revisited (Figure 5a, bottom panel): a north-south axis, denoting an anomalous (stronger or weaker) westerly flow towards Europe, and a northwest-southeast axis exhibiting an anomalous meridional flow towards Europe. Temporally these patterns are stable for several decades (Figure 5a, top panel). The 16th century indicated by (i) is dominated by the anomalous meridional flow pattern, switching to the westerly pattern from ∼1600 to 1650 (ii in Figure 5a, top panel). Note that this westerly pattern is mainly in its negative phase, so continuing an anomalous meridional flow. For the Late Maunder Minimum period (∼1680 to 1715, iii) the axis turns again towards the northwest-southeast orientation and the position of the northwestern center moves from Iceland to the British Islands. For the 20th century the axis shows again a north-south orientation.

During summer a different picture with a northwest-southeast and a southwest-northeast orientation of the axis of teleconnectivity is captured (Figure 5b, bottom panel). A west-east orientation can also be found, but this is a rare event and therefore not of primary consideration. For the northwest-southeast orientation, main air masses stem from western Russia (positive phase) or the southern Atlantic (negative phase). The southwest-northeast corresponds to a flow regime from Greenland (positive phase) or North Africa (negative phase). Temporally the southwest-northeast orientation, corresponding to an anomalous stronger or weaker north-south flow, was mainly found in the 17th century, which was dominated by the Maunder Minimum (Figure 5b, top panel). From 1720 onwards the climate system stays in the northwest-southeast mode. The anticorrelations are less pronounced in summer compared to winter (not shown).
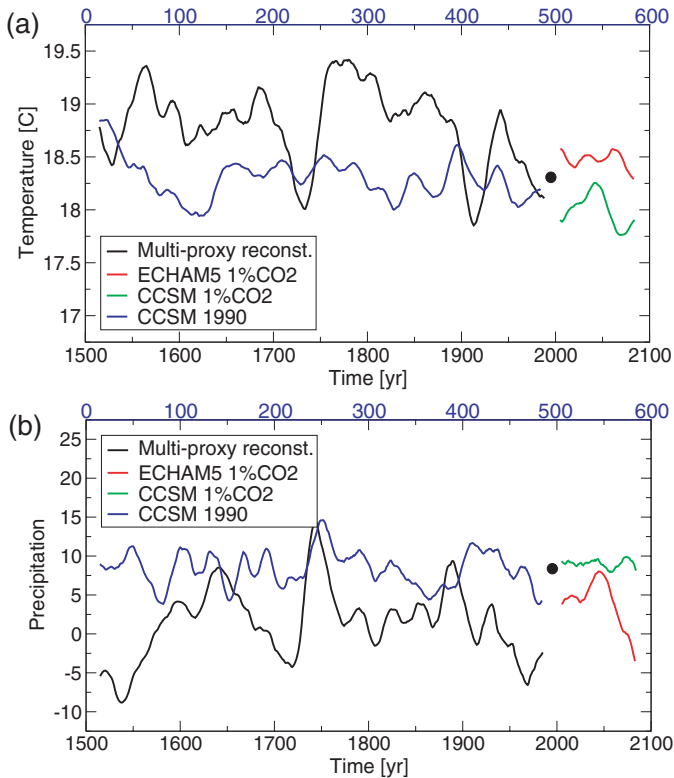
Fig. 4 Filtered time series for the difference JJA-DJF (a) European temperature and (b) European precipitation (unit: mm per 3 months). The time series are adjusted to the period 1990–2000 (denoted by the black dot). A 31-yr triangular filter is used emphasising the low-frequency variability in the time series. The multi-proxy reconstructions are based on Luterbacher et al. (2004) and Pauling et al. (2006). Note also that the CCSM 1990 simulation is for perpetual 1990 conditions, thus the top blue x-axis shows model years

The orientations of the teleconnectivity in the CCSM 1990 simulation behave differently. The CCSM 1990 shows a northwest-southeast axis and a north-south axis (Iceland to Azores) in winter, which is similar to the reconstructions, but there is also a north-south anticorrelation from Scandinavia to the eastern part of the Mediterranean Sea (Figure 6a). Temporally, the axis orientation is not stable in time for decades which is also in contrast to the reconstructions. The summer (Figure 6b) behaves temporally similar to winter, but also exhibits the southwest-northeast axis found in the reconstructions. Overall the simulated teleconnection evolution appears more noisy and less structured than the reconstruction teleconnections (Figure 5) for both seasons.

In contrast to the CCSM 1990 simulation, the teleconnection patterns in the scenario simulations are more time stable over several decades for both seasons (Figure 7). The ECHMA5 1% CO_2 resembles the reconstruction modes, whereas in the CCSM 1% CO_2 the position of the northwestern center of the northwest-to-southeast mode in winter is moved to Britain Isles. In summer the southeast center of the CCSM 1% CO_2 simulation is moved to the Iberian peninsula, in contrast to the reconstructions and the other simulations where this center of action is located in the eastern part of the Mediterranean Sea. Whether or not
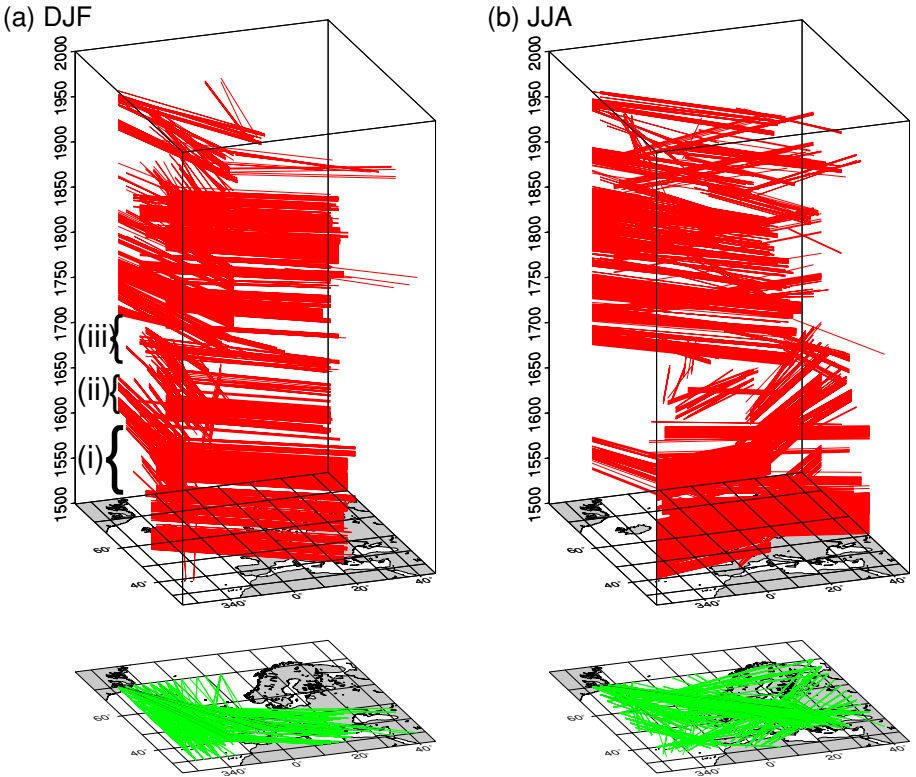
Fig. 5 The temporal evolution of the axis of teleconnections measured by the teleconnectivity of the reconstructed 500 hPa geopotential height (Luterbacher et al. 2002b): (a) DJF and (b) JJA. Bottom panels show the projection of all axes in the Atlantic-European region. The axes connect the centers of action within particular teleconnection modes. Special periods mentioned in the text are indicated by (i), (ii), and (iii)

this is a model deficiency or a real signal to the 1% CO_2 increase can not yet be concluded. Ensemble simulations with more than two models, in order to minimise the influence of specific model formulations, could help answer this question.

Combining the results of Figure 2 through Figure 7, we find for the cold spell during the 17th century, corresponding to the Maunder Minimum that winters were colder and drier, and summers were colder and wetter than today (Luterbacher et al. 2001). An abrupt seasonality change in temperature and precipitation occurred at or near the end of the Maunder Minimum. In both seasons the atmospheric circulation changed to a more meridional mode during the Maunder Minimum where the axis, connecting the centers of action, exhibits a northwest-southeast orientation in winter and a southwest-northeast orientation in summer. Nevertheless, one has to mention that the Maunder Minimum is not the only cold period; also the end of the 16th and 19th centuries colder seasons compared to today are observed with similar shifts of teleconnection patterns. Moreover, the teleconnection patterns are more time stable in the reconstruction. A more variable temporal behaviour of the simulated teleconnectivity of CCSM 1990 is observed and could be due to model deficiencies and/or the constant external forcing compared with the reconstructions. The reconstruction method itself could also be the source of generating stability over several decades by focusing on only a few
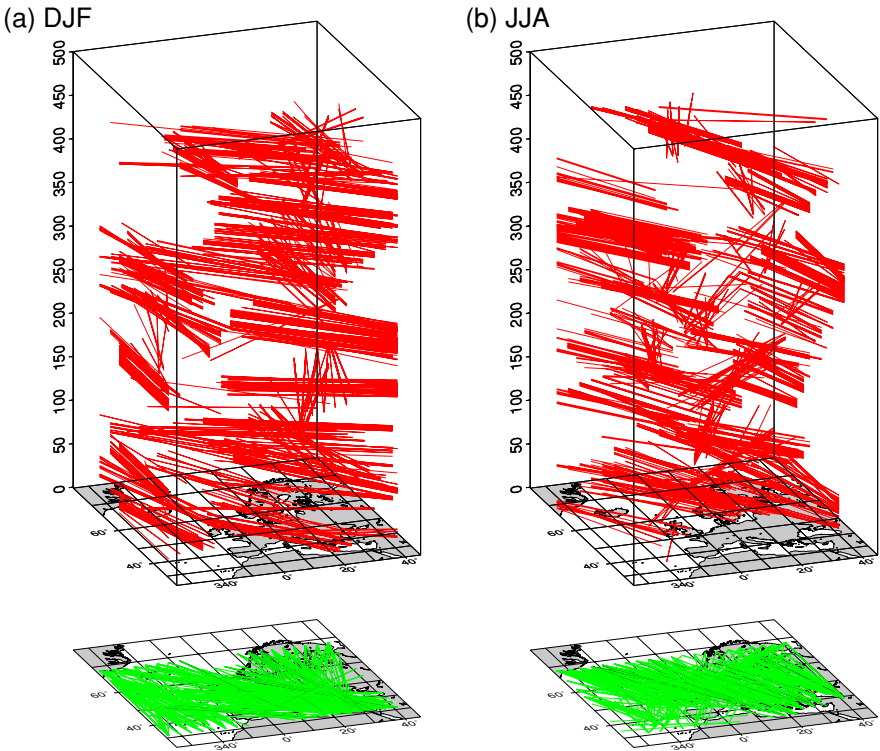
Fig. 6 Same as Figure 5, but for the 500-year long CCSM simulation with perpetual 1990 conditions

patterns of variability. But, because the reconstructions incorporate external forcing ranging from natural (solar and volcanic) to anthropogenic forcing (greenhouse gas emissions) and because the scenario simulations show a greater time stability of the teleconnection pattern (compared with the CCSM 1990) we favor an influence of external forcing, thus we hypothesise that time-dependent external forcing (solar, volcanic and greenhouse gases) might help in stabilising the mode temporally.

4 Climate variability in the Alps

With the steadily growing data base, reconstructions of climate parameters are performed for the European Alps (Casty et al. 2005b; Frank and Esper 2005; Büntgen et al. 2005). Figures 8 and 9 show the winter (DJF) and summer (JJA) temperature and precipitation for the Alpine areas, respectively. In winter, the temperature shows periods with stronger interannual variations around 1600 and a decrease in this variability in the second half of the 20th century (Figure 8a). In summer, where two independent reconstructions are available, the interannual variations are nearly unchanged, except for the period 1800–1830 which was dominated by strong volcanic eruptions, e.g., 1815 eruption of Tambora (Figure 8b). Comparing both reconstructions, stronger variability is found within the multi-proxy reconstruction (Casty et al. 2005b). This is likely due to the fact that although the tree-ring reconstruction has a
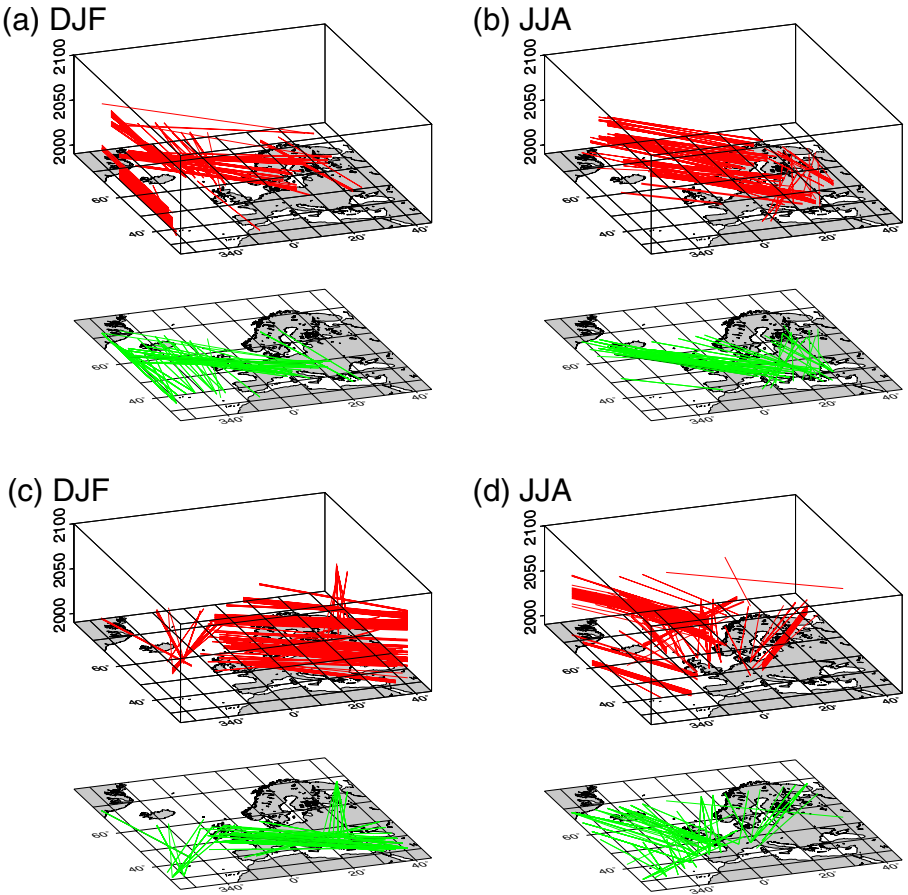
Fig. 7 Same as Figure 5, but for the (a,b) ECHAM5 1% CO_2 and the (c,d) CCSM 1% CO_2

maximum response towards summer temperatures, it also integrates some effects of previous month temperature variability. In contrast to the interannual behaviour the winter precipitation shows enhanced year-to-year variations towards the end of the 19th and the whole 20th century (Figure 8c). In summer, the behaviour is vice versa, with a decrease in variability on these time scales in the 18th through 20th centuries compared with the period before (Figure 8d). Winter uncertainties are rather high prior to 1770 with values of around 190 mm per 3 months (Casty et al. 2005b) and explain at least part of the decreased variability of the reconstructed precipitation sums for the 1500–1850 period. Summer uncertainties are smaller than for winters (80 mm per 3 months) and the decrease of variability towards the 20th century could not be traced back to a weak performance of the reconstruction. However Pfister (1992) states that historical data, used during the pre-1688 period, often emphasize extreme conditions. This may provide a misleading sense of the true seasonal or annual mean climate anomalies.

The filtered time series show that the pre-20th century Alpine winter temperatures were generally colder than those of the 1901–2000 period (Figure 9a). The lowest temperatures
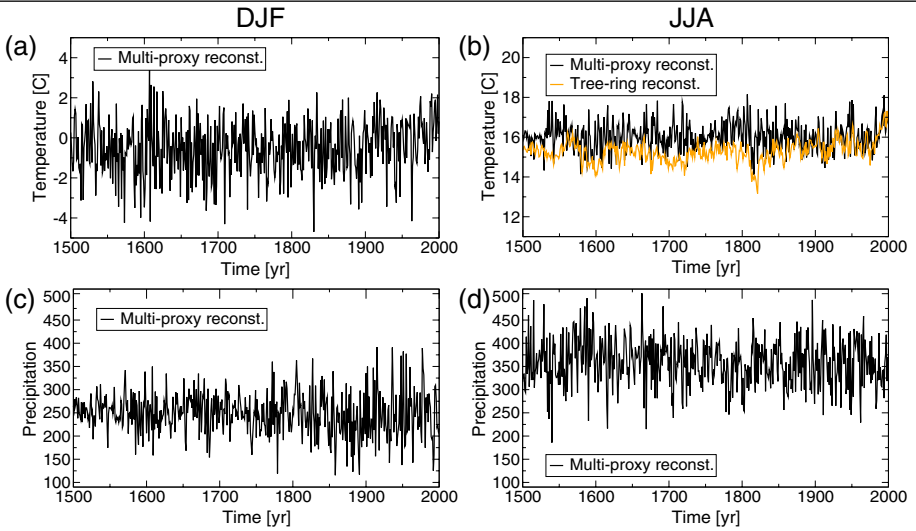
Fig. 8 Unfiltered time series of Alpine temperature and precipitation (unit: mm per 3 months) for (a,c) DJF and (b,d) JJA. The time series are adjusted to the period 1961–1990. The multi-proxy reconstructions (black lines) are based on Casty et al. (2005b) and the tree-ring reconstruction (yellow line) on Büntgen et al. (2005)
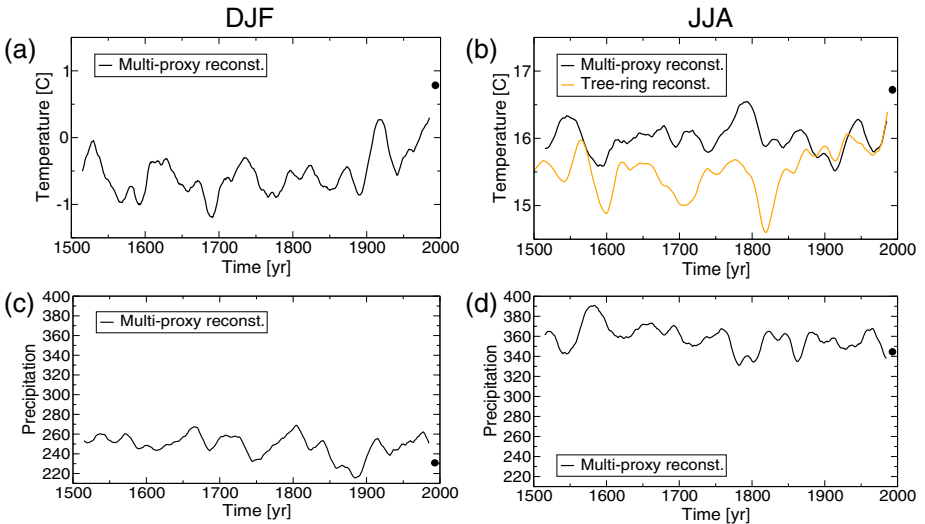
Fig. 9 Filtered time series of Alpine temperature and precipitation (unit: mm per 3 months) for (a,c) DJF and (b,d) JJA. The time series are adjusted to the period 1961–1990. A 31-yr triangular filter is used emphasising the low-frequency variability in the time series. The multi-proxy reconstructions (black lines) are based on Casty et al. (2005b) and the tree-ring reconstruction (yellow line) on Büntgen et al. (2005). To show the tendency of the last decades (which are partly excluded by the filter) the mean from 1986–2000 is denoted by dots for both variables and seasons, respectively

were experienced during the last decades of the 17th century, which is in agreement with the coldest phase over Europe back to 1500 (Luterbacher et al. 2001, 2004). Winters in the 1690s were extremely harsh in the Alpine area with temperature anomalies of the order of $-1.2\,°C$ compared to $0\,°C$ for the 20th-century mean. Less intense cold periods are reconstructed for the second half of the 16th century and at the end of the 19th century.

A strong transition to a warming in Alpine winters is found from around 1890 to 1915. A cooling is then experienced in the mid-20th century followed by an unprecedented upward trend until recent times (illustrated by dots in Figure 9 that represent the mean of the last 15 years).

In summer the two filtered proxy time series are again analysed and compared. The major difference between the multi-proxy and the tree-ring reconstruction is that the latter shows a clear trend from 1800 to 2000 starting from a lower temperature mean the century before. Again, this amplitude difference could partly be related to the fact that the tree-ring reconstructions also integrates temperature information from before the vegetation period. This extended response period likely reflects lower frequency, inter-decadal scale variability (Figure 9b). Therefore, a better agreement between the two reconstructions could be achieved by comparing the tree-ring reconstruction with the smoothed annual Alpine multi-proxy reconstruction. Moreover, both reconstructions are calibrated against different data. The use of the new homogenised temperatures series of Switzerland (Begert et al. 2005) for both reconstructions data set could also lead to a better agreement. For the multi-proxy reconstruction, warm Alpine summers were experienced around 1550, periodically in the 17th century, the second half of the 18th century, in the mid 20th century, and from 1970 onward (Figure 9b). Except for 1550s, the tree-ring reconstruction resembles this multi-decadal behaviour of the multi-proxy reconstruction, even though the multi-proxy reconstruction and the tree-ring reconstruction are not exactly parallel. For both reconstructions cold summer periods are found at the end of the 16th century, the end of the 17th century, the early 18th century, and the beginning of the 20th century. Summarizing, the discrepancies between the multi-proxy and the tree-ring reconstruction can be traced back to the differing seasonalities represented by the reconstructions, the use of different (predictand) instrumental data, and finally, differing calibration methods during different calibration periods (Büntgen et al. 2005).

For both seasons the reconstructed precipitation time series show that strong decadal to interdecadal changes are superimposed on a general downward trend until the end of the 19th century (Figure 9c,d). The driest period in winter is at the turn of the 20th century followed by a strong upward trend within the 20th century. Very wet summers occurred from 1550 to 1600. The recent downward trend of precipitation over the Alps after 1970 is a result of the trend in the NAO to its positive phase in winter. Statistically significant negative correlations of around -0.5 are found during this period (Casty et al. 2005b). During summer the Azores High gets more pronounced, contributing to the downward trend in precipitation over the Alps (Dünkeloh and Jacobeit 2003; Xoplaki et al. 2004).

To get an idea of the future behaviour of the Alps under global climate change, time slice simulations with a regional model are carried out. In the A2 simulation (2071 to 2100) the winter and summer temperatures show an average rise of about $3°C$ and $4°C$, respectively (Figure 10a,b). Comparing the control time slice 1961–1990 with the A2 scenario, the interannual variability is unchanged in winter, whereas a strong increase on these time scales in summer is observed (Schär et al. 2004). Precipitation behaves differently; in winter a small average increase is simulated in the A2 scenario (Figure 10c). The simulated trend in winter precipitation for the control period 1961–1990 is consistent with the observed trend (Schmidli et al. 2002) and the reconstruction (Figure 9c); thus it may be explained by internal variability. In summer the mean precipitation shows a small decrease compared with the mean of the control simulation (Figure 10d). The interannual variability of precipitation remains unchanged in winter, but increases in summer, comparing the A2 with the control simulation.
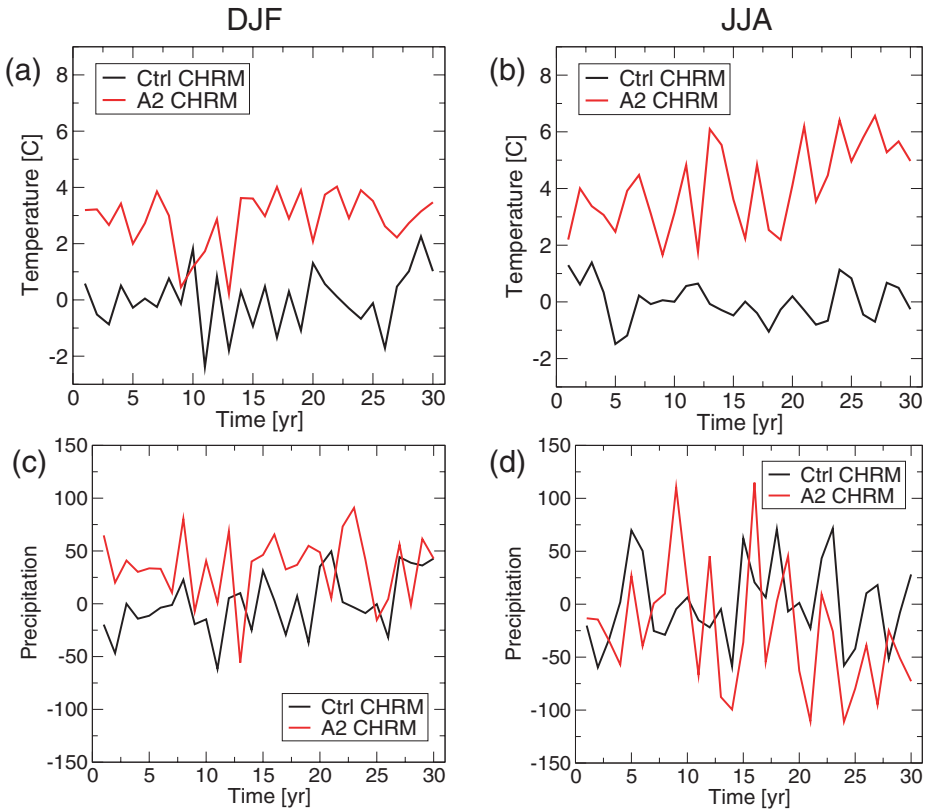
Fig. 10 Temperature (a,b) and precipitation (c,d) anomalies of regional simulations for the control time-slice 1961-1990 and the A2 scenario from 2071–2100: (a,c) DJF, (b,d) JJA. Anomalies are taken with respect to the mean of the control simulation 1961-1990. The unit of precipitation is mm per 3 months

5 Summary and conclusions

To improve the understanding of natural climate variability and to assess future climate change, both reconstructions and model simulations are analysed for the Atlantic-European and the Alpine regions.

The time series for temperature and precipitation show variations on interannual to decadal time scales. The recent upward temperature trend for Atlantic-European region is unprecedented over the last 500 years for winter and summer, resembling findings from Jones and Mann (2004) for the Northern Hemisphere and will continue for the next 100 years under the constraint that greenhouse gas emissions will rise (simulated by two coupled GCMs with a 1% CO_2 increase per year). The precipitation signal is not as clear, as the future simulations do not agree in tendency. Going back in time, distinct cold periods are found in the reconstructions, which are separated from the coupled GCM simulation forced with constant 1990 conditions (CCSM 1990). This is mainly due to the difference in radiative forcing over the last 500 years, which was lower at certain stages than the 1990 values used in the simulations. The overlaid reconstructed decadal variability, however, is not distinguishable from the CCSM 1990, leading to a signal detection problem as mentioned by Yoshimori et al. (2005). Recently, von Storch et al. (2004) mentioned that regression methods used in

Northern Hemisphere reconstructions of this kind underestimate low-frequency variability, which leads to the conclusion that the real climate variability shows stronger decadal fluctuations and therefore it might be distinguishable from CCSM 1990. However, recent work (Mann et al. 2005; Goosse et al. 2005) suggests that the results of von Storch et al. (2004) may be overstated, implying that the decadal fluctuations reconstructed may be relatively accurate. In this case the signal detection problem would remain. The changes in seasonality show that the reconstructions have a broader range than the model simulations, resembling the results of Jones et al. (2003). A clear signal in the future could not be detected; as the two simulations again do not agree.

Illustrated by the teleconnectivity we showed that low-frequency changes of large-scale atmospheric circulation flow control at least part of the temperature and precipitation variability, e.g., the meridional circulation in the late Maunder Minimum connected with an anomalously cold period and more zonal flow regime with warm temperatures in the 20th century. Temporally, differences between the reconstructed and the simulated teleconnectivity using CCSM 1990 are likely to be due to the constant external forcing of CCSM 1990. Because the scenario simulations show temporally stable axes of teleconnection patterns over several decades, similar to the reconstructions, we hypothesise that time-dependent external forcing (solar, volcanic and greenhouse gases) might support a temporal stabilisation of the patterns. Future investigations of an ensemble of transient model simulations from 1500 onwards will help to address this question in more detail. It will also give us the possibility to test the reconstruction method in order to exclude exclude those, which are the source of stabilization.

Analysing the low-frequency behaviour of temperature and precipitation, the Alpine area shows stronger amplitudes than the Atlantic-European region in summer and winter. However, this result likely derives from the smaller area considered and does not necessarily imply that mountainous regions are more sensitive to large-scale variability and climate change. Projections for the future climate with a regional model show, beside a clear temperature increase in both seasons, a change in interannual variability in summer. Temperature and precipitation show broader distributions, which could be partly explained by a soil moisture precipitation feedback mechanism (Schär et al. 1999, 2004). However, the reconstructions show an opposite behaviour, comparing the period after 1900 (which is already influenced by increasing greenhouse gas emissions) with the centuries before. Still, it can not be decided whether or not this is due to the underestimation of variability of regression techniques used for the reconstructions, or the regional model's overestimation of the variability, or the past warming was small compared with the expected future warming. A further improvement of the reconstruction methods as well as multi-model ensemble approaches (using different regional models nested in different global models) could give a more comprehensive picture in future.

References

Appenzeller C, Stocker TF, Anklin M (1998) North Atlantic Oscillation dynamics recorded in Greenland ice cores. Science 282:446–449

Arakawa A, Lamb VR (1981) A potential enstrophy and energy conserving scheme for the shallow water equations. Mon Wea Rev 109:18–36

Bauer E, Claussen M, Brovkin V, Huenerbein A (2003) Assessing climate forcings of the Earth system for the past millennium. Geophys Res Lett 30, DOI:10.1029/2002GL016639

Begert M, Schlegel T, Kirchhofer W (2005) Homoteneous temperature and precipitation series of Switzerland from 1864 to 2000. Int J Climatol 25:65–80

Blackmon ML, Boville B, Bryan F, Dickinson R, Gent Kiehl J, Moritz R, Randall D, Shukla J, Solomon S, Bonan G, Doney S, Fung I, Hack J, Hunke E, Hurrell J, Kutzbach J, Meehl J, Otto-Bliesner B, Saravanan R, Schneider EK, Sloan L, Spall M, Taylor K, Tribbia J, Washington W (2001) The community climate system model. Bull Am Meteorol Soc 82:2357–2388

Böhm R, Auer I, Brunetti M, Maugeri M, Nanni T, Schöner W (2001) Regional temperature variability in the European Alps: 1760–1998 from homogenized instrumental series. Int J Climatol 21:1779–1801

Bradley R, Jones PD (1993) Little Ice Age" summer temperature variations: Their nature and relevance to recent global warming trends. The Holocene 3:367–376

Briffa KR, Jones PD, Bartholin TS, Eckstein D, Schweingruber FH, Karlen W, Zetterberg P, Eronen M (1992) Fennoscandian summers from AD 500: Temperature changes on short and long timescales. Clim Dyn 7:111–119

Briffa KR, Osborn TJ, Schweingruber FH, Harris IC, Jones PD, Shiyatov SG, Vaganov EA (2001) Low-frequency temperature variations from a northern tree-ring density network. J Geophys Res 106:2929–2941

Büntgen U, Esper J, Frank DC, Nicolussi K, Schmidhalter M (2005) A 1052-year tree-ring proxy for Alpine summer temperatures. Clim Dyn 25:141–153

Casty C, Handorf D, Raible CC, Luterbacher J, Weisheimer A, Xoplaki E, Gonzalez-Rouco JF, Dethloff K, Wanner H (2005a) Recurrent climate winter regimes in reconstructed and modelled 500 hPa geopotential height fields over the North Atlantic-European sector 1659–1990. Clim Dyn 24:809–822, DOI:10.1007/s00382-004-0496-8

Casty C, Wanner H, Luterbacher J, Esper J, Böhm R (2005b) Temperature und precipitation variability in the European Alps since 1500. Int J Climatol 25:1855–1880

Cheng W, Beck R, Rooth C (2004) Multi-decadal thermohaline variability in an ocean-atmosphere general circulation model. Clim Dyn 22:573–590, DOI:10.1007/s00382-004-400-6

Cook ER, D'Arrigo RD, Mann ME (2002) A well-verified, multiproxy reconstruction of the winter North Atlantic Oscillation index since AD 1400. J Climate 15:1754–1764

Cook ER, Esper J, D'Arrigo RD (2004) Extra-tropical Northern Hemisphere land temperature variability over the past 1000 years. Quat Sci Rev 23:2063–2074

Crowley TJ (2000) Causes of climate change over the past 1000 years. Science 289:270–277

Dünkeloh A, Jacobeit J (2003) Circulation dynamics of Mediterranean precipitation variability 1948–98. Int J Climatol 23:1843–1866

Esper J (2000) Long term tree-ring variations in Junipers at the upper timberline in the Karakorum (Pakistan). The Holocene 10:253–260

Esper J, Cook ER, Schweingruber FH (2002a) Low-frequency signals in long tree-line chronologies for reconstructing past temperature variability. Science 295:2250–2253

Esper J, Frank DC, Wilson RJS (2004) Climate reconstructions: Low-frequency ambition and high-frequency ratification. EOS, Trans Am Geophys Union 85:113,120

Esper J, Schweingruber FH, Winiger M (2002b) 1300 years of climate history for Western Central Asia inferred from tree-rings. The Holocene 12:267–277

Esper J, Shiyatov SG, Mazepa VS, Wilson RJS, Graybill DA, Funkhouser G (2003) Temperature-sensitive Tien Shan tree ring chronologies show multi-centennial growth trends. Clim Dyn 21:699–706

Frank DC, Esper J (2005) Temperature reconstructions and comparison with instrumental data from a tree-ring network for the European Alps. Int J Climatol 25:1437–1454

Frei C, Christensen JH, Deque M, Jacob D, Jones RG, Vidale PL (2003) Daily precipitation statistics in regional climate models: Evaluation and intercomparison for the European Alps. J Geophys Res 108(D3), 4124, DOI: 10.1029/2002JD002287

Gibson JK, Kallberg P, Uppala S, Hernandez A, Nomura A, Serrano A (1999) ERA description, Version 2 Technical report, ERA-15 Project Report Series, No. 1, ECMWF, Reading, UK. p. 74

Goosse H, Crwoley TJ, Zorita E, Ammann H, Renssen CM, Driesschaert E (2005) Modelling the climate of the last millennium: What causes the differences between simulations. Geophys Res Lett 32, L06710, DOI:10.1029/2005GL022368

Grötzner A, Latif M, Barnett TP (1998) A decadal cycle in the North Atlantic ocean as simulated by the ECHO coupled GCM. J Climate 11:831–847

Guiot J, Nicault A, Rathgeber C, Edouard J, Guibal F, Pichard G, Till C (2005) Last-millennium summer-temperature variations in western Europe based on proxy data. Holocene 15:489–500

Hagemann S, Duemenil-Gates, L (2001) Validation of the hydrological cycle of ECMWF and NCEP reanalyses using the MPI hydrological discharge model. J Geophys Res 106:1503–1510

Hansen J, Lacis A, Ruedy R, Sato M (1992) Potential climate impact of Mount Pinatubo eruption. Geophys Res Lett 19:215–218

Hurrell, JW (1995) Decadal trends in the North Atlantic Oscillation: Regional temperatures and precipitation. Science 269:676–679

Hurrell JW, Kushnir Y, Ottersen G, Visbeck M (2003) *The North Atlanitc Oscillation: Climate Significance and Environmental Impact*, Vol. 134. Geophysical Monograph Series. p. 279

Hurrell JW, Loon HV (1997) Decadal variations in climate associated with the North Atlantic Oscillation. Clim Change 36:301–326

IPCC (2001) *Climate Change 2001: The Scientific Basis*. Cambridge, UK and New York, NY, USA: Cambridge University Press. Contribution of Working Group I to the Third Assessment Report of the Intergovenmental Panel on Climate Change, p. 881

Jacobeit J, Wanner H, Luterbacher J, Beck C, Philipp A, Sturm K (2003) Atmospheric circulation variability in the North-Atlantic-European area since the mid-seventeenth century. Clim Dyn 20:341–352

Jones PD, Briffa KR, Barnett TP, Tett SFB (1998) High-resolution palaeoclimatic records for the last millennium: Interpretation, integration and comparison with General Circulation Model control-run temperatures. The Holocene 8:455–471

Jones PD, Briffa KR, Osborn TJ (2003) Changes in the Northern Hemisphere annual cycle: Implications for paleoclimatology. J Geophys Res 108, DOI:10.1029/2003JD003695

Jones PD, Mann ME (2004) Climate over past millennia. Rev Geophys 42, RG2002, DOI:10.1029/2003RG000143

Jones RG, Murphy JM, Hassell DC, Taylor R (2001) Ensemble mean changes in a simulation of the European climate of 2071–2100 using the new Hadley Centre Regional modelling system HadAM3H/HadRM3H, Technical report, Hadley Centre, Exeter, UK, available at http://prudence.dmi.dkl

Kalnay E, Kanamitsu M, Kistler R, Collins W, Coauthors (1996) The NCEP/NCAR 40 year reanalysis project. Bull Am Meteor Soc 77:437–471

Kiehl JT, Hack JJ, Bonan GB, Boville BA, Williamson DL, Rasch PJ (1998) The National Center for Atmospheric Research Community Climate Model: CCM3. J Clim 11:1131–1149

Kistler R, Kalnay E, Collins W, Saha S, Coauthors (2001) The NCEP-NCAR 50-year reanalysis: Monthly means CD-ROM and documentation. Bull Am Meteor Soc 77:437–471

Latif M, Roeckner E, Botzet M, Esch M, Haak H, Hagemann S, Jungclaus J, Legutke S, Marsland S, Mikolajewicz U (2004) Reconstructing, monitoring, and predicting multidecadal-scale changes in the North Atlantic Thermohaline Circulation with sea surface temperature. J Clim 17:1606–1614

Luterbacher J, Dietrich D, Xoplaki E, Grosjean M, Wanner H (2004) European seasonal and annual temperature variability, trends, and extremes since 1500. Science 303:1499–1503

Luterbacher J, Rickli R, Xoplaki E, Tinguely C, Beck C, Pfister C, Wanner H (2001) The late Maunder Minimum (1675–1715) – a key period for studying decadal scale climatic change in Europe. Clim Change 49:441–462

Luterbacher J, Schmutz C, Gyalistras D, Xoplaki E, Wanner H (1999) Reconstruction of monthly NAO and EU indices back to AD 1675. Geophys Res Lett 26:2745–2748

Luterbacher J, Xoplaki E, Dietrich D, Jones PD, Davies TD, Portis D, Gonzalez-Rouco JF, von Storch H, Gyalistras D, Casty C, Wanner H (2002a) Extending North Atlantic Oscillation reconstructions back to 1500. Atmos Sci Lett 2:114–124

Luterbacher J, Xoplaki E, Dietrich D, Rickli R, Jacobeit J, Beck C, Gyalistras D, Schmutz C, Wanner H (2002b) Reconstruction of sea level pressure fields over the Eastern North Atlantic and Europe back to 1500. Clim Dyn 18:545–561

Mann ME, Bradley RS, Hughes MK (1998) Global-scale temperature patterns and climate forcing over the past six centuries. Nature 392:779–787

Mann ME, Rutherford S, Wahl ER, Ammann CM (2005) Testing the fidelity of methodologies used in proxy-based reconstructions of past climate. J Clim 18:4097–4107

Marshall J, Johnson H, Goodman J (2001) A study of the interaction of the North Atlantic Oscillation with ocean circulation. J Clim 14:1399–1421

Marsland SJ, Haak H, Jungclaus JH, Latif M, Roeske F (2003) The Max-Planck-Institute global ocean/sea ice model with orthogonal curvilinear coordinates. Ocean Model 5:91–127

Meehl GA, Washington WM, Wigley TML, Arblaster JM, Dai A (2003) Solar and greenhouse gas forcing and climate response in the twentieth century. J Clim 16:426–444

Mitchell TD, Carter TR, Jones PD, Hulme M, New, M (2004) A comprehensive set of high-resolution grids of monthly climate for Europe and the globe: The observed record (1901–2000) and 16 scenarios (2001–2100). Technical Report Working Paper 55, Tyndall Center for Climate Change Research

Moberg A, Sonechkin DM, Holmgren K, Datsenko NW, Karlen W (2005) Highly variable Northern Hemisphere temperatures reconstructed from low- and high-resolution proxy data. Nature 433:613–617

New M, Hulme M, Jones PD (2000) Representing twentieth-century space-time climate variability. Part II: Development of 1901–1996 monthly grids of terrestrial surface climate. J Clim 13:2217–2238

Overpeck J, Hughen K, Hardy D, Bradley R, Case R, Douglas M, Finney, B, Gajewski K, Jacoby G, Jennings A, Lamoureux S, Lasca A, MacDonald G, Moore J, Retelle M, Smith S, Wolfe A, Zielinski G (1997) Arctic environmental change of the last four centuries. Science 278:1251–1256

Pauling A, Luterbacher J, Casty C, Wanner H (2006) 500 years of gridded high-resolution precipitation reconstructions over Europe and the connection to large-scale circulation. Clim Dyn 26:387–405

Pfister C (1992) Monthly temperature and precipitation in Central Europe 1525–1979: Quantifying documentary evidence on weather and its effects. In: Bradley RS, Jones PD (eds) Climate since A.D. 1500. Routledge, London

Pope DV, Gallani M, Rowntree R, Stratton A (2000) The Impact of new physical parameterizations in the Hadley Centre climate model HadAM3. Clim Dyn 16:123–146

Raible CC, Luksch U, Fraedrich K (2004) Precipitation and Northern Hemisphere Regimes. Atmos Sci Lett 5:43–55, DOI:10.1016/j.atmoscilet.2003.12.001

Raible CC, Luksch U, Fraedrich K, Voss R (2001) North Atlantic decadal regimes in a coupled GCM simulation. Clim Dyn 18:321–330

Raible CC, Stocker TF, Yoshimori M, Renold M, Beyerle U, Casty C, Luterbacher J (2005) Northern Hemispheric trends of pressure indices and atmospheric circulation patterns in observations, reconstructions, and coupled GCM simulations. J Clim 18:3968–3982

Renold M, Beyerle U, Raible CC, Knutti R, Stocker TF, Craig T (2004) Climate modeling with a Linux cluster, EOS, Trans Am Geophys Union 85:292

Rind D, Lean J, Healy R (1999) Simulated time-dependent climate response to solar radiative forcing since 1600. J Geophys Res 104:1973–1990

Roeckner E, Bäuml G, Bonaventura L, Brokopf R, Esch M, Giorgetta M, Hagemann S, Kirchner I, Kornblueh L, Manzini E, Rhodin A, Schlese U, Schulzweida U, Tompkins A (2003) The atmospheric general circulation model ECHAM5: Part I: Model description, Technical Report 349, Max-Planck-Institut, Hamburg, Germany

Schär C, Lüthi D, Beyerle U, Heise E (1999) The soil-precipitation feedback: A process study with a regional climate model. J Clim 12:722–741

Schär C, Vidale PL, Lüthi, D, Häberli C, Liniger MA, Appenzeller C (2004) The role of increasing temperature variability in European summer heatwaves. Nature 427:332–336

Schmidli J, Schmutz C, Frei C, Wanner H, Schär C (2002) Mesoscale precipitation variability in the Alpine region during the 20th century. Int J Climatol 22:1049–1074

Shindell DT, Schmidt GA, Miller RL, Mann ME (2003) Volcanic and solar forcing of climate change during the preindustrial era. J Clim 16:4094–4107

Shindell DT, Schmidt GA, Miller RL, Rind D (2001) Northern Hemisphere winter climate response to greenhouse gas, ozone, solar, and volcanic forcing. J Geophy Res 106:7193–7210

Terray L, Valcke S, Piacentini A (1998) The OASIS coupler user guide, version 2.2, Technical Report TR/CMGC/98–05, CERFACS

Ulbrich U, Christoph M (1999) A shift of the NAO and increasing storm track activity over Europe due to anthropogenic Greenhouse gas forcing, Clim Dyn 15:551–559

Vidale PL, Lüthi D, Frei C, Seneviratne SI, Schär C (2003) Predictability and uncertainty in a regional climate model. J Geophys Res 108, DOI:10.1029/2002JD002810

Vinther BM, Johnsen SJ, Andersen KK, Clausen HB, Hansen AW (2003) NAO signal recorded in the stable isotopes of Greenland ice cores. Geophys Res Lett 30(7), 1387, DOI: 10.1029/2002GL016193

von Storch H, Zorita E, Jones J, Dimitriev Y, Gonzalez-Rouco F, Tett S (2004) Reconstructing past climate from noisy data. Science 306:679–682, DOI:10.1126/science.1096109

Wallace JM, Gutzler DS (1981) Teleconnections in the geopotential height field during the Northern Hemisphere winter. Mon Wea Rev 109:782–812

Wanner H, Brönnimann S, Casty C, Gyalistras D, Luterbacher J, Schmutz C, Stephenson DB, Xoplaki E (2001) North Atlantic Oscillation—concepts and studies. Survey Geophys 22:321–382

Wild M, Calanca P, Scherrer SC, Ohmura A (2003) Effects of polar ice sheets on global sea level in high-resolution greenhouse scenarios, J Geophys Res 108, DOI:10.1029/2002JD002451

Wolff JO, Maier-Reimer E, Legutke S (1997) The Hamburg Ocean primitive equation model HOPE. Technical Report 13, Deutsches Klimarechenzentrum, Hamburg, Germany

Xoplaki E, Gonzalez-Rouco JF, Luterbacher J, Wanner H (2004) Wet season Mediterranean precipitation variability: Influence of large-scale dynamics and trends. Clim Dyn 23:63–78

Xoplaki E, Luterbacher J, Paeth H, Dietrich D, Steiner N, Grosjean M, Wanner H (2005) European spring and autumn temperature variability and change of extremes over the last half millennium. Geophys Res Lett 32, L15713, DOI: 10.1029/2005GL023424

Yoshimori M, Stocker TF, Raible CC, Renold M (2005) Internal and externally-forced varibilities in an ensemble of climate simulations of the Maunder Minimum. J Clim 18:4253–4270

Challenges posed by and approaches to the study of seasonal-to-decadal climate variability

**Cornelia Schwierz · Christof Appenzeller ·
Huw C. Davies · Mark A. Liniger · Wolfgang Müller ·
Thomas F. Stocker · Masakazu Yoshimori**

Abstract The tasks of providing multi-decadal climate projections and seasonal plus sub-seasonal climate predictions are of significant societal interest and pose major scientific challenges. An outline is presented of the challenges posed by, and the approaches adopted to, tracing the possible evolution of the climate system on these various time-scales. First an overview is provided of the nature of the climate system's natural internal variations and the uncertainty arising from the complexity and non-linearity of the system. Thereafter consideration is given sequentially to the range of extant approaches adopted to study and derive multi-decadal climate projections, seasonal predictions, and significant sub-seasonal weather phenomena. For each of these three time-scales novel results are presented that indicate the nature (and limitations) of the models used to forecast the evolution, and illustrate the techniques adopted to reduce or cope with the forecast uncertainty. In particular, the contributions (i) appear to exemplify that in simple climate models uncertainties in radiative forcing outweigh uncertainties associated with ocean models, (ii) examine forecast skills for a state-of-the-art seasonal prediction system, and (iii) suggest that long-lived weather phenomena can help shape intra-seasonal climate variability. Finally, it is argued, that co-consideration of all these scales can enhance our understanding of the challenges associated with uncertainties in climate prediction.

C. Schwierz (✉) · H. C. Davies
Institute for Atmospheric and Climate Science, ETH Zürich, Switzerland
e-mail: cornelia.schwierz@env.ethz.ch

C. Appenzeller · M. A. Liniger · W. Müller
Federal Office of Meteorology and Climatology (MeteoSwiss), Switzerland

W. Müller
Present Address: MPI for Meteorology, Hamburg, Germany

T. F. Stocker · M. Yoshimori
Climate and Environmental Physics, Physics Institute, University of Bern, Switzerland

M. Yoshimori
Present Address: Center for Environmental Prediction, Rutgers University, USA

1 Introduction

In the context of possible anthropogenically-induced climate change considerable effort is being devoted to providing projections of the evolution of the climate system over the 21st century (e.g., IPCC 2001). These projections should in principle not only yield an indication of the development of a climate mean but also supply the associated behaviour of and change of that variability (e.g., Mearns et al. 1984; Schneider 2000). Indeed it is possible that climate change could be manifested at least in part by changes in the nature and amplitude of the variability. Thus it is important to improve both our understanding and our predictive capability of climate variability.

Here the focus is on the atmospheric component of the climate system and on multi-decadal, seasonal, and sub-seasonal time-scales. In this time-range key processes influencing the variation and change range from the direct and indirect effects of increased greenhouse gas emissions, the longer-term memory of the oceans, atmosphere-ocean and atmosphere-land surface interactions, and the internal dynamics of the atmosphere itself.

In the following sections, an overview is provided of the challenges associated with developing projections on these different time-scales. In Section 2 summaries are given of the concepts of climate variability; the prediction-model hierarchy; forecast uncertainty and the probabilistic approach to quantify forecast uncertainty. The subsequent sections are devoted to consideration of the methods and challenges pertaining to each time-scale, and providing novel results that exemplify the complexity and temporal interrelations and specific intricacies. The individual sections comprise a discussion of the utility of a hierarchy of climate models to reduce the uncertainty of climate projections on the multi-decadal time scales (Section 3); the ingredients of current schemes for seasonal prediction and the quantitative assessment of forecast skill (Section 4); and a discussion of the dynamics of significant sub-seasonal weather phenomena and their linkage to climate variation (Section 5). Finally some comments are proffered on the synergies that exist between the procedures employed on these different time-scales and possible avenues for future research (Section 6).

2 Basic concepts

2.1 Climate variability, impacts and trends

Climate varies naturally on a vast range of time-scales under the influence of both external forcing or internal variability of the system. Internal variability occurs, because in a system of components with non-linear interactions and very different response times the components tend to vary constantly and not achieve a state of inter-component equilibrium. The response of the climate to external forcings and to the internal variability is further complicated by feedbacks and non-linear responses of the components (IPCC 2001). On the regional scale, climate variability often manifests itself in geographically anchored spatial patterns with changing amplitude (and sign). These patterns determine the local climatic conditions and hence it is also highly desirable to understand and predict them accurately.

The strongest large-scale climate variation on seasonal to inter-annual time-scales has its origin in the tropical-subtropical Pacific and is known as the El Niño/Southern Oscillation (ENSO, see reviews of Philander 1990; Trenberth et al. 1998), that typically occurs every 2–7 years. The ENSO phenomenon consists of a coupled interplay between the atmosphere and ocean. It is associated with a see-saw in atmospheric pressure between the eastern and western Pacific and the occurrence of warm ocean-temperature anomalies in the upper few hundred

meters of the eastern and central tropical Pacific. Marked shifts in weather conditions, in particular precipitation patterns, are associated with ENSO and are not only located in the central Pacific, but also over adjacent continents (Trenberth and Hurrell 1994) and in more removed regions around the globe (Diaz and Markgraf 2000). For Europe there is only a limited direct impact of the equatorial Pacific (Fraedrich 1994; van Oldenborgh et al. 2000; Merkel and Latif 2002), and it has nonlinear (Lin and Derome 2004) and nonstationary (Greatbatch et al. 2004) characteristics.

In the North-Atlantic European area other climate variations such as the North Atlantic Oscillation (NAO) have more substantial impact (for a detailed review see Hurrell et al. 2003 and references therein). Indeed, the NAO is the major winter climate mode, accounting for about one third of the statistically derived inter-annual variability of the mid-tropospheric large-scale flow in mid-latitudes. It is often defined with an index based upon the sea-level pressure anomaly difference between the Azores and Iceland. During the positive phase, a stronger south-westerly flow advects warmer and humid air towards Northern Europe. In the negative phase, the flow is weaker and more zonally oriented. The NAO provides a statistically well-defined pattern to study the predictability of the European winter climate. Unlike the impact of ENSO on the Pacific-American sector, the processes determining the evolution of the NAO remain controversial (Hurrell et al. 2003). In addition, the higher modes of variability are significant for the local climatic variations in the Euro-Atlantic sector (e.g., Pavan et al. 2000b; Scherrer et al. 2006). Most of the existing studies on the mechanisms behind Euro-Atlantic climate variability have however focussed on explaining NAO variability.

Evidence indicates that most of the NAO variability evolves from internal non-linear extratropical atmospheric dynamics. The autocorrelation of the NAO index exhibits a de-correlation time-scale of 8–10 days (Stephenson 2000; Feldstein 2000), and this can be viewed as the fundamental time scale for the short-term NAO component. In this context the long-lived synoptic phenomena (weather regimes) can modulate the seasonal or monthly-mean flow pattern. An example of such a weather phenomenon is atmospheric blocking, i.e. long-lasting quasi-stationary high-pressure systems with typical life-times of 7–15 days (e.g., Croci-Maspoli et al. 2006). On longer time-scales, these weather components exhibit little coherence and it has been cautioned that the observed longer-term NAO fluctuations might be the statistical residue of the averaged short-term contributions (Wunsch 1999; Stephenson 2000). However, this so-called "climate noise paradigm" (Leith 1973; Hasselmann 1976; Madden 1976) falls short of explaining the increased winter NAO variability of the last decades of the 20th century (see Hurrell et al. 2004 and references therein). Hurrell et al. (2004) attribute it to a combination of a tropically forced signal and a "noise" component, and Gillett et al. (2003) hypothesise that the observed positive trend of the NAO over the last 30 years is attributable to the increasing concentration of atmospheric greenhouse gases (GHGs).[1] Potentially relevant one-way or coupled interactions with other components of the climate system include (i) the mid-latitude ocean (see Bjerknes 1964; Rodwell et al. 1999 and others), (ii) the tropical ocean (Hoerling et al. 2001; Bader and Latif 2003), (iii) the Indian ocean (Hurrell et al. 2004), and (iv) the stratosphere (Thompson and Wallace 2001; Baldwin and Dunkerton 2001). There are decadal signals in the NAO variability (Appenzeller et al. 1998), and the detection of such long-term trends and variability must rely on observations and proxy historical reconstructions (Luterbacher et al. 2002). Model simulations in unforced control conditions

---

[1] Viewed in perspective of the latest NAO data up to 2004/05 Gillett's hypothesis probably needs to be modified (C. Deser, pers. comm.).

can help decide whether the observed recent trends might merely be irregular events. To further resolve questions of this nature, a hierarchy of models needs to be developed and employed.

2.2 Remarks on the complexity of the model hierarchy

The choice of the prediction model and its degree of complexity depends on both the scientific focus and the available computational resources. This dichotomy influences the selection of the range of processes, the climate components, the parametrized processes and the model resolution. A whole range of models of varying complexity exists and the most commonly applied categories and their specific properties are introduced here.

Dynamical models are founded on the physical laws that govern the oceanic and atmospheric system and are designed to simulate weather or climate on a range of spatial and temporal scales, by solving numerically the governing fluid-dynamic and thermodynamic equations. Unresolved processes in such models (e.g. cloud microphysics, convection) are represented by grid-box parametrisations or introduced by empirical statistical relationships. The model hierarchy comprises three main types of models:

(i) For numerical weather prediction (NWP) up to the 5–10 day scale, the ocean component is often treated as merely a fixed lower boundary or represented in a slab-type manner, whereas the dynamics of the atmosphere is represented in some considerable detail. Current NWP models operate at horizontal resolutions of $\sim$7 km (regional) and $\sim$50 km (global). On the weather time scale, the sea surface temperature (SST) variability is mainly a result of the surface wind stress.

(ii) For seasonal prediction an improved representation of the ocean processes is necessary. Both NWP models of slightly coarser spatial resolution and atmosphere-ocean general circulation models, AOGCMs, are employed, with a dynamical ocean coupled to the atmosphere and often a refined parametrisation of land surface processes. Currently seasonal predictions are conducted at ECMWF[2] at $\sim$150 km resolution for both atmosphere and ocean. The limited resolution of such a global description of the coupled system requires a reduction in complexity with a focus on the processes thought to be most relevant for the corresponding spatial and temporal scales.

(iii) In modelling past and future climate on time scales of many decades to centuries the synoptic-scale weather is invariably regarded as a noise component, whereas the ocean is accorded high spatial resolution, of currently $\sim$100–300 km (e.g. OGCMs). Projections on decadal to century time-scales are usually undertaken in the following sequence of steps: (1) construction of emission scenarios for the various radiatively active species; (2) translation of the emissions to the atmospheric concentrations using gas-cycle and chemistry-transport models, and then, if necessary, to radiative forcing or albedo; and (3) projection of the forcing on climate using comprehensive three-dimensional climate models (IPCC 1990, 1996, 2001).

For even longer time scales, the complexity of models is systematically reduced (e.g. by averaging certain dimensions in space). This leads to the formulation of climate models of reduced complexity (Stocker et al. 1992), or Earth System Models of Intermediate Complexity (EMICs, Claussen et al. 2002). A reduction in complexity or resolution decreases the computational demands (see also Stocker and Marchal 2001; Claussen et al. 2002; Stocker and Knutti 2003), and can be prompted by physical considerations based upon the relative importance of the physical processes. However the presence of non-linear and inter-scale

---

[2] European Center for Medium–Range Weather Forecasts.

interactions can render this procedure questionable, unless careful and specific comparisons with models of higher complexity are undertaken.

Dynamical models explicitly use the physical equations and thereby attempt to accurately capture events in terms of their physical causes and effects. In contrast *statistical models* do not seek to represent physical processes. Statistical models are essentially based upon exploiting long observational data sets to identify key relationships between the ocean and atmosphere in the past. They range from simple approaches that refine persistence (Colman and Davey 2003), analogue or linear regression techniques, sophisticated schemes utilising nonlinear canonical correlation analysis, and probabilistic schemes (Mason and Mimmack 2002) or Markov chains (Pasmanter and Timmermann 2003). A comprehensive comparison of results derived using these various approaches to forecast one particular event – the 1997/98 ENSO event – is given by Barnston et al. (1999a) and Landsea and Knaff (2000).

Most statistical models are based on the stationarity assumption and imply that the governing processes do not change with time and retain their statistical characteristic in principle into the future. Therefore, such statistical models cannot be employed to study the functioning of climate change processes and are strongly limited in anticipating unexpected changes in the climate system. Further, these models typically tend to be designed and trained for one particular quantity and time-scale in one particular location (e.g. ENSO index). Dynamical models require the initial state of the climate system with an accuracy as high as possible, while statistical models are based on a high-quality historical record.

To summarise, the prediction and validation of climate variability for each scale is beset with its own characteristic difficulties. Computational costs are linked to the degree of the model's comprehensiveness in representing the primary physical processes and their space-time resolution. It is important to note however, that there are limits to the reduction of complexity for an adequate representation of climate variability, e.g. the need to represent as realistically as possible atmospheric transients in climate experiments.

2.3 Types of uncertainty

Foundational to the assessment of climate projections is the recognition that they are linked to various intrinsic and inevitable uncertainties (Reilly et al. 2001; Allen et al. 2001), and below we set out the rudiments of three types. Together the three sources of uncertainty contribute to the uncertainty of a prediction (cf. Figure 1).

Type I uncertainty relates to the selection or construction of emission scenarios and the implications for the radiative forcing and is mainly relevant for decadal to centennial climate projections (cf. for instance Sutton 2005). Nakićenović et al. (2000) proposed 40 different emission scenarios (SRES) that were to be viewed as "images of how the future might unfold". The scenarios took into account "demographic development, socio-economic development, and technological change" (although no political intervention), but "probabilities or likelihood were not assigned to individual scenarios". For 35 selected scenarios the total radiative forcing from 1990 to 2100 ranges from about 3.1 to 8.1 Wm^{-2} (Wigley and Raper 2001). Thus differing emission scenarios result in uncertainty related to radiative forcing. However the absence of an assigned probability to the scenarios makes it difficult to quantify the uncertainty (Schneider 2001; Grübler and Nakicenovic 2001), and the high dimensionality of the phase space militates simulating all possible settings with GCMs.

Type II uncertainty is linked directly to the nature of the climate system. The system is highly non-linear and its evolution is irregular, and forecasts are subject to imperfectly known initial and boundary conditions. Slightly different representations of the initial state or forcing
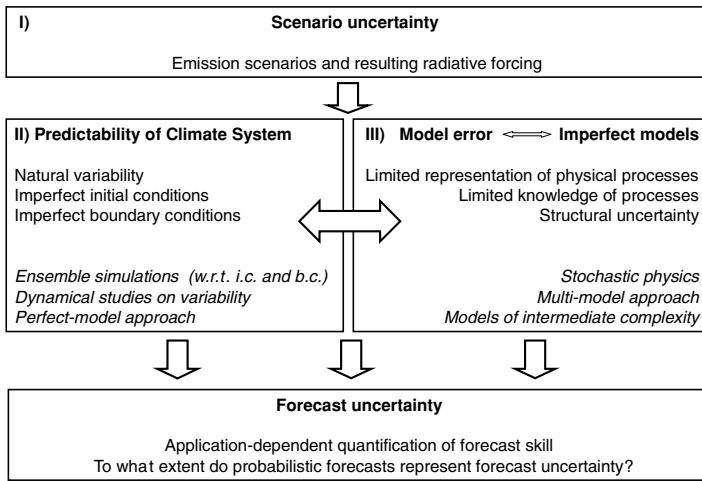
Fig. 1 Schematic illustration of the three components of forecast uncertainty (bold), that are discussed in Section 2.3. The assigned keywords refer to the contributions of each type. Also mentioned are some modelling approaches and related research areas (italic) that are elaborated further in Sections 3 to 5. Refer to text for details

can lead to very different but equally feasible projections into the future. A preliminary estimate of the *climate sensitivity* to a change in an individual forcing can be obtained by measuring the impact upon some pertinent parameter.[3] Cubasch et al. (2001) calculate climate sensitivity from 15 atmospheric GCMs coupled to mixed-layer ocean models. The resulting values range from 2.0 to 5.1 °C, and their final estimated values based on "expert elicitation" range from 1.5 to 4.5 °C. Such an estimate of this type of uncertainty is neither fully objective nor is it accompanied by probabilistic representations. Moreover (cf. Section 2.1), the climate system exhibits an intrinsicly chaotic behaviour. Hence climate variability is often sustained by stochastic, unpredictable or unresolved processes. The degree of forecast uncertainty is dependent on the actual state of the atmosphere, i.e. modulated by natural climate variability.

Type III arises from the fact that the representation of the climate system in a weather or climate model is inevitably incomplete and inadequate. The models carry uncertainty due to (i) the chosen formulation of model equations of the prediction models themselves (so-called structural uncertainty); (ii) the limited representation of physical processes, e.g. due to resolution or due to our limited knowledge of the relevant processes and (iii) the non-linear interactions between climate components themselves. The complexity of the climate system (type II) and the model imperfection (type III) are thus intimately linked.

For type III uncertainty due to an imperfect knowledge of processes can be exemplified by the estimation of the radiative forcing. For the well-mixed greenhouse gases (GHGs) the radiative forcing from pre-industrial to present can be inferred with a relatively high confidence. However the forcing due to other radiatively active species is not well constrained (Ramaswamy et al. 2001). In particular, the radiative forcing due to the indirect effects of tropospheric aerosol has the largest uncertainty (Haywood and Boucher 2000; Knutti et al. 2002;

---

[3] For instance the equilibrium climate sensitivity to CO_2 changes is defined as the equilibrium response of the global mean temperature to the forcing that results from a doubling of the atmospheric CO_2 concentration. It is inversely proportional to the strength of the feedback processes in the system that act to counter a change in forcing IPCC:1990,IPCC:1996,IPCC:2001.

Anderson et al. 2003a), followed by mineral dust (Ramaswamy et al. 2001). Ramaswamy et al. (2001) presented the uncertainty range for the indirect effect of tropospheric aerosol as -2 to 0 Wm^{-2}, with an extreme value being nearly comparable in magnitude to the GHG radiative forcing of 2.4 Wm^{-2}. This uncertainty originates essentially from the combination of a lack of global and long-term observations and a poor understanding of the underlying processes. Uncertainties in other forcings such as the direct effect of tropospheric aerosols and tropospheric ozone could be similarly large if they are added together (IPCC 2001).

Together these three types of uncertainty place a limit upon the predictability of the system and determine the reliability of the prediction.

2.4 Probabilistic forecasts, errors and uncertainty

In view of the foregoing it is highly desirable to quantify the forecast uncertainty (Palmer et al. 2005) and to assess the flow-dependent predictability of the atmosphere-climate system. To this end it has become customary to produce probabilistic estimates of the projected development. A traditional deterministic forecast given by a certain value for the predicted quantity (e.g. temperature will be 25 °C) carries no information on the uncertainty. In contrast, probabilistic forecasts can provide a quantitative indication of the level of uncertainty inherent in the prevailing climatic configuration. They usually result in an estimate of the probability density function (PDF) for the predicted quantity (e.g. a forecast histogram for temperature) or the probability for the incidence of a particular event (e.g. probability for the temperature to be above 25 °C). Provided an estimate is available of the range of uncertainty in input (e.g. emissions) and model parameters, the strategy is to try and cover the largest possible area of model phase space so as to provide probabilistic estimates of a projected development.

A *probabilistic forecast* can be obtained in various ways. (i) Statistical forecasting systems can be set up not only for the mean tendency but also for a direct prediction of the PDF moments. However, this requires the derivation of equations governing the evolution of the mean and higher-order statistical moments, and moreover the interdependency of the moments poses difficulties regarding the cut-off (i. e. the closure problem), cf. Ehrendorfer 1997 and references therein. (ii) Sampling the PDF by multiple integrations of the prediction model. This *ensemble strategy* (e.g., Palmer 1993; Palmer et al. 2005) requires performing a large number of model runs with slightly altered conditions so as to mimic the forementioned uncertainties (I)–(III). Specifically, *single-model ensembles* can be obtained by multiple integrations with slightly different initial and boundary conditions. This approach provides information on the single-model prediction uncertainty from uncertain starting conditions (Tracton and Kalnay 1993; Palmer and Anderson 1994; Stern and Miyakoda 1995). Additionally, the uncertainty due to unresolved processes can be described by introducing a stochastic component during the integration (Buizza et al. 1999) or by implementing so-called stochastic-dynamic subgrid models (Palmer et al. 2005). The degree of inter-model uncertainty can be assessed by comparing results obtained with different models (*multi-model ensemble*). This has been a key feature of successive IPCC assessments. (iii) Assigning an error bar to each variable and process. This requires tracing the evolution of the assigned error bars with the dynamical equations to derive a non-linear estimate of the uncertainty range (*forward modelling*, cf. Section 3.3). This approach is difficult when non-linear interactions dominate and it is also not trivial to estimate the (model dependent) error bars.

Available computer resources limit the use of comprehensive climate models to obtain single-model ensemble runs to evaluate their sensitivity to the representation or specification of particular processes. However complementary strategies can be adopted to at least partially circumvent this shortcoming. First a novel approach geared to exploiting the computational

resources available via grid computing (Allen 1999; Allen and Stainforth 2002; Stainforth 2005) enables ensemble simulations to be undertaken with a single but relatively complex GCM using differing physical parametrizations (cf. Section 3.2). Second a somewhat more simplified climate model with less detailed physical representations and spatial resolution that is concomitantly much more computationally efficient can be deployed in an ensemble mode (cf. Section 3.3).

However, one should be aware that the error and uncertainty estimates are obtained in the self-contained model world. This prompts the caveat "Can we estimate the uncertainty in our uncertainty estimates? [...] Ultimately, all uncertainty is quantified within a given modeling paradigm and our forecasts need never reflect the uncertainty in a physical system." (Smith 2002).

Finally note that quantitative information on the uncertainty can be crucial for many end-user applications. The intrinsic dynamic predictability limit of the atmosphere must be sharpened or tailored to match the end-users' needs, since different applications often depend upon and require different metrics of uncertainty. More details on ensemble forecasting and the definition of model skill is outlined in Section 4.2.

In the subsequent sections consideration will be given sequentially to the range of extant approaches adopted to derive multi-decadal climate projections, seasonal predictions, and sub-seasonal weather phenomena that significantly contribute to seasonal climate variability. For each of these three time-scales novel results are presented that give an indication of the nature (and limitations) of the models used to forecast the evolution, and the techniques adopted to reduce or cope with the forecast uncertainty.

3 Multi-decadal climate projections, models and uncertainty

In this section the focus is on climate projections for decadal and centennial time-scales. Particular attention is devoted to the deployment of a hierarchy of climate models to assess and reduce the uncertainty that accompanies such predictions, and the results derived with such a hierarchy can in principle increase our understanding of model uncertainties provided care is excersised in their interpretation.

3.1 Models of reduced complexity

Figure 2 provides an overview of both the atmosphere and ocean component of a hierarchy of models of varying complexity. Notwithstanding the caveats of reduced complexity models mentioned in Section 2.2, a range of these models have been and are currently used to study specific aspects of the climate system and to examine the accompanying sensitivity (cf. Figure 2). Examples are energy balance models (EBMs), radiative-convective models (RCMs), statistical dynamical models (SDMs), and quasi–geostrophic (QG) models. EBMs are based on vertically-integrated energy balance equations, and further averaging may be made in horizontal directions (e.g., Budyko 1969; Sellers 1969; North et al. 1981). They may also include a moisture balance equation when coupled to ocean models. Transport in EBMs is usually parametrised by eddy diffusion. RCMs solve vertical radiative energy transfer equations with a prescribed convective adjustment scheme deployed to maintain vertical stability (e.g., Manabe and Strickler 1964; Manabe and Wetherald 1967; Ramanathan and Coakley 1978). SDMs employ somewhat more sophisticated parametrisations than EBMs and represent the statistical behaviour of synoptic-scale processes with empirically-based

Dimension		*O c e a n*			
		0	**1**	**2**	**3**
A t m o s p h e r e	**0**	global EBM Saltzman-type models pulse response models neural network	global mixing models geochemical box models UD/EB models ***MAGICC, HILDA***	THC models (lat/z) wind-driven circulation models (lat/long) deep ocean models (lat/long)	OGCM
	1	EBM (lat) RCM (z)	-	ocean (lat/z) + EBM (lat) ***Bern2.5D***	-
	2	EBM (lat/long)	SDM (lat/z) + diffusion ocean, ***MIT 2-D***	ocean (lat/z) + SDM (lat/long), ***CLIMBER-2*** ocean (lat/z) + QG atm. (lat/z), ***MoBidiC***	OGCM + EBM (lat/long) ***UVic*** FG ocean + EBM (lat/long) ***Bern3D***
	3	AGCM + SST	-	AGCM + mixed layer	QG atm. + QG ocean ***Q-GCM*** QG atm. + OGCM ***EcBilt-CLIO*** A/OGCM

Fig. 2 A hierarchy of climate models and their substitutes categorised in terms of resolved spatial dimensions in atmosphere and ocean components. The names of specific models are given in bold italics. The table is intended to present examples of existing models and is not complete. Abbreviations are explained in the text. Modified from Stocker and Knutti (2003)

relations (e.g., Saltzman 1978). A rigorous approximation to the dynamical equations is made in QG models (e.g., Gallée et al. 1991; Opsteegh et al. 1998; Hogg et al. 2003).

Examples of ocean model components of reduced complexity are 1-D upwelling-diffusion (UD) models and zonally averaged thermohaline circulation (THC) models (e.g., Marotzke et al. 1988; Wright and Stocker 1991). Examples of dynamically simplified 3-D models are frictional geostrophic (FG) models (e.g., Maier-Reimer and Mikolajewicz 1992; Edwards and Marsh 2005; Müller et al. 2005) and QG models (e.g., Hogg et al. 2003).

In some applications, substitutes of climate models are used that take the form of pulse response models. The latter assume a linearity of the response but dramatically increase the computational efficiency (Joos and Bruno 1996). Alternatively a neural-network approach formally removes the linearity assumption but does not necessarily replicate the system's non-linear characteristics (Knutti et al. 2003).

In the next sub-sections we review approaches of assessing uncertainty using models of different complexity.

3.2 Uncertainty assessment with GCMs

Beyond observational validation of individual models there have been concerted international efforts to evaluate the performance of GCMs with model intercomparison projects. Such projects involve the coordinated conduct of experiments, and examples include atmospheric GCM simulations with prescribed, historical sea surface conditions (AMIP, cf. Gates et al. 1999) and coupled GCM simulations with a historical, scenario, or idealized forcing (CMIP, cf. Covey et al. 2003). These studies reveal the range, similarities and differences in model behaviour and help to pinpoint the important processes whose better representation can improve GCMs. While such an approach is fundamental to capture the structural uncertainty

(see type III, Section 2.3), it is not designed to assess parametric uncertainty (the uncertainty associated with model parameter values).

Parametric uncertainty was systematically investigated by Murphy et al. (2004) in a single atmospheric GCM coupled to a mixed-layer ocean model. It involved an ensemble simulation of the present-day climate with 53 different model set-ups with 29 key parameters being varied separately. The relative reliability of different model set-ups was assessed based on the deviation of simulated climate from observations. Climate sensitivity (cf. 2.3) was then estimated by linearly combining the climate feedback parameters, weighted according to the models' "diagnosed" reliability. A PDF of climate sensitivity was obtained from $\sim 10^6$ random combinations of values for the model parameters. With this observational constraint the 5–95% confidence interval of climate sensitivity narrowed from 1.5–5.3 °C to 2.4–5.4 °C. However the validity of the linear combination of climate feedback parameters can be questioned (Stainforth 2005), and on the basis of results with a "grand ensemble" of 1000 GCM simulations a case can be made for a much wider range of climate sensitivity, 1.9−11.5 °C. A caveat is that the latter range was not constrained by observations and hence reflects simply the à priori PDFs.

Allen et al. (2000) and Stott and Kettleborough (2002) evaluated the uncertainty in predictions of future warming by using an empirical linear relationship between the 20th century and the mid-21st century warming in models with a hierarchy of complexities. The mid-21st century warming is scaled based on the simulated 20th century warming so that the latter becomes consistent with observations. This scaling was done in a reduced spatio-temporal space applying optimal fingerprinting (or optimal detection method; cf. Weaver and Zwiers 2000; Zwiers 2002). The strength of the method is that the prediction is minimally affected by the uncertainty in climate sensitivity and ocean heat uptake. In other words, the models are not required to simulate the amplitude of the response accurately, but merely its structure. A limitation is that this approach is not applicable if for example the balance between GHG and sulphate aerosol forcing changes with time. In addition, the projection does not take into account the abrupt climate change that could result from non-linear effects. Furthermore, the method cannot, by design, account for the forcing uncertainty. In summary, significant progress has been made during the last few years in the assessment of uncertainty with GCMs despite the obstacle posed by the severe computational cost of those models.

3.3 Uncertainty assessment with reduced complexity models

3.3.1 Forward modeling to assess uncertainty

To provide a probabilistic "guidance" to the estimates given in Cubasch et al. (2001), Wigley and Raper (2001) assigned, based on IPCC (2001), PDFs to input and model parameters that have large uncertainty: aerosol forcing, climate sensitivity, ocean vertical diffusivity, and carbon cycle feedback. The procedure followed was to integrate a UD/EB model with various combinations of parameters ($\sim 10^6$ simulations in total) to yield PDFs for the future temperature change. With an estimated 5–95% confidence interval of warming from 1990 to 2100 the change ranges from 1.7 to 4.9 °C. Note however that the derived uncertainty range mainly reflects the subjectively determined à priori PDFs of input and model parameters, and hence is not an objective quantity. In addition, the absence of ocean and atmospheric dynamics in the model set-up limits determination of the full uncertainty.

3.3.2 Inverse modeling to assess uncertainty

The application of inversion procedures are common in many geophysical settings. Typically they involve the estimate of unknown parameters of a system with given input and output, or an estimate of the input with given system and a known output. For linear systems a direct inversion is often possible. However one has to adopt the approach of indirect inversion if the system is non-linear (e.g. the climate system), or if neither the input nor parameters are known (e.g. sulphate aerosol forcing and ocean mixing parameters). In a climate modelling setting this entails adjusting the unknown parameter values to minimise the residuals (– difference between the simulated and observed values) by repeatedly performing forward simulations. In effect observations are used to constrain the range of unknown or uncertain parameters using the so-called Bayesian approach. This approach requires, by design, a large number of ensemble members, and current computational cost prohibits its application to coupled GCMs. An example with a reduced complexity model will be given later (Section 3.4).

Recently, several studies with different types of reduced complexity models exploited the inverse approach to assess the uncertainty associated with radiative forcing, climate sensitivity, and ocean mixing. Andronova and Schlesinger (2001) used a similar type of model as Wigley and Raper (2001), and conducted $\sim 10^4$ simulations. Using mean and interhemispheric difference in near-surface air temperature as constraining variables, the estimated 5–95% confidence interval for total sulphate aerosol forcing and climate sensitivity range from -0.54 to -0.13 Wm^{-2} and 1.0 to 9.3 °C, respectively. Forest et al. (2002) used a zonally averaged 2-D SDM coupled to a mixed-layer ocean model in which temperature anomalies diffused into the deep ocean, and conducted $\sim 10^1$ simulations. Using latitude-height air temperature, and global mean near-surface air temperature and ocean heat uptake as the constraining variables, the estimated 5–95% confidence intervals for total anthropogenic aerosol forcing, climate sensitivity, and effective ocean diffusivity range from -0.3 to 0.95 Wm^{-2}, 1.4 to 7.7 °C, and 1.8×10^{-4} to 56.0×10^{-4} $m^2 s^{-1}$, respectively. Knutti et al. (2002) used a similar model as Stocker and Schmittner (1997), and conducted $\sim 10^4$ simulations. Using global mean observational records of both near-surface air temperature and ocean heat uptake as constraining variables, their estimated 5–95% confidence interval for indirect aerosol forcing ranges from -1.2 to 0 Wm^{-2}. The a priori uncertainty range for climate sensitivity from 1 to 10 °C was not narrowed. The number of ensemble members can be increased to the order of $\sim 10^6$ by introducing a neural network to serve as a model substitute (Knutti et al. 2003). Noting that indirect aerosol forcing has the largest uncertainty among radiative forcing agents, the results of the latter studies constitute a reduction in the uncertainty of this effect in comparison to the forward modeling approach (Anderson et al. 2003a). However these studies do not place a strong constraint upon the climate sensitivity and the value of the ocean mixing parameter with the given large uncertainties in forcing.

3.3.3 Ensemble kalman filtering

As noted earlier there are large uncertainties associated with the representation of unresolved processes in climate models. Annan et al. (2005) and Hargreaves et al. (2004) applied a data assimilation technique with an ensemble Kalman filter to derive an objective estimate of uncertainty in parameters of a 3-D FG ocean model coupled to a 2-D EBM. In the usual data assimilation framework, state variables such as temperature and salinity were adjusted to minimise the difference between simulations and observations (i.e. the residuals) at every assimilation point. This adjustment results in state variables 'approaching' observations. The relation between model parameter values and the residuals were obtained by conducting

an ensemble simulation with different parameter sets. In turn this information was used to update or adjust the model parameters towards optimal values so that residuals are minimised. In these studies, the modern steady state is considered to constrain 12 model parameters. The advantage of this method is that it requires a moderate number of ensemble members of 54 although the sensitivity of the results to this number is not presented. The method was shown to be orders of magnitude more efficient than the 1000-member Monte Carlo simulations of Edwards and Marsh (2005). An ensemble simulation with the estimated model parameter uncertainty range under a generic 1% annual increase of atmospheric CO_2 exhibits a qualitatively similar spread of future THC as Knutti and Stocker (2002).

3.4 Reduction of uncertainty

The Bayesian approach applied to reduced complexity models is a powerful tool to assess the uncertainty in forcing and model parameters. Moreover the availability of more observational data in the future will serve to constrain more tightly the uncertain parameters and thereby result in a reduction in the corresponding value of the uncertainty.

To demonstrate this possibility, we extend the ensemble approach of Knutti et al. (2002) using a global EBM coupled to a 1-D diffusion ocean model. The concept of the experiment is schematically depicted in Figure 3. It entails four steps. First, the model is integrated to obtain a surrogate of observational records from 1765 to 2100, and thereafter an uncertainty range is added to this 'true record' by assuming a reasonable magnitude for the internal variability. Second, à priori PDFs are assigned for climate sensitivity, ocean vertical diffusivity, and radiative forcing based on IPCC (2001) as in Knutti et al. (2002). Third, 10,000 model simulations are performed to obtain à posteriori PDFs for parameters that are consistent with the observational substitute. Fourth, future forcings are projected using the posteriori PDFs to obtain PDFs of future warming. Figures 4a and b show the PDFs of future warming for
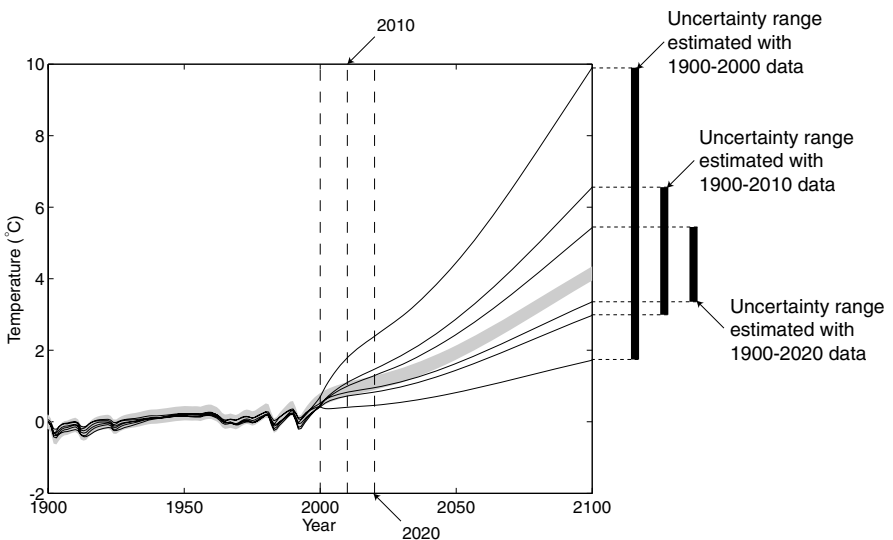
Fig. 3 Schematic diagram of the 'perfect model' experiments in demonstrating the reduction of uncertainty assuming the existence of longer observational records. Each thin curve represents an ensemble member. Shading represents the sum of an observational substitute ('true answer') and assumed internal variability
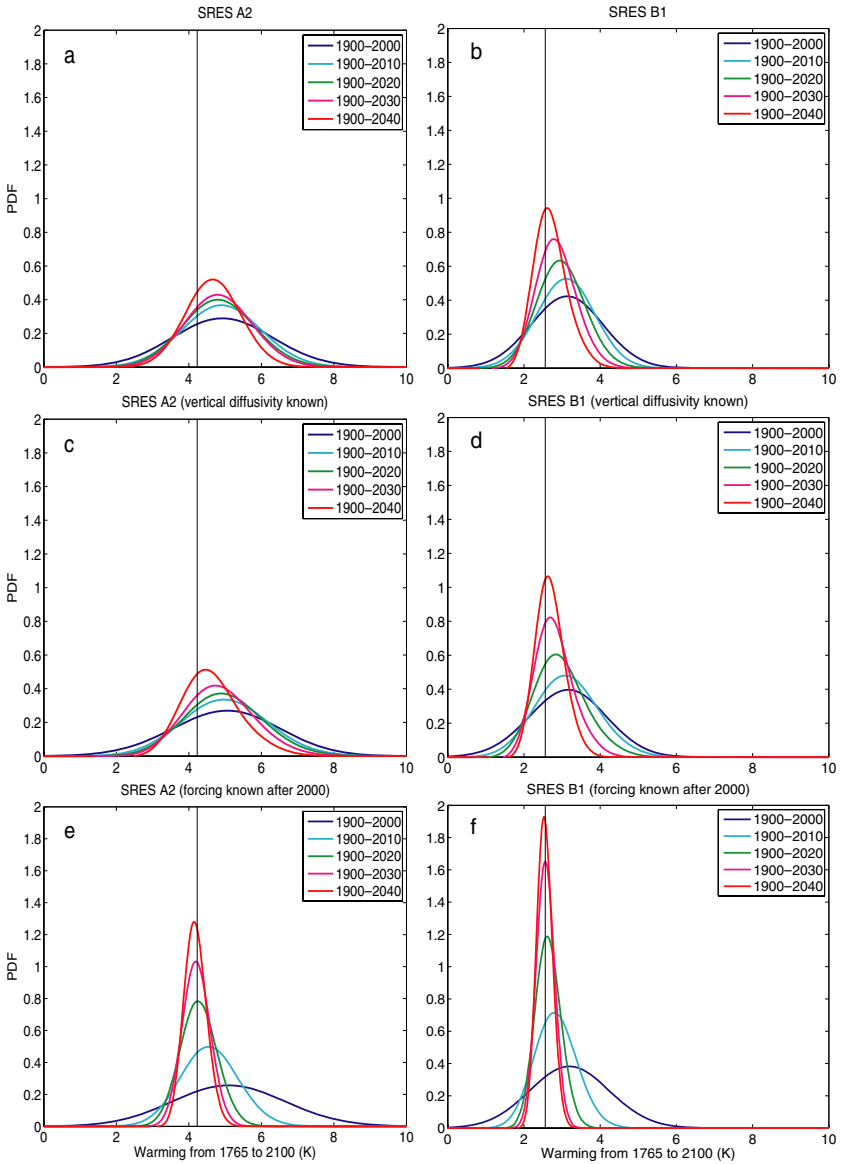
Fig. 4 Projected probability density functions (PDFs) for warming from 1765 to 2100 after the removal of climate sensitivity, ocean vertical diffusivity, and radiative forcing that do not match the 'true answer' (a substitute of observational records). The ranges of years in the upper right corner represent the periods of near surface air temperature record used to constrain the uncertain parameters. Note that the same period is used for the ocean heat content except that the starting year is 1955 instead of 1900. Vertical lines represent 'true answers'. (a) SRES A2 scenario; (b) SRES B1 scenario; (c) same as in (a) but the ocean vertical diffusivity is assumed to be known; (d) same as in (b) but the ocean vertical diffusivity is assumed to be known; (e) same as in (a) but forcing is assumed to be known after year 2000; (f) same as in (b) but forcing is assumed to be known after year 2000. See text for further details

scenarios SRES A2 and B1, respectively. PDFs narrow moderately with the use of longer observational records.

Figures 4c and d show the results subject to the assumption of perfect knowledge of ocean vertical diffusivity. The results exhibit few differences from Figures 4a and b, implying that the impact of the uncertainty in ocean vertical diffusivity on temperature changes is small relative to other uncertainties. Figures 4e and f show the results when we assume perfect knowledge of radiative forcing after the year 2000. Here the results narrow dramatically the PDFs and thereby reduce the uncertainty range. This result points to the importance to focus efforts in quantifying the radiative forcing for the next decades. The figures also reveal that PDFs are biased from true values when the parameters are not well constrained by observations (cf. Figure 3).

Another possible avenue of future research is to increase the number of variables to further constrain uncertainty parameters. For example recent observational studies (Curry et al. 2003) showed that the anthropogenic signal is evident in the salinity field in the Atlantic Ocean during the past four decades. This suggests that the salinity field could serve as a potential constraint.

Here the focus was on estimating the uncertainty of climate projections. Next, we continue to address probabilistic methods and introduce quantitative statistical measures of forecast uncertainty, with a specific focus on the interface to operational application and the end-user perspective. This will be exemplified on the seasonal time-scale.

4 Seasonal climate prediction

4.1 The rationale

A major addition to the forecasting repertoire of weather services in recent years has been the development of operational techniques for seasonal climate predictions. It is argued that sustained large-scale surface (ocean and land-surface) forcing can exert a coherent and conceivably predictable atmospheric response on seasonal time-scales. Indeed the atmosphere itself exhibits coherent large-scale climate variations on this time-scale. Likewise it has been suggested that well-recognised atmospheric flow phenomena or features that are confined to specific regions/layers but that are sustained on quasi-seasonal time-scales can influence the seasonal patterns in the far-field. Two possible examples are the equatorially-based Madden-Julian Oscillation and the stratospheric polar annular oscillation.

Seasonal forecasts are derived using either statistical or dynamical models or a combination (for an overview see Goddard et al. 2003). In practice elements of the statistical and dynamical approaches are combined in a seasonal forecasting system (e.g., Palmer et al. 2005). For example a serial approach utilises a statistical model to generate oceanic boundary conditions for the atmospheric dynamical model (Colman and Davey 2003). Likewise the output of dynamical models can be subject to statistical post-processing to compensate for model drift or to counter known limitations such as resolution. Such a model calibration requires an adequate number of forecasts performed from initial states in the past ("hindcasts"). Most dynamical models or hybrid forecasting systems based upon a mix of statistical and dynamical ingredients exhibit a low signal-to-noise ratio.[4] Hence the desire to derive estimates of forecast uncertainty in the probabilistic framework (Palmer 1993).

---

[4] Ratio of the variability related to external forcing and the unpredictable part of internal variability.

4.2 Ensemble prediction and multi-model approach

One approach to this end is to perform multiple integrations with a specific dynamical model (cf. Section 2.4). One such example is the ECMWF Seasonal Forecast System 2 (Anderson et al. 2003b). It comprises a state-of-the-art coupled atmosphere-ocean model with the resolution of the atmospheric component being higher than standard GCMs and lower than that of the ECMWF's daily weather forecasting configuration. It produces 40 ensemble members, and runs operationally on a monthly basis with hindcasts available from 1987 onward.

Figure 5 shows the results from a typical seasonal ensemble forecast. Each line represents the predicted daily temperature anomaly for the individual members. Clearly care is required in the interpretation of such forecasts, noting that the ensemble mean does not encapsulate all useful information. It is evident that in this particular example there is a very low signal-to-noise ratio throughout, indicating a ly less-predictable situation. Note that the signal-to-noise-ratio depends on the averaging of the data and would be different for monthly and seasonal means. Naively it might be expected that the spread of the members would increase with integration time. Here, however the spread does not increase steadily, reflecting a temporally varying predictability.

Another approach to garner more information for the post-processing statistics is to incorporate data from many different models. In effect such a multi-model prediction system (Fraedrich and Leslie 1987; Pavan and Doblas-Reyes 2000; Kharin and Zwiers 2003) can shed light on the uncertainties due to model formulations. This additional step leads to the concept of multi-model ensemble prediction systems (Harrison et al. 1995; Palmer and Shukla 2000; Shukla et al. 2000) that co-consider model-based and initial data uncertainties. Improvement in the performance using such a multi-model ensemble formulation has been shown for seasonal forecasts (Doblas-Reyes et al. 2000; Graham et al. 2000; Palmer et al.

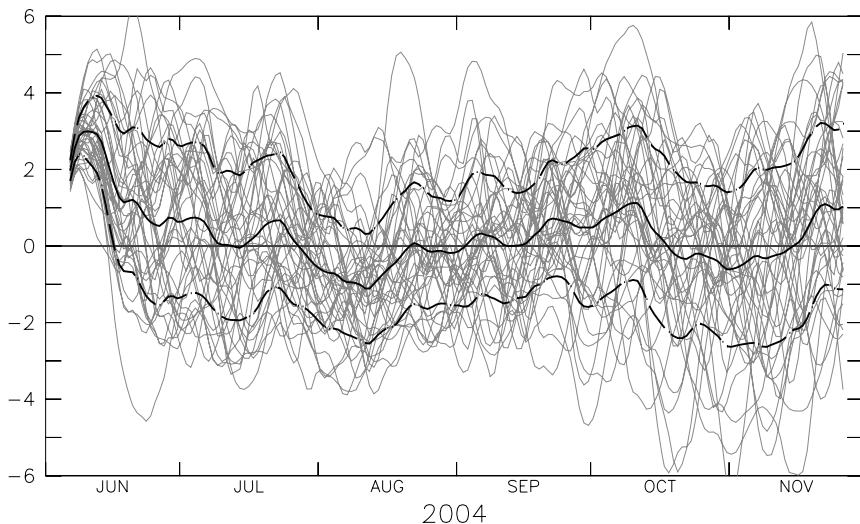**Fig. 5** Forecast initialized at 1 June 2004 for a point in NW-USA for the 2 m temperature. Shown are all 40 individual members (grey), the ensemble mean (solid line) with $+/-$ standard deviation (dashed) as anomaly versus the 1987 till 2001 model climatology. The forecast is based on the operational ECMWF seasonal forecast system 2. The daily values are smoothed using a 14 day running average

2004). However the relative merit of using a larger ensemble with a single model versus an ensemble derived from different (possibly inferior) models remains an open issue (Hagedorn et al. 2005; Doblas-Reyes et al. 2005). In this parallel approach, the forecasts of (ideally) independent sources and models are directly combined, e.g. as linear combination (Barnston et al. 1999b; Coelho et al. 2004) The technique of weighting the forecast models depending on their past performance (Thompson 1977) is still controversial since it is difficult to measure the model quality in its full phase space (Pavan and Doblas-Reyes 2000).

4.3 Forecast verification and skill scores

The difficulty of dealing with probabilistic forecasts is evident from inspection of Figure 5: How can such a noisy ensemble be quantitatively compared with a single observation? This illustrates the challenge in designing suitable verification procedures, and there are a range of measures (scores) for probabilistic forecast quality, i.e. the error relative to the corresponding observation.

Examples are Brier Scores (BS) or the Relative Operating Characteristics (for details see Swets 1973; Wilks 1995). These scores apply to forecasts for a specific kind of event (e.g. the probability that the temperature exceeds a certain threshold value), and are therefore termed dichotomous scores. Other more general scores are multi-categorical and provide both a measure of the shape as well as the central tendency of the whole probability density function (PDF), e.g. the probabilities that the temperature exceeds a range of different threshold values. One example is the ranked probability score (RPS) (Epstein 1969; Murphy 1969, 1971). It is an extension of the BS to multiple probabilistic categories. The RPS is usually calculated in probability space and not in physical space. For example, the threshold value for the RPS must not necessarily be a physical value but could also be defined relative to its statistical recurrence time in the past (i.e. quantile).

The comparison of the forecast performance with a reference forecast is measured by the skill score (SS). Formally the skill score describes the benefit of a forecast score S over the reference forecast score S_{ref} relative to a perfect forecast score S_{perf} ($=0$), i.e.

$$SS = \frac{S - S_{\text{ref}}}{S_{\text{perf}} - S_{\text{ref}}} = 1 - \frac{S}{S_{\text{ref}}} \qquad (1)$$

As a reference forecast, usually a climatological, persistence or random forecast is employed. A positive skill score indicates an improvement with respect to the reference forecast, a negative skill a degradation.

A particular problem of systems with small ensemble size is that a comparison between the scores suffers from different discretization of the forecast and reference forecast probabilities. This leads to a negative bias of the expected skill score for systems with small ensemble size, commonly referred to as the equitability problem (e.g., Mason 2004). For the examples presented here (Sections 4.4 and 4.5) the skill score is evaluated by a newly defined modification which is referred to as debiased version of the standard RPSS (RPSS$_D$, Müller et al. 2005a). The proposed modification involves the re-sampling of the reference forecast. For forecasts with no skill, the RPSS$_D$ gives values of zero even for systems with small ensemble sizes.

4.4 Potential predictability on seasonal time scales

In this sub-section we illustrate some of the points made above in the context of two particular settings. The first is the observationally-based forecast approach (FA). Here we deploy it in

the context of the ECMWF ERA-40 reanalysis data. The data set forms both the (quasi-) observations and defines the climatological distribution used as "reference" forecast. The second is the perfect model approach (PMA). In this setting the reference forecast is based on all single predicted ensemble members of the model climatology, and each single ensemble member is treated once as observation. In effect the PMA estimates the *potential predictability* of the system. It is independent of the real world observations and assumes that the model fully represents the climate system. By construction it exhibits no systematic model drifts, and provides a measure of mean shift and signal-to-noise ratio between the actual forecast and the model climatology.

For many applications, station-based forecasts are needed. As an approximation the forecast skill ($RPSS_D$) of the 2m mean temperature is examined from a grid-point perspective. Figure 6 shows an example of the potential seasonal predictability of the operational ECMWF seasonal forecast system 2 for the period 1987–2002. In the FA (Figure 6a) high skill scores are found over the oceans, in particular over the tropics. Highest values are located in the El Niño region in the eastern tropical Pacific, whereas the western Pacific, the Indian Ocean and the tropical Atlantic show somewhat lower, but mostly significant positive skill. The heterogeneous patterns in the region of Indonesia are mostly due to the differences between the land-sea masks of the forecast model and the verification data set (ERA40). In the extra-tropics, the Pacific basin exhibits wide regions of significant skill. For the Atlantic basin, the
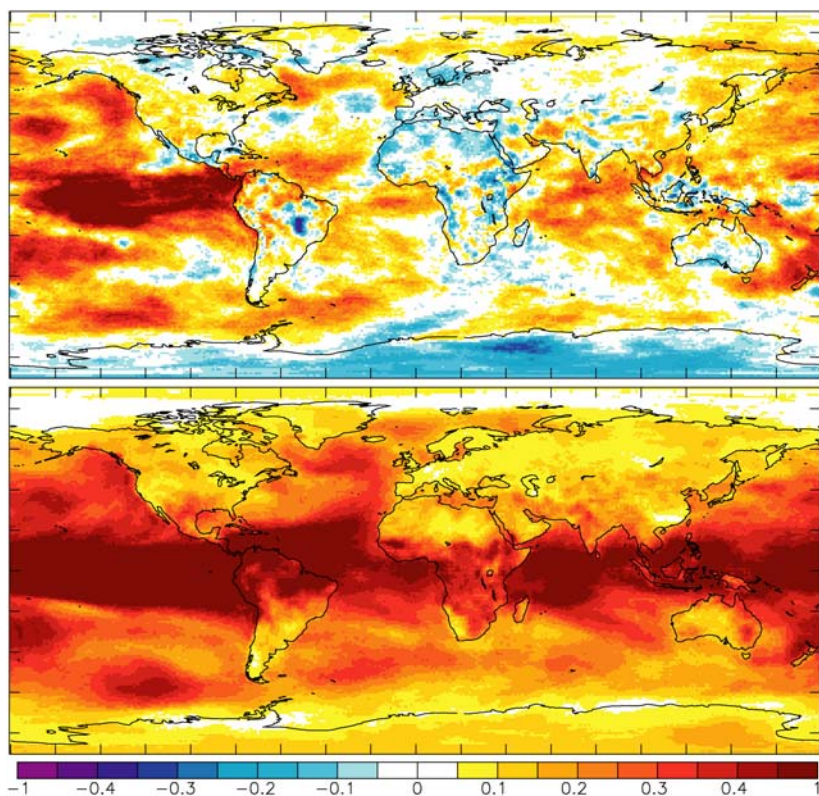

Fig. 6 The $RPSS_D$ of the 3-monthly mean 2 m temperature with lead time of 1 month from 1987 till 2002 for the ECMWF seasonal forecast system 2. Shown are (a) the FA and (b) the PMA for all starting months

values are closer to zero. Relevant for Europe, there is a band-like structure of a weak positive signal across the northern Atlantic reaching from Newfoundland to the Bay of Biscay. Over land, the skills are lower throughout. Highest values are found over Northern America, and along the Pacific coast of Asia. Most other continents, in particular Europe, are associated with negative or non-significant values.

The potential predictability estimated by the PMA supports these findings (Figure 6b). The tropical oceans feature high potential predictability. In the extratropics, the oceans show reduced but still significant positive values. Over land, the PMA implies a higher predictability in the tropics than extratropics (e.g. over Africa and Southern America). A comparison to the FA shows, that this potential is not realised in the actual forecast skill. A better agreement between PMA and FA is found in the extratropics with very limited, but significant, skill values. In particular over the European region the skill scores are in the order of less then 10%, both for PMA and FA.

## 4.5 Forecasting climate indices (ENSO and NAO)

Accurate extended-range predictions of regional and global climate indices are highly desirable in the context of impact research and applications. Here we discuss and compare the forecast skills for the ENSO and NAO index.

Coupled atmosphere-ocean models as well as statistical models yield a significant positive level of forecast skill for ENSO up to a lead time of 12 months (for a review see Latif et al. 1998). The predictions depend critically on the phase of the ENSO (Fedorov 2002; Vitart et al. 2003; McPhaden 2004). In a comparative study of the forecast for the 1997/98 El Niño, Landsea and Knaff (2000) examined 12 deterministic statistical and dynamical models and found no skill beyond persistence on seasonal to inter-annual time scales for any model. More generally, van Oldenborgh et al. (2003) compared the ECMWF seasonal forecast system 1 and 2 (Anderson et al. 2003b) against a statistical and a persistence model of the form of Knaff and Landsea (1997) for the full period 1987–2001. In terms of skill, the statistical methods perform similar to the dynamical models in the winter months. However, in the summer months the skill scores of the statistical models are strongly reduced ("spring barrier"). Among all models, the lowest skill score is achieved by the persistence model in the summer months.

For the NAO, operational statistical and more recently dynamical forecasting systems suggest only moderate skill. The statistical properties of the time series enables statistical forecasts based directly on the time series (Stephenson et al. 2000). Other efforts have focused on the role of the Atlantic SST (Czaja and Frankignoul 1999, 2002; Peng et al. 2003), Eurasian snow cover (Cohen and Entekhabi 1999) and more recently the lower stratosphere (Baldwin and Dunkerton 2001; Baldwin et al. 2003). Recent modeling studies (Rodwell et al. 1999; Rodwell and Folland 2002) and statistical approaches (Saunders and Qian 2002) provide enhanced forecast skill with preceding summer/autumn SST. However, some authors explain the skill as a statistical artefact (Bretherton and Battisti 2000). Several studies investigate dynamical systems on the skill of NAO predictions (Doblas-Reyes et al. 2003; Müller et al. 2005b) and find very limited, but positive, skill values. Other large-scale variability patterns in the Euro-Atlantic sectors exhibit higher predictability, probably due to a more direct ocean forcing (Pavan et al. 2000a,b).

As an illustration, the skill for ENSO and NAO forecasts is calculated for the ECMWF seasonal forecasts system 2 (Figure 7). For the NAO, the skill scores are much lower than for the ENSO forecasts, with values of around 25% for the FA and much lower (8%) for PMA. Both values are statistically significant as derived using a Monte Carlo approach. This

Fig. 7 The RPSS$_D$ of (a) ENSO and (b) NAO index for winter (DJF) averages from 1987 till 2001 for the ECMWF seasonal forecast system 2 started at November 1st. The verification is undertaken in the FA (light grey) and the PMA (black). The horizontal red lines denote the statistical significance level of 95%
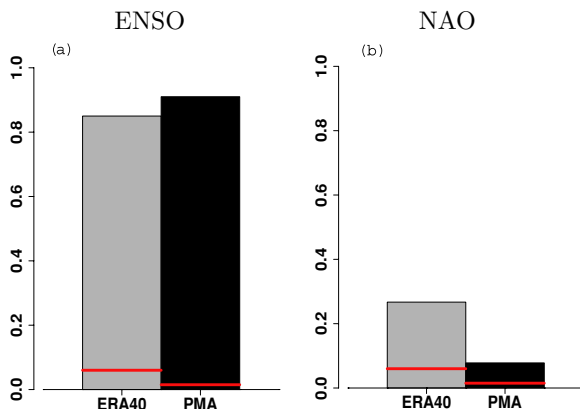
indicates that the potential predictability of this climate pattern is lower than the actually achieved skill over this period. Indeed, skill scores of this magnitude are very sensitive to the sample size and the NAO skill mainly originates from a few well-predicted events (Doblas-Reyes et al. 2003; Müller et al. 2005b). The limited number of available hindcasts for the operational ECMWF system 2 (15 years) is a major constraint for the verification.

The intra-seasonal dynamics of the above patterns of climate variability is at the heart of the following Section 5.

5 Patterns of intra-seasonal variability and weather regimes

5.1 The rationale

The regional impact of climate change is communicated through the leading modes of climate variability. To assess their behaviour under future climate change and to quantify the reliability of climate projections it is necessary to identify the dynamical and physical mechanisms that underly climate variability (Sutton 2005).

As indicated in Section 2.1, weather regimes such as atmospheric blocking, can have a significant impact on the patterns of inter-annual variability. This is supported by their large persistence of ∼10 days; their spatial extent ($\mathcal{O}(10^6)$ km^2); and their significant disturbance to the ambient climatic conditions. In effect blocking systems are associated with a reduction of the in-situ zonal wind, and a deflection of transient cyclonic systems away from their customary tracks with an accompanying marked redistribution of precipitation (Rex 1950a, b, Trigo et al. 2004). Hence the correct prediction of intra-annual and intra-seasonal variability and the associated uncertainty hinges to some extent on the predictability of the blocking phenomenon. The processes involved in blocking formation are complex and occur on a range of scales (see later), and their correct prediction, particularly their onset and breakdown remains difficult (Anderson 1993; D'Andrea et al. 1998; Oortwijn 1998).

It is therefore instructive: to consider the relation between blocking and modes of climate variability; to explore the cause-and-effect relationship between blocking and regional climate patterns; and to review some of the notions on the underlying dynamics of blocking, that might be crucial for the correct representation of blocking in models.

5.2 Blocking occurrence and climate variability patterns

Climatologically for the Northern Hemisphere, the main centers of blocking activity are found over the oceanic basins with a secondary peak over Eurasia (Sausen et al. 1995; Lupo and Smith 1995; Wiedenmann et al. 2002; Schwierz et al. 2004). Some significant correlations have been noted between blocking frequency and large-scale patterns of climate variability. For example in the Pacific, the occurrence of intra-seasonal variations has been associated with tropical SST anomalies with enhanced blocking occurring during the La Niña phases (Wiedenmann et al. 2002), and it is further speculated that this might be reflected in the PNA pattern. However, other studies associate the intra-seasonal PNA variations to the Madden-Julian Oscillation (MJO), while ENSO seems more closely linked to higher order patterns of variability (Karoly et al. 1989; Frederiksen and Zheng 2004). In the Atlantic, the negative NAO phase is correlated with blocking occurrence in the west and central North Atlantic (Shabbar et al. 2001), while the positive NAO phase is associated with blocking over the Western European and Scandinavian region (Scherrer et al. 2006). The opposing phases of the higher modes of variability in the Atlantic region (EOF2-4, together accounting for ~42% of variability) are even more clearly separating specific regions of European blocking occurrence (Scherrer et al. 2006). Interestingly the phase-separated blocking regions are significantly correlated in all 4 EOFs, for the daily as well as for the seasonal NAO-index. This indicates that a large amount of inter-annual variability of the Euro-Atlantic region results from intra-seasonal processes (Zheng and Frederiksen 2004; Frederiksen and Zheng 2004), where also tropical phenomena (such as the MJO) may play a role.

5.3 Temporal relationship between NAO and euro-atlantic blocking

The statistical correlations between NAO and Euro-Atlantic blocking, even though significant, do not point directly to a cause-and-effect relationship. This requires a more dynamically-based approach. One possibility is to investigate the evolution of the blocking system in relation to the contemporaneous strength of a variability pattern. To this end consider the Atlantic region and the relationship of blocking with the NAO pattern.

Individual winter blocks with a minimum life-time of 5 days are identified with the ERA40 data set (1958–2002), their location logged on a 6-hourly basis and their track determined from onset to breakdown (cf. Schwierz et al. 2004). Each block located entirely within the Euro-Atlantic region [90°W:50°E] is recorded and this yields a total of 178 cases. Likewise a similar procedure is followed for blocks located in the Pacific region [110°E:110°W], and there are 211 cases in this category. With this data set it is possible to record the temporal evolution of mean-flow climate parameters (such as the NAO index) during the life cycle of the block.

Figure 8 shows the NAO index value throughout the life time of the blocking systems. (Note individual blocking systems differ in their duration, and hence the index is plotted against the relative blocking life time ranging from 0–100%). The NAO indices at a particular step in the life cycle are then averaged over (i) all blocks in the Euro-Atlantic region, and (ii) blocks in the Pacific, and a distinction is made between classes of blocks lasting less/more than 10 days.

The figure reveals several interesting features. In the Euro-Atlantic sector long-lasting blockings are clearly associated with the negative NAO phase, cf. the spatial distributions shown in Croci-Maspoli et al. (2006), whereas the blocks in the 5–10 day category exhibit no such dependence. (For the Pacific sector there is no clearly detectable relationship of blocks with the NAO index.) A particularly significant feature in the Euro-Atlantic sector
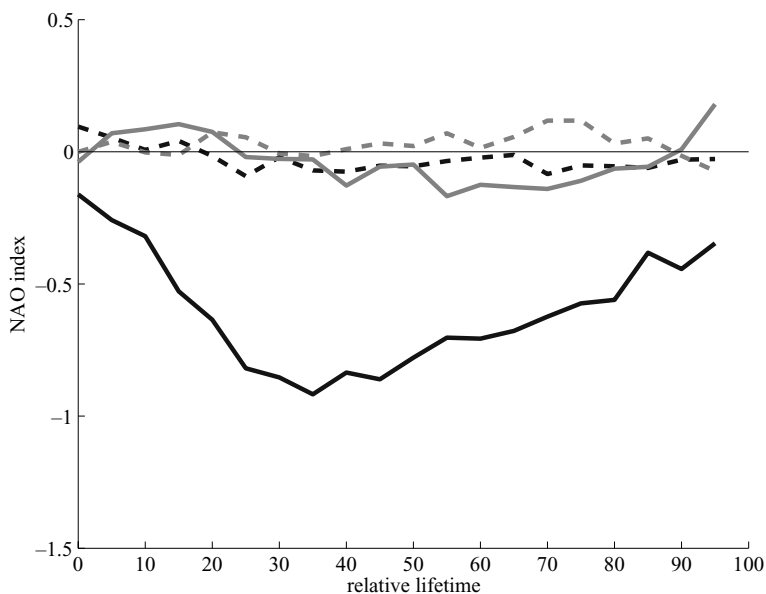
Fig. 8 Development of the median NAO index (daily data, in units of the standard deviation) during the blocking life cycles (relative life time of block in %) for winter (DJF) and for blocks with 5 day minimum life time, for the Euro-Atlantic region (black) and the Pacific region (grey). Blocking are grouped by their life-times between 5–10 days (dashed) and life-times greater than 10 days (solid). Refer to text for further details. The index is that of the Climate Prediction Center CPC `http://www.cpc.ncep.noaa.gov`

relates to the relative temporal development of the NAO and long-lasting blocks (>10 days). In effect the NAO index decreases (i.e. strengthens markedly) during the life cycle of the block with the block starting to form in a near neutral NAO environment. Typically as the blocks develop, the mean value of their contemporaneous NAO index decreases and reaches its minimum at ∼35% of the blocking life-time. Subsequently as the block decays, the NAO index also increases back toward a more neutral state. In essence these results indicate a striking temporal relationship between the evolution of a synoptic-scale block that appears to lead the progression of the large-scale flow into a significant NAO negative phase in the Atlantic region.

5.4 Dynamics of blocking, physical processes

To address the question to what degree the phenomenon of blocking can be represented in climate models, it is instructive to consider the dynamical processes and interactions central to the formation, maintenance and breakdown of blocks. In particular current blocking theories provide a hint of the spatial resolution and nature of the model formulation necessary to simulate this intra-seasonal climate phenomenon.

The characteristic shift from a more zonal flow regime to the blocked flow state has been linked to the existence of multiple stable flow equilibria and resonance (Charney and DeVore 1979; Legras and Ghil 1985). In effect multiple equilibria can be viewed as attractors – "fixed points" – in phase space providing a predilection for certain flow regimes with specific implications for predictability (cf. the studies using Lorenz-type models) (Yamane and Yoden 1997; Corti and Palmer 1997; Palmer 1999). Also it has been argued that the influence of

topography upon the zonal mean flows can destabilise the flow and lead the system to oscillate from one attractor to another (Haines and Hannachi 1995).

A related group of studies link blocks to the amplification of stationary planetary-scale waves (Cerlini et al. 1999; Liu 1994; Da Silva and Lindzen 1993; Hansen and Sutera 1993; Nigam and Lindzen 1989), and the importance of non-linear interactions with large-scale travelling waves has been stressed (Egger 1978). For blocking, the constructive interference of land-sea contrast (thermal forcing) and topographic forcing seems to be crucial (Ji and Tibaldi 1983; Tung and Lindzen 1979; Egger 1978), and no long-lasting events (>6 days) were possible without mountains in numerical sensitivity experiments (Mullen 1989a). From mountain torque and angular momentum analyses, Lott et al. (2004a; b) also concluded, that the jet streams' interactions with large-scale topography play a key-role for hemispheric and regional variability on the 20–30-day time-scale.

There is evidence that certain large-scale mechanisms precondition the atmosphere so as to favour blocking formation. Da Silva and Lindzen (1993) and Nigam and Lindzen (1989) showed that the stationary wave amplitude is sensitive to small shifts in the subtropical jet and the sharpness of the jet. Preconditioning by teleconnection patterns involves a tropical diabatic vorticity anomaly with a subsequent global-scale Rossby-wave train into the extra-tropics (Hoskins and Karoly 1981; Simmons et al. 1983; Hoskins and Sardeshmukh 1987).

A more local view of blocking maintenance is the so-called eddy-straining hypothesis that relates to the modification of the mean flow by the eddies (Berggren et al. 1949; Shutts 1983; Mullen 1987; Vautard et al. 1988). More recent studies by Tsou and Smith (1990), and Lupo and Smith (1995) and others confirm the feedback from eddies to the mean flow in the case of blocking events.

It has been shown, that moist cloud-diabatic processes induced by transient synoptic systems and orographic forcing can act to maintain blocking anomalies Schwierz (2001). Transient disturbances are also believed to play a crucial role in the onset and breakdown of the blocking anomalies. Deep upstream cyclogenesis appears to trigger Atlantic blocking. Ji and Tibaldi (1983), Crum and Stevens (1988), and Lupo and Smith (1995) found a positive correlation between the intensity of blocking anticyclones and the intensity of the precursor cyclone development.

It is evident from the above that many components of the climate system potentially play a role in the dynamics of blocking. From a predictability perspective, elements such as topography, cyclones, moist processes, tropical and stratospheric forcings need to be resolved and represented appropriately.

5.5 Predictability of blocking and climate patterns

Difficulties in forecasting block occurrence might well relate to the intrinsic predictability of the associated climate regime. Studies have been undertaken using a range of approaches from experiments with state-of-the-art NWP models to probabilistic methods, such as (i) seasonal ensemble hindcasts of Euro-Atlantic wintertime variability (Pavan et al. 2000b), (ii) assessment of predictability of blocking with ensemble methods (Frederiksen et al. 2004; Mauritsen and Källén 2004; Pelly and Hoskins 2003; Watson and Colucci 2002), (iii) the multi-model approach (Pavan and Doblas-Reyes 2000; Doblas-Reyes et al. 2003) (cf. also Section 4.2), and also (iv) climate simulations and GCM intercomparison projects (Sausen et al. 1995; Tibaldi et al. 1997; D'Andrea et al. 1998; Doblas-Reyes et al. 1998).

Some standard model deficiencies can impact on the prediction of blocks and intra-seasonal variability. For example in GCMs these include: an excessive zonality of jet streams; greater than normal storm track activity and undersimulation of low-frequency planetary and

stationary waves. For the prediction of blocks themselves it has been noted that there is: –a general tendency to underestimate blocking activity (frequency), particularly for extended forecast times Jung (2005); –a lack of long-lived blocks (D'Andrea et al. 1998); –a tendency of Atlantic blocking to be shifted east, since transients penetrate too far east and south as the jet stream becomes too zonal (Doblas-Reyes et al. 1998) (Pacific blocking predictions do not show this tendency). Moreover forecast model errors differ significantly in the skill in representing Pacific and Atlantic blocks (Tibaldi et al. 1994), and indeed the skill of the (ECMWF) seasonal model prediction is higher in the Pacific than in the Atlantic (Pavan et al. 2000a). This in turn might betoken the fact that different processes for blocking formation prevail for the two main NH blocking regions.

A regime-dependent component has been found in forecast error fields (Molteni and Tibaldi 1990), and the systematic model errors of 500-hPa geopotential height are related to the inability to predict blocking (Mauritsen and Källén 2004). This has ramifications for quantifying forecast uncertainty, and in particular the difficulties in correctly predicting the onset and break-down of blocking periods have profound implications. In the medium range, major forecast failures are associated with regime transitions, that affect the statistical properties of the errors (Trevisan et al. 2001).

For long-range or seasonal prediction, the presumed linkage of sea-surface temperature (SST) anomalies to patterns of climate variability and blocking is noteworthy and relates to the paradigm of preconditioning the atmosphere towards specific regimes of variability. Earlier studies hinted at the impact of Pacific SST anomalies on blocking location (Mullen 1989b). In the North Pacific, low-frequency (blocking) variability is enhanced during La Niña winters and hence potential predictability during El Niño winters is increased (Chen and van den Dool 1999). Using GCM experiments, Cassou et al. (2004) and Mathieu et al. (2004) find that tropical and extra-tropical Atlantic SST anomalies can significantly affect the excitation of North Atlantic climate regimes such as the NAO and blocking. The influence of ENSO-modulated SST anomalies on Euro-Atlantic blocking can be limited by the model's ability to correctly represent planetary wave propagation from the Pacific into the Atlantic (Pavan et al. 2000b).

5.6 Further comments and challenges

In this section we have emphasised the issue of predictability and illustrated the challenge of climate variability prediction from a process-based standpoint. The range and interaction of processes and the need to represent them sufficiently accurately is a major difficulty for prediction. Here this was pinpointed in the context of the need for a better fundamental understanding of the synoptic processes underlying the onset, maintenance and breakdown of blocks (sic. weather regimes) and their non-linear two-way interaction with the pattern of climate-scale variability.

For example the co-development of an individual blocking event and a negative NAO phase has been shown to be linked to the life time of the block. The implication is that a model should adequately represent the processes relevant for blocking (wave interactions, diabatic heating, interactions with the ocean or stratosphere).

Sensitivity studies with climate models of parameters such as resolution, physical parametrisation, moisture content, surface schemes, representation of ocean and tropical processes might help to investigate the link between predictability of climate and weather regimes. And indeed there are indications that some of the model errors for blocking can be alleviated by increased resolution (Doblas-Reyes et al. 1998) and improvements in the physical parametrisation (Molteni and Tibaldi 1990).

6 Final remarks

A major difficulty in predictions and the assessment of uncertainty is the determination and separation of influencing factors on climate variability and change. These comprise a forced component (GHGs), internal sources (such as QBO, NAO, PNA, ENSO, feedback with eddies), residual weather "noise" and their non-linear interactions.

It has been argued here that a hierarchy of models is a powerful approach to estimate and assess the uncertainty. Dynamical models have been combined with models of reduced complexity, and with statistical models. Beneficial for the assessment is an overlap between the model evaluations. For instance models used in NWP can be combined with GCMs for climate and seasonal time scales to determine the accurate representation of processes (Section 5). Such GCMs in connection with reduced-complexity and statistical models, which are often used in an ensemble mode, are efficient in the estimation of errors. In addition such an overlap can lend credence to the applicability of the less-detailed models (cf. Section 3). However, long-term projections – in particular when undertaken with statistical models – rely on assumptions such as stationarity and ergodicity which are not fulfilled for instance for dramatic changes in circulation patterns. (cf. Section 2). Climate models, especially with reduced complexity and relaxed non-linearity, will not necessarily foresee a major change in dominant circulation regimes (Smith 2002).

6.1 Internal, natural, and regional variability

Hence, the application of a model hierarchy is also beset with problems. In climate studies, the internal variability of the climate system sets a level of background noise to attempts to estimate or predict an external or anthropogenic signal (Manabe and Stouffer 1996; Stouffer et al. 2000). A prediction by a single climate simulation or any parameter estimation that uses observational records as a constraint is subject to the uncertainties due to this internal variability and stochastic uncertainties (Murphy et al. 2004). These uncertainties are expected to increase if one goes to regional scales.

It has been argued that the externally forced signal may be preferentially projected onto the existing large scale modes of variability inherent in the climate system by changing the probability distribution of weather regimes (Palmer 1998, 1999; Corti et al. 1999; Monahan et al. 2000). Considering the impact of these large scale modes of variability on regional climate (Hurrell 1995, 1996; Thompson and Wallace 2001) as well as on the THC (Latif et al. 2000; Delworth and Dixson 2000; Schmittner et al. 2000), the understanding of underlying mechanisms of internal variability is important for (i) the justification of the choice of a model of reduced complexity and (ii) the extension of uncertainty assessment toward regional scales. In addition, the spatial inhomogeneity of radiative forcing, e.g. by tropospheric aerosols, which is represented as a globally uniform radiative forcing in reduced complexity models, may have a non-negligible impact on regional-scale climate change.

6.2 Reduced complexity models

The potential utility of a reduced complexity models is enhanced if its response overlaps and replicates that of comprehensive model. An example of such an overlap is the projection of future changes in the thermohaline circulation (THC). The fate of the THC in a warming world has attracted considerable attention due to its significant global and regional impact. Stocker and Schmittner (1997) used a multi-basin, zonally-averaged ocean model coupled to a 1-D EBM and conducted a series of experiments with different boundary conditions.

They found that the reduction of the THC depends on the rate of increase in GHG forcing. A similar result, albeit in a much smaller parameter space, was derived with a 3-D fully coupled GCM (Stouffer and Manabe 1999). The THC system is highly nonlinear, and hence a large number of ensemble members are necessary to obtain a robust picture. Indeed, many GCMs project quite different strengths of the future THC (as well as modern simulations). Knutti and Stocker (2002), using a similar model as Stocker and Schmittner (1997), conducted an ensemble of 100 simulations with different noise sequences which represent the atmospheric internal variability. For that particular model setting they showed that the predictability of THC is severely limited when the system approaches the instability threshold or bifurcation point.

6.3 Structural uncertainty

GCMs, albeit expensive, are believed to be better suited for the use in projections of future climate change. However, reduced complexity models are very useful to assess uncertainty with probabilistic representations and ensemble methods. It is also possible for those models to objectively optimise the model parameter values, and hence reduce the parametric uncertainties. For reduced complexity models to serve as GCM substitutes, it is desirable to direct more effort towards the structural uncertainties. It remains a challenge to assess how much uncertainty or error could be introduced by reducing the complexity of models. Of course, structural uncertainty does not only exist in reduced complexity models but also in GCMs. With regard to THC projections, for example, these are poor representation of western boundary currents, deep convection, and flow over shallow sills. It is hoped that these weaknesses in GCMs are continuously improved as our understanding on fundamental processes and computational power increase. A hierarchy of climate models is useful and necessary, but more studies, particularly in quantification of the structural uncertainty, are highly desirable.

6.4 Operational application and challenges

Seasonal climate forecasting has recently become operational at many weather centers around the globe. Such forecasts provide potentially useful information to support decision makers in the governmental and private sectors. Substantial effort is also undertaken to improve applications in other sectors such as agricultural or health sectors (Palmer et al. 2004). But many issues still need to be resolved. Assuming that the current models do adequately represent the key processes and interactions Figure 6 suggests that the potential predictability is high in tropical regions but rather small in the extra-tropical European region. From an application perspective the following issues seem to be particularly important. First the climate system itself needs to be potentially predictable in the region and for the quantity of interest. Second, the current forecast systems still suffer from not being fully reliable systems. This indicates that the way the spread of the ensemble system is generated needs to be improved. One approach to do so is the use of a multi-model system as described in Section 4.2. Finally, the climate models used need to be able to represent the relevant processes that control climate variability on seasonal time scales. An example is the development of blocking systems (cf. Section 5).

Increased understanding of processes acting at this interface between weather and climate is needed to bridge the gap between the time-scales. "Since they are the only patterns arising from intraseasonal variability that contribute significantly to the interannual variability of the seasonal-mean field, they are the major patterns that one should pay prime attention to

in medium-range weather forecasting, in order to improve dynamical seasonal forecasts" (Zheng and Frederiksen 2004). Potential shortcomings of the current models in representing the salient physical mechanisms need to be identified. A combination of (i) data diagnosis, (ii) sensitivity studies on resolution, parametrisations, moisture fields, surface schemes, ocean and tropical representations, undertaken with a hierarchy of models, (iii) theoretical considerations and (iv) the application of probabilistic methods are instrumental in this purpose. Together with the necessity to integrate the various research efforts in the relevant fields.

References

Allen M (1999) Do-it-yourself climate prediction. Nature 401(6754):642

Allen M, Raper S, Mitchell J (2001) Uncertainty in the IPCC's third assessment report. Science 293(5529):430–433

Allen MR, Stainforth DA (2002) Towards objective probabilistic climate forecasting. Nature 419(6903):228

Allen MR, Stott PA, Mitchell JFB, Schnur R, Delworth TL (2000) Quantifying the uncertainty in forecasts of anthropogenic climate Change. Nature 407(6804):617–620

Anderson JL (1993) The climatology of blocking in a numerical forecast model. J Climate 6(6):1041–1056

Anderson TL, Charlson RJ, Schwartz SE, Knutti R, Boucher O, Rodhe H, Heintzerberg J (2003a) Climate forcing by aerosols – a Hazy picture. Science 300(5622):1103–1104

Anderson DL, Stockdale T, Balmaseda M, Ferranti L, Vitard F, Doblas-Reyes FJ, Hagedorn R, Jung T, Vidard A, Troccoli A, Palmer TN (2003b) Comparison of the ECMWF seasonal forecast systems 1 and 2, including the relative performance for the 1997/8 El Niño, vol. 404 of ECMWF Technical Memorandum. ECMWF, p. 93

Andronova NG, Schlesinger ME (2001) Objective estimation of the probability density function for climate sensitivity. J Geophys Res 106(D19):22605–22611

Annan JD, Hargreaves JC, Edwards NR, Marsh R (2005) Parameter estimation in an intermediate complexity earth system model using an ensemble Kalman filter. Ocean Model 8(1–2):135–154

Appenzeller C, Stocker F, Anklin M (1998) North Atlantic Oscillation dynamics recorded in Greenland Ice Cores. Science 282:446–449

Bader J, Latif M (2003) The impact of decadal-scale Indian Ocean sea surface temperature anomalies on Sahelian rainfall and the North Atlantic Oscillation. Geophys Res Let 30:1–4

Baldwin MP, Dunkerton TJ (2001) Stratospheric harbingers of anomalous weather regimes. Science 294(5542):581–584

Baldwin MP, Stephenson DB, Thompson DWJ, Dunkerton TJ, Charlton AJ, OíNeill A (2003) Stratospheric memory and skill of extended-range weather forecasts. Science 301:636–640

Barnston AG, Glantz MH, He YX (1999a) Predictive skill of statistical and dynamical climate models in SST forecasts during the 1997–1998 El Niño episode and the 1998 La Niña onset. Bull Am Meteor Soc 80(2):217–243

Barnston AG, Leetmaa A, Kousky VE, Livezey RE, O'Lenic E, Van den Dool H, Wagner AJ, Unger DA (1999b) NCEP Forecasts of the El Niño of 1997/1998 and its U.S. Impacts. Bull Am Meteor Soc 80(9):1829–1852

Berggren R, Bolin B, Rossby CG (1949) An aerological study of zonal motion, its perturbations and breakdown. Tellus 1:14–37

Bjerknes J (1964) Atlantic air-sea interaction. Adv Geophys 10:1–82

Bretherton CS, Battisti DS (2000) An interpretation of the results from atmospheric general circulation models forced by the time history of the observed sea surface temperature distribution. Geophys Res Let 27(6):767–770

Budyko MI (1969) Effect of solar radiation variations on climate of earth. Tellus 21(5):611–619

Buizza R, Miller M, Palmer TN (1999) Stochastic representation of model uncertainties in the ECMWF ensemble prediction system. Quart J Roy Meteor Soc 125(560):2887–2908

Cassou C, Terray L, Hurrell JW, Deser C (2004) North Atlantic winter climate regimes: Spatial asymmetry, stationarity with time, and oceanic forcing. J Climate 17(5):1055–1068

Cerlini PB, Corti S, Tibaldi S (1999) An intercomparison between low-frequency variability indices. Tellus A 51(5):773–789

Charney JG, DeVore JG (1979) Multiple flow equilibria in the atmosphere and blocking. J Atmos Sci 36:1205–1216

Chen WY, van den Dool HM (1999) Significant change of extratropical natural variability and potential predictability associated with the El Nino/Southern Oscillation. Tellus A 51(5):790–802

Claussen M, Mysak LA, Weaver AJ, Crucifix M, Fichefet T, Loutre M-F, Weber SL, Alacamo J, Alexeev VA, Berger A, Calov R, Ganopolski A, Goosse H, Lohmann G, Lunkeit F, Mokhov II, Petoukhov V, Stone P, Wang Z (2002) Earth system models of intermediate complexity: Closing the gap in the spectrum of climate system models. Clim Dyn 18(7):579–586

Coelho CAS, Pezzulli S, Balmaseda M, Doblas-Reyes FJ, Stephenson DB (2004) Forecast calibration and combination: A simple bayesian approach for ENSO. J Clim 17:1504–1516

Cohen J, Entekhabi D (1999) Eurasian snow cover variability and northern hemisphere climate predictability. Geophys Res Let 26(3):345–348

Colman AW, Davey MK (2003) Statistical prediction of global sea-surface temperature anomalies. Int J Climatol 23(14):1677–1697

Corti S, Palmer T (1997) Sensitivity analysis of atmospheric low-frequency variability. Quart J Roy Meteor Soc 123(544):2425–244

Corti S, Molteni F, Palmer TN (1999) Signature of recent climate change in frequencies of natural atmospheric circulation regimes. Nature 398(6730):799–802

Covey C, AchuaRao KM, Cubasch U, Jones P, Lambert SJ, Mann ME, Phillips TJ, Taylor KE (2003) An overview of results from the coupled model intercomparison project. Global and Planetary Change 37:103–133

Croci-Maspoli M, Schwierz C, Davies HC (2006) A multi-faceted climatology of atmospheric blocking and its recent linear trend. J Clim (in press)

Crum FA, Stevens DE (1988) A case study of atmospheric blocking using isentropic analysis. Mon Wea Rev 116(1):223–241

Cubasch U, Meehl GA, Boer GJ, Stouffer RJ, Dix M, Noda A, Senior CA, Raper S, Yap KS (2001) Projections of future climate change. In: Houghton JT, Ding Y, Griggs DJ, Noguer M, van der Linden PJ, Dai X, Maskell K, Johnson CA (eds) Climate change 2001: The scientific basis. Cambridge, UK and New York, NY, USA: Cambridge University Press, Chapt. 9, pp. 525–582. Contribution of Working Group I to the Third Assessment Report of the Intergovenmental Panel on Climate Change, p. 881

Curry R, Dickson B, Yashayaev I (2003) A change in the freshwater balance of the Atlantic Ocean over the past four decades. Nature 426(6968):826–829

Czaja A, Frankignoul C (1999) Influence of the North Atlantic SST on the atmospheric circulation. Geophys Res Let 26(19):2969–2972

Czaja A, Frankignoul C (2002) Observed impact of Atlantic SST anomalies on the North Atlantic Oscillation. J Clim 15(6):606–623

Da Silva AM, Lindzen RS (1993) The effect of concentrated PV gradients on stationary waves. J Atmos Sci 50(1):43–61

D'Andrea F, Tibaldi S, Blackburn M, Boer G, Déqué M, Dix MR, Dugas B, Ferranti L, Iwasaki T, Kitoh A, Pope V, Randall D, Roeckner E, Straus D, Stern W, van den Dool H, Williamson D (1998) Northern Hemisphere atmospheric blocking as simulated by 15 atmospheric general circulation models in the period 1979–1988. Clim Dyn 14(6):385–407

Delworth TL, Dixson KW (2000) Implications of recent trend in the Arctic/North Atlantic Oscillation for the North Atlantic thermohaline circulation. J Climate 13(21):3721–3727

Diaz HF, Markgraf V (2000) El Niño and the southern Oscillation: Multiscale variability and global and regional impacts. Cambridge University Press.

Doblas-Reyes FJ, Deque M, Piedelievre JP (2000) Multi-model spread and probabilistic seasonal forecasts in PROVOST. Quart J Roy Meteor Soc 126(567):2069–2087

Doblas-Reyes FJ, Déqué M, Valerbo F, Stephenson DB (1998) North Atlantic Wintertime intraseasonal variability and its sensitivity to GCM horizontal resolution. Tellus 50A:573–595

Doblas-Reyes FJ, Hagedorn R, Palmer TN (2005) The rationale behind the success of multi-model ensembles in seasonal forecasting – II. Calibration and combination. Tellus 57A:234–252

Doblas-Reyes FJ, Pavan V, Stephenson DB (2003) The skill of multi-model seasonal forecasts of the wintertime North Atlantic Oscillation. Clim Dyn 21(5–6):501–514

Edwards NR, Marsh R (2005) Uncertainties due to transport-parameter sensitivity in an efficient 3-d ocean-climate model. Clim Dyn 24(4):415–433

Egger J (1978) Dynamics of blocking highs. J Atmos Sci 35(10):1788–1801

Ehrendorfer M (1997) Predicting the uncertainty of numerical weather forecasts: A review. Meteor Zeitschr 6:147–183

Epstein ES (1969) A scoring system for probability forecasts of ranked categories. J Appl Meteor 8:985–987

Fedorov AV (2002) The response of the coupled tropical ocean-atmosphere to westerly wind bursts. Quart J Roy Meteor Soc 128(579):1–23

Feldstein SB (2000) The timescale, power spectra and climate noise properties of teleconnection patterns. J Clim 13:4430–4440

Forest CE, Stone PH, Sokolov AP, Allen MR, Webster MD (2002) Quantifying uncertainties in climate system properties with the use of recent climate observations. Science 295(5552):113–117

Fraedrich K (1994) ENSO impact on Europe – a review. Tellus 46A:541–552

Fraedrich K, Leslie LM (1987) Combining predictive schemes in short-term forecasting. Mon Wea Rev 115(8):1640–1644

Frederiksen CS, Zheng X 2004 Variability of seasonal-mean fields arising from intraseasonal variability. Part 2, application to NH winter circulations. Clim Dyn 23(2):193–206

Frederiksen JS, Collier MA, Watkiins AB (2004) Ensemble prediction of blocking regime transitions. Tellus 56A(5):485–500

Gallée H, van Ypersele JP, Fichefet T, Tricot C, Berger A (1991) Simulation of the last glacial cycle by a coupled, sectorially averaged climate-ice sheet model 1. The climate model. J Geophys Res 96(D7):13139–13161

Gates WL, Boyle JS, Covey C, Dease CG, Doutriaux CM, Drach RS, Fiorino M, Gleckler PJ, Hnilo JJ, Marlais SM, Phillips TJ, Potter GL, Santer BD, Sperber KR, Taylor KE, Williams DN (1999) An overview of the results of the atmospheric model intercomparison project (AMIP I). Bull Am Meteorol Soc 80(1):29–55

Gillett NP, Graf HF, Osborn TJ (2003) Climate Change and the North Atlantic Oscillation. In: Hurrell JW, Kushnir Y, Ottersen G, Visbeck M (eds) The North Atlantic Oscillation: Climate significance and environmental impact, Vol. 134 of geophysical monograph. Washington, DC, USA: American Geophysical Union, pp 193–209

Goddard L, Barnston AG, Mason SJ (2003) Evaluation of the IRI's 'net assessment" seasonal climate forecasts 1997–2001. Bull Am Meteor Soc 84(12):1761–1781

Graham RJ, Evans ADL, Mylne KR, Harrison MSJ, Robertson KB (2000) An assessment of seasonal predictability using atmospheric general circulation models. Quart J Roy Meteor Soc 126(567):2211–2240

Greatbatch RJ, Lu J, Peterson A (2004) Nonstationary impact of ENSO on Euro-Atlantic winter climate. Geophys Res Let 31, doi:10.1029/2003GL018542

Grübler A, Nakicenovic N (2001) Identifying dangers in an uncertain climate. Nature 412(6842):15

Hagedorn R, Doblas-Reyes FJ, Palmer TN (2005) The rationale behind the success of multi-model ensembles in seasonal forecasting. – I. Basic concept. Tellus 57A:219–233

Haines K, Hannachi A (1995) Weather regimes in the Pacific from a GCM. J Atmos Sci 52(13):2444–2462

Hansen AR, Sutera A (1993) A comparison between planetary-wave flow regimes and blocking. Tellus 45A(4):281–288

Hargreaves JC, Annan JD, Edwards NR, Marsh R (2004) An efficient climate forecasting method using an intermediate complexity earth system model and the ensemble Kalman filter. Clim Dyn 23(7–8):745–760

Harrison MSJ, Palmer TN, Richardson TN, Buizza DS, Petroliagis T (1995) Joint ensembles from the UKMO and ECMWF models. In: ECMWF seminar proceedings, predictability, Vol. 2. pp 61–120

Hasselmann K (1976) Stochastic climate models: 1. Theory. Tellus 28(6):473–485

Haywood J, Boucher O (2000) Estimates of the direct and indirect radiative forcing due to tropospheric aerosols: A review. Rev Geophys 38(4):513–543

Hoerling MP, Hurrell J, Xu TY (2001) Tropical origins for recent North Atlantic climate change. Science 292:90–92

Hogg AM, Dewar WK, Killworth PD, Blundell JR (2003) A quasi-geostrophic coupled model (Q-GCM). Mon Wea Rev 131(10):2261–2278

Hoskins BJ, Karoly DJ (1981) The steady linear response of a spherical atmosphere to thermal and orographic forcing. J Atmos Sci 38:1179–1196

Hoskins BJ, Sardeshmukh PD (1987) A diagnostic study of the dynamics of the Northern- Hemisphere winter of 1985–1986. Quart J Roy Meteor Soc 113(477):759–778

Hurrell JW (1995) Decadal trends in the North Atlantic Oscillation: Regional temperatures and precipitation. Science 269(5224):676–679

Hurrell JW (1996) Influence of variations in extratropical wintertime teleconnections on Northern Hemisphere temperature. Geophys Res Lett 23(6):665–668

Hurrell J, Kushnir Y, Ottersen G, Visbeck M (2003) An overview of the North Atlantic Oscillation. In: Hurrell JW, Ottersen G, Visbeck M (eds) The North Atlantic Oscillation, pp 1–36

Hurrell J, Hoerling MP, Phillips AS, Xu T (2004) Twentieth century North Atlantic climate change. Part I: assessing determinism. Clim Dyn 23:371–389

IPCC (1990) Climate change: The IPCC scientific assessment. Cambridge, UK: Cambridge University Press. Report Prepared for IPCC by Working Group 1, p 365

IPCC (1996) Climate change 1995: The science of climate change. Cambridge, UK: Cambridge University Press. Contribution of Working Group I to the Second Assessment Report of the Intergovernmental Panel on Climate Change, p 572

IPCC (2001) Climate change 2001: The scientific basis. Cambridge, UK and New York, NY, USA: Cambridge University Press. Contribution of Working Group I to the Third Assessment Report of the Intergovenmental Panel on Climate Change, p 881

Ji LR, Tibaldi S (1983) Numerical simulations of a case of blocking – the effects of orography and land sea contrast. Mon Wea Rev 111(10):2068–2086

Joos F, Bruno M (1996) Pulse response functions are cost-efficient tools to model the link between carbon emissions, atmospheric CO_2 and global warming. Phys Chem Earth 21:471–476

Jung T (2005) Systematic errors of the atmospheric circulation in the ECMWF forecasting system. Quart J Roy Meteor Soc 131(607):1045–1073

Karoly DJ, Plumb RA, Ting MF (1989) Examples of the horizontal propagation of quasi-stationary waves. J Atmos Sci 46(18):2802–2811

Kharin VV, Zwiers FW (2003) Improved seasonal probability forecasts. J Clim 16(11):1684–1701

Knaff JA, Landsea CW (1997) An El Niño Southern Oscillation climatology and persistence (CLIPER) forecasting scheme. Wea Forecasting 12(3):633–652

Knutti R, Stocker TF (2002) Limited predictability of the future thermohaline circulation close to an instability threshold. J Climate 15(2):179–186

Knutti R, Stocker TF, Joos F, Plattner G-K (2002) Constraints on radiative forcing and future climate change from observations and climate model ensembles. Nature 416(6882):719–723

Knutti R, Stocker TF, Joos F, Plattner G-K (2003) Probabilistic climate change projections using neural networks. Clim Dyn 21(3–4):257–272

Landsea CW, Knaff JA (2000) How much skill was there in forecasting the very strong 1997–98 El Niño?. Bull Am Meteor Soc 81(9):2107–2119

Latif M, Anderson D, Barnett T, Cane M, Kleeman R, Leetmaa A, O'Brien J, Rosati A, Schneider E (1998) A review of the predictability and prediction of ENSO. J Geophys Res-Oceans 103(C7):14375–14393

Latif M, Roeckner E, Mikolajewicz U, Voss R (2000) Tropical stabilization of the thermohaline circulation in a greenhouse warming simulation. J Climate 13(11):1809–1813

Legras B, Ghil M (1985) Persistent anomalies, blocking and variations in atmospheric predictability. J Atmos Sci 42(5):433–471

Leith CE (1973) The standard error of time–average estimates of climatic means. J Appl Meteor 12:1066–1069

Lin H, Derome J (2004) Nonlinearity of the extratropical response to tropical forcing. J Clim 17:2597–2608

Liu Q (1994) On the definition and persistence of blocking. Tellus 46A(3):286–298

Lott F, Robertson AW, Ghil M (2004a) Mountain torques and Northern Hemisphere low-frequency variability. Part I: Hemispheric aspects. J Atmos Sci 61(11):1259–1271

Lott F, Robertson AW, Ghil M (2004b) Mountain torques and Northern Hemisphere low-frequency variability. Part II: Regional aspects. J Atmos Sci 61(11):1272–1283

Lupo AR, Smith PJ (1995) Climatological features of blocking anticyclones in the Northern-Hemisphere. Tellus 47A(4):439–456

Luterbacher J, Xoplaki E, Dietrich D, Rickli R, Jacobeit J, Beck C, Gyalistras D, Schmutz C, Wanner H (2002) Reconstruction of sea level pressure fields over the Eastern North Atlantic and Europe back to 1500. Clim Dyn 18:545–561

Madden RA (1976) Estimates of the natural variability of time-averaged sea-level pressure. Mon Wea Rev 104:942–952

Maier-Reimer E, Mikolajewicz U (1992) The Hamburg large scale geostrophic ocean general circulation model (Cycle 1). Technical Report 2, Deutsches Klimarechenzentrum.

Manabe S, Stouffer RJ (1996) Low-frequency variability of surface air temperature in a 1000-year integration of a coupled atmosphere-ocean-land surface model. J Climate 9(2):376–393

Manabe S, Strickler RF (1964) Thermal equilibrium of the atmosphere with a convective adjustment. J Atmos Sci 21(4):361–385

Manabe S, Wetherald RT (1967) Thermal equilibrium of the atmosphere with a given distribution of relative humidity. J Atmos Sci 24(3):241–259

Marotzke J, Welander P, Willebrand J (1988) Instability and multiple steady states in a meridional-plane model of the thermohaline circulation. Tellus 40A:162–172

Mason SJ (2004) On Using "Climatology" as a reference strategy in the brier and ranked probability skill scores. Mon Wea Rev 132:1891–1895

Mason SJ, Mimmack GM (2002) Comparison of some statistical methods of probabilistic forecasting of ENSO. J Clim 15(1):8–29

Mathieu PP, Sutton B, Dong RT, Collins M (2004) Predictability of winter climate over the North Atlantic European region during ENSO events. J Climate 17:1953–1974

Mauritsen T, Källén E (2004) Blocking prediction in an ensemble forecasting system. Tellus A 56(3):218–228

McPhaden MJ (2004) Evolution of the 2002/03 El Niño. Bull Am Meteor Soc 85(5):677–695

McPhaden MJ, Yu X (1999) Equatorial waves and the 1997–1998 El Niño. Geophys Res Lett 26(19):2961–964

Mearns LO, Katz RW, Schneider SH (1984) Extreme high-temperature events - changes in their probabilities with changes in mean temperature. J Clim Appl Met 23(12):1601–1613

Merkel U, Latif M (2002) A high resolution AGCM study of the El Niño impact on the North Atlantic/European sector. Geophys Res Lett 29(9):1291, doi:10.1029/2001GL013726

Molteni F, Tibaldi S (1990) Regimes in the wintertime circulation over northern extratropics. II: Consequences for dynamical predictability. Quart J Roy Meteor Soc 116:1263–1288

Monahan AH, Fyfe JC, Flato GM (2000) A regime view of Northern Hemisphere atmospheric variability and changes under global warming. Geophys Res Lett 27(8):1139–1142

Müller SA, Joos F, Edwards NR, Stocker TF (2006) Water-mass distribution and ventilation time scales in a cost-efficient, 3-dimensional ocean model. J Clim (in press)

Mullen SL (1987) Transient eddy forcing of blocked flows. J Atmos Sci 44:3–22

Mullen SL (1989a) The impact of orography on blocking frequency in a general-circulation model. J Climate 2(12):1554–1560

Mullen SL (1989b) model experiments on the impact of pacific sea surface temperature anomalies on blocking frequency. J Climate 2(9):997–1013

Müller WA, Appenzeller C, Doblas-Reyes FJ, Liniger MA (2005a) A debiased ranked probability skill score to evaluate probabilistic forecasts with small ensemble sizes. J Clim 18(10):1513–1523

Müller WA, Appenzeller C, Schär C (2005b) Probabilistic seasonal prediction of the winter North Atlantic Oscillation and its impact on near surface temperature. Clim Dyn 24(2–3):213–226

Murphy AH (1969) On the ranked probability skill score. J Appl Meteor 8:988–989

Murphy AH (1971) A note on the ranked probability skill score. J Appl Meteor 10:155–156

Murphy JM, Sexton DMH, Barnett DN, Jones GS, Webb MJ, Collins M, Allen MR, Stainforth DJ (2004) Quantification of modelling uncertaities in a large ensemble of climate change simulations. Nature 430(7001):768–772

Nakićenović N, Alcamo J, Davis G, de Vries B, Fenhann J, Gaffin S, Gregory K, Grübler A, Jung TY, Kram T, La Rovere EL, Michaelis L, Mori S, Morita T, Pepper W, Pitcher H, Price L, Raihi K, Roehrl A, Rogner H-H, Sankovski A, Schlesinger M, Shukla P, Smith S, Swart R, van Rooijen S, Victor N, Dadi Z (2000) IPCC Special Report on Emissions Scenarios. Cambridge, UK and New York, NY, USA: Cambridge University Press. p 599

Nigam S, Lindzen RS (1989) The sensitivity of stationary waves to variations in the basic state zonal flow. J Atmos Sci 46(12):1746–1768

North GR, Cahalan RF, Coakley JA (1981) 'Energy-balance climate models. Rev Geophys Space Phys 19(1):91–121

Oortwijn J (1998) Predictability of the onset of blocking and strong zonal flow regimes. J Atmos Sci 55:973–994

Opsteegh JD, Haarsma RJ, Selten F, Kattenberg A (1998) ECBILT: A dynamic alternative to mixed boundary conditions in ocean models. Tellus 50A:348–367

Palmer TN (1998) Nonlinear dynamics and climate change: rossby's legacy. Bull Am Meteor Soc 79(7):1411–1423

Palmer TN (1993) Extend-range atmospheric prediction and the lorenz model. Bull Am Meteor Soc 74(1):49–65

Palmer TN (1999) A nonlinear dynamical perspective on climate prediction. J Climate 12(2):575–591

Palmer TN, Alessandri A, Andersen U, Cantelaube P, Davey M, Delecluse P, Deque M, Diez E, Doblas-Reyes FJ, Feddersen H, Graham R, Gualdi S, Gueremy JF, Hagedorn R, Hoshen M, Keenlyside N, Latif M, Lazar A, Maisonnave E, Marletto V, Morse AP, Orfila B, Rogel P, Terres JM, Thomson MC (2004) Development of a European multimodel ensemble system for seasonal-to-interannual prediction (DEMETER). Bull Am Meteor Soc 85(6):853–874

Palmer TN, Anderson DLT (1994) The prospects for seasonal forecasting – a review paper. Quart J Roy Meteor Soc 120(518):755–793

Palmer TN, Shukla J (2000) Editorial to DSP/PROVOST special issue. Quart J Roy Meteor Soc 126(567):1989–1990

Palmer TN, Shutts GJ, Hagedorn R, Doblas-Reyes F, Jung T, Leutbecher M (2005) Representing model uncertainty in weather and climate prediction. Ann Rev Earth and Plan Sci 33:163–193

Pasmanter RA, Timmermann A (2003) Cyclic Markov chains with an application to an intermediate ENSO model. Nonlin Proc Geophys 10:197–210

Pavan V, Doblas-Reyes FJ (2000) Multi-model seasonal hindcasts over the Euro-Atlantic: Skill scores and dynamic features. Clim Dyn 16(8):611–625

Pavan V, Tibaldi S, Brankovic C (2000a) Seasonal prediction of blocking frequency: Results from winter ensemble experiments. Quart J Roy Meteor Soc 126(567):2125 –2142

Pavan V, Molteni F, Brankovic C (2000b) Wintertime variability in the Euro-Atlantic region in observations and in ECMWF seasonal ensemble experiments. Quart J Roy Meteor Soc 126(567):2143–2173

Peixoto JP, Oort AH (1984) Physics of climate. Rev Mod Phys 56(3):365–429

Pelly JL, Hoskins BJ (2003) How well does the ECMWF ensemble prediction system predict blocking?. Quart J Roy Meteor Soc 129(590):1683–1702

Peng SL, Robinson WA, Li SL (2003) Mechanisms for the NAO responses to the North Atlantic SST tripole. J Clim 16(12):1987–2004

Philander SGH (1990) El Niño, La Niña and the Southern Oscillation. Academic Press, San Diego, CA

Ramanathan V, Coakley JA (1978) Climate modelling through radiative-convective models. Rev Geophys Space Phys 16:465–489

Ramaswamy V, Boucher O, Haigh J, Hauglustaine D, Haywood J, Myhre G, Nakajima T, Shi GY, Solomon S (2001) Radiative forcing of climate change. In: Houghton JT, Ding Y, Griggs DJ, Noguer M, van der Linden PJ, Dai X, Maskell K, Johnson CA (eds) Climate Change 2001: The Scientific Basis. Cambridge, UK and New York, NY, USA: Cambridge University Press, Chapt. 6, pp 349–16. Contribution of Working Group I to the Third Assessment Report of the Intergovenmental Panel on Climate Change, p 881

Reilly J, Stone PH, Forest CE, Webster MD, Jacoby HD, Prinn RG (2001) Uncertainty and climate change assessments. Science 293(5529):430–433

Rex DF (1950a) Blocking action in the middle troposphere and its effect upon regional climate. I. An aerological study of blocking. Tellus 2:169–211

Rex DF (1950b) Blocking action in the middle troposphere and its effect upon regional climate. II. The climatology of blocking action. Tellus 2:275–301

Rodwell MJ, Folland CK (2002) Atlantic air-sea interaction and seasonal predictability. Quart J Roy Meteor Soc 128(583):1413–1443

Rodwell MJ, Rowell DP, Folland CK (1999) Oceanic forcing of the wintertime North Atlantic Oscillation and European climate. Nature 398(6725):320–323

Saltzman B (1978) A survey of statistical-dynamical models of the terrestrial climate. Adv Geophys 20:183–303

Saunders MA, Qian BD (2002) Seasonal predictability of the winter NAO from North Atlantic sea surface temperatures. Geophys Res Lett 29(22):2049, doi:10.1029/2002GL014952

Sausen R, König W, Sielmann F (1995) Analysis of blocking events from observations and ECHAM model simulations. Tellus 47(4):421–438

Scherrer SC, Croci-Maspoli M, Schwierz C, Appenzeller C (2006) Two-dimensional indices of atmospheric blocking and their statistical relationship with winter climate patterns in the Euro-Atlantic region. Int J Clim 26(2):233–249

Schmittner A, Appenzeller C, Stocker TF (2000) Enhanced Atlantic freshwater export during El Niño. Geophys Res Lett 27:1163–1166

Schneider SH (2000) Adaptation: sensitivity to natural variability, agent assumptions and dynamic climate changes. Climatic Change 45(1):203–221

Schneider SH (2001) What is 'dangerous' climate change? Nature 411(6833):17–19

Schwierz C (2001) Interactions of greenland-scale orography and extra-tropical synoptic-scale flow. Ph.D. thesis, ETH Zürich, Institute for Atmospheric and Climate Science. Dissertation Nr. 14356

Schwierz C, Croci-Maspoli M, Davies HC (2004) A perspicacious indicator of atmospheric blocking. Geophys Res Lett 31(6):L06125, doi: 10.1029/2003GL019341

Sellers WD (1969) A global climatic model based on the energy balance of the earth-atmosphere system. J Appl Meteorol 8:392–400

Shabbar A, Huang J, Higuchi K (2001) The relationship between the wintertime North Atlantic Oscillation and blocking episodes in the Northern Atlantic. Int J Clim 21(3):355

Shukla J, Anderson J, Baumhefner D, Brankovic C, Chang Y, Kalnay E, Marx L, Palmer T, Paolino D, Ploshay J, Schubert S, Straus D, Suarez M, Tribbia J (2000) Dynamical seasonal prediction. Bull Am Meteor Soc 81(11):2593–2606

Shutts GJ (1983) The propagation of eddies in diffluent jetstreams: Eddy vorticity forcing of "blocking" flow fields. Quart J Roy Meteor Soc 109:737–761

Simmons AJ, Wallace JM, Branstator GW (1983) Barotropic wave propagation and instability, and atmospheric teleconnection patterns. J Atmos Sci 40(6):1363–1392

Smith LA (2002) What might we learn from climate forecasts? P Natl Acad Sci USA 99(Suppl. 1):2487–2492. Suppl. 1.

Stainforth DA, Aina T, Christensen C, Collins M, Faull N, Frame DJ, Kettleborough JA, Knight S, Martin A, Murphy JM, Plani C, Sexton D, Smith LA, Spicer RA, Thorpe AJ, Allen MR (2005) Uncertainty in predictions of climate change response to rising levels of greenhouse gases. Nature 433:403–406

Stephenson DB (2000) Is the North Atlantic Oscillation a random walk? Int J Climatol 10:1–18

Stephenson DB, Pavan V, Bojariu R (2000) Is the North Atlantic Oscillation a random walk? Int J Climatol 20(1):1–18

Stern W, Miyakoda K (1995) Feasibility of seasonal forecasts inferred from multiple GCM simulations. J Clim 8(5):1071–1085

Stocker TF, Wright DG, Mysak LA (1992) A zonally averaged, coupled ocean-atmosphere model for paleoclimate studies. J Clim 5(1):773–797

Stocker TF, Knutti R (2003) Do simplified climate models have any useful skill? CLIVAR Exchanges 8(1):7–10

Stocker TF, Marchal O (2001) Recent progress in paleoclimate modeling: Climate models of reduced complexity. PAGES News 9(1):4–7

Stocker TF, Schmittner A (1997) Influence of CO_2 emission rates on the stability of the thermohaline circulation. Nature 388(6645):862–865

Stott PA, Kettleborough JA (2002) Oringins and estimates of uncertainty in predictions of twenty-first century temperature rise. Nature 416(6882):723–726

Stouffer RJ, Hegerl G, Tett S (2000) A comparison of surface air temperature variability in three 1000-yr coupled ocean-atmosphere model integrations. J Climate 13(3):513–537

Stouffer RJ, Manabe S (1999) Response of a coupled ocean-atmosphere model to increasing atmospheric carbon dioxide: Sensitivity to the rate of increase. J Climate 12(8: Part I):2224–2237

Sutton R (2005) Informing adaptation: New challenges for the climate modelling community. Weather 60(7):186–189

Swets JA (1973) The relative operating characteristic in psychology. Science 182:990–1000

Thompson PD (1977) How to improve accuracy by combining independent forecasts. Mon Wea Rev 105:228–229

Thompson DWJ, Wallace JM (2001) Regional climate impacts of the Northern Hemisphere Annular Mode. Science 293(5527):85–89

Tibaldi S, D'Andrea F, Tosi E, Roeckner E (1997) Climatology of Northern Hemisphere blocking in the ECHAM model. Climate Dyn 13:649–666

Tibaldi S, Tosi E, Navarra A, Pedulli L (1994) Northern and Southern-Hemisphere seasonal variability of blocking frequency and predictability. Mon Wea Rev 122(9):1971–2003

Tracton MS, Kalnay E (1993) Operational ensemble prediction at the national meteorological center – practical aspects. Wea Forecasting 8(3):379–398

Trenberth KE, Branstator GW, Karoly D, Kumar A, Lau NC, Ropelewski C (1998) Progress during TOGA in understanding and modeling global teleconnections associated with tropical sea surface temperatures. J Geophys Res-Oceans 103(C7):14291–14324

Trenberth KE, Hurrell JW (1994) Decadal atmosphere-ocean variations in the Pacific. Clim Dyn 9(6):303–319

Trevisan A, Pancotti F, Molteni F (2001) Ensemble prediction in a model with flow regimes. Quart J Roy Meteor Soc 127(572):343–358

Trigo RM, Trigo IF, DaCamara CC, Osborn TJ (2004) Climate impact of the European winter blocking episodes from the NCEP/NCAR Reanalyses. Clim Dyn 23(1)

Tsou CH, Smith PJ (1990) The role of synoptic/planetary-scale interactions during the development of a blocking anticyclone. Tellus 42A:174–193

Tung KK, Lindzen RS (1979) A theory of stationary long waves. Part I: A simple theory of blocking. Mon Wea Rev 107(6):714–734

van Oldenborgh GJ, Balmaseda M, Ferranti L, Stockdale T, Anderson D (2003) Did the ECMWF seasonal forecast model outperform a statistical model over the last 15 years?. Vol. 418 of ECMWF Technical Memorandum. ECMWF, p 32

van Oldenborgh GJ, Burgers G, Klein Tank A (2000) On the El Niño teleconnection to spring precipitation in Europe. Int J Climatol 20:565–574

Vautard R, Legras B, Déqué M (1988) On the source of midlatitude low-frequency variability. 1. A statistical approach to persistence. J Atmos Sci 45(20):2811–2843

Vitart F, Balmaseda MA, Ferranti L, Anderson D (2003) Westerly wind events and the 1997/98 El Niño event in the ECMWF seasonal forecasting system: A case study. J Clim 16(19):3153–3170

Watson JS, Colucci SJ (2002) Evaluation of ensemble predictions of blocking in the NCEP global spectral model. Mon Wea Rev 130(12):3008–3021

Weaver AJ, Zwiers FW (2000) Uncertainty in climate change. Nature 407(6804):571–572

Wiedenmann JM, Lupo AR, Mokhov II, TEA (2002) The climatology of blocking anticyclones for the Northern and Southern Hemispheres: Block intensity as a diagnostic. J Climate 15(23):3459–3473

Wigley TML, Raper SCB (2001) Interpretation of high projections for global-mean warming. Science 293(5529):451–454

Wilks DS (1995) Statistical methods in the atmospheric sciences, Vol. 59 of International Geophysics Series. Academic Press

Wright DG, Stocker TF (1991) A zonally averaged ocean model for the thermohaline circulation. Part I: Model development and flow dynamics. J Phys Oceanogr 21(12):1713–1724

Wunsch C (1999) The interpretation of short climate records, with comments on the North Atlantic Oscillation and Southern Oscillations. Bull Am Met Soc 80(2):245–255

Yamane S, Yoden S (1997) Predictability variation and quasi-stationary states in simple non-linear systems. J Met Soc Jap 75(2):557–568

Zheng X, Frederiksen CS (2004) Variability of seasonal-mean fields arising from intraseasonal variability: part 1, methodology. Clim Dyn 23(2):177–191

Zwiers FW (2002) The 20-year forecast. Nature 416(6882):690–691

Global warming and the summertime evapotranspiration regime of the Alpine region

Pierluigi Calanca · Andreas Roesch · Karsten Jasper · Martin Wild

Abstract Changes of the summer evapotranspiration regime under increased levels of atmospheric greenhouse gases are discussed for three Alpine river basins on the basis of a new set of simulations carried out with a high-resolution hydrological model. The climate change signal was inferred from the output of two simulations with a state-of-the-art global climate model (GCM), a reference run valid for 1961–1990 and a time-slice simulation valid for 2071–2100 under forcing from the A2 IPCC emission scenario. In this particular GCM experiment and with respect to the Alpine region summer temperature was found to increase by 3 to 4 °C, whereas precipitation was found to decrease by 10 to 20%. Global radiation and water vapor pressure deficit were found to increase by about 5% and 2 hPa, respectively. On this background, an overall increase of potential evapotranspiration of about 20% relative to the baseline was predicted by the hydrological model, with important variations between but also within individual basins. The results of the hydrological simulations also revealed a reduction in the evapotranspiration efficiency that depends on altitude. Accordingly, actual evapotranspiration was found to increase at high altitudes and to the south of the Alps, but to decrease in low elevation areas of the northern forelands and in the inner-Alpine domain. Such a differentiation does not appear in the GCM scenario, which predicts an overall increase in evapotranspiration over the Alps. This underlines the importance of detailed simulations for the quantitative assessment of the regional impact of climate change on the hydrological cycle.

1 Introduction

Assessing the impact of global warming on the hydrological cycle of the Alpine region is not only important from the point of view of the exploitation of water resources but also

P. Calanca (✉) · K. Jasper
Agroscope FAL Reckenholz, Swiss Federal Research Station for Agroecology and Agriculture, CH-8046 Zürich, Switzerland
e-mail: pierluigi.calanca@fal.admin.ch

A. Roesch · M. Wild
Institute for Atmospheric and Climate Science, Swiss Federal Institute of Technology, CH-8092 Zürich, Switzerland

with regard to the management of forests as well as agricultural ecosystems. It is nowadays acknowledged that agriculture and forestry provide key services to society, such as the protection of the landscape and the preservation of biodiversity (Behringer et al. 2000).

The functioning of ecosystems is constraint by water and energy fluxes and feeds back on them (Eagleson 2002). Atmospheric carbon dioxide (CO_2), light and temperature determine the maximum rate for the growth of plants (Monteith 1981; Thornley and Johnson 1990), whereas the soil moisture status sets an upper limit to the actual productivity (Taylor et al. 1983). The physiology of plants is so tightly related to water fluxes, that the ratio between actual and potential evapotranspiration is in fact a good measure for the ratio between actual and potential productivity (Doorenbos and Kassam 1979).

Analyses of global records have provided some evidence that the climatic warming observed in particular since 1976 has been accompanied by an increase in precipitation and river discharge in most of the extratropics (Houghton et al. 2001). Other studies (e.g. Brutsaert and Parlange 1998; Golubev et al. 2001; Ohmura and Wild 2002; Roderick and Farquhar 2002) have revealed a statistically significant decrease in pan evaporation over more or less the same period, but it is not clear whether this has been followed by a decrease in actual evapotranspiration over land areas. Wild et al. (2004) have noticed that a decrease in evapotranspiration between 1960 and 1990 could explain why the surface temperature has increased over this period of time despite a clear decline in global radiation.

Concerning the response of evapotranspiration to global warming, there is little information available in the Third Assessment Report of the Intergovernmental Panel on Climate Change (Houghton et al. 2001). According to experiments with global climate models (GCMs), elevated greenhouse gas concentrations will foster the hydrological cycle, but increasing aerosol load could lead to a reversal of this response, with an overall decrease of precipitation and evapotranspiration (Roeckner et al. 1999; Liepert et al. 2004; Feichter et al. 2004).

Recent studies addressing the shifts induced by global warming in the climate of the Alpine region have basically considered temperature and precipitation (Gyalistras et al. 1998) as well as snow cover (Beniston et al. 2003). Other studies have examined the impacts on ecosystems (Bugmann 2003; Riedo et al. 2000, 2001). So far, however, only a few investigations have looked in detail at alterations of the hydrological regime of Europe (Arnell 1999) and of Alpine watersheds (see Jasper et al. 2004).

It is often assumed that in mountain areas evapotranspiration will increase in a warmer global climate (Beniston 2003). This probably holds true on an annual basis. However, with respect to the summer season the limiting effects of progressively larger soil moisture deficits can not be neglected. Jasper et al. (2004 and 2006) have shown that under future climatic conditions critical soil water levels over protracted periods of time could occur with a higher likelihood even in the relatively wet summer climate of northeastern Switzerland.

The objective of this work is to examine the effect of climate change on the summertime evapotranspiration regime of three Alpine river basins characterized by distinct precipitation climates. As noted by Beniston (2003), the current spatial resolution of GCM is too crude to adequately represent the topographic details of the Alpine region. On the other hand, variations in topographic characteristics (aspect, slope and altitude), soil texture and vegetation are primary drivers of water flows in complex terrain (Beven 2001) and are therefore important for understanding the regional variability of evapotranspiration (Gurtz et al. 1999).

For this reason, simulations with a state-of-the-art GCM are complemented by an experiment with a high-resolution, spatially-distributed hydrological model. This makes it possible to quantify the impact of climate change on the altitudinal distribution of potential and actual

evapotranspiration and to disclose regional differences in the response, both across the Alpine region as well as within individual river basins.

2 The target areas

The location of the three Alpine river basins considered for the analysis is shown in Figure 1. The catchment of the river Thur, in north eastern Switzerland, has an area of roughly 1700 km^2. Altitude ranges from 360 to about 2500 m above sea level (m asl), with an average of 770 m asl. The mean slope is of 9°. About 60% of the area is classified as agricultural land, and 20% are covered by forests. Loam, silt loam and sandy loam are, in the order, the dominant soil types.

The basin of the upper Ticino is located just to the south of the main ridge of the Alps. It has an area of 1500 km^2. Altitude varies from 220 to 3400 m asl, with a mean of 1700 m asl. More than 80% of the surface is located above 1000 m asl, and about half of it is covered by forests. Loamy sand, sandy and silt loam and loam are the main soil types. The mean slope is of 28°.

The third target area is a sub-basin of the river Rhone located in the upper Valais (Figure 1). This basin has an area of 1660 km^2 and extends in altitude from 500 to 4000 m asl. The average altitude is close to 2000 m asl, and the average slope is of 25°. About 25% of the surface is covered by forests, while another 15% is used for agriculture. Due to its altitudinal extent a significant percentage of the surface is without vegetation.

With respect to climate, the three basins present distinct characteristics. Most important are the disparities in precipitation (Schwarb et al. 2001a,b). Annual rainfall amounts to 1470 and 1820 mm in the Thur and Ticino basins, respectively, but only to 1060 mm in the Rhone area. In the two former watersheds, the seasonality of precipitation is pronounced. The main rain season begins in April/May and ends in September/October, and in both catchments there is a clear inflection of mean rainfall rates during the months of June and July. Monthly total amounts show little seasonal variations in the Rhone area.

Contrasting patterns are also recovered with regard to the altitudinal distribution of summer precipitation (Figure 2). The altitudinal gradient is pronounced in the basin of the river Thur, but comparatively small in the Ticino and the Rhone areas.

3 The models

As in Jasper et al. (2004), the present works relies on the Water Flow and Balance Simulation Model (WaSiM-ETH) (Schulla 1997; Schulla and Jasper 2000). WaSiM-ETH consists of a set of modules dedicated to the following tasks: temporal and spatial interpolation of meteorological fields, evaluation of potential and actual evapotranspiration, simulation of snow accumulation and snow melt, simulation of soil and groundwater dynamics, determination of runoff routing (Schulla and Jasper 2000; Jasper et al. 2004).

The dynamics of the unsaturated zone is described by the Richards equation. Soil retention characteristics and hydraulic conductivity are specified according to van Genuchten (1980) with parameters taken from Carsel and Parrish (1988). Soils are classified according to the scheme of the Soil Conservation Service (1975).

Evapotranspiration is computed in two steps. The model first estimates potential evapotranspiration using the Penman-Monteith equation (Monteith and Unsworth 1990), with canopy resistance set to a minimum. Potential evapotranspiration is then reduced to actual
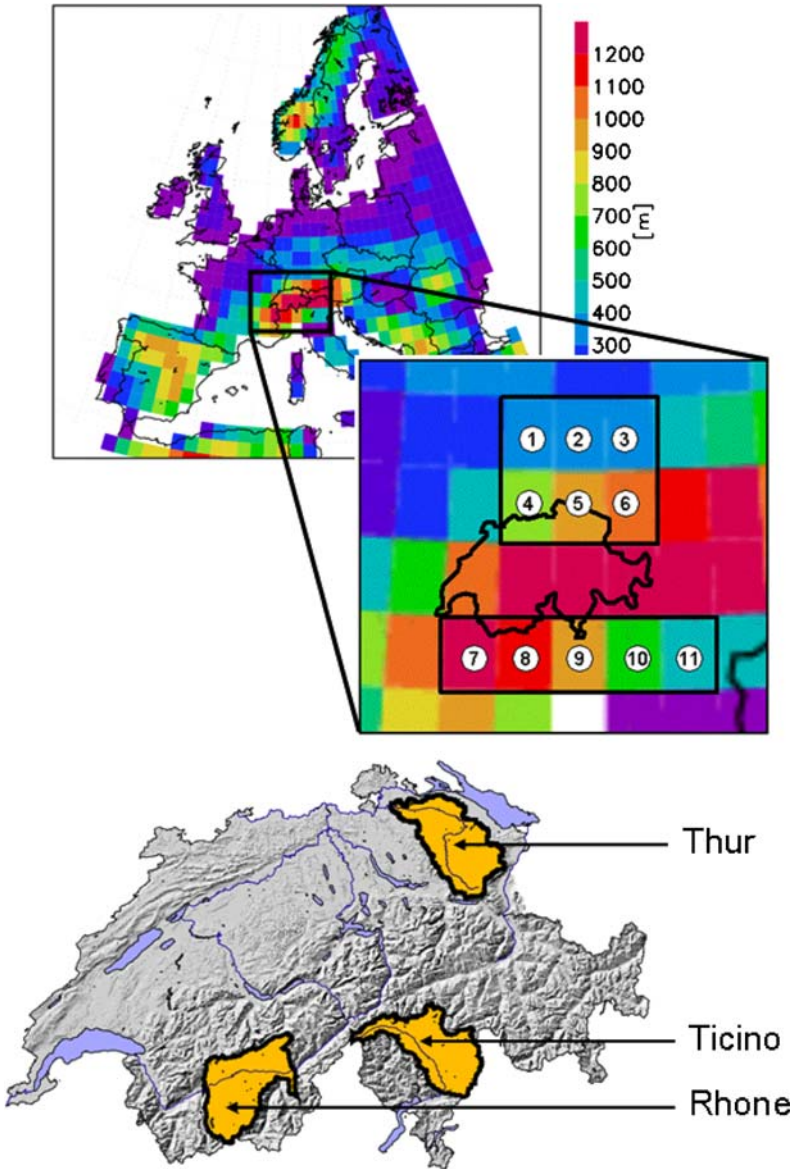
Fig. 1 Location of the river basins examined in the present study within the Alpine region and Europe. The panel on top shows continental Europe with the ECHAM5/T106 topography. The panel in the center displays part of the Alpine region with Switzerland and grid cells considered for deriving a representative climate change signal for the three watersheds shown in the bottom panel
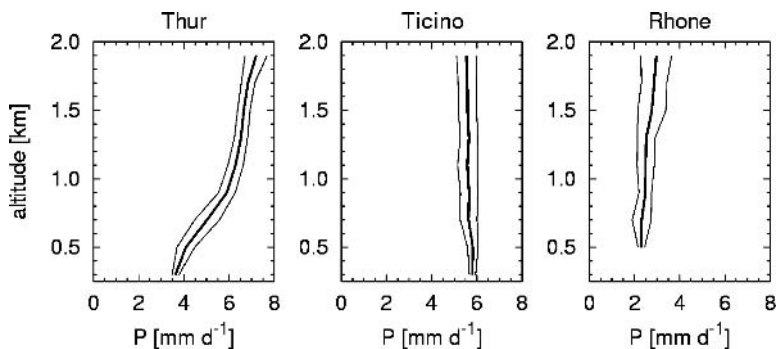
Fig. 2 Altitudinal distribution of summer mean precipitation within the basins of the rivers Thur, Ticino and Rhone (from left to right). The heavy line indicates the mean value within altitudinal classes of 200 m thickness, while the two thin lines give the range of the standard deviation

evapotranspiration, depending on whether or not the plant-available water falls short of a given critical level (Schulla 1997; Jasper et al. 2004). The critical level is defined in terms of an equivalent matric potential of $-3.5 \cdot 10^4 \, \text{J kg}^{-1}$. Vegetation characteristics with fixed seasonality are provided via look-up tables.

In our application the model was run at a horizontal resolution of 1 km $\times$ 1 km and with a daily time step. This choice gives a comparable accuracy as for simulations performed at a horizontal resolution of 100 m $\times$ 100 m and an hourly time step (Jasper et al. 2006). Overall, model setup, calibration and validation follow Jasper et al. (2004).

Gridded information on vegetation and soil texture was derived from the land-use statistics and the map of soil aptitudes of the Swiss Federal Statistical Office (1998 and 2000). The land-use statistics are originally provided on a 250 m $\times$ 250 m grid and include 74 land-use categories. For the purpose of hydrological modeling, these were aggregated into 15 main land-use classes.

Baseline simulations were driven with daily meteorological data obtained from the Swiss Federal Office for Meteorology (MeteoSwiss) for the years 1981–2000. The data stem from different observational networks: the automatic network, operational since 1978; the conventional network, providing synoptic observations three times a day; and the precipitation monitoring network, including a few hundreds rain gauges. The data were merged and projected onto the model grid using a combination of local regression against altitude and spatial interpolation with inverse-distance weighting (Schulla 1997).

Daily meteorological fields for the scenario experiment were generated using results from an experiment with ECHAM5, the latest version of the GCM of the Max-Planck Institute for Meteorology in Hamburg (Roeckner et al. 2003). Following the recommendations of Roeckner et al. (2004) the model was run at a horizontal resolution of T106 (approximately 110 km $\times$ 110 km in mid latitudes) and with 31 vertical levels (31L).

In ECHAM5, turbulent fluxes are computed using a bulk formulation. A factor linearly depending on the soil moisture is used to reduce evapotranspiration when the soil water content drops below 75% of the field capacity (Wild et al. 1997).

The two experiments performed with ECHAM5/T106L31 were a baseline simulation for the period 1961–1990 and a scenario run for the period 2071–2100. The global analyses of Rayner et al. (2003) were used to specify the distribution of sea-surface temperature and sea-ice cover for the baseline run. For the scenario experiment, these were modified by adding the long-term anomaly from a coupled transient run with version 3 of the Hadley Centre GCM
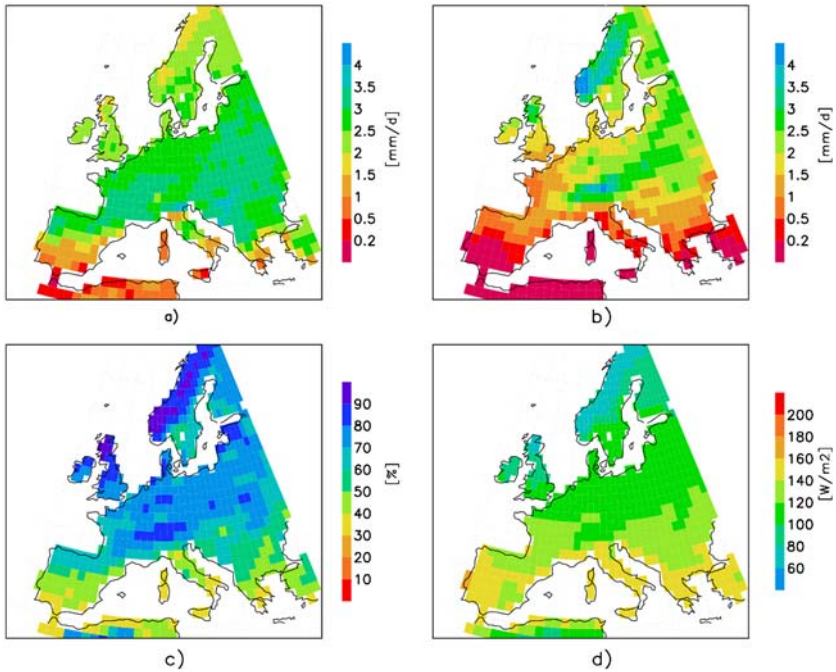
Fig. 3 Summer climate over continental Europe as simulated for the baseline period (1961–1990) by ECHAM5/T106L31: (a) evapotranspiration; (b) precipitation; (c) relative soil moisture (volumetric soil moisture divided by field capacity); (d) net radiation

that was carried out as part of the European project PRUDENCE (http://prudence.dmi.dk/). Concentrations of greenhouse gases were specified according to the A2 scenario of the Special Report on Emission Scenarios (SRES) (Nakicenovic and Swart 2000).

A scenario for the absolute changes in monthly mean temperature and global radiation and for the relative changes in precipitation and water vapour pressure was prepared by calculating the differences, respectively the ratios of the corresponding monthly climatologies in the 2071–2100 and 1961–1990 time slices. The scenario was applied to the daily fields used on input to WaSiM-ETH in the baseline simulation to create series of daily fields valid for 2081–2100. The monthly mean signal was assumed to nominally hold true for the 15th of each month, and linear interpolation was used to estimate the climate change signal on other dates.

4 The European climate as simulated by ECHAM5

We now proceed by reviewing the results of the ECHAM5/T106L31 experiments. Figure 3 shows the present-day summer climate over continental Europe. The spatial patterns of precipitation, soil moisture and evapotranspiration reflect the transition from the semi-arid climate of the Mediterranean area to the wet climate of central and northern Europe. Limiting soil water conditions are basically restricted to the Mediterranean basin. Extreme conditions are simulated for southern Spain, Italy and Greece, where relative soil water levels falls short of 50%. Over central Europe the net radiation field is rather uniform. Net radiation varies from about 150 W m^{-2} in the south to less than 100 W m^{-2} in the high latitudes.
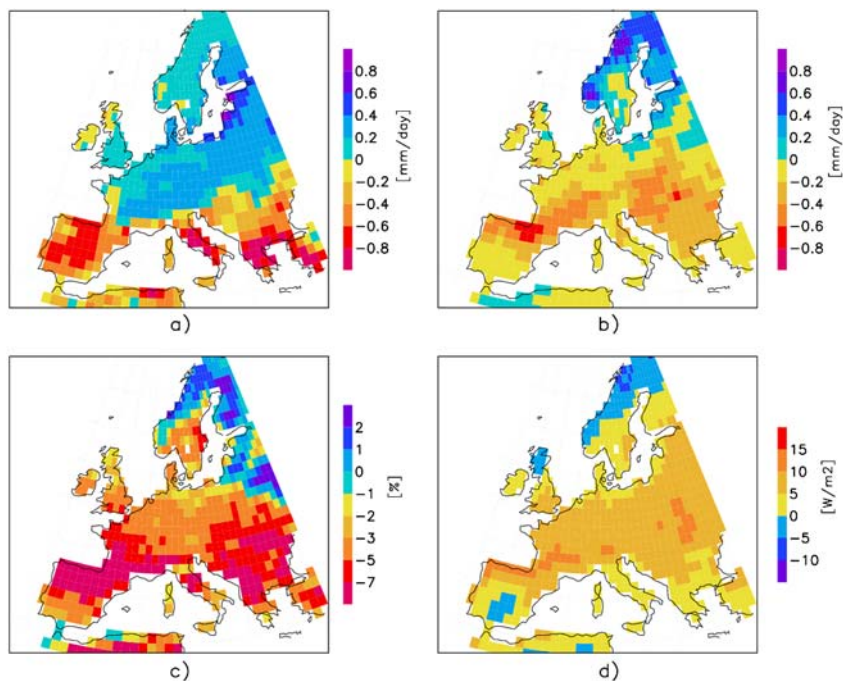
Fig. 4 Same as Figure 3 but for the change in seasonal mean conditions between baseline and scenario

The change in summer climate obtained by forcing ECHAM5/T106L31 with the greenhouse gas concentrations of the IPCC A2 scenario is displayed in Figure 4. With few exceptions (southern Spain and northern Scandinavia) there is an increase in net radiation of roughly $10\,\text{W m}^{-2}$.

Summer precipitation is seen to decrease over most of continental Europe. The largest signal (more than $-0.2\,\text{mm d}^{-1}$) is found along a belt roughly stretching from northern Spain to the Black Sea and basically including the Alps. The corresponding reduction in the relative soil moisture content is of the order 5%, with peaks of more than 7% in parts of Spain, Italy the Balkans and Greece.

Concerning the impact of global warming on evapotranspiration, Figure 4 suggests a sharp transition from positive ($+0.1$ to $+0.5\,\text{mm d}^{-1}$) in the north to negative changes (of the order of $-0.5\,\text{mm d}^{-1}$) in the south. In areas with soil moisture levels exceeding 75% of the field capacity (basically all of central and northern Europe) evapotranspiration increases by about $+0.3\,\text{mm d}^{-1}$. For the forelands on the northern side of the Alps the simulations predict an increase in actual evapotranspiration of 0.2 to $0.3\,\text{mm d}^{-1}$.

We now turn our attention to the Alpine region. Table 1 presents the values for the shift in summer temperature, relative humidity, global radiation and precipitation for the two sectors of the ECHAM grid most likely representing the conditions of our three target areas (Figure 1).

According to these figures, the effect of climate change on temperature and precipitation is more pronounced to the south than to the north of the Alps. This agrees with the results of other studies (Houghton 2001; Jasper et al. 2004). Changes in the summer mean relative humidity are small. They nevertheless give rise to a change in summer mean vapor pressure

Table 1 Change in summer climate between 1961–1990 and 2071–2100 as projected by ECHAM5/T106L31 for six grid-cells on the northern side and five grid-cells on the southern side of the main Alpine ridge

Domain	Grid-cell	Coordinates	Altitude [m.a.s.l.]	ΔT [C]	ΔRH [%]	ΔGl/Gl [%]	ΔP/P [%]
North	1	7.31–8.44 E, 48.22–49.35 N	262	3.5	−2.9	2.6	−8.4
	2	8.44–9.56 E, 48.22–49.35 N	301	3.6	−3.2	2.8	−2.7
	3	9.56–10.69 E, 48.22–49.35 N	320	3.7	−3.2	2.6	−6.9
	4	7.31–8.44 E, 47.10–48.22 N	484	3.6	−2.9	2.5	−17.6
	5	8.44–9.56 E, 47.10–48.22 N	744	3.8	−2.1	4.3	−15.5
	6	9.56–10.69 E, 47.10–48.22 N	949	3.8	−1.5	5.2	−11.7
South	7	6.19–7.31 E, 44.86–45.98 N	1256	4.3	−2.7	5.6	−25.0
	8	7.31–8.44 E, 44.86–45.98 N	1195	4.4	−2.7	3.8	−20.6
	9	8.44–9.56 E, 44.86–45.98 N	903	4.4	−2.7	1.3	−15.5
	10	9.56–10.69 E, 44.86–45.98 N	620	4.6	−3.1	1.0	−16.8
	11	10.69–11.81 E, 44.86–45.98 N	489	4.6	−2.1	0.9	−12.3

The location of the-grid cells is shown in Figure 1. T is the temperature, RH the relative humidity, Gl the global radiation and P the precipitation. The change in temperature and relative humidity is given in absolute values; the change in global radiation and precipitation is relative to the baseline

deficit of approximately +1.5 hPa. Changes in global radiation are comparable to those in net radiation, and are of the order of +3 to +5% relative to the baseline.

Variations of the climate change signal within the two domains are moderate, even though the change in precipitation and global radiation is slightly dependent on altitude. This suggests that the choice of grid-cells for defining the scenario for the hydrological simulations is probably not crucial. This is particularly true for the domain to the north of the Alps, and eventually grid-cell number 5 was selected to represent the Thur basin.

With respect to the domain to the south of the Alps, the choice is less straightforward. Grid cells number 7 to 9 are all characterized by a mean altitude around 1000 m asl, whereas the baseline climate of grid cells 10 and 11 presents many of the characteristic features of the Mediterranean climate. As a compromise, grid-cell number 9 was selected to represent both the Ticino and Rhone basins.

5 The evapotranspiration regime of the Alpine region

On an annual basis, in the Alps as in other mountain regions there is an obvious decrease of evapotranspiration with increasing altitude. As noted by Menzel et al. (1998) and Körner (2004) this is fully explained by the altitudinal reduction of the length of the vegetation period. If seasonal evapotranspiration is divided by the number of snow-free days, the altitudinal gradient almost disappears.

This feature of the present-day climate of the Alpine region, which applies to both potential and actual evapotranspiration, is satisfactorily reproduced by the baseline simulations with WaSiM-ETH (Figure 5). The daily mean evapotranspiration calculated for domains of the Thur and Ticino varies from about 4 mm d^{-1} at low elevations to about 3 mm d^{-1} at heights close to 2000 m asl, in good agreement with the range of values given by Körner (2004, Figure 9.4) for the Austrian Alps (about 5 mm d^{-1} at 1000 m asl, and 3.7 mm d^{-1} at 2500 m asl).
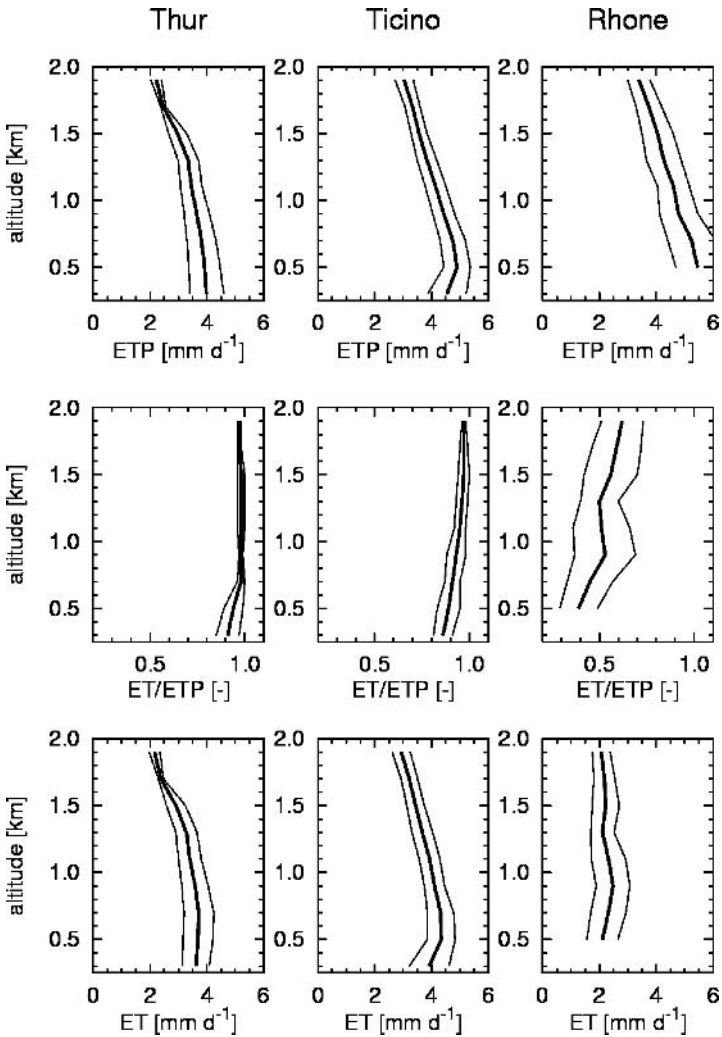
Fig. 5 Altitudinal distribution of summer mean potential evapotranspiration (upper row), evapotranspiration efficiency (middle row) and actual evapotranspiration (lower row) within the basins of the rivers Thur, Ticino and Rhone (from left to right). The data are from the baseline simulation with WaSiM-ETH. As in Figure 2, the heavy line indicates the mean value within altitudinal classes of 200 m thickness, while the two thin lines give the range of the standard deviation

In all three basins, potential evapotranspiration decreases with increasing altitude. (The altitudinal increase in potential evapotranspiration in the Ticino basin up to about 500 m asl reflects the change in land-use, from prevailing agricultural areas to forest). This follows despite the altitudinal increase in global radiation (Marty et al. 2002), and suggest that at higher elevations the maximum evapotranspiration rate is limited by temperature, vapor pressure deficit and wind speed.

Owing to higher values of the incoming solar radiation (up to 200 W m^{-2} as compared to 150 W m^{-2}. See also Z'graggen 2001), potential evapotranspiration is larger in the Rhone area than in the other two basins.
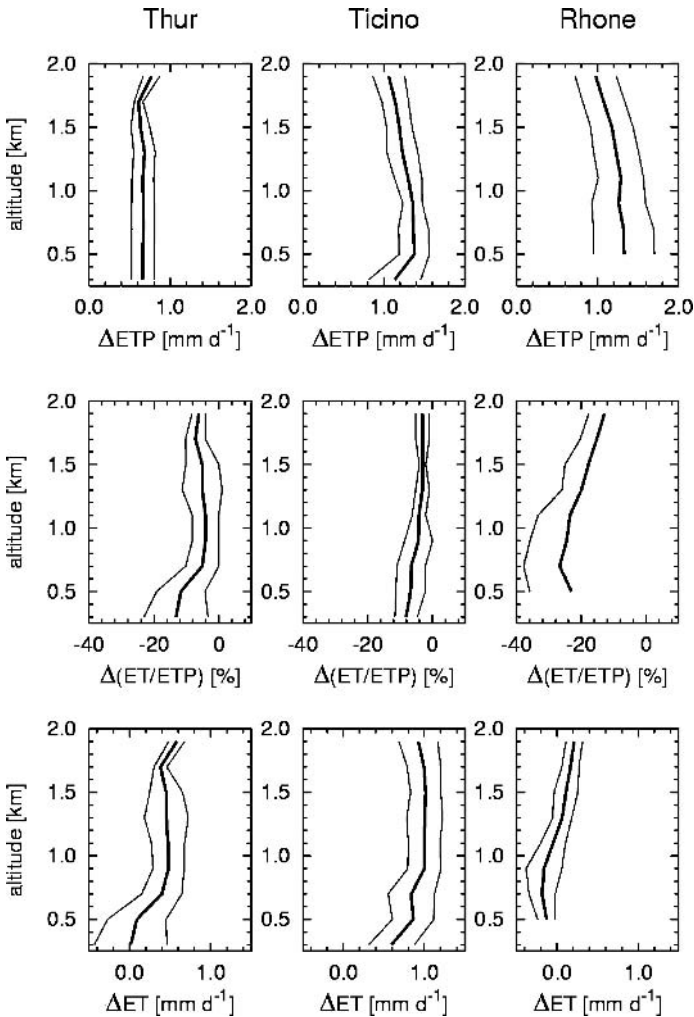
Fig. 6 Same as Figure 5 but for the change between baseline and scenario as projected by WaSim-ETH

The present-day precipitation distribution in the three watersheds was already discussed in Section 2. The contrasting amounts of rainfall seen in Figure 2 suggest divergent soil moisture regimes. This is reflected in the distribution of the evapotranspiration efficiency, with values of more than 0.7 in the Thur and Ticino basins, but of only 0.5 in the Rhone area.

The spatial variability of the evapotranspiration efficiency is more pronounced in the Rhone area than in the basins of the Thur and Ticino, reflecting lower soil water contents. Since the sensitivity of the evapotranspiration efficiency to changes in soil moisture is largest when soil water content falls short of the critical threshold, most pronounced spatial variations are found in the region with the most arid climate (Rhone area).

In all three basins the effect of climate change is to strengthen the summer mean potential evapotranspiration, less markedly in the Thur basin, most substantially in the Ticino and Rhone areas (Figure 6). Both the increase in global radiation (roughly $+10\,\mathrm{W\ m^{-2}}$, see
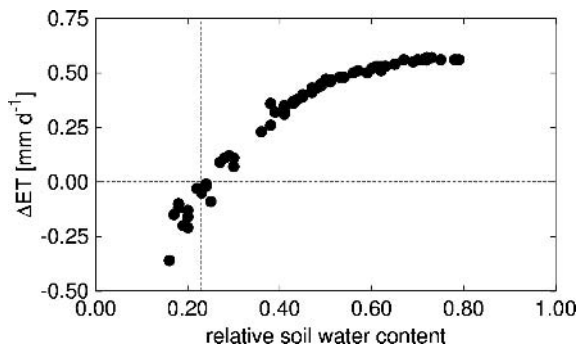
Figure 4 and Table I) as well as the intensification of the vapor pressure deficit ($+1$ to $+2$ hPa) contribute to foster potential evapotranspiration, because the energy and aerodynamic term in the Penman-Monteith equation (Monteith and Unsworth 1990) are typically of the same order of magnitude.

For all three areas we observe a reduction in evapotranspiration efficiency. This reflects a drop in soil moisture availability that, with regard to the Thur and Ticino basins, has already been discussed in detail by Jasper et al. (2004). It is interesting to note that while the decline in the evapotranspiration efficiency within the Ticino basin is minimal at all altitudes, there is a pronounced shift toward markedly lower efficiencies not only in the Rhone area, but also at low altitudes within the basin of the river Thur.

Concerning the Ticino basin, the reduction of the evapotranspiration efficiency has only a marginal impact on the actual evapotranspiration, which overall increases by the same amount (approximately 1 mm d^{-1}) as the potential evapotranspiration. The same holds true with regard to the Thur basin for elevations above 700 m asl. However, a substantial decline in the actual evapotranspiration results for extended areas within the basin of the river Rhone, and at low elevations within the Thur basin.

Plotting the change in actual evapotranspiration against the soil water content simulated for present-day conditions (Figure 7) suggests that the latter is a good predictor of the former. Processes leading to critical soil water conditions under contemporary climatic conditions are discussed by Jasper et al. (2006).

Finally it is worth mentioning that, with regard to low elevations within the Thur basin, the change in evapotranspiration is not only opposite to the overall trend in this same area (with an overall increase of about 8% relative to the baseline) but also contrary to the increase predicted by ECHAM5/T106L31 for the northern forelands of the Alpine chain (about 10% relative to the scenario). This shows that within the Alpine region water fluxes can respond very differently to one and the same forcing, stressing the necessity of detailed hydrological simulations for down-scaling the results of a GCM experiment.

6 Summary and concluding remarks

In this paper we studied the impact of climate change on the summer evapotranspiration regime of three Alpine river basins that were chosen to cover a broad spectrum of climatic conditions.

The analysis was carried out with a high-resolution, spatially-distributed hydrological model. Meteorological fields for the baseline simulation were derived from actual

observations. Scenarios for the simulation of future climatic conditions where recovered from the output of corresponding experiments carried out with ECHAM5/T106L31.

The simulations suggest that increased levels of solar radiation and reduced air humidity intensify the summer mean potential evapotranspiration. Changes in air humidity are predicted in the order of 5% and, at first sight, appear to be unimportant. Nevertheless, they affect potential evapotranspiration in a consistent way. It is unfortunate that air humidity is often neglected in scenarios utilized for impact studies; based on our experience, we recommend that global radiation and air humidity be routinely included in regional climate scenarios.

While ECHAM predicts an increase in evapotranspiration over the entire Alpine region, the simulations with WaSiM-ETH indicate less uniform patterns of change, with an increase in the area to south of the Alps, but a decrease in the inner-Alpine domain and at low elevations in the northern forelands. It has been pointed out by Jasper et al. (2006) that consideration of the spatial distribution of soil moisture as affected by slope, land-use and soil type is necessary to understand this differential response to one and the same forcing. With respect to the Alpine region, a minimum spatial resolution of 1 km × 1 km or higher is required to adequately represent the dominant modes of spatial heterogeneity.

There is no doubt that the present results reflect the specific scenario used to force the hydrological model. In our study, the climate change signal was extracted from the results of an experiment with ECHAM5/T106L31. Thanks to improved parameterizations (Roeckner et al. 2003) and enhanced vertical resolution (Roeckner et al. 2004), the impact of global warming on precipitation and soil moisture is less pronounced here than in studies based on previous versions of ECHAM (Wild et al. 1996).

Overall, changes in summer mean climate as simulated by ECHAM5/T106L31 for the Alpine region are in line with those predicted by other GCMs (Houghton et al. 2001). However, the signal is stronger than found in regional climate scenarios derived by statistical downscaling from global fields (Jasper et al. 2004).

One has also to bear in mind that our scenario did not include changes in the inter-annual variability of the Alpine climate. This is a crucial point, because in GCMs this variability depends on the representation of the soil-atmosphere feedback (Schär et al. 2004). Whether this is simulated in a realistic way by ECHAM5 (as by other GCMs) remains to be verified. In general, a better representation of the hydrological cycle in GCMs is badly needed for quantifying the soil-atmosphere feedback in a more reliable way.

We also did not contemplate changes in the occurrence of extreme events. Understanding the effect of climate change on the characteristics of extreme events (frequency and intensity) is fundamental for risk assessments. By looking at a variety of climate scenarios Fuhrer et al. (2006) arrived at the conclusion that the most remarkable trend in summer climate was a decrease in the frequency of wet days and shorter return times of heat waves. As shown by Calanca (2004), summer mean soil moisture levels are very sensitive with respect to changes in the frequency of wet days. Had we taken this into account in our analysis, we would have found a more systematic and substantial decrease in actual evapotranspiration that suggested by the present results.

References

Arnell N (1999) The effects of climate change on the hydrological regimes in Europe. Global Environ Change 9:5–23

Behringer J, Buerki R, Fuhrer J (2000) Participatory integrated assessment of adaptation to climate change in Alpine tourism and mountain agriculture. Integr Assess 1:331–338

Beniston M (2003) Climatic change in mountain regions: A review of possible impacts. Climatic Change 59:5–31

Beniston M, Keller F, Koffi B, Goyette S (2003) Estimates of snow accumulation and volume in the Swiss Alps under changing climatic conditions. Theor Appl Clim 76:125–140

Beven KJ (2001) Rainfall-runoff modelling. The Primer. John Wiley and Sons, Chichester, p 360

Brutsaert W, Parlange MB (1998) Hydrologic cycle explains the evaporation paradox. Nature 396:30

Bugmann H (2003) Predicting the ecosystems effects of climate change. In: Canham CD, Cole JJ, Lauenroth WK (eds) Models in ecosystem science, Princeton University Press, Princeton, pp 385–409

Calanca P (2004) Interannual variability of summer mean soil moisture conditions in Switzerland during the 20th century: A look using a stochastic soil moisture model. Water Resourc Res 40:W12502, doi:10.1029/2004WR003254

Carsel RF, Parrish RS (1988) Developing joint probability distributions of soil water retention characteristics. Water Resources Res 24(5):755–769

Doorenbos J, Kassam AH (1979) Yield Response to Water, FAO Irrigation and Drainage Paper 33, Food and Agriculture Organization of the United Nations, Rome, p 193.

Eagleson PS (2002) Ecohydrology. Darwinian expression of vegetation form and function. Cambridge University Press, Cambridge, p 443

Feichter J, Roeckner E, Lohmann U, Liepert BG (2004) Nonlinear aspects of the climate response to greenhouse gas and aerosol forcing. J. Climate 17:2384–2398

Fuhrer J, Beniston M, Fischlin A, Frei Ch, Goyette S, Jasper K, Pfister Ch (2006) Climate risks and their impact on agriculture and forests in Switzerland. Clim Change DOI: 10.1007/s10584-006-9106-6 (this issue).

Golubev VS, Lawrimore JH, Groisman PY, Speranskaya NA, Zhuravin SA, Menne MJ, Peterson TC, Malone RW (2001) Evaporation changes over the contiguous United States and the former USSR: A reassessment. Geophys Res Lett 28:2665–2668

Gurtz J, Baltensweiler A, Lang H (1999) Spatially distributed hydrotope-based modelling of evapotranspiration and runoff in mountainous basins. Hydrol Process 13:2751–2768

Gyalistras D, Schär C, Davies HC, Wanner H (1998) Future Alpine climate. In: Cebon P, Dahinden U, Davies HC, Imboden D, Jäger CG (eds) Views from the Alps: Regional perspectives on climate change. MIT Press, Boston, pp 171–223

Houghton JT, Ding Y, Griggs DJ, Noguer M, van der Linden PJ, Dai X, Maskell K, Johnson CA (eds) (2001) Climate Change 2001, The Scientific Basis, Contribution of Working Group I to the Third Assessment Report of the Intergovernmental Panel on Climate Change. Cambridge University Press, Cambridge, p 881.

Jasper K, Calanca P, Gyalistras D, Fuhrer J (2004) Differential impacts of climate change on the hydrology of two Alpine river basins. Clim Res 26:113–129

Jasper K, Calanca P, Fuhrer J: (2006) Changes in summertime soil water patterns in complex terrain due to climatic change. J Hydrology (in press)

Körner C (2004) Alpine plant life, 2nd edn. Springer, Berlin, and 4 colour plates, p 344

Liepert BG, Feichter J, Lohmann U, Roeckner E (2004) Can aerosols spin down the water cycle in a warmer and moister world? Geophys Res Lett 31:L06207, doi:10.1029/2003GL019060

Marty C, Philipona R, Fröhlich C, Ohmura A (2002) Altitude dependence of surface radiation fluxes and cloud forcing in the Alps: Results from the Alpine surface radiation budget network. Theor Appl Climatol 72:137–155

Menzel L, Lang H, Rohmann M (1998) Mean Annual Evapotranspiration 1973–1992, Hydrological Atlas of Switzerland, Plate 4.1, Federal Office of Topography, Bern

Monteith JL (1981) Climatic variation and the growth of crops. Quart J Roy Meteor Soc 107:749–774

Monteith JL, Unsworth MH (1990) Principles of environmental physics, 2nd edn. Edward Arnold, London, p 291

Nakicenovic N, Swart R (eds) (2000) Emission Scenarios. Special Report of the Intergovernmental Panel on Climate Change, Cambridge University Press, Cambridge, p 570

Ohmura A, Wild M (2002) Is the hydrological cycle accelerating? Science 298:1345–1346

Rayner NA, Parker DE, Horton EB, Folland CK, Alexander LV, Rowell DP, Kent EC, Kaplan A (2003) Global analyses of sea surface temperature, sea ice, and night marine air temperature since the late nineteenth century. J Geophys Res 108(D14):4407, doi:10.1029/2002JD002670

Riedo M, Gyalistras D, Fuhrer J (2000) Net primary production and carbon stocks in differently managed grasslands: Simulation of site-specific sensitivity to an increase in atmospheric CO_2 and to climate change. Ecol Model 134:207–227

Riedo M, Gyalistras D, Fuhrer J (2001) Pasture response to elevated temperature and doubled CO_2 concentration: Assessing the spatial pattern across an alpine landscape. Clim Res. 17:19–31

Roderick ML, Farquhar GD (2002) The cause of decreased pan evaporation over the past 50 years. Science 298:1410–1411

Roeckner E, Bengtsson L, Feichter J, Lelieveld J, Rodhe H (1999) Transient climate change simulations with a coupled atmosphere-ocean GCM including the tropospheric sulfur cycle. J Clim 12:3004–3032

Roeckner E, Bäuml G, Bonaventura L, Brokopf R, Esch M, Giorgetta M, Hagemann S, Kirchner I, Kornblueh L, Manzini E, Rhodin A, Schlese U, Schulzweida U, Tompkins A (2003) The Atmospheric General Circulation Model ECHAM5. Part I: Model Description. Max Planck Institute for Meteorology, Report No. 349, Hamburg, p 127

Roeckner E, Brokopf R, Esch M, Giorgetta M, Hagemann S, Kornblueh, L, Manzini E, Schlese U, Schulzweida U (2004) The Atmospheric General Circulation Model ECHAM. Part II: Sensitivity of Simulated Climate to Horizontal and Vertical Resolution. Max Planck Institute for Meteorology, Report No. 354, Hamburg, p 56

Schär C, Vidale DL, Lüthi D, Frei C, Häberli C, Liniger MA, Appeazeller C (2004) The role of increasing temperature variability in European summer heatwaves. Nature 427:332–336

Schulla J (1997) Hydrologische modellierung von Flussgebieten zur Abschätzung der Folgen von Klimaänderungen, Zürcher Geographische Schriften, vol 69. Swiss Federal Institute of Technology, Zurich, p 161

Schulla J, Jasper K (2000) WaSiM-ETH: Model Description, Internal Report, Swiss Federal Institute of Technology, Zurich, p 166

Schwarb M, Frei C, Schär C, Daly C (2001a) Mean Annual Precipitation Throughout the European Alps 1971–1990, Hydrological Atlas of Switzerland, Plate 2.6, Federal Office of Topography, Bern

Schwarb M, Frei C, Schär C, Daly C (2001b) Mean Seasonal Precipitation Throughout the European Alps 1971–1990, Hydrological Atlas of Switzerland, Plate 2.7, Federal Office of Topography, Bern

Soil Conservation Service (1975) Soil taxonomy: A basic system of soil classification for making and interpreting soil surveys. Agricultural Handbook no. 436, U.S. Department of Agriculture

Swiss Federal Statistical Office (1998) Arealstatistik 1992/1997. Neuchâtel, Switzerland

Swiss Federal Statistical Office (2000) Digital map of the soil aptitudes. Neuchâtel, Switzerland

Taylor HM, Jordan WR, Sinclair TR (eds) (1983) Limitations to efficient water use in crop production. American Society of Agronomy, Crop Science Society of America, Soil Science Society of America, Madison, Wisconsin, p 538

Thornley JHM, Johnson IR (1990) Plant and crop modelling. Clarendon Press, Oxford, p 669

Van Genuchten MT (1980) A closed-form equation for predicting the hydraulic conductivity of unsaturated soils. Soil Sci Soc Am J 44:892–898

Wild M, Dümenil L, Schulz JP (1996) Regional climate simulation with a high resolution GCM: Surface hydrology. Climate Dynamics 12:755–774

Wild M, Ohmura A, Cubasch U (1997) GCM simulated surface energy fluxes in climate change experiments. J Climate 10:3093–3110

Wild M, Ohmura A, Gilgen H (2004) On the consistency of trends in radiation and temperature records and implications for the global hydrological cycle. Geophys Res Lett 31:L11201, doi:10.1029/2003GL019188

Z'graggen L (2001) Strahlungsbilanz der Schweiz, Doctor of Natural Sciences Thesis Dissertation No. 14158, Swiss Federal Institute of Technology, Zurich, p 196

Climate risks and their impact on agriculture and forests in Switzerland

**J. Fuhrer · M. Beniston · A. Fischlin · Ch. Frei ·
S. Goyette · K. Jasper · Ch. Pfister**

Abstract There is growing evidence that, as a result of global climate change, some of the most severe weather events could become more frequent in Europe over the next 50 to 100 years. The paper aims to (i) describe observed trends and scenarios for summer heat waves, windstorms and heavy precipitation, based on results from simulations with global circulation models, regional climate models, and other downscaling procedures, and (ii) discuss potential impacts on agricultural systems and forests in Switzerland. Trends and scenarios project more frequent heavy precipitation during winter corresponding, for example, to a three-fold increase in the exceedance of today's 15-year extreme values by the end of the 21st century. This increases the risk of large-scale flooding and loss of topsoil due to erosion. In contrast, constraints in agricultural practice due to waterlogged soils may become less in a warmer climate. In summer, the most remarkable trend is a decrease in the frequency of wet days, and shorter return times of heat waves and droughts. This increases the risk of losses of crop yield and forage quality. In forests, the more frequent occurrence of dry years may accelerate the replacement of sensitive tree species and reduce carbon stocks, and the projected slight increase in the frequency of extreme storms by the end of the century could increase the

J. Fuhrer (✉) · K. Jasper
Agroscope FAL Reckenholz, Swiss Federal Research Station for Agroecology and Agriculture, Air Pollution/Climate Group, Reckenholzstrasse 191, CH-8046 Zurich, Switzerland
e-mail: juerg.fuhrer@fal.admin.ch

M. Beniston · S. Goyette
Department of Geosciences, University of Fribourg, Fribourg, Switzerland

A. Fischlin
Department of Environmental Sciences, Institute of Terrestrial Ecology, Swiss Federal Institute of Technology ETHZ, Schlieren/Zurich, Switzerland

Ch. Frei
Department of Environmental Sciences, Institute for Atmospheric and Climate Science, Swiss Federal Institute of Technology ETHZ, Zurich, Switzerland

Ch. Pfister
Institute of History, University of Bern, Bern, Switzerland

risk of windthrow. Some possible measures to maintain goods and services of agricultural and forest ecosystems are mentioned, but it is suggested that more frequent extremes may have more severe consequences than progressive changes in means. In order to effectively decrease the risk for social and economic impacts, long-term adaptive strategies in agriculture and silviculture, investments for prevention, and new insurance concepts seem necessary.

1 Introduction

1.1 Scope and aim

Climate risks arise from complex interactions between climate, environment, social and economic systems, and they represent combinations of the likelihood of climate events and their consequences for society and the environment. Society can be affected either directly or indirectly. Recent examples of direct effects in Europe were the flood damage caused by extreme rainfall in spring 1999 (Christensen and Christensen 2002), or the excess death particularly in France during the heat wave in 2003 (Valleron and Boumendil 2004). The present article deals with potential indirect effects, which may occur via impacts on the provision of goods and services to society by agricultural systems and forests. Historical events recorded in Switzerland show that heavy precipitation and droughts were most important for agricultural crop and forage production (Pfister 1999). Typically, impacts of isolated events on croplands, i.e. yield loss, were of short-term nature and could largely be alleviated by financial compensations. In the case of forests, winter storms are considered key climate risks, particularly in pre-alpine and alpine areas. Effects of climate extremes on forests can have both short-term and long-term implications for standing biomass, tree health and species composition (Dale et al. 2001; Bush et al. 2004), and similar principles apply to semi-natural grasslands (Grime et al. 1994). A climate extreme can thus be considered an ecological disturbance in semi-natural terrestrial ecosystems, and they are implicated as mechanistic drivers of species diversity, nutrient cycling or carbon (C) stocks (Parmesan 2000). Consequently, the frequency of climate extremes is important with respect to the development and succession of ecosystems.

The types of extreme climatic events considered in this article have significant damage potentials at the local and at the regional scales under today's climate. But their importance could increase over time, because extreme weather events may become more frequent as part of global climate change (e.g., IPCC 2001). The link between climatic extremes and climatic change is elusive because a few isolated events are difficult to relate in a statistically meaningful way to changes in mean climatic conditions (e.g., Frei and Schaer 2001; Beniston and Stephenson 2004).

The focus of this article is on climatological and ecological aspects. The aim is first to review information from the Swiss research program NCCR 'Climate' (Swiss National Center of Competence in Research 'Climate') and from other sources concerning temporal and spatial trends and scenarios for extremes in precipitation, temperature and wind, and secondly to relate their current and projected occurrence to possible implications for agricultural land and forests in Switzerland.

1.2 Climatic extremes and their simulation

There are different possibilities to define 'extreme events'. In a statistical sense, a climate extreme can be characterized by (1) the frequency of occurrence of anomalous weather (IPCC

2001), and an 'extreme' refers to the tail ends of a probability density function, for instance an event that occurs below the 10% or above the 90% quantile, or (2) the intensity of an event, which is described through the exceedance of a quantity measured per unit of time and/or area beyond some threshold. Alternatively, climate extremes can be characterized based on their socio-economic and/or ecological relevance, which implies the definition of specific thresholds beyond which serious impacts may occur in the systems concerned (Meehl et al. 2000). Regardless of the definition used, the characteristics of what is called an 'extreme weather event' may vary from place to place.

The assessment of extreme events and their implications is difficult because of issues of scale. Several studies documented those impacts of climate changes that are of greater magnitude when fine-scale scenarios are used compared to coarse-scale scenarios (e.g., Carbone et al. 2003; Doherty et al. 2003). Many of the processes determining the development and evolution of extremes (especially heavy precipitation and wind storms) are on spatial scales finer than what can be explicitly resolved by current general circulation models (GCMs) with their grid spacing of 150–400 km. The simplified representation of these processes in the GCM's parameterizations raises concerns about the reliability of GCM scenarios on extreme events (e.g. Giorgi et al. 2001; Huntingford et al. 2003). Moreover, depending on the scope of the assessment, there can be a mismatch of spatial scales between what can be provided by a GCM and what is needed for impact modelling. This mismatch is particularly relevant when output and input variables refer to different surface types or different topographic environments (e.g., upstream vs. downstream slopes). Statistical and numerical modelling methods have been proposed to downscale GCM outputs to regional scales (Mearns et al. 2004; Wilby et al. 2004). The numerical approach by Regional Climate Models (RCMs) aims at a more explicit simulation of the relevant physical processes of extreme events and a better representation of the topographic and physiographic detail. Thus, RCMs with a resolution of 50 km are promising tools for the development of scenarios for extreme events at the sub-continental scale, and for application in impact modeling at smaller scales (e.g., Christensen et al. 2002). RCMs have been found to reproduce patterns in the climatology of extremes, which could not be expected from the use of GCMs alone (e.g. Huntingford et al. 2003; Frei et al. 2003; Kleinn et al. 2005). As an example, Figure 1 depicts a regional climatology of heavy precipitation in autumn for the European Alps. Here, simulations for present climate with a 50 km RCM (CHRM, Vidale et al. 2003) with boundary conditions from a GCM control experiment (HadAM3H, Pope et al. 2000) are compared with observations (Frei and
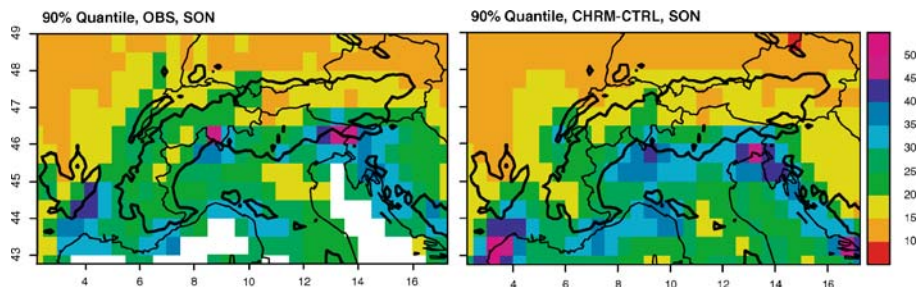
Fig. 1 Climatology of heavy precipitation in the Alpine region, as simulated by a control run with CHRM (right), and observations (left). The regional climate model CHRM (Vidale et al. 2003) was forced with HadAM3H (Jones et al. 2001) for control conditions (1961–1990). Observations are from high-resolution rain gauges upscaled to the climate model resolution (Frei and Schär 1998; Frei et al. 2003). The parameter shown is the 90% quantile of daily precipitation totals (in mm) for September to November

Schär 1998). Clearly, there are errors in magnitude and exact location of the pattern, but the visual correspondence is remarkable, given the complex distribution associated with details in topography and land-sea distribution.

Damage from windstorms may be fostered by strong sustained winds, but a large part of the small-scale impacts is due to gusts, and damage to infrastructures varies approximately exponentially with the speed of wind gusts (Dorland et al. 1999). Thus, data on finer spatial scales of a few kilometers is required. Statistical analysis of extremes in wind speed based on observed data can provide useful information on the return period for a given area (see Palutikof et al. 1999, for a review of methods); however, the relationship to the potential estimated damage can be established only for areas close to the observation station since spatial interpolation of the winds yields unreliable results. One alternative is given by the use of numerical models such as the Canadian RCM (Caya and Laprise 1999), and the application of multiple self-nesting with a RCM to obtain a fine resolution. The so-called 'medium' resolution RCMs (resolution ∼50 km) cannot be used directly as such to infer the change in wind speed at the very fine scales. As a second step, numerical downscaling of re-analysis data using RCMs with a wind gust parameterization is necessary to reproduce the strong winds in a number of documented storms (e.g., Goyette et al. 2001, 2003). Simulated hourly means may then be compared with observations if grid spacing is on the order of 1–2 km. In addition, hourly maximum wind speed may be compared if a gust parameterization is implemented in the model. As an example, Figure 2 shows the maximum wind speed field simulated for February 27, 1990, on a 2 km horizontal grid over Switzerland using multiple self-nesting methodologies after downscaling the NCEP-NCAR re-analysis data (Kalnay et al. 1996). Maximum winds exceeding $40 \, \text{m s}^{-1}$ correspond well to observed forest damage areas.

1.3 Linking climate scenarios to ecosystem models

Results from climate models can either be used for numerical downscaling making use of nested RCMs (e.g., Goyette et al. 2003), or in combination with local weather data through statistical downscaling to the temporal and spatial resolution of a few kilometers (e.g., Wilby
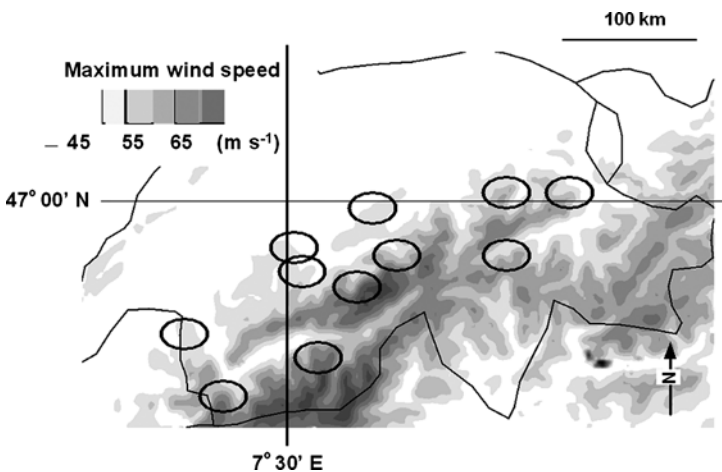

Fig. 2 Relationship between wind speed and storm damage to Swiss forests. Maximum wind speed simulated by the 2 km Canadian RCM during the 'Vivian' storm on February 27, 1990. Grey tones indicated in inset intervals of 5 m s^{-1}. Circles indicate main forest damage areas according to Schüepp et al. (1994)

et al. 1998; Gyalistras and Fischlin 1999). Downscaled monthly scenarios can be converted to daily and hourly scenarios by stochastic weather generation (e.g., Gyalistras et al. 1994, 1997; Zhang et al. 2004). These can then be used to force ecosystem models at a high spatial (e.g., 1 × 1 km) and temporal resolution (e.g., 1 h) (Riedo et al. 1999; Gyalistras and Fischlin 1999). Thus, with the current representation of meso-scale details across complex topographies, the spatial and/or temporal resolution more closely matches the requirements of many ecosystem impact assessments at the scales of interest to decision makers and practitioners, for instance at catchment or landscape scales.

2 Extreme events in Switzerland and their evolution in a changing climate

2.1 Heavy precipitation

Europe has experienced pronounced changes in precipitation during the 20th century. Analyses of instrumental data revealed an increase in mean wintertime precipitation from central Europe to Scandinavia (e.g., Schönwiese et al. 1994; Hanssen-Bauer and Forland 2000; Osborn et al. 2000). For the Mediterranean region a tendency towards decreasing annual means is noted, yet with strong regional variations (e.g., Esteban-Parra et al. 1998; Buffoni et al. 1999; Xoplaki et al. 2000), and for the whole basin, a general downward trend of 2.2 mm month^{-1} decade^{-1} in wet season (October–March) precipitation occurred since the 1960s (Xoplaki et al. 2004). In Switzerland, in the northern and western parts the changes consist in a 20–30% increase of mean winter precipitation, while no significant changes were noted for the other parts of the country (Schmidli et al. 2002). There is evidence from a number of European data analyses that the wintertime changes are associated with an increase in intensity and frequency of rainfall (Klein Tank and Können 2003; Haylock and Goodess 2004). These shifts are also evident in many statistics of Swiss precipitation measurements (Schmidli and Frei 2005). For example, Figure 3 illustrates the observed increase in the occurrence of intense precipitation events in northern Switzerland. It is not possible to make clear statements about systematic changes in extremes due to statistical limitations associated with these very rare events (Frei and Schär 2001). Nevertheless, observational analyses suggest, for the 20th century, a trend towards more vigorous precipitation events in winter over central and northern Europe, including Switzerland.

Knowledge of possible future changes in heavy precipitation events on a regional scale is derived primarily from RCMs. Representative for the results of a range of recent model integrations (e.g., Räisänen et al. 2004; Frei et al. 2006) we present here results from two RCMs: CHRM is the climate version of the former weather forecasting model of the German and Swiss weather services and is operated at ETH Zurich (Vidale et al. 2003), and HadRM3H is the model of the UK Met Office Hadley Centre (Jones et al. 2001; Noguer et al. 1998). Results are from model integrations over the entire European continent, with a resolution of ∼50 km. The boundary conditions were taken from HadCM3 and the IPCC SRES emission scenario A2 (Nakicenovic et al. 2000), where atmospheric CO_2 concentration reaches twice the value of year 2000 in about 2090. Results for the CHRM are from a 30-year integration for present (1961–1990) and future (2071–2100) conditions, while those for HadRM3H are from three independent members of a GCM ensemble in each of the two periods. Figure 4 shows the relative change in precipitation statistics. It reveals distinct regional and seasonal patterns of change. In winter, both rain-day frequency and intensity (Figure 4a,c) exhibit an increase north of about 45°N, while the rain-day frequency (but not intensity) decreases to the south. This is consistent with an increase of mean winter precipitation by 10–30% over
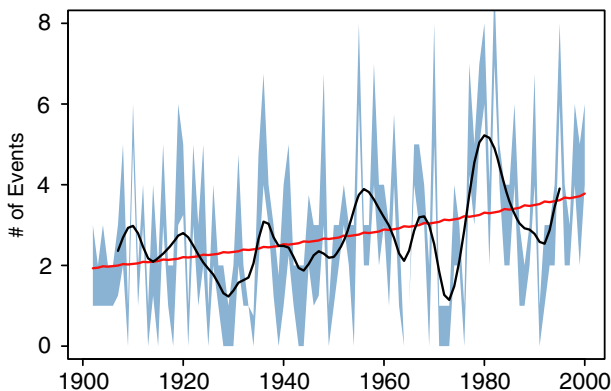
Fig. 3 Evolution of the number of heavy precipitation events per winter in northern Switzerland (days, when the daily total exceeds the climatological 90% quantile). Blue shaded: inter-quartile range from 35 stations; bold black line: smoothed time series (smoothing window is 11 years); red line: long-term trend estimated from the pooled data using logistic regression. The trend corresponds to an increase by 75% over the 20th century and is statistically significant at the 5% level (Schmidli and Frei 2005). (Courtesy of J. Schmidli, ETH Zurich)

most of central and northern Europe, and a decrease over the Mediterranean (not shown). These changes are reflected in changes for intense and heavy precipitation. For example, the 90% quantile, i.e. the typical rainfall with a recurrence of 20–30 days, increases by about 20% over northern Europe in winter.

An analysis for extreme events based on the method of extreme value statistics (see Frei et al. 2006 for details) was undertaken for the HadRM3H integration and is displayed in Figure 5. For winter, the HadRM3H model reveals an increase in the 5-year maximum 5-day precipitation event by 10–30% over large areas of central and northern Europe, including Switzerland (Figure 5a). This change corresponds roughly to a three-fold increase in frequency, i.e. the 15-year event of today's climate would become a 5-year event.

In summer, the most remarkable change is a strong decrease in the frequency of wet days (Figure 5b), for instance to about half in the Mediterranean, which goes along with a 20–50% decrease of mean summer precipitation (not shown). There is no similar tendency of drying in rainfall intensity. For example, a central part of Europe including Switzerland, which undergoes significant drying in the mean, shows a slight increase in the 90% quantile (Figure 4f) and the 5-year return period of extreme rainfall (Figure 5b). Yet the changes for extremes are at the border of statistical significance.

The results from the selected model integrations are very similar to results found in other RCM experiments (e.g., Durman et al. 2001; Christensen and Christensen 2003; Räisänen et al. 2004; Frei et al. 2006) in terms of their seasonal distribution and their larger-scale geographic pattern. However, the magnitude of change and the smaller-scale pattern vary considerably between RCMs. Hence, although a general increase of heavy precipitation during wintertime is noted in the simulations for the territory of Switzerland, there remains considerable uncertainty about the magnitude of this increase, even under a prescribed emission scenario. Moreover, little can be said today about regional differences within the country. Particularly uncertain are current scenarios of heavy precipitation for the summer season, where results for Central Europe vary even in the sign between different models (Räisänen et al. 2004; Frei et al. 2006). However, it is interesting to see the similarity among many models: the frequency of extreme precipitation events decreases modestly, or even increases,
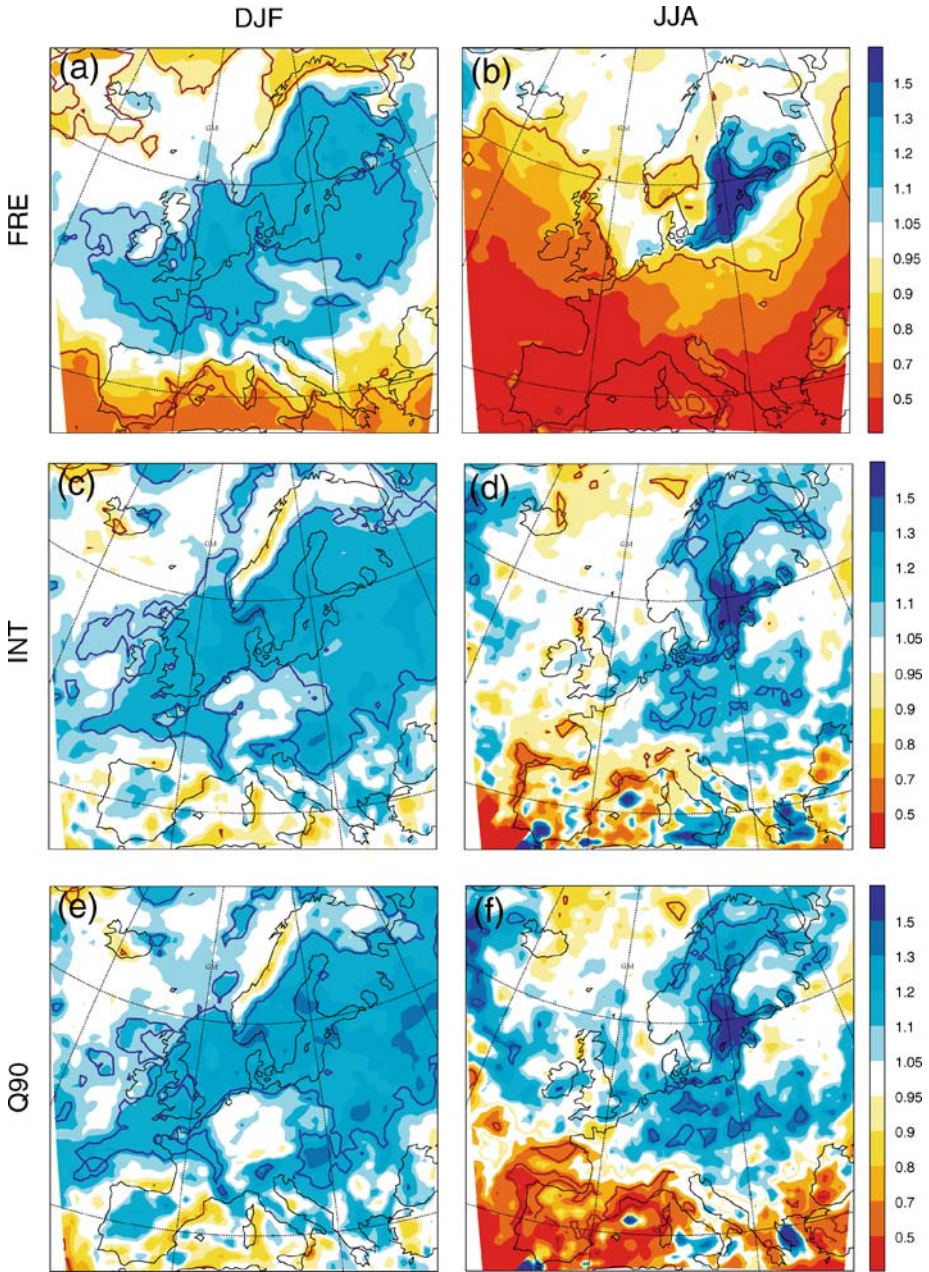
Fig. 4 Change in selected statistics of daily precipitation between 1961–1990 and 2071–2100. Scenario from the regional climate model CHRM with boundary forcing from HadAM3H and the SRES A2 emission scenario. The panels depict the ratio between future and present climate for wet-day frequency (a, b), wet-day intensity (c, d) and 90% quantile of daily precipitation (e, f), for winter (DJF, a, c, e) and summer (JJA, b, d, f). Blue colors for increase and yellow/red colors for decrease. Thick contour lines delineate areas where the change is statistically significant at the 5% level, according to a non-parametric resampling test (Courtesy of S. Fukutome, ETH Zurich)
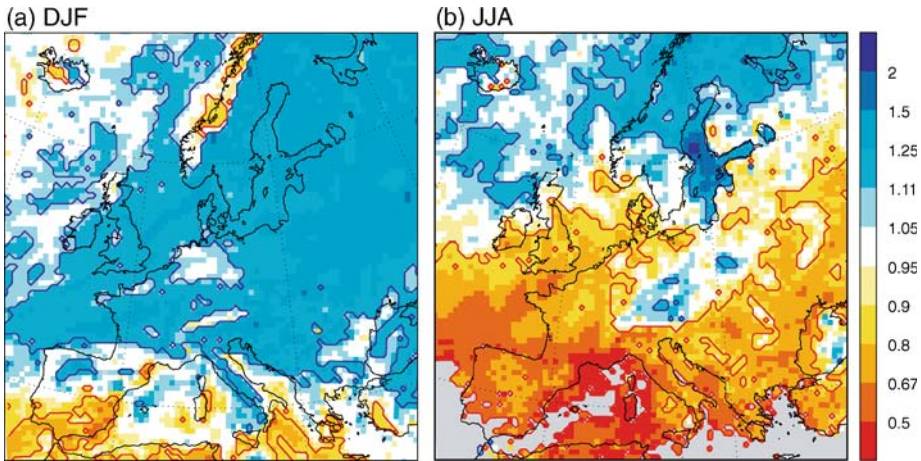
Fig. 5 Change in the 5-year extreme of 1-day precipitation totals in winter (a) and summer (b). The change is expressed as a ratio between future (2071–2100) and present (1961–1990) climate. Blue for increase, red for decrease. The blue and red contours delineate the two-sided 5% significance

despite a decrease in the frequency of average events (Christensen and Christensen 2003; Pal et al. 2004; Frei et al. 2006).

2.2 Heat waves and droughts

The record heat wave that affected many parts of Europe during the course of the summer of 2003 has been seen as typical of summers that may commonly occur in Switzerland towards the end of the 21st century (e.g., Beniston 2004a; Schär et al. 2004). The 2003 event stands out as a 'climatic surprise', in the sense that the departure from the mean 1961–1990 temperature is far greater than any recorded anomalies since the beginning of the 20th century". Figure 6 illustrates the course of annual values of summer maximum temperatures (i.e., daily maximum temperatures averaged for June, July, and August) at Basel, Switzerland, which puts 2003 into a long-term perspective.

Differences between current (1961–1990) and future (2071–2100) climates based on the IPCC A2 emission scenario and simulated by the HIRHAM4 model (Christensen et al. 1998), for example, suggest that warmer conditions will invade most of Europe, with summers in the Iberian Peninsula and southwestern France warming by 5–6 °C on average. Model-based statistics show increases in the 90%-quantile of maximum temperature that are greater than the rise in mean summer daily maxima, suggesting a change in the variance of the temperature distribution; this results in higher temperature extremes and a greater heat-wave frequency. To illustrate this point, Figure 7 shows the shift in summer maxima between the 1961–90 reference period and 2071–2100 for the RCM grid-point closest to the city of Basel. A shift by 6 °C in both mean and 90%-quantile is observed between the two 30-year periods, with a greater inter-annual variability in the scenario simulations. Mean and 90% quantile for the 2003 event are superimposed to highlight the fact that the recent heat wave in Europe closely mimicked summers that are expected to occur in Switzerland towards the end of the 21st century with the SRES A2 scenario. Because higher temperatures stimulate evapotranspiration (see accompanying paper by Calanca et al. 2006) the trend in temperature, combined with the downward trend in summer precipitation, will significantly increase the risk of droughts.
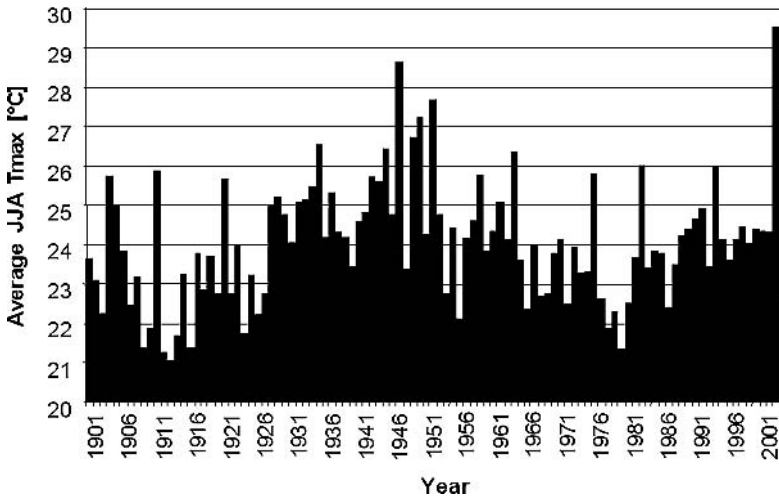
Fig. 6 Development of summer (JJA) daily maximum temperatures recorded at Basel, Switzerland, from 1901–2003
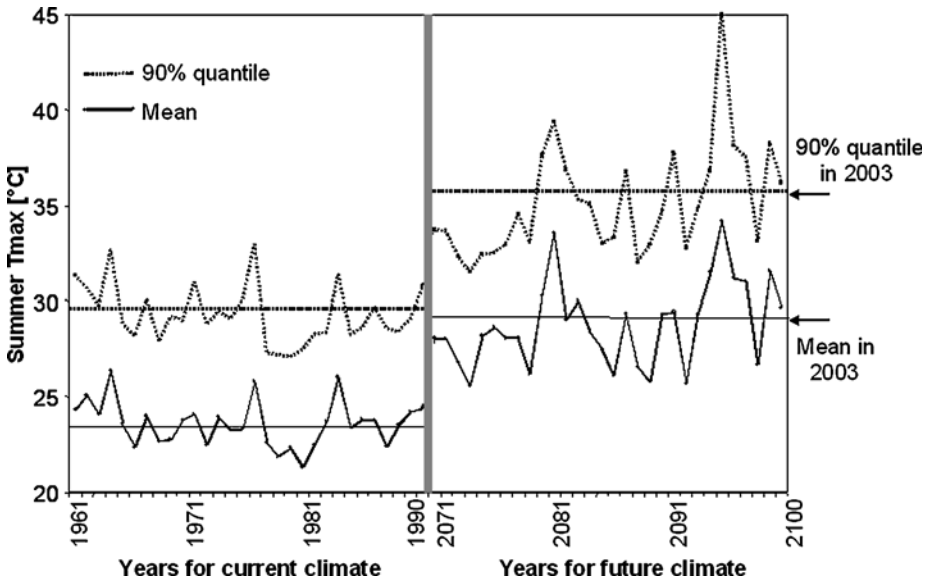
Fig. 7 Changes in mean and 90% quantile of summer (JJA) maximum temperatures in Basel, Switzerland, between current (1961–1990) and future (2071–2100) climates. Dashed and dotted lines show 30-yr means for each period. The arrow shows the temperature in 2003

2.3 Wind storms

Storms in the North Atlantic are capable of generating strong winds and gusts that have the potential to cause significant impacts (e.g., Beniston 2004b). During the last 25 years, a number of storms caused extensive damage in Western Europe including the Burns' Day storm in the UK on January 25, 1990 (McCallum and Norris 1990), the 'Vivian' storm in

Switzerland on February 27, 1990 (Schüepp et al. 1994), and the 'Lothar' storm that struck France and Switzerland on December 25–26, 1999 (Wernli et al. 2002). On the basis of a large documentary data set for the last 500 years, Pfister (1999) concluded that extremely violent storms such as Vivian (1990) occurred once in every century. Accordingly, the occurrence of 'Lothar' within the same decade of the 1990s was somewhat surprising. These storms are generated by cyclones whose climatology has been examined by a number of studies based on observations (e.g., Hanson et al. 2004; Alexandersson et al. 2000; McCabe et al. 2001; WASA Group 1998; Schmith et al. 1998; Heino et al. 1999), and also through simulations with GCMs for the current climate (e.g., Lambert et al. 2002), as well as for a future climate (e.g., Stephenson and Held 1993; Hall et al. 1994; Knippertz et al. 2000). The results suggest that during 1979–2000 there has been a general increase in weak cyclones and strong storms in the northern North Atlantic; however, the WASA Group (1998) concluded that the storminess has not increased in recent years beyond the bounds of natural variability. But for the period 1959–97, McCabe et al. (2001) have shown that there has been a significant decrease in the frequency of mid-latitude and high-latitude cyclones, and that storm intensity has increased in both the high and mid-latitudes. Similarly, modeling studies have shown that in a warmer climate cyclone activity undergoes a shift towards the north and west over Europe and the north-eastern Atlantic, which is accompanied by several weak cyclones and an increase in deep cyclones (Carnell and Senior 1998; Knippertz et al. 2000); an increase in mean wind speeds and in wind speed extremes have also been diagnosed. A consensus among many studies is the possibility that gale frequency will increase in the future in Northern Europe, independent of the emission scenario (Parry 2000; IPCC 2001). Extreme value analysis using the Canadian GCM outputs suggested increased wind speed extremes over Europe with warming, which is related to the negative pressure anomaly over northern parts of Europe (Zwiers and Kharin 1998). Generally, similar conclusions about the changes in the flow fields can be drawn from the equilibrium (e.g., $2 \times CO_2$) and from time-dependent greenhouse-gas-induced climate change simulations. The models selected to analyze the precipitation and temperature changes based on the SRES A2 emission scenario have also been used to draw some general conclusions regarding changes in wind speed (Christensen et al. 2002). Results show an overall positive change in the mean wind speed fields over Western Europe. Leckebusch and Ulbrich (2004) found that global model simulations (HadCM3) with present GHG forcing reproduced realistic patterns of the storm track density. Changes occur in particular with respect to the SRES A2 scenario for extreme cyclone systems where track density tends to increase. Moreover, analyses of the responses of RCMs driven by a series of GCMs have shown that the changes in the mean wind field patterns are also in accordance with results of their driving models. Similar numerical approaches may allow projections of damage for future climates. Based on the output produced with HIRHAM4, analysis of changes in wind direction between the 1961–1990 and 2071–2100 indicates that north-westerly flows from December through February increase on average by up to 7% with a corresponding decrease of south-westerly flows over Switzerland (Christensen et al. 2002). This would suggest a slight increase in the occurrence of 'extreme' windstorms similar to 'Vivian' and 'Lothar'.

3 Implications of climate extremes for agriculture

3.1 Heavy precipitation

More frequent heavy precipitation events in the Alpine region (see Section 2.1) may sig-nificantly increase the risk of damage from flooding, erosion, debris flow or land slides. In

Switzerland, floods in the past were most severe in autumn 1868 and in late August 1987, as defined by material losses equivalent to >300 Million Swiss Francs (value in 2000), or more than 50 victims (Pfister 2004). It is noteworthy that the major part of these losses was attributable to a few particularly severe events, such as those of 1987 and 1993 (see also Frei et al. 2001; OcCC 2003). According to the structure of today's economy, most of the financial losses associated with these events concerned public infrastructure such as river embankments, streets, bridges and railways. But heavy precipitation can also have important non-monetary adverse effects on agriculture, for instance, through the loss of fertile topsoil by erosion (Williams et al. 2001). Soil erosion is particularly sensitive to the intensity of individual precipitation events (Pruski and Nearing 2002); hence, the projected increase in the frequency and intensity of rainfall could significantly increase the risk of erosion from croplands in sloped terrain, unless preventive measures were taken. Moreover, heavy precipitation can cause soil waterlogging, which can cause crop damage through anoxic soil conditions, increased incidence of plant diseases, or impaired workability (Rosenzweig et al. 2002). As given in FAT (1996), soil water content (SWC) above field capacity (FC) impedes or delays fieldwork due to restricted operation of machinery, which can be costly for the farmers. Waterlogging of soils becomes most critical during periods with frequent or sustained intense rainfall, as for instance during May 1999 when heavy precipitation coincided with snowmelt (Grebner and Roesch 1999) resulting in large-scale flooding and in excessive SWC in Switzerland. The pre-alpine Thur river basin (1700 km^2) with currently 55% of the surface being used for agriculture was selected for analyzing the implications for SWC of shifts in the seasonality of precipitation. Simulations with a distributed hydrological model (WASIM-ETH; Schulla 1997) revealed a decrease in area-mean SWC for an ensemble of climate projections for the next 100 years, with largest changes towards the end of the growing season, but also in early spring (Jasper et al. 2004). From the mean seasonal pattern of SWC for the period 2081–2100 (Figure 8), it can be estimated that from March to May the number of days with SWC exceeding FC varies from 51 days (CSIRO [B2] scenario) down to 0 (HadCM3 [A2] scenario). For sites with slopes larger than 3°, SWC is always smaller than the FC threshold because of subsurface flows (Jasper et al. 2006). Thus, on average the occurrence of waterlogged soils during March, April and May could decline with climate warming due to the change in the partitioning of solid to liquid precipitation (Kleinn 2002), earlier and reduced springtime snowmelt, and increased potential evapotranspiration. Even one single extreme rainfall would not significantly increase the number of critical days because of sufficiently rapid soil drying under the warmer conditions (data not shown).

3.2 Heat waves and drought

Historically, heat waves have not been a major issue with respect to effects on crops and grasslands, but they may become more frequent and intense (see Section 2.2), with higher maximum temperatures, and thus become more relevant for agricultural production. Besides direct effects of heat on plants, high temperatures stimulate potential evapotranspiration (Calanca et al. 2006), which contributes to more rapid soil water depletion (Jasper et al. 2004).

Unlike heat, agricultural drought resulting from a lack of precipitation has been an important issue in the past. Using a stochastic soil moisture model, Calanca (2004) found that in 20 out of the past 100 years SWC during the growing season in northern Switzerland was close to the permanent wilting point, suggesting potential crop losses due to drought. Number and timing of these years closely matched historic records of yield losses (Schorer
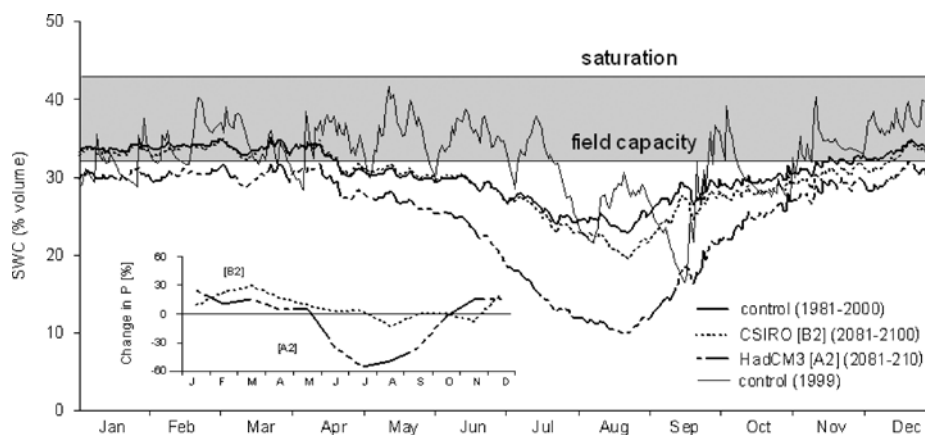
Fig. 8 Seasonal pattern of mean daily volumetric soil water content (SWC) for farmland on loamy soils and gentle slopes ($<3°$) in the Swiss Thur basin simulated with the runoff and water balance model WaSiM-ETH (e.g., Schulla 1997; Jasper et al. 2006). Data are results of the control run (1981–2000) and the 2081–2100 projections obtained by using two different climate scenarios (HadCM3 (A2) and CSIRO (B2)) (see Jasper et al. 2006). Inset: Projected changes in mean monthly precipitation (P)

1992; Pfister 1999). Drought in 1947 had the most devastating effect on Swiss agriculture because of its long duration (July to October) and its large geographical extent. Wheat yields in northwestern and central Europe dropped by 25–35% relative to the long-term average, and fodder became scarce and expensive throughout the continent (FAO data, cited in Schorer 1992). In contrast to the droughts in 1952 and 1953, import of forage into Switzerland was limited because of the concurrent crop losses in neighboring European countries (Schorer 1992). More recently, in 2003 yields of various crops and fodder cereals decreased by an average of 20% relative to the mean for 1991–99 (Keller and Fuhrer 2004). Low forage production during the second half of the season resulted in a shortage of fodder, which was compensated by increased imports at a reduced tax. Overall, the extreme weather in 2003 lowered the national net revenue of farmers from plant production by 11.1%, equivalent to about 500 Million Swiss Francs, while the fluctuations in supply had no effect on final prices of agricultural goods (Swiss Federal Office for Agriculture 2003). Hence, an isolated extreme event may not have lasting economic consequences.

To estimate future risks due to low SWC, Jasper et al. (2004) estimated for both northern and southern Switzerland an increase in average annual ET by 9–23% by 2071–2100, relative to 1981–2000, with largest changes during the summer months (see also Calanca et al. 2006). Combined with the projected reduction in summer precipitation (Schmidli and Frei 2005), this trend increases the likelihood of episodic drought. This is supported by preliminary estimates of the probability of the occurrence of agricultural drought on the Swiss Central Plateau from currently about 10–15% to over 50% towards the end of the century (Calanca 2006).

Effects of more frequent drought concern not only croplands, but also permanent grasslands, which in Switzerland cover around 75% of the agricultural land and sustain domestic meat and dairy production. The value associated with animal production was estimated at 5.2 billion Swiss Francs, or 68% of the total value of agricultural production (Swiss Farmers' Union 2001). Using a simple grassland model, Calanca and Fuhrer (2005) showed that grassland productivity could benefit in the future from moderately increased temperatures,

higher radiation, and elevated CO_2. But if changes in the thermal and hydrological conditions were more pronounced and similar to the conditions in 2003, grassland production could become strongly water-limited. The authors estimated that the costs for setting up fixed irrigation systems for the entire grassland area of Switzerland would amount to 0.3 billion Swiss Francs annually, which is substantial but still a reasonable amount when compared to the present value of grassland production. Alternatively, fodder imports would be necessary from regions with more favorable conditions.

Effects of drought include not only decreased productivity, but also declining quality resulting from the formation of gaps in the sward, which can be colonized by weeds (cf. Lüscher et al. 2005); in turn, this has negative implications for animal nutrition. While in managed systems this effect can be addressed by farmers' interventions such as re-seeding, in semi-natural grasslands with little or no influence of management natural re-colonization following perturbation by drought is considered a primary driver of vegetation dynamics. A study by Stampfli and Zeiter (2004) in southern Switzerland (Ticino) confirmed that more frequent droughts might drive grassland vegetation changes with local colonization and extinction, as suggested earlier by Grime et al. (1994). Hence, increased frequency of drought has important economic effects in productive grassland systems and ecologically relevant effects in semi-natural systems.

4 Implications of climate extremes for forests

4.1 Wind storms

Storm is considered the most important natural disturbance agent in European forests. It is responsible for one third of total unplanned fellings (Brassel and Brändli 1999). Since 1868 European forests were impacted at least 16 times by the effects of several severe storms (Schelhaas et al. 2003), and 10 times since the early 1950s with windthrow of over 20 million m³; damages in 1990 and 1999 were by far the worst of all these years (UN/ECE Timber Committee 2000). Apparently, windthrow damage in Europe has increased in the past century; yet, loss of timber was typically smaller than annual timber harvests (Schelhaas et al. 2003). An exception was storm 'Lothar' in 1999, which was among the four most extreme events since 1500 (Pfister 1999) and threw 12.7×10^6 m³ in Switzerland, which is equivalent to 2.8 times the average annual timber harvest (e.g. Dobbertin et al. 2002). Wind velocities on top of the Jura Mountains near Geneva exceeded 200 km h⁻¹, and in other areas of Switzerland winds were measured at 240 km h⁻¹. The total amount of damage was estimated at more than 750 million Swiss Francs, plus another 38 million due to damages to individual trees and fruit trees (WSL/BUWAL 1999). Because of the large spatial extent, the abundance of windthrown timber affected the European market: roundwood markets were temporarily in chaos after the 'Lothar' event, with sharply falling prices (UN/ECE Timber Committee 2000). Similar to the effects of storms in 1990 on markets for wood products, fluctuations in supply and price were absorbed during primary processing and there were little distinguishable effects in prices or sales for sawn wood, panels and pulp. Greater market calamity was mitigated through sector solidarity.

Besides the loss of timber, windthrow can also have positive ecological effects (Schönenberger 2001), but where damage levels exceed harvesting or salvage harvesting costs are high, e.g. in mountainous terrain, adverse effects of wind storms outweigh any positive ones resulting from wood utilization (Widmer et al. 2004). As it dries, the wind-blown wood presents ideal conditions for massive fires and insect outbreaks, thus threatening
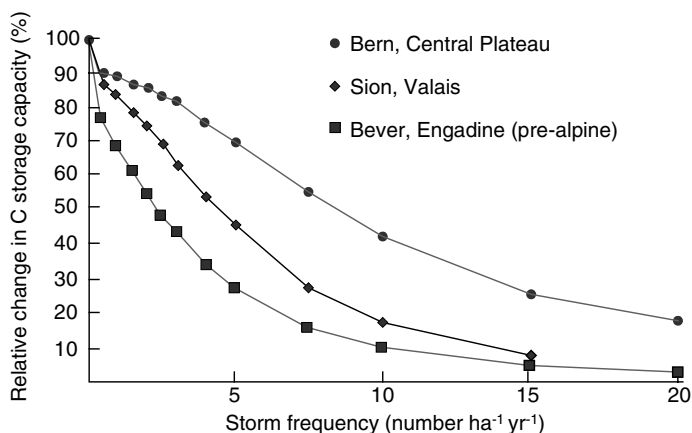
Fig. 9 Change in average carbon storage capacity (t C ha^{-1}) of young to middle-aged stands in relation to increasing frequency of storms (number of storm events ha^{-1} yr^{-1}) simulated by FORCLIM 2.6–4.0 for selected Swiss sites (Bern - Swiss Plateau, Bever - Subalpine Upper Engadine, Sion – Rhône Valley)

forests not affected by the storms themselves. More frequent disturbance by windthrow can also have long-term consequences. To quantitatively assess effects of changed storm frequency on species composition and C stocks, the FORCLIM model (Fischlin et al. 1995; Bugmann 1996) was used to simulate impacts on forest structure and maximum C-stocks. The most recent FORCLIM version 2.6–4.0 features (i) a refined response to climatic drivers, notably their variability, supporting the simulation of transient forest responses in a physically and ecologically consistent manner (based on work by Gyalistras 1997; Gyalistras and Fischlin 1999), (ii) an improved carbon cycle submodel simulating litter and soil carbon derived from Perruchoud et al. (1999), and (iii) a submodel simulating disturbances (fire, storms, avalanches, rockfall, landslides, and insect damage), derived from Mäder (1999). FORCLIM 2.6–4.0 was forced with several levels of storm frequencies, assuming an exponentially distributed storm severity up to those of 'Vivian' and 'Lothar'. The frequency in terms of events per year and surface area was gradually increased from 0 up to a maximum of 20 times the historical base line estimate (Schmidtke 1997; Schelhaas et al. 2003; Jungo et al. 2002). The results shown in Figure 9 demonstrate that even a small increase in storm frequency can lead to significant impacts of considerable economic relevance in the short-term, similar to the ones caused by the storm 'Lothar', and a long-term reduction in C stock. Diversity might increase, as long as the frequency of disturbance remains at the moderate levels projected by the storm scenarios (not shown). At the sub-alpine site Bever in the Upper Engadine an increase by only 7% appears to be sufficient to significantly reduce forest C stocks over a 1000-year simulation period. This is in contrast to results obtained for a 40-year period with the forest scenario model MASSIMO and the soil C model YASSO showing that an increase in storm frequency by 30% has only a small impact on the national C budget of forests (Thürig et al. 2005). The discrepancy between the two studies suggests that longer time periods need to be considered to detect the effects of changes in storm frequency and possibly other disturbances on forests.

Storm damage to forests depends not only on storm frequency and intensity, but also on the topography of the site, the specific properties of the stand, and the site conditions (cf. Mayer 1989; BUWAL 2005). Based on the experience gained from the storms 'Vivian' and 'Lothar', monocultures of coniferous species are more sensitive than those of deciduous

species (BUWAL 2005), and stands with a high fraction of coniferous trees and high average breast height-diameter seem to be most vulnerable (Dobbertin et al. 2002). Thus, from an economic point of view, windstorms are of particular importance because older trees with a higher value are preferentially affected, as opposed to the probability of damage from drought or snow, which is high for young stands and gradually decreases with age (Kuboyama and Oka 2000). The data for damage by 'Lothar' underline the importance of stand composition in determining storm risks, which can be addressed by silvicultural measures (BUWAL 2005). Finally, the chemical environment influences the risk of windthrow (BUWAL 2005). Data for beech (*Fagus sylvatica* L.) and spruce (*Picea abies* L.) suggested that uprooting after 'Lothar' was inversely related to soil base saturation. In beech stands, the latter was positively related to nitrogen concentrations in foliage, thus indicating that the sensitivity of trees to storm could be highest at sites with acid soils and receiving high atmospheric nitrogen inputs (Braun et al. 2003).

4.2 Heat waves and droughts

The immediate response of trees to dry spells such as the one in 2003 can be documented by site-specific physiological measurements. A survey of net ecosystem C fluxes revealed that the extreme conditions pushed many forest ecosystems from being a net C sink to being a net C source (Ciais et al. 2005). Thus, heat waves can affect the regional terrestrial C balance and, through an increase in net CO_2 emission, cause a biological feedback to the climate system (e.g., Fischlin 1997). However, data from a 100-year-old mixed deciduous forest near Basel suggested that several tree species investigated, particularly oak (*Quercus petraea* (Matt.) Liebl.), did not experience severe water stress at this site in 2003 (Leuzinger et al. 2005). Although mean stomatal conductance and rates of maximum net photosynthesis decreased considerably in mid-August across all species, daily peak values of sap flow remained surprisingly constant in oak over the whole period, and it decreased to only about half of the early summer maxima in beech and European hornbeam (*Carpinus betulus* L). Elevated CO_2 had only a minor effect on the water status of the trees. Compared to the previous year, leaf longevity was greater in 2003, but the seasonal increase in stem basal area reached only about 75%. Consequently, more frequent exceptionally dry summers could have a more serious impact at this site than a single event and would give oak trees a competitive advantage.

In the long run, a change in the frequency of hot any dry years could affect tree species composition and diversity in Swiss forests (Keller et al. 2002). Simulations using FORCLIM 2.6–4.0 demonstrated significant changes in species dominance over time in a mixed deciduous forest on the Swiss Plateau currently dominated by European beech (Figure 10). The climate change scenarios in this application implied that by ∼2080 every second summer would be as warm or warmer than in 2003 (Schär et al. 2004). Not surprisingly, the forest established under the new climate is typical of xeric conditions with the dominance of more drought-tolerant species such as oak (*Q. robur* L.) and chestnut (*Castanea sativa* MILL.). This change in species dominance was more pronounced than found earlier in simulations with scenarios characterized by less frequent extremes (Fischlin and Gyalistras 1997; Lischke et al. 1998), thus suggesting that more frequent extremes accelerates species replacement. The scenario also caused a transitory loss of C towards the end of this century, which was only fully compensated for by the end of the 23rd century.

These simulation results are corroborated by recent experimental and observational evidence. Drought stress is thought to be a frequent cause for tree defoliation, but effects of dry years on forests are lagged. Consequences of an occasional extremely warm and dry year
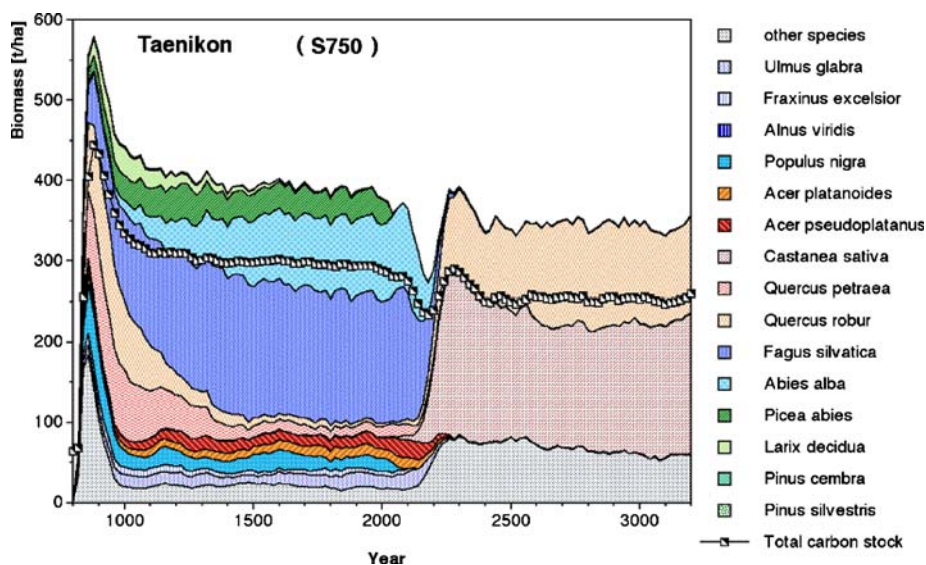
Fig. 10 Long-term changes in tree species composition (t biomass ha^{-1}) of a deciduous forest dominated by European beech in response to climate change. Transient simulations with FORCLIM 2.6–4.0 for the mesic site Taenikon on the Swiss Plateau. The initial start-up phase begins in year 800 under base-line climate (Gyalistras 2003). Superimposed is a climate change sensitivity derived by statistical downscaling from a HADCM3 (SRES A2) run for the means. Estimates of changes in the variances of temperature and precipitation for present (1970–2000) and future (2070–2100) were derived from Schär et al. (2004). The S750 stabilization scenario (Houghton et al. 1995) was used to compute the actual transient climate change scenario by the method of Gyalistras and Fischlin (1999).

can usually be observed only during the subsequent year(s). For instance, crown condition inventories in Bavaria revealed increased needle and leaf loss across all species in 2004 as a result of the 2003 summer (LWF 2004); beech and oak (*Q. spp.*) were most strongly affected, while deep-rooting species such as silver fir (*Abies alba* MILL.) were less affected. Both broadleaved and coniferous species reacted to the conditions of the previous year with sprouting in 2004. A statistical analysis of temporal relations across Swiss forests by Zierl (2004) revealed significant impacts of drought on crown conditions for all deciduous tree species under consideration, i.e. beech, fir, European ash (*Fraxinus excelsior* L.), and oak, but only weak correlations were found for spruce and no relations were found for fir and Scots pine (*Pinus sylvestris* L.). In the largest inner-alpine valley of Switzerland (Valais), defoliation and mortality in Scots pine observed in each year during 1996–2002 was related to the precipitation deficit and hot conditions of the previous year (Rebetez and Dobbertin 2004). These authors suggested that an increase in the frequency of warm years could be critical for ecosystems with Scots pine as the dominant species. Warm and dry years may also favor insect calamities of economic relevance (e.g., bark beetle infestations; Wermelinger and Seifert 1999) in areas with increased amounts of dead or damaged wood. Finally, lack of precipitation together with high temperatures alters the disturbance regime by forest fires. Today, forest fires are already a serious threat in southern Switzerland, and for this region Reinhard et al. (2005) reported an increasing trend over the past 32 years in most climatic variables favoring forest fires; with increasing drought frequency, this problem may spread to regions north of the Alps.

5 Discussion and conclusions

Extreme events, i.e., extremely rare climatic events under current conditions, have potentially great impacts on ecological, economic and social systems, with a strong interdependence between them. In many regions of Europe, ecosystems play an important role in providing goods and services to the society; in Switzerland, agricultural production systems cover about 60% of domestic consumption, and the value of annual production is roughly 7 billion Swiss Francs. Together with forests, agroecosystems improve the livelihood and aesthetic value of rural landscapes. Forests cover about 28% of the land surface and provide 4.5 million m^3 of timber annually, and the forestry sector offers about 85,000 jobs, equivalent to 3.1% of the total workforce. In pre-alpine and alpine regions forests are of vital relevance by protecting settlements, roads and other infrastructures from avalanches and landslides. Moreover, forests have a high ecological conservation value, similar to semi-natural grasslands and wetlands, since they harbor about 50% of all species occurring in Switzerland, they play an important role in the cycling of water and nutrients at the watershed level, and they act as large-scale C sinks. Finally, a recent study estimated the economic value of Swiss forests for recreational uses alone at 10.5 billion Swiss Francs per year (about 2.4% of GDP, Ott and Baur 2005). Hence, negative effects of climate extremes on agriculture and forests are relevant, and increasing frequencies would create considerable strain on the society to maintain their goods and services. Effects of past isolated extreme events on Swiss agriculture and forests are well documented, but the analysis presented here shows that there is growing evidence for an increasing likelihood of climatic extremes. Effects of individual events could overlap with the recovery process from previous events, thus mutually augmenting the detrimental impacts upon the system concerned.

The assessment of climate risks depends on both the skills to simulate these events at various scales, and the understanding of the responses of the target system. One of the major advances made recently in projecting climate risks concerns the improvement in linking the larger-scale climate simulation to small-scale effects. Extreme events are often related to large-scale synoptic conditions, but the scales at which impacts occur can vary from local to regional. For instance, large-scale continental storms can generate strong winds and gusts, which are most damaging at very small scales of a few km^2 down to a few hectares. Thus, physically consistent downscaling is an important and challenging task, but it is highly relevant to assess future climate risks at the scales at which societal responses take place. This is of particular relevance in regions with a complex terrain such as that of the European Alps. The work summarized here documents the advancement in these skills, and the progress made in linking extremes to global change scenarios. Smaller-scale patterns still vary considerably between RCMs, but current RCM integrations provide quantitative scenarios of the regional future change, which are valuable for examining possible impact mechanisms, until more formal regional probabilistic scenarios become available.

The review shows that already during the 20th century, the likelihood for extremes has increased. Instrumental data reveal remarkable changes in precipitation characteristics in central Europe, which are difficult to explain by changes in the large-scale circulation alone (Widmann and Schär 1997; Hanssen-Bauer and Forland 2000; Schmith 2000). Clearly, the uncertainty attached to future scenarios of precipitation extremes remains large, and sufficiently long RCM simulations exist for only a small set of GCM boundary conditions, but there is considerable agreement for an increase in wintertime precipitation extremes, and physical arguments have been advanced to explain this tendency (e.g., Trenberth 1999). Episodes that inflict catastrophic flooding may increase with climate warming, in spite of less summertime precipitation (Christensen and Christensen 2002; Allen and Ingram 2002).

For agriculture, the projected increase in the frequency of heavy rainfall during winter and spring may cause a considerable loss of topsoil from croplands, particularly in areas with sloped terrain such as the pre-alpine and alpine regions of Switzerland, and in the presence of inappropriate cultivation practices, soil compaction, overgrazing, or construction (Grimm et al. 2002). This type of risk can be mitigated effectively by taking measures to cover and protect the soil surface, for instance by avoiding fallow periods, intercropping, or application of conservation tillage or no-till. Such measures can be implemented quickly and at low costs. In addition, larger amounts of winter precipitation could cause excess soil moisture during the early part of the growing season, which could delay fieldwork, as suggested by Rosenzweig et al. (2002); however, the results for Switzerland suggest that related risks are reduced to some extent by more rapid soil drying in the warmer climate. Hence, in this region and in other pre-alpine and alpine areas of Europe, the potential of agriculture may be sufficiently large to cope with the exposure of cropland to more frequent intense precipitation.

The more serious threat relates to the projected scarcity of soil water during the growing season (Jasper et al. 2004). Crops currently cultivated in Switzerland have been selected for cultivation in temperate, humid conditions. Thus, their sensitivity to precipitation deficits during the main growing season is high, as demonstrated by the yield losses in the most affected areas in 2003. Currently, in the absence of any insurance system for crop losses due to drought, measures taken by the Federal administration are necessary to alleviate economic losses of individual farmers. However, the consequences of more frequent situations like in 2003 would weigh heavily on agriculture. Increasing return times of droughts could exceed the financial capacities for government interventions. Consequently, adaptive measures would be necessary to avoid or to cope with drought risks, including altered crop and cultivar selection, improved nutrient and water management at the local and regional scale, or increased storage of fodder. However, such measures would require long-term planning and investments (e.g., irrigation equipment).

Main effects of climate extremes on pre-alpine and alpine forests include short-term loss of timber due to windstorms, and drought effects on tree vitality, as well as long-term effects on services such as biodiversity, C sequestration, soil and water conservation, and protection. Increasing storm frequency would have immediate economic implications for the forest owners and the lumber industry, as observed after 'Lothar' in 1999, but the effects on many forests may take place during century-long phases of drastic changes before new and more stable phases can be reached again. More frequent periods of droughts would affect forest health and succession, as already observed in the dry Valais, and long-term simulations show how species replacement could alter several services. Environmental stresses such as drought are supposed to be predisposing mechanisms of forest decline by making trees more vulnerable to damaging agents such as fungal disease insects (cf. Zierl 2004). A concurrent increase in storm frequency and dry spells could accelerate species replacement taking place in response to a gradual increase in mean temperature. Thus, suitable management of forests over the typical time horizon of decades could become a crucial challenge. It may require measures such as selective tree harvesting and repeated re-planting of sensitive seedlings, regardless of how well-adapted they might be as adults under the then altered climatic conditions, or reforestation of stands or even entire forest districts. To cope with increased risks of windthrow, management of the species composition of forest stands, proper thinning, and maintenance of optimal soil physical and chemical properties would also be essential measures (BUWAL 2005).

In conclusion, projections emerging from the improved understanding of the evolution of the global climate system and of the resulting regional aspects show that what lies ahead may well exceed past risks. There is now better evidence for an increasing likelihood of extreme precipitation and windstorms during winter, or heat waves during summer, with an improved

spatial resolution of these projections for the Alpine region. More frequent extremes are likely to be at least as important, if not more important than a gradual change in climate, and this will affect both agricultural systems and forests in Switzerland. This poses great challenges for society, and the lessons learned for instance in 1999 (storm 'Lothar') or 2003 (heat wave) should be given appropriate scientific and political consideration, particularly in view of the long replacement times of infrastructure ($\sim$30 yrs), land-use ($\sim$decadal), or the long response times of forests growth ($\sim$50–100 yrs), succession (several hundred yrs), or soil formation (many centuries). To ignore the change in climatic risks may turn out to be increasingly difficult, and adaptation to become more costly. To secure ecosystem goods and services within the limits set by biophysical, economic and societal constraints, shifts in agricultural and silvicultural practices, new insurance schemes, or investments in preventive measures will be necessary. However, some indirect consequences may remain for the socio-economic development, and for the esthetic value of the landscape in pre-alpine and alpine regions.

References

Alexandersson H, Tuomenvirta H, Schmith T, Iden K (2000) Trends of storms in NW Europe derived from an updated pressure data set. Clim Res 14:71–73

Allen MR, Ingram WJ (2002) Constraints on future changes in climate and the hydrologic cycle. Nature 419:224–232

Beniston M (2004a) The 2003 heat wave in Europe. A shape of things to come? Geophys Res Lett 31:2022–2026

Beniston M (2004b) Climatic change and its impacts – an overview focusing on Switzerland. Advances in global change research, vol. 19. Kluwer Academic Publisher, Dordrecht, p 297

Beniston M, Stephenson DB (2004) Extreme climatic events and their evolution in a changing climatic conditions. Global Planet Change 44:1–9

Brassel P, Brändli UB (eds) (1999) Schweizerisches Landesforstinventar: Ergebnisse der Zweitaufnahme 1993–1995. Eidgenössische Forschungsanstalt für Wald, Schnee und Landschaft (WSL), Birmensdorf and Bundesamt für Umwelt, Wald und Landschaft, Bern, Verlag Haupt, Bern, Switzerland, p 442

Braun S, Schindler C, Volz R, Flückiger W (2003) Forest damages by the storm 'Lothar' in permanent observation plots in Switzerland: the significance of soil acidification and nitrogen deposition. Water Air Soil Pollut 142:327–340

Buffoni L, Maugeri M, Nanni T (1999) Precipitation in Italy from 1833 to 1996. Theor Appl Climatol 63:33–40

Bugmann HKM (1996) A simplified forest model to study species composition along climate gradients. Ecology 77:2055–2074

Bush, MB, Silman MR, Urrego DH (2004) 48,000 years of climate and forest change in a biodiversity hot spot. Science 303:827–829

BUWAL (2005) Lothar – Ursächliche Zusammenhänge und Risikoentwicklung. Umwelt-Materialien Nr. 184, Swiss Federal Office of Environment, Forest and Landscape, Bern, Switzerland, p 145

Calanca PL (2004) Interannual variability of summer mean soil moisture conditions in Switzerland during the 20th century: a look using a stochastic soil moisture model. Water Resour Res 40, doi: 10.1029/2004WR003254

Calanca PL (2006) Climate change and drought occurrence in the Alpine region: how severe are becoming extremes? Global Planetary Change, in press

Calanca PL, Fuhrer J (2005) Swiss agriculture in a changing climate: grassland production and its economic value. In: Haurie A, Viguier L (eds) The coupling of climate and economic dynamics – essays on integrated assessment, advances in global change research, vol. 22. Springer, Dordrecht, NL, pp 341–353

Calanca PL, Roesch A, Jasper K, Wild M (2006) Global warming and the summertime evapotranspiration regime of the Alpine region. Clim Change, (this issue) DOI 10.1007/s10584-006-9103-9

Carnell RE, Senior, CA (1998) Changes in mid-latitude variability due to increasing greenhouse gases and sulphate aerosols. Clim Dyn 14:369–383

Caya D, Laprise R (1999) A semi-implicit semi Lagrangian regional climate model: the Canadian RCM. Mon. Weather Rev 127:341–362

Christensen JH, Carter TR, Giorgi F (2002) PRUDENCE employs new methods to assess European climate change. EOS 83:147

Christensen JH, Christensen OB (2003) Severe summertime flooding in Europe. Nature 421:805–806

Christensen OB, Christensen JH, Machenhauer B, Botzet, M (1998) Very high-resolution regional climate simulations over Scandinavia – present climate. J Clim 11:3204–3229

Ciais Ph, Ciais Reichstein M, Viovy N, Granier A Ogée J, Allard V, Buchmann N, Aubinet M, Bernhofer Chr, Carrara A, Chevallier F, De Noblet D, Friend A, Friedlingstein P, Grünwald T, Heinesch B, Keronen P, Knohl A, Krinner G, Loustau D, Manca G, Matteucci G, Miglietta F, Ourcival JM, Pilegaard K, Rambal S, Seufert G, Soussana JF, Sanz MJ, Schulze ED Vesala T, Valentini R (2005) European-wide reduction in primary productivity caused by the heat and drought in 2003. Nature 437:529–533

Dale, VH, Joyce LA, McNulty S, Neilson RP, Ayres MP, Flannigan MD, Hanson PJ, Irland LC, Lugo AE, Peterson CJ, Simberloff D, Swanson FJ, Stocks BJ, Wotton BM (2001) Climate change and forest disturbances. Bioscience 51:723–734

Dobbertin M, Seifert H, Schwyzer A (2002) Standort und Bestandesaufbau waren mitentscheidend für das Ausmass der Sturmschäden. Wald und Holz 83:39–42

Dorland C, Tol RSJ, Palutikov JP (1999) Vulnerability of the Netherlands and Northwest Europe to storm damage under climate change. Clim Change 43:513–535

Durman CF, Gregory JM, Hassell DC, Jones RG, Murphy JM (2001) A comparison of extreme European daily precipitation simulated by a global and a regional climate model for present and future climates. Quat J Roy Meteorol Soc 127:1005–1015

Esteban-Parra MJ, Rodrigo FS, Castro-Diez Y (1998) Spatial and temporal patterns of precipitation in Spain for the period 1880–1992. Int J Climatol 18:1557–1574

FAT (1996) Wetterrisiko und verfügbare Feldarbeitstage in der Schweiz. FAT-Berichte 490: Swiss Federal Research Station for Agricultural Economy and Engineering, Tänikon, Switzerland, p 5

Fischlin A (1997) Biospheric feedbacks in the global climate system. J Environ Qual 26:2

Fischlin A, Bugmann H, Gyalistras D (1995) Sensitivity of a forest ecosystem model to climate parameterization schemes. Environ Pollut 87:267–282

Fischlin A, Gyalistras D (1997) Assessing impacts of climatic change on forests in the Alps. Global Ecol Biogeogr Lett 6:19–37

Frei C, Christensen JH, Déqué M, Jacob D, Jones RG, Vidale PL (2003) Daily precipitation statistics in regional climate models: evaluation and intercomparison for the European Alps. J Geophys Res 108(D3):4124, doi: 10.1029/2002JD002287

Frei C, Davies HC, Gurtz J, Schär C (2001) Climate dynamics and extreme precipitation and flood events in Central Europe. Integr Assessm 1:281–299

Frei C, Schär C (1998) A precipitation climatology of the Alps from high-resolution rain-gauge observations. Int J Climatol 18:873–900

Frei C, Schär C (2001) Detection probability of trends in rare events: theory and application to heavy precipitation in the Alpine region. J Clim 14:1568–1584

Frei C, Schöll R, Schmidli J, Fukutome S, Vidale PL (2006) Future change of precipitation extremes in Europe: an intercomparison of scenarios from regional climate models. J Geophys Res 111, D06105, doi: 10.1029/2005JD005965

Giorgi F, Hewitson B, et al. (2001) Regional climate information – evaluation and projections. In: Climate change 2001. The scientific basis. The Third Assessment Report of the Intergovernmental Panel on Climate Change (IPCC), pp 581–638

Goyette S, Beniston M, Caya D, Laprise JPR, Jungo P (2001) Numerical investigation of an extreme storm with the Canadian Regional Climate Model: the case study of windstorm 'VIVIAN', Switzerland, February 27, 1990. Clim Dyn 18:145–178

Goyette S, Brasseur O, Beniston M (2003) Application of a new wind gust parameterisation. Multi-scale case studies performed with the Canadian RCM. J Geophys Res 108:4374–4390

Grebner D, Roesch T (1999) Zusammenhänge und Beurteilung der Hochwasserperiode in der Schweiz vom 11. bis 15. Mai 1999. Wasser, Energie, Luft 5/6:127–132

Grime JP, Willis AJ, Hunt R, Dunnett NP (1994) Climate-vegetation relationships in the Bibury road verge experiments. In: Leigh RA, Johnston AE (eds) Long-term experiments in agricultural and ecological sciences. CAB International, Wallingford, UK, pp 271–285

Grimm M, Jones RJA, Montanarella L (2002) Soil erosion risk in Europe. Report EUR 19939 EN, Office for Official Publications of the European Communities. Luxemburg, p 40

Gyalistras D (1997) Projecting scenarios of climatic change and future weather for ecosystem models: derivation of methods and their application to forests in the Alps. PhD Dissertation ETH No. 12065, Swiss Federal Institute of Technology: Zürich, Switzerland, p 103

Gyalistras D (2003) Development and validation of a high-resolution monthly gridded temperature and precipitation data set for Switzerland (1951–2000). Clim Res 25:55–83

Gyalistras D, Fischlin A (1999) Towards a general method to construct regional climatic scenarios for model-based impacts assessments. Petermanns Geogr Mitt 143:251–264

Gyalistras D, Fischlin A, Riedo M (1997) Herleitung stündlicher Wetterszenarien unter zukünftigen Klimabedingungen. In: Fuhrer J (ed), Klimaänderung und Grünland, Vdf Hochschulverlag AG and der ETH Zurich, Zurich, pp 207–276

Gyalistras D, von Storch H, Fischlin A, Beniston M (1994) Linking GCM-simulated climatic changes to ecosystem models: case studies of statistical downscaling in the Alps. Clim Res 4:167–189

Hall NMJ, Hoskins BJP, Valdes J, Senior CA (1994) Storm tracks in a high-resolution GCM with doubled carbon dioxide. Quart J Roy Meteor Soc 120:1209–1230

Hanssen-Bauer I, Forland EJ (2000) Long-term trends in precipitation and temperature in the Norwegian Arctic: can they be explained by changes in atmospheric circulation patterns? Clim Res 10:143–153

Hanson CE, Palutikov JP, Davies TD (2004) Objective cyclone climatologies of the North Atlantic-a comparison between the ECMWF and NCEP reanalyses. Clim Dyn 22:757–769

Haylock MR, Goodess CM (2004) Interannual variability of extreme European winter rainfall and links with mean large-scale circulation. Int J Climatol 24:759–776

Heino R, Brázdil R, FØrland E, Tuomenvirta H, Alexandersson H, Beniston M, Held C, IM (1999) Large-scale dynamics and global warming. Bull Amer Meteor Soc 74:228–241

Houghton JT, Meira Filho LG, Bruce J, Lee H, Callander BA, Haites E, Harris N, Maskell K (eds) (1995) Climate change 1994: Radiative forcing of climate change and an evaluation of the IPCC IS92 emission scenarios. Reports of Working Groups I and III of the Intergovernmental Panel on Climate Change (IPCC), forming part of the IPPC Special Report to the first session of the Conference of the Parties to the UN Framework Convention on Climate Change. Cambridge University Press, Cambridge, p 339

Huntingford C, Jones RG, Prudhomme C, Lamb R, Gash HHC, Jones DA (2003) Regional climate-model predictions of extreme rainfall for a changing climate. Quart J Roy Meteorol Soc 129:1607–1621

IPCC (2001) In: Houghton JT, Ding DJ, Griggs DJ, Noguer M, van der Linden PJ, Xiasou D (eds), Climate change 2001. The scientific basis. Cambridge University Press, Cambridge and New York, p 944

Jasper K, Calanca PL, Gyalistras D, Fuhrer J (2004) Differential impacts of climate change on the hydrology of two alpine river basis. Clim Res 26:113–129

Jasper K, Calanca PL, Fuhrer J (2006) Changes in summertime soil water patterns in complex terrain due to climatic change. J Hydrology 327:550–563

Jones R, Murphy J Hassell D, Taylor R (2001) Ensemble mean changes in a simulation of the European climate of 2071–2100, using the new Hadley Centre regional climate modelling system HadAM3H/HadRM3H. Hadley Centre Report 2001, available from www.prudence.dmi.dk (accessed 10/06/2005)

Jungo P, Goyette S, Beniston M (2002) Daily wind gust speed probabilities over Switzerland according to three types of synoptic circulation. Int J Climatol 22:485–499

Kalnay E, Kanamitsu M, Kistler R, Collins W, Deaven D, Gandin L, Iredell M, Saha S, White G, Woollen J, Zhu Y, Leetmaa A, Reynolds B, Chelliah M, Ebisuzaki W, Higgins W, Janowiak J, Mo KC, Ropelewski C, Wang J, Jenne Roy, Joseph Dennis (1996) The NCEP/NCAR 40-year reanalysis project. Bull Am Meteorol Soc 77:437–472

Keller F, Fuhrer J (2004) Landwirtschaft im Hitzesommer 2003. Swiss Agric Res 11:403–410

Keller F, Lischke H, Mathis T, Möhl A, Wick L, Ammann B, Kienast F (2002) Effects of climate, fire, and humans on forest dynamics: forest simulations compared to the paleological record. Ecol Model 152:109–127

Klein Tank AMG, Können GP (2003) Trends in indices of daily temperature and precipitation extremes in Europe, 1946–1999. J Clim 16:3665–3680

Kleinn J (2002) 'Climate change and runoff statistics in the Rhine basin: a process study with a coupled climate-runoff model', Doctor of Natural Sciences Thesis Dissertation No. 14663, Swiss Federal Institute of Technology, Zurich, p 114

Kleinn J, Frei C, Gurtz J, Lüthi D, Vidale PL, Schär C (2005) Hydrological simulations in the Rhine basin, driven by a regional climate model. J Geophys Res 110:D04102, doi: 10.1029/2004JD005143

Knippertz P, Ulbrich U, Speth P (2000) Changing cyclones and surface wind speeds over the North Atlantic and Europe in a transient GHG experiment. Clim Res 15:109–122

Kuboyama H, Oka H (2000) Climate risks and age-related damage probabilities – effects on the economically optimal rotation length for forest stand management in Japan. Silva Fenn 34:155–166

Lambert S, Sheng J, Boyle J (2002) Winter cyclone frequencies in thirteen models participating in the Atmospheric Model Intercomparison Project (AMIP 1). Clim Dyn 19:1–16

Leckebusch GC, Ulbrich U (2004) On the relationship between cyclones and extreme windstorm events over Europe under climate change. Global Planet Change 44:181–193

Leuzinger S, Zotz G, Asshoff R, Körner C (2005) Responses of deciduous forest trees to severe drought in Central Europe. Tree Physiol 25:641–650

Lischke H, Guisan A, Fischlin A, Williams J, Bugmann H (1998) Vegetation responses to climate change in the Alps: modeling studies. In: Cebon P, Dahinden U, Davies HC, Imboden DM, Jäger CC (eds), Views from the Alps: regional perspectives on climate change. MIT Press, Boston, Massachusetts, pp 309–350

Lüscher A, Fuhrer J, Newton PCD (2005) Global atmospheric change and its effect on managed grassland systems. In: McGolloway DC (ed), Grassland – a global resource. Wageningen Academic Publishers, pp 251–264

LWF (2004) Waldzustandsbericht 2004. Bayrisches Staatsministerium für Landwirtschaft und Forsten. http://www.lwf.bayern.de/ (accessed 10/06/2005)

Mäder J (1999) Effekte externer Störungen auf den Sukzessionslauf subalpiner Wälder: Modellierung und Analyse. Master of Environmental Sciences Thesis, Institute of Terrestrial Ecology, Swiss Federal Institute of Technology, Zurich, p 62

Mayer H (1989) Windthrow. Phil Trans R Soc Lond B 324:267–181

McCabe G J, Clark MP, Serreze M (2001) Trends in northern hemisphere surface cyclone frequency and intensity. J Clim 14:2763–2768

McCallum E, Norris WJT (1990) The storms of January and February 1990. Meteorol Mag 119:201–210

Mearns LO, Giorgi F, Whetton P, Pabon D, Hulme M, Lal M (2003) Guidelines for use of climate scenarios developed from Regional Climate Model experiments. Technical Report. The IPCC Data Distribution Centre, Norwich, UK, p 38

Meehl GA, Karl T, Easterling DR, Changnon S, Pielke R, Changnon D, Evans J, Groisman PY, Knutson TR, Kunkel KE, Mearns LO, Parmesan C, Pulwarty R, Root T, Sylves RT, Whetton P, Zwiers F (2000) An introduction to trends in extreme weather and climate events: observations, socioeconomic impacts, terrestrial ecological impacts, and model projections. Bull Am Soc Meteorol 81:413–416

Nakićenović N, Alcamo J, Davis G, de Vries B, Fenhann J, Gaffin S, Gregory K, Grübler A, Jung TY, Kram T, La Rovere EL, Michaelis L, Mori S, Morita T, Pepper W, Pitcher H, Price L, Raihi K, Roehrl A, Rogner HH, Sankovski A, Schlesinger M, Shukla P, Smith S, Swart R, van Rooijen S, Victor N, Dadi Z (2000) IPCC special report on emissions scenarios. Cambridge University Press, Cambridge and New York, p 599

Noguer M, Jones RG, Murphy JM (1998) Sources of systematic errors in the climatology of a regional climate model over Europe. Clim Dyn 14:691–712

OcCC (2003) Extremereignisse und Klimaänderung, Organe Consultatif sur lse Changements climatiques, Bern, Switzerland, p 88

Osborn TJ, Hulme M, Jones PD, TA Basnett (2000) Observed trends in the daily intensity of United Kingdom precipitation. Int J Climatol 20:347–364

Ott W, Baur M (2005) Der monetäre Erholungswert des Waldes, Umwelt-Materialien Nr. 193, Bundesamt für Umwelt, Wald und Landschaft (BUWAL), Bern, Switzerland, p 68

Pal JS, Giorgi F, Bi X (2004) Consistency of recent European summer precipitation trends and extremes with future regional climate projections. Geophys Res Lett 31:L13202, doi: 10.1029/2004GL019836

Palutikof JP, Brabson BB, Lister DH, Adcock ST (1999) A review of methods to calculate extreme wind speeds. Meteor Appl 6:119–132

Parmesan C, Root TL, Willing MR (2000) Impacts of extreme weather and climate on terrestrial biota. Bull Am Soc Meteorol 81:443–449

Parry ML (ed) (2000) Assessment of potential effects and adaptation for climate change in Europe: the Europe ACACIA project. Jackson Environment Institute, University of East Anglia, Norwich, UK, p 320

Perruchoud D, Joos F, Fischlin A, Hajdas I, Bonani G (1999) Evaluating time scales of carbon turnover in temperate forest soils with radiocarbon data. Global Biogeochem Cycle 13:555–573

Pfister C (1999) Wetternachhersage. 500 Jahre Klimavariationen und Naturkatastrophen 1496–1995. Verlag Paul Haupt, Bern, p 304

Pfister C (2004) Von Goldau nach Gondo. Naturkatastrophen als identitätsstiftende Ereignisse in der Schweiz des 19. Jahrhunderts. In: Pfister C, Summermatter S (eds) Katastrophen und ihre Bewältigung. Perspektiven und Positionen. Paul Haupt, Bern, Switzerland, pp 53–78

Pope DV, Gallani M, Rowntree R, Stratton A (2000) The impact of new physical parameterizations in the Hadley Centre climate model: HadAM3. Clim Dyn 16:123–146

Pruski FF, Nearing MA (2002) Runoff and soil-loss responses to changes in precipitation: a computer simulation study. J Soil Water Conserv 57:7–16

Räisänen J, Hannson U, Ullerstig A, Döscher R, Graham LP, Jones C, Meier HEM, Samuelsson P, Willén U (2004) European climate in the late twenty-first century: regional simulations with two global models and two forcing scenarios. Clim Dyn 22:13–31

Rebetez M, Dobberin M (2004) Climate change may already threaten Scots pine stands in the Swiss Alps. Theor Appl Climatol 79:1–9

Reinhard M, Rebetez M, Schlaepfer R (2005) Recent climate change: rethinking drought in the context of forest fire research in Ticino, South of Switzerland. Theor Appl Climatol, DOI 10.1007/s00704–005-0123-6

Riedo M, Gyalistras D, Fischlin A, Fuhrer J (1999) Using an ecosystem model linked to GCM-derived local weather scenarios to analyze effects of climate change and elevated CO_2 on dry matter production and partitioning, and water use in temperate managed grasslands. Global Change Biol 5:213–223

Rosenzweig C, Tubiello FN, Goldberg R, Mills E, Bloomfield J (2002) Increased crop damage in the US from excess precipitation under climate change. Global Environ Change 12:197–202

Schär C, Vidale PL, Lüthi D, Frei C, Häberli C, Liniger M, Appenzeller C (2004) The role of increasing temperature variability in European summer heat waves. Nature 427:332–336

Schelhaas MJ, Nabuurs GJ, Schuck A (2003) Natural disturbances in the European forests in the 19th and 20th centuries. Global Change Biol 9:1620–1633

Schmidli J, Frei C (2005) Trends of heavy precipitation and wet and dry spells in Switzerland during the 20th century. Int J Climatol 25:753–771

Schmidli J, Schmutz C, Frei C, Wanner H, Schär C (2002) Mesoscale precipitation in the Alps during the 20th century. Int J Climatol 22:1049–1074

Schmidtke H, Scherrer HU (1997) Sturmschäden im Wald. vdf Hochschulverlag AG an der ETH Zürich, Zurich, p 38

Schmith T (2000) Global warming signature in observed winter precipitation in Northwestern Europe. Clim Res 17:263–274

Schmith T, Kaas E, Li T-S (1998) Northeast Atlantic winter storminess 1875–1995 re-analysed. Clim Dyn 14:529–536

Schönenberger W (2001) Trends in mountain forest management in Switzerland. Schweiz Z Forstwes 152:152–156

Schönwiese C-DJ, Rapp T Fuchs, M Denhard (1994) Observed climate trends in Europe 1891–1990. Meteorol Zeitschrift N.F.3:22–28

Schorer M (1992) Extreme Trockensommer in der Schweiz und ihre Folgen für Natur und Wirtschaft. Geographica Bernensia G 40, Institute of Geography, University of Bern, p 192

Schubert M, Perlwitz J, Blender R, Fraedrich K, Lunkeit F (1998) North Atlantic cyclones in CO_2-induced warm climate simulations: frequency, intensity, and tracks. Clim Dyn 14:827–837

Schüepp M, Schiesser HH, Huntrieser H, Scherrer HU, Schmidtke H (1994) The winterstorm 'VIVIAN' of 27 February 1990: about the meteorological development, wind forces and damage situation in the forests of Switzerland. Theor Appl Climatol 49:183–200

Schulla J (1997) Hydrologische Modellierung von Flussgebieten zur Abschätzung der Folgen von Klimaänderungen, Zürcher Geographische Schriften 69: Swiss Federal Institute of Technology (ETH), Zürich, p 187

Stampfli A, Zeiter M (2004) Plant regeneration directs changes in grassland composition after extreme drought: a 13-year study in southern Switzerland. J Ecol 92:568–576

Stephenson DB, Held IM (1993) GCM response of Northern winter stationary waves and storm tracks to increasing amounts of carbon dioxide. J Clim 6:1859–1870

Swiss Federal Office of Agriculture (2003) Agrarbericht 2003. Bern, Switzerland

Thürig E, Palosuo T, Bucher J, Kaufmann E (2005) The impact of windthrow on carbon sequestration in Switzerland: a model-based assessment. Forest Ecol Manage 210:337–350

Trenberth KE (1999) Conceptual framework for changes of extremes of the hydrological cycle with climate change. Clim Change 42:327–339

UN/ECE Timber Committee (2000) Forest Products Annual Market Review 1999–2000. Timber Bulletin, Vol. LIII, ECE/TIM/BULL/53/3, United Nations, Geneva, Switzerland, p 228

Valleron A-J, Boumendil A (2004) Epidemillionlogy and heat waves: analysis of the 2003 episode in France. Compt Rend Biol 327:1125–1141

Vidale PL, Lüthi D, Frei C, Seneviratne S, Schär C (2003) Predictability and uncertainty in a Regional Climate Model. J Geophys Res 108(D18):4586, doi: 10.1029/2002JD002810

WASA Group (1998) Changing waves and storms in the north-east Atlantic? Bull Am Meteor Soc 79:741–760

Wermelinger B, Seifert M (1999) Temperature-dependent reproduction of the spruce bark beetle Ips typographus, and analysis of the potential population growth. Ecol Entomol 24:103–110

Wernli H, Dirren S, Liniger M A, Zillig M (2002) Dynamical aspects of the life cycle of the winter storm 'Lothar' (24–26 December 1999). Quart J Roy Meteor Soc 128:405–429

Widmer O, Said S, Miroir J, Duncan P, Gaillard JM, Klein F (2004) The effects of hurricane 'Lothar' on habitat use of roe deer. For Ecol Manage 195:237–242

Widmann M, Schär C (1997) A principal component and long-term trend analysis of daily precipitation in Switzerland. Int J Climatol 17:1333–1356

Wilby RL, Charles SP, Zorita E, Timbal B, Whetton P Mearns LO (2004) Guidelines for use of climate scenarios developed from statistical downscaling methods. Technical Report. The IPCC Data Distribution Centre, Norwich, UK, p 27

Wilby RL, Wigley TML, Conway D, Jones PD, Hewitson BC (1998) Statistical downscaling of general circulation model output: a comparison of methods. Water Resour Res 34:2995–3008

Williams AN, Nearing M, Habeck M, Southworth J, Pfeifer R, Doering OC, Lowenberg-Deboer J, Randolph JC, Mazzocc MA (2001) Global climate change: implications of extreme events for soil conservation strategies and crop production in the midwestern United States. In: Stott DE, Mohtar RH, Steinhardt GC (eds), Sustaining the global farm. Proceedings of the 10th international soil conservation organization meeting, Purdue University, West Lafayette, pp 509–515

WSL/BUWAL (1999) Lothar. Der Orkan (1999) Ereignisanalyse. Eidg. Forschungsanstalt WSL und Bundesamt für Umwelt, Wald und Landschaft BUWAL (Hrsg.), 2001, Birmensdorf, Bern, p 391

Xoplaki E, Gonzalez-Rouco JF, Luterbacher J Wanner H (2004) Wet season Mediterranean precipitation variability: influence of large-scale dynamics and trends. Clim Dyn 23:63–78

Xoplaki E, Luterbacher J, Burkard R, Patrikas I, Maheras P (2000) Connection between the large-scale 500 hPa geopotential height fields and precipitation over Greece during wintertime. Clim Res 14:129–146

Zhang X-C, Nearing MA, Garbrecht JD, Steiner JL (2004) Downscaling monthly forecasts to simulate impacts of climate change on soil erosion and wheat production. Soil Sci Soc Am J 68:1376–1385

Zwiers FW, Kharin VV (1998) Changes in the extremes of the climate simulated by CCC GCM2 under CO_2 doubling. J Clim 11:2200–2222

Zierl B (2004) A simulation study to analyse the relations between crown condition and drought in Switzerland. For Ecol Manage 188:25–38

The coupling of optimal economic growth and climate dynamics

**Olivier Bahn · Laurent Drouet · Neil R. Edwards ·
Alain Haurie · Reto Knutti · Socrates Kypreos ·
Thomas F. Stocker · Jean-Philippe Vial**

Abstract In this paper, we study optimal economic growth programs coupled with climate change dynamics. The study is based on models derived from MERGE, a well established integrated assessment model (IAM). We discuss first the introduction in MERGE of a set of "tolerable window" constraints which limit both the temperature change and the rate of temperature change. These constraints, obtained from ensemble simulations performed with the Bern 2.5-D climate model, allow us to identity a domain intended to preserve the Atlantic thermohaline circulation. Next, we report on experiments where a two-way coupling is realized between the economic module of MERGE and an intermediate complexity "3-D-" climate model (C-GOLDSTEIN) which computes the changes in climate and mean temperature. The coupling is achieved through the implementation of an advanced "oracle based

O. Bahn
GERAD and MQG, HEC Montréal, Montréal (Qc), H3T 2A7, Canada
e-mail: olivier. bahn@hec.ca

L. Drouet · A. Haurie · J.-P. Vial
LOGILAB-HEC, University of Geneva, 1211 Geneva, Switzerland
e-mail: laurent.drouet@hec.unige.ch
e-mail: alain.haurie@hec.unige.ch
e-mail: jean-philippe.vial@hec.unige.ch

N. R. Edwards
Earth Sciences, CEPSAR, Open University, Milton Keynes, MK7 6AA, UK
e-mail: n.r.edwards@open.ac.uk

R. Knutti
National Center for Atmospheric Research, Boulder, CO 80305, USA
e-mail: knutti@ucar.edu

S. Kypreos
Paul Scherrer Institute, 5232 Villigen, Switzerland
e-mail: socrates.kypreos@psi.ch

T. F. Stocker
Climate and Environmental Physics, Physics Institute, University of Bern, 3012 Bern, Switzerland
e-mail: stocker@climate.unibe.ch

optimization technique" which permits the integration of information coming from the climate model during the search for the optimal economic growth path. Both cost-effectiveness and cost-benefit analysis modes are explored with this combined "meta-model" which we refer to as GOLDMERGE. Some perspectives on future implementations of these approaches in the context of "collaborative" or "community" integrated assessment modules are derived from the comparison of the different approaches.

1 Introduction

The building of integrated assessment models of climate change has followed two main approaches. In one strand of research, we find highly aggregated and integrated models where the economy, the climate system and the damage evaluation form components of a modular dynamical system. The integrated climate-economy system behavior is then simulated over a long time horizon, for specified economic policies. An optimization technique is used to identify a cost-effective or an efficient global climate policy. The archetypal models having this structure are the DICE family of models (Nordhaus, 1993; Nordhaus and Boyer, 2000), MERGE (Manne et al. 1995), and more recently ICLIPS (Toth et al. 2003), among many others. In all these models the description of climate dynamics is highly simplified and reduces to a relatively small number of difference equations describing the carbon cycle, the greenhouse gas forcing and the resulting average surface air temperature. Another strand of integrated assessment modeling effort is typically represented by the MIT integrated global system model (IGSM) (Prinn et al. 1999) where the assessment tool is composed of loosely interconnected modules, such as a detailed multi-region computable general equilibrium model to describe the world economy and a high-resolution general circulation model to describe the climate dynamics. There is no hard-linking between the different modules. In such a system, each module is run more or less independently with boundary conditions that are specified by taking into account the results of simulations performed on the other models composing the system. The coupling between these heterogeneous classes of models is therefore a challenge which has been recognized by the Collaborative Integrated Assessment Model (CIAM[n]) research framework (Jaeger et al. 2002) and first tackled explicitly by Leimbach and Jaeger (2004).

   The aim of this paper is to present methods that permit the integration into a relatively detailed optimal economic growth model of information concerning climate change that is provided by a relatively detailed, spatially resolved climate model. A guiding objective in the research reported here has been to combine the methodological elegance of highly integrated models with the sectoral relevance of systems combining state-of-the-art models of climate and economics. The economic model that we use follows the Ramsey-Solow long-term optimal economic growth paradigm and forms part of MERGE, a well established IAM developed to study the economic dimension of climate change. On the climate side we use (i) the Bern 2.5-D model (Stocker et al. 1992; Stocker and Schmittner 1997) which is well known in the climate community and (ii) C-GOLDSTEIN (Edwards and Marsh 2005) which is a novel higher dimensional intermediate complexity model lending itself to relatively fast simulations of climate histories. In the first approach the Bern 2.5-D model is used to propose a combined constraint on temperature change and its rate of change to attempt to avoid a breakdown of the Atlantic thermohaline circulation (THC). This constraint is added to MERGE which is then run in a cost-effectiveness mode. In a sense, the detailed climate model is used to identify a "tolerable window" (TW) constraint that is introduced in the IAM. The second approach is more ambitious as it establishes a direct dialogue between two specialized

modules: the first module is concerned with the economic growth dynamics, the accumulation of GHGs (carbon cycle dynamics) and the damage due to climate change; the other module deals with the climate dynamics per se. A cost-effectiveness and a cost-benefit analysis are thus conducted by implementing an "oracle-based" optimization technique that establishes a coordination between these two modules. This direct coupling between detailed economic and climate models has been made possible by two scientific advances: (a) the building of computationally efficient intermediate complexity climate models that lend themselves to fast simulations, and (b) the development of oracle-based optimization techniques that converge in relatively few calls to the oracles. The implementation of such a combination of advanced optimization and climate modeling techniques opens new avenues in the development of IAMs and will thus be presented in some detail.

The remainder of the paper is organized into three parts. In the first part, we review the structure of MERGE. In the second part, we address the issue of constraining the economic development path through climate change limits that are intended to avoid the occurrence of a threshold event, namely the collapse of the THC. These constraints are identified via an ensemble simulation conducted with the Bern 2.5-D climate model. In the third part, we report on experiments where the economic growth module of MERGE is directly coupled with a higher dimensional climate model with fully 3-D ocean dynamics. In conclusion we discuss possible further applications and extensions of the approach.

2 The MERGE modeling framework

The Model for Evaluating the Regional and Global Effects of greenhouse gas reduction policies (MERGE) was introduced by Manne et al. (1995). MERGE comprises nine geopolitical regions and four modules (energy, macroeconomic, climate and damage modules) as displayed in Figure 1.

The energy module is a bottom-up process model. It describes the energy supply sector of each region, in particular the generation of electricity and the production of non-electric energy. It captures price-dependent substitutions of energy forms and energy technologies to comply with greenhouse gas (GHG) emission abatements. The macroeconomic module is a top-down macroeconomic growth model. It balances the rest of the economy of a given region using a nested constant elasticity of substitution production function. It captures
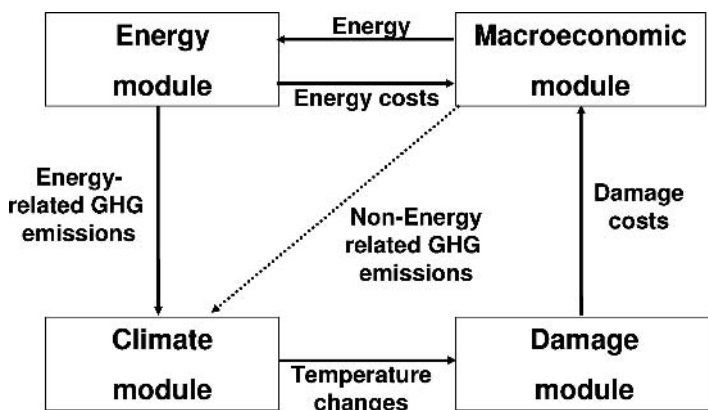

Fig. 1 Overview of the MERGE modules.

macroeconomic feedbacks between the energy system and the rest of the economy, for instance impacts of higher energy prices on economic activities. The regional models yield anthropogenic emissions of CO_2, CH_4 and N_2O. The climate module computes changes in atmospheric GHG concentrations, impacts on the Earth's radiative forcing balance and finally mean surface air temperature (SAT) changes. Finally, the damage module assesses how temperature changes cause commensurate economic losses, distinguishing among market damages (damages that can be valued using market prices) and non-market damages (e.g. damages caused to biodiversity that do not have direct market values). A discussion of the evaluation of climate change damage in MERGE is given by Manne and Richels (2005).

The mathematical formulation of the regional energy-economy modules is an optimization problem, where the economic equilibrium is determined by a single optimization. More precisely, the model maximizes a welfare function defined as the net present value of the logarithm of regional consumption (adjusted for non-market damages when following a cost-benefit approach). It aggregates the regional welfare functions into a global welfare function using Negishi weights (Negishi 1972). The regional submodels are further linked by international trade of oil, gas, synthetic fuels, industrial-energy-intensive products, emission permits, and an aggregate good expressed in a monetary unit that represents all other (non-energy) traded goods. A global constraint ensures that international trade is balanced.

We use here version 4.6 of MERGE in which the climate module parameters have been revised in accordance with the findings of the IPCC as described by Bahn et al. (2004). Uncertainty in climate-module response is reduced to uncertainty in two key parameters, the basic atmospheric sensitivity to radiative forcing (the equilibrium temperature change for a doubling of CO_2 above pre-industrial level) and a timescale for the lag of the atmospheric temperature behind its equilibrium value, principally as a result of heat uptake by the ocean. In the case studies we present, the climate sensitivity ranges between 2 and 4 °C in accordance with IPCC (2001b), whereas the lag time is set to 60 years, a mean value obtained from an ensemble of 1000 runs of C-GOLDSTEIN (Edwards and Marsh 2005). Notice also that, for the sake of simplicity, the model version we use does not consider endogenous technological progress in the energy sector.

3 Tolerable window constraints derived from the Bern 2.5-D climate model

In this section, we introduce tolerable window constraints derived from the Bern 2.5-D climate model. The German Advisory Council on Climate Change (WBGU)[1] proposed to limit temperature increase (relative to pre-industrial levels) by 2 °C and rate of temperature increase by 0.2 °C per decade (WBGU 2003). This position has recently been echoed by the European Council.[2] In this section, rather than using subjectively defined values we introduce objectively defined constraints limiting the probability of a THC collapse. These constraints are designed using an ensemble of simulations performed with the Bern 2.5-D model.

3.1 TW constraints to preserve the ATLANTIC THC

The imposition of TW constraints designed to preserve the Atlantic THC has been considered by several authors, (Bahn et al. 2004; Bruckner and Zickfeld 2004; Keller et al. 2004). We

---

[1] Wissenschaftlicher Beirat der Bundesregierung Globale Umweltveränderungen.

[2] EU Council 7631/04.

follow here the approach of Bahn et al. (2004) (henceforth BEKS) who have proposed simple climate constraints designed to prevent the collapse of the THC. We shall describe briefly how these constraints are obtained and present new numerical results where uncertainty is explicitly taken into account in the decision-making process.

To estimate the level and rate of GHG emissions likely to induce a collapse of the THC, BEKS used the Bern 2.5-D climate model which is based on 2-dimensional (latitude-depth) representations of the flow in each of the Pacific, Atlantic and Indian Oceans, connected via a 2-dimensional (longitude-depth) representation of the Southern Ocean (Stocker et al. 1992). The model also includes a 1-layer energy and moisture balance representation of the atmosphere (Schmittner and Stocker 1999) and a thermodynamic representation of sea ice. In the version used here, GHG forcing is parameterized as a change in radiative forcing at the top of the atmosphere.

Constraints were derived from an ensemble of 25000 Monte-Carlo simulations with values of climate sensitivity and GHG concentrations chosen randomly within specified bounds but with future emissions scaled to SRES scenario Bl (very similar values for the TW constraints were obtained using SRES A2). Only simulations which matched observed global mean surface warming from 1900 to 2000 and observed ocean heat uptake from 1955 to 1995 were retained, around 10% of the total number; for details see Knutti et al. (2003). This set was used to derive approximate conditions for a collapse of the THC, defined here as a decrease of over 50% in the maximum integrated northward water-mass flux in the Atlantic. Note that since the circulation has a qualitatively bimodal behaviour (Knutti and Stocker 2002), our choice of 50% for the threshold value should have little effect on the results. As found by Stocker and Schmittner (1997) both the maximum absolute warming and the maximum warming rate need to be considered, although the sensitivity of the THC to warming rate is not found in all models (Lenton et al. 2005). BEKS thus applied linear constraints to these two quantities as follows: the limit on absolute warming increases linearly between $0.70\,°C$ in 2000 and $1.42\,°C$ in 2100, whereas the limit on warming rate decreases linearly between $0.24\,°C$ in 2000 and $0.13\,°C$ in 2100.

3.2 Numerical results

Using the version of MERGE described in section 2, BEKS analysed climate policies preserving the Atlantic THC, namely policies that impose constraints (as defined above) on maximum absolute warming and maximum warming rate. These policies (denoted P*) were contrasted with a business-as-usual scenario, without any GHG emission control, and a Kyoto-like GHG reduction policy. Of specific importance for these scenarios is the uncertainty in the response of the physical climate system (encapsulated here in the climate sensitivity). This uncertainty can be addressed using a scenario-by-scenario analysis: separately considering several cases where all parameters are perfectly known (the perfect foresight situation), for example, a case denoted *L with "low" climate sensitivity ($2\,°C$) and a case denoted *H with "high"[3] climate sensitivity ($4\,°C$). This scenario-by-scenario approach has been used by BEKS. In the present paper we deal with the uncertainty characterizing the climate sensitivity by implementing a "stochastic programming" approach that considers simultaneously the different scenarios for the uncertain climate parameter without the assumption of perfect foresight. We assume

---

[3] With respect to the current uncertainty range proposed by (IPCC, 2001b) (1.5 to 4.5°C). It is, however, worth noticing that our high case is not a worst case scenario, as new studies (Knutti et al. 2002; Stainforth et al. 2005; Knutti et al. 2006; Stott et al. 2006) indicate that the climate sensitivity range might be higher.
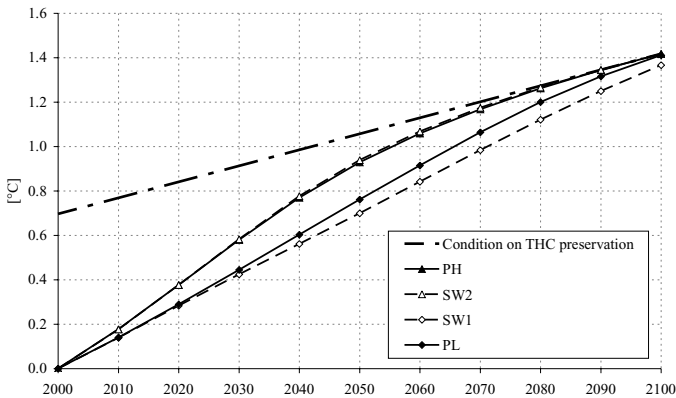
Fig. 2 Warming (from 2000) for the THC preservation scenarios (denoted PL and PH in the scenario-by-scenario approach, and SW1 and SW2 in the stochastic programming approach), as well as necessary condition for preserving the THC in terms of maximum warming. Cases PL and SW1 (resp. PH and SW2) correspond to low (resp. high) climate sensitivity assumptions.

a particular future date (2030)[4] at which a perfect knowledge of climate sensitivity will be obtained. The stochastic process describing the unfolding of uncertainty is then represented by a two-stage event tree. This consists of a first stage, or trunk, that describes the measures (e.g., GHG abatement) to be implemented when climate sensitivity is still uncertain (between 2000-2030), and a second stage, or branches, that describe recourses (i.e., revised GHG abatement levels) to be implemented once perfect knowledge is obtained. Branches correspond to alternative settings for the uncertain climate parameter (corresponding to cases *L and *H) that define two states of the world (SW1 and SW2, respectively). Following the PDF generated by the Bern 2.5-D model, the probabilities used are: 20% for SW1 and 80% for SW2. We will also examine the effect of alternative probability distributions.

We assume also that there is a social planner (world regulator) that monitors the Earth's warming and is able to impose worldwide GHG emission reductions such that the necessary conditions on THC preservation are respected. Figure 2 displays the evolution of the warming[5] which constitutes the more demanding condition for the THC preservation. For the scenario SW1, the THC preservation constraint becomes binding by 2120 (the model's horizon).

The stochastic approach proposes to policy makers a "hedging" climate policy.[6] This corresponds to a single trajectory for GHG emissions up to the date at which uncertainty is resolved (here, 2030). Following this trajectory corresponds to a "least regret" strategy that balances present regret of imposing premature and costly emission reduction (when climate sensitivity is low) with future regret of neglected reduction in the past (when climate sensitivity is high). This strategy is defined by maximizing the sum of the welfare of the two states of the world weighted by their respective probability of occurrence. Figure 3 displays the resulting world energy-related CO_2 emissions under the different THC preservation scenarios.

---

[4] In contrast to several other studies such as Keller et al. (2004) which assume a longer learning time.

[5] Between 2000 and 2030, the computation of the warming in the SW1 (resp. SW2) case uses the emissions of the hedging path (see below) and assumes a low (resp. high) climate sensitivity.

[6] See for instance F.L. Toth and M. Mwandosya, "Decision-making Frameworks", pp. 612–614, in (IPCC, 2001a).
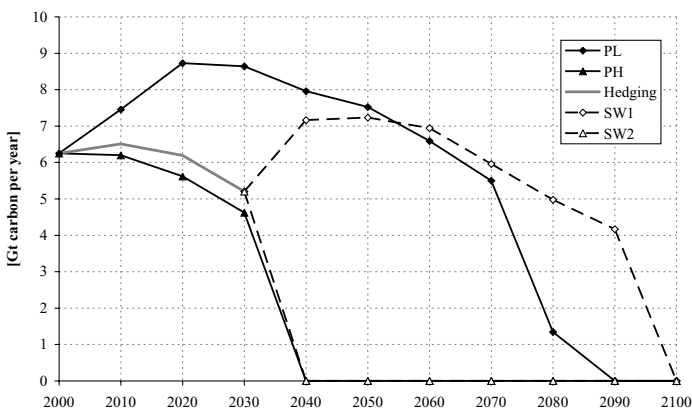
Fig. 3 World energy-related CO_2 emission trajectories under the THC preservation scenarios (denoted PL and PH in the scenario-by-scenario approach; and Hedging, SW1 and SW2 in the stochastic programming approach). Cases PL and SW1 (resp. PH and SW2) correspond to low (resp. high) climate sensitivity assumptions.

Figure 3 shows, for the stochastic programming approach, a unique emission path between 2000 and 2030 (before the resolution of climate uncertainties), whichever state is finally realized (SW1 or SW2). This corresponds to the hedging strategy which, in this case, closely follows the PH emission path. After 2030, once the true climate sensitivity is known, the stochastic programming approach also proposes an optimal path to adapt to the assumed true state. In the low climate sensitivity case (SW1), emissions are allowed to increase until 2050 (to compensate for early reductions) and are reduced afterwards, albeit less quickly than in the PL emission path. In the high climate sensitivity case (SW2), emissions are required to reduce to zero as early as 2040, as in the PH emission path. Such a drastic abatement can only be more severe when assuming a climate sensitivity higher than 4°C, a possibility that has been recognized in recent studies. The fact that the hedging path follows the PH emission trajectory is not simply a result of the high probability associated with SW2. To demonstrate this we have conducted a sensitivity analysis, assuming alternative probability settings for the two states of the world (SW1 and SW2, respectively): (50%, 50%), (70%, 30%) and (90%, 10%). Emissions in 2030 are respectively 5.3, 5.4 and 5.5 Gt C, very close to the value of 5.2 Gt C found when assuming a (20%, 80%) probability distribution. This is explained by the fact that one must be able to reduce emissions to zero by 2040 when climate sensitivity is revealed to be high. In a sense, the stochastic programming approach here is close to a maximin approach, where the social planner's decisions (levels of abatement) are driven by the consideration of the worst possible outcome (high climate sensitivity).

This example has demonstrated that TW constraints based on information obtained from more advanced climate models can be included in an economic growth model coupled with a simple climate model (in this case the integrated assessment model MERGE). However, the temperature change (in MERGE) is still predicted by a "zero-dimensional" climate module. There is therefore a lack of consistency between the model (Bern 2.5-D) that is used to delineate the TW constraints and the climate model (within MERGE) used to simulate the climate-economy feedbacks. In the next section we consider how this situation can be improved by allowing a two-way exchange of information between economic and climate models, so that the two models share a consistent representation of climate change.

4 An oracle-based optimization approach for the coupling of MERGE
with the C-GOLDSTEIN climate model

In this section we describe a general method permitting a coupling between independent and specialized models in order to build an IAM. The method exploits a recently developed mathematical programming method, the "Oracle Based Optimization Technique" (OBOT), that permits a coherent dialogue between models. In the implementation described here, one module gives a description of the world economy and carbon-cycle dynamics and is obtained from MERGE. A second module is a 3-D climate model of reduced complexity. The result is an all-encompassing model with an economic sub-model, a climate sub-model and a master program which controls the optimization procedure through a consistent dialogue between the models.

   In previous experiments with this approach reported by Drouet et al. (2005a,b) a coupling has been realized between the economic part of the DICE model and the C-GOLDSTEIN climate model. The implementation of OBOT described here for the coupling of MERGE with C-GOLDSTEIN represents a significant advance. Not only is MERGE a far more comprehensive and detailed model of the global energy economy than DICE but furthermore, by coupling climate and economic models both of which have some spatial resolution, we have made an important step towards an IAM with spatially resolved feedback between climate and economy. In the remainder of this section we first briefly recall the main features of the C-GOLDSTEIN model, then present OBOT, the two coupling modes, namely cost-effectiveness (CE) and cost-benefit (CB) and finally the results obtained from this coupling.

4.1 The C-GOLDSTEIN climate model

C-GOLDSTEIN is a flexible geometry, efficient, frictional geostrophic, 3-D global ocean model with eddy-induced and isopycnal mixing coupled with an energy and moisture balance atmosphere and a dynamic and thermodynamic sea-ice component. The model dynamics and behaviour are described briefly by Drouet et al. (2005a), and more fully by Drouet et al. (2005b). With an integration speed of one or two thousand years per hour on a modern PC (Pentium-IV, 2.4 GHz), it is an order of magnitude less efficient than the Bern 2.5-D model, but 3 or 4 orders of magnitude faster than conventional, high-resolution models such as HadCM3 (Gordon et al. 2000) and 1 or 2 orders of magnitude faster than other intermediate complexity models such as ECBILT-CLIO (Haarsma et al. 2001) or the UVic model (Weaver et al. 2001), which has a very similar atmosphere. This efficiency is mainly a result of low spatial resolution and simplified dynamics. For the studies described here, the ocean component is configured with 8 vertical levels and 36 by 36 cells in the horizontal. Gross features of the global-scale ocean circulation and climate can be reasonably well represented, particularly when model parameters are automatically calibrated with respect to observational data by performing large numbers of simulations (Hargreaves et al. 2005). For the experiments reported here, however, we use default values for model parameters since our focus is on the demonstration of the coupling technique. All components share the same horizontal grid, but the model atmosphere has only one vertical level, so that atmospheric processes are represented by a vertical balance of energy and moisture plus simple horizontal transport by anisotropic diffusion and fixed advection by the wind. Atmospheric radiative forcing is parameterised by a polynomial function of temperature and humidity with a greenhouse gas forcing term proportional to the log of the ratio of CO_2 concentration compared to its pre-industrial value. Feedbacks involving changes in atmospheric circulation and precipitation patterns, and feedbacks involving the land surface, are relatively poorly represented or ignored. Sea-ice

height and areal coverage are similarly governed by a vertical heat and freshwater balance, plus advection by surface currents with a diffusive term to represent unresolved processes. Given these dynamical simplifications, the model is most suitable for studies of large-scale ocean circulation and long-term climate change, and for probabilistic climate-change studies and integrated assessment modelling. The model forms a component of the Grid Enabled Integrated Earth System Model (GENIE) project[7] in the context of which an Earth System Model with more detailed representations of atmosphere, land-ice, ocean biogeochemistry and land-surface processes is under development.

For the experiments reported here temporal variability in solar forcing is ignored and the model approaches an equilibrium state, after a few thousand years of integration, which is essentially independent of the initial conditions and can be taken to represent the preindustrial climate. The model is then integrated forwards with observed atmospheric CO_2 concentrations from 1795 to 1995 to produce an initial condition for the coupled runs.

4.2 The oracle based optimization technique

The optimization of large-scale systems through decomposition techniques has given rise to important developments related to non-differentiable optimization, column generation and cutting plane techniques. The version of an *Oracle Based Optimization Technique* (OBOT) that we use was first proposed by Goffin et al. (1992). Since then several improvements and implementation advances have been made as described by Péton and Vial (2001) and Babonneau et al. (2005).

In the world of convex optimization, one searches for the minimum of a convex function over a convex set of admissible values for the variables. OBOT converges to the optimum by sending a sequence of query points which are proposed values for the decision variables. If the query point is not feasible (that is, it violates the imposed constraints) an "oracle" sends back information in the form of a separating plane which places the query point in one half-space and the admissible set in the other. If the query point is feasible, another "oracle" sends back information in the form of the value reached by the optimization criterion and the gradient of this function at the query point (which defines a supporting hyperplane for the epigraph of the function). From this sequence of "cutting planes" one is able to construct a polyhedral approximation of a so-called "localization set" which always contains the optimal values for the variables and the criterion function. Among possible strategies, one can choose the query point at the "center" of the current localization set. The localization set then shrinks rapidly and it has been proved that the optimum will be found with the desired level of accuracy in a manageable computational time.

The method that we implement is called *Analytic Center Cutting Plane Method* (ACCPM) in reference to the way one defines the center where one selects the query point. In this method, the criterion and the constraints do not have to be explicitly defined. An implicit definition permitting a computation of a value of the function at a query point and an evaluation of its gradient at this point will suffice. It is this feature which makes the approach very attractive to couple models pertaining to different spheres.

The convergence of ACCPM towards the global optimum, as well as its rate of convergence, has been established for convex optimization problems only. In the present application, the economic model is convex, but we have no guarantee that the climate model shares this property. However, once the two models have found compatible, feasible climate and

---

[7] See http://www.genie.ac.uk

emission variables, we can assert that the objective value of the economic model is attainable and provides an upper bound to a global optimum. It may also improve upon alternative local optima. This is the situation that prevails at the end of the optimization process in our application.

In proving that the best point found by ACCPM is a local optimum we would face two difficulties. The first one is that the cutting planes are imprecise as they are computed by finite differences, and are thus subject to error. The second difficulty stems from the fact that sensitivity analysis in a non-convex model provides information that is only valid in a neighborhood of that point, but may be invalid farther away. To cope with this second difficulty, we have implemented a simple scheme that tests whether the cutting plane created at the current query point invalidates the current best solution. If it does, we simply shift the cutting plane to preserve feasibility of the best solution. This allows for convergence of the method. In the present case, as well as in the similar applications mentioned earlier, we very seldom encountered contradictory cutting planes.

Note that even if we could compute exact derivatives in the climate model, local optimality could only be guaranteed by discarding remote cutting planes, in the spirit of a trust-region approach (Moré, 1983; Schramm and Zowe, 1992), and proving optimality via local cutting planes only. At present, little has been done to extend cutting plane schemes to the non-convex case. Our approach is a pragmatic substitute for a rigorous trust-region scheme, taking into account that the multiple simulations of the climate model required to calculate damage gradients are computationally expensive, ruling out the possibility of using the large numbers of query points required by other algorithms such as the differential evolutional algorithm considered by Keller et al. (2004).

4.3 Two modes of coupling

We give here briefly the principles of OBOT when applied to the coupling of an economic growth model with a climate model in two different modes of analysis, namely cost-effectiveness (CE) and cost-benefit (CB) modes. The coupling yields a new meta-IAM which is now denoted GOLDMERGE-CE or GOLDMERGE-CB according to the coupling mode that is used. The method of solution is similar for the two modes but the information exchanged between the oracles and the optimization module differs slightly. These differences and the two reduced-order problems driven by the coupling variables are discussed in the next two subsections. More details on the technical aspects can be found in Drouet et al. (2005a) and Drouet et al. (2005b). We use the economic modules and the carbon-cycle description of MERGE version 4.6 as described in Section 2.

4.3.1 The oracles in the cost-effectiveness mode

In cost-effectiveness mode the coupling variables between the two modules are essentially the atmospheric CO_2 concentrations, denoted as a vector C with a component for each decade from 2010 to 2100. Constraining these variables controls the "economy oracle". We thus obtain an optimal growth path which maximizes the total discounted welfare criterion and satisfies these concentration constraints. The sensitivity of the optimized criterion to variations in the C constraints is provided by duality analysis. The "climate oracle" C-GOLDSTEIN, receiving, as input, the concentration schedule C, computes the average surface air temperature (SAT) and its decadal rate of change. The master program has to find the concentration schedule C which optimizes the economy under a constraint of $2\,°C$ on the average SAT change over the whole planning horizon and $0.2\,°C$ on its change over each decade. This

corresponds to the rate of temperature change constraint proposed by the WBGU and alluded to at the beginning of section 3. The sensitivity of the temperature changes to marginal modifications of C is obtained by calling C-GOLDSTEIN several times with perturbed C vectors (effectively using a finite-difference approximation to the derivative).

The reduced-order optimization problem solved by OBOT can be summarized by:

$$\max_{C \in \mathbb{R}^n} \{ U(C) \,|\, \phi(C) \le \bar{\phi} \}, \tag{1}$$

where U is the optimum value for the welfare criterion (actually a linear combination of the welfare of each region) in the economic growth model, ϕ is the rate of temperature change by decade computed by the climate module with a forcing of the concentration C and $\bar{\phi} = 0.2$ is the upper-bound value defined by the tolerable window constraint. Notice that satisfaction of the constraint on the rate of temperature change ($0.2\,^\circ$C per decade) implies automatically that the constraint on a global temperature change of $2\,^\circ$C will be satisfied over the century.

4.3.2 The oracles in the cost-benefit analysis mode

In cost-benefit mode the economic damage depending on temperature changes is included in the computation of the welfare function. The coupling variables, denoted by the vector X, represent (i) the concentration schedule C from 2010 to 2100 by decade and (ii) the decadal changes in temperature T over the same horizon:

$$X = (C, \delta T) \in \mathbb{R}^{2n}, \tag{2}$$

where $n = 10$ is the number of periods of the time horizon. The economy oracle MERGE receives the concentrations C and the temperature changes δT and replies to this query by sending the optimal value of the global welfare function $U(X)$ corresponding to the given constraints on concentration and the given temperature changes. In addition, the economic oracle sends back a gradient vector which is easily obtained from duality analysis in the economic model, as in the cost-effectiveness mode. The climate oracle C-GOLDSTEIN computes the SAT from the concentrations C and replies to the query by the value of the "gap function" $\Theta(X)$ defined as follows:

$$\Theta(X) = \phi(C) - \delta T, \tag{3}$$

where $\phi(C)$ is the SAT change from 2000 computed by the climate module with the forcing of the concentrations C. The jacobian matrix $\nabla \Theta(X)$ is also sent back and is equal to $\gamma = (\nabla \phi(\bar{C}), -I)$ where I is the identity matrix. The subgradient $\nabla \phi(\bar{C})$ is evaluated numerically by C-GOLDSTEIN by finite difference approximation. The value of the function Θ must be non-positive. Therefore OBOT solves the reduced order optimization problem which is formulated as follows:

$$\max_{X \in \mathbb{R}^{2n}} \{ U(X) \,|\, \Theta(X) \le 0 \}, \tag{4}$$

where $U(X)$ is the optimum value for the economy model and $\Theta(X)$ is the gap function defined above. In summary, then, damages are included in the welfare function in the CB mode, in which case, the temperature changes are not explicitly constrained. On the contrary, temperature constraints are explicitly included in the CE mode.

4.4 GOLDMERGE results

To compare the GOLDMERGE results with those of MERGE itself, as described in Section 2, we set the climate sensitivity parameters to a common value of 2.75 °C and the timescale for the lag of atmospheric temperature behind its equilibrium to 60 years. Note that the forcing due to CH_4 and NO_2 gases is taken into account in the MERGE climate module whereas in C-GOLDSTEIN it is not. While this extra forcing effect could relatively easily be accounted for in C-GOLDSTEIN its neglect is unlikely to significantly alter our conclusions since the effect of the extra gases amounts to an SAT change of only about 0.2 °C over the whole time horizon. Results are reported separately for cost-effectiveness and cost-benefit modes which are denoted by the suffices CE and CB.

4.4.1 GOLDMERGE-CE

Figure 4b shows the resulting CO_2 concentrations at the optimum in GOLDMERGE-CE and MERGE-CE. GOLDMERGE-CE CO_2 concentrations reach a level of 692 ppmv in 2100 whereas MERGE-CE concentrations reach only 560 ppmv. Figure 4a reveals the world CO_2 energy-related emissions. These are strongly related to the CO_2 concentration levels since they are computed by the MERGE energy module. Emissions follow roughly the same path during the first periods, then MERGE-CE CO_2 emissions start to decrease in 2050 whereas GOLDMERGE-CE emissions only decrease in 2070. In 2100, a gap of 6 GtC/year exists between the two emissions curves. Figures 4c and 4d show the temperature and warming rate trajectories. The warming rate attains the level of 0.2 °C per decade in 2050 in both models, then the constraint on temperature rate stays active until 2100. Differences for the
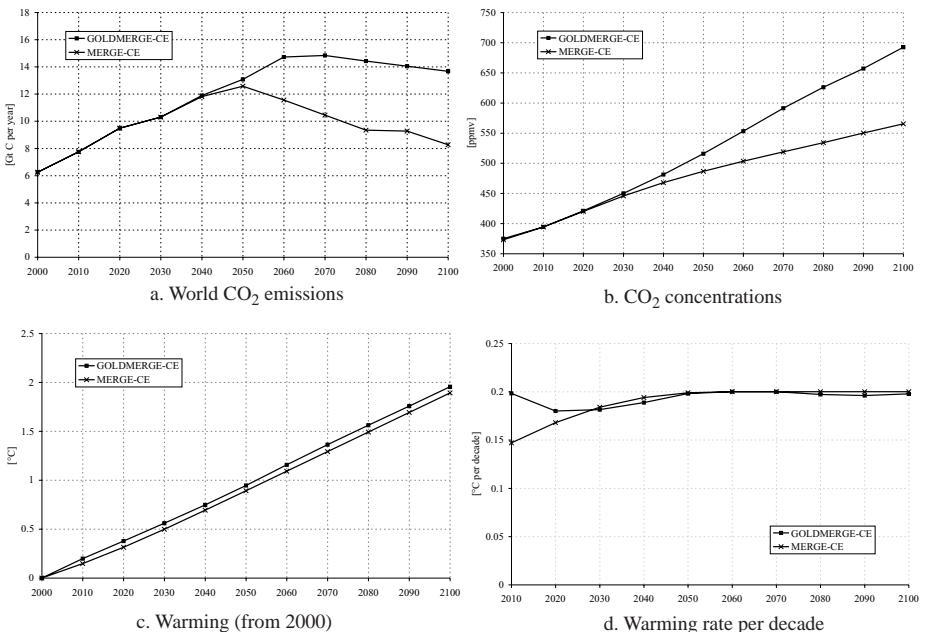

Fig. 4 World energy-related CO_2 emissions and atmospheric CO_2 concentrations trajectories and warming from 2000 for MERGE in cost-effectiveness mode (MERGE-CE) and GOLDMERGE-CE.

first period can be explained by the initial climate system inertia which is not the same in the two climate modules. In C-GOLDSTEIN, the initial inertia comes from the initial CO_2 forcing used to simulate climate change from the preindustrial era to 2000. In the MERGE climate module, this is parameterised using an additional radiative forcing parameter which defines a lower initial forcing (and hence a lower temperature change of 0.15 °C in 2010). The cumulative temperatures in Figure 4c reflect this difference by a small gap between the two curves. In summary, the difference in predicted climate response between the models appears mainly in the difference in the CO_2 concentration paths. The gap between the two paths increases with time while the warming rates remain the same due to the constraint. Since the equilibrium climate sensitivities and the warming rates are the same, the larger emissions in GOLDMERGE-CE necessarily imply a larger transient heat uptake by the ocean. Although the ocean lag timescale was chosen to make the response of the two models similar, the behaviour of the more complex model cannot readily be matched by the simple climate module within MERGE. The more realistic climate module is thus allowing larger emissions only to release more heat in the long-term future, beyond the planning horizon. As mentionned in the beginning of the section, the forcing due to other GHGs that are included in MERGE may also be an explanation of the divergence of the two concentration paths.

4.4.2 GOLDMERGE-CB

The difference in solution (computation) time between the CE and CB approaches is not significant even though the number of coupling variables is twice as large in the CB case. The coupling variables, temperatures and CO_2 concentrations, are plotted in Figure 5. CO_2 concentrations are very close in the two models beginning at 373 ppmv in 2000 and reaching 749 ppmv for GOLDMERGE-CB and 745 ppmv for MERGE-CB in 2100. Temperatures have the same dissimilarities described in the previous section. Figure 5d details the decadal temperature change rates. In C-GOLDSTEIN the warming rate stays around 0.2 °C with a slight decrease in 2030 and an increase in the following decades to reach a level of 0.27 °C in 2100. The evolution of the rate of temperature change in MERGE appears smoother. Energy-related CO_2 emissions are plotted in Figure 5a. The two paths are very close, as for the CO_2 concentrations paths (Figure 5b), but GOLDMERGE-CB CO_2 emissions are slightly lower from 2020 to 2070 then increase quickly after 2070 to exceed the MERGE-CB curve. In summary, the difference in predicted climate response between the models is summarized in the warming rates while the CO_2 concentration paths are similar. Interestingly, this is in constrast to the cost-effectiveness approach discussed previously. It may be that in this case the increasing rate of warming permitted by the trade-off between damage and abatement costs is masking the larger potential for long-term heat storage in the more complex model.

4.5 New perspectives offered by GOLDMERGE

The experiments with the coupling of the two models MERGE and C-GOLDSTEIN, as described above, show that the method is effective in this extended modelling framework. An interesting opportunity offered by this approach will be to exploit the spatial distribution of the climate variable evolutions provided in the output of C-GOLDSTEIN in order to produce genuine regional damage functions that could influence the economic growth path in the different regions. In Figure 6 we show the spatial distribution of land surface temperature change in 2100 obtained from C-GOLDSTEIN for the case GOLDMERGE-CB.
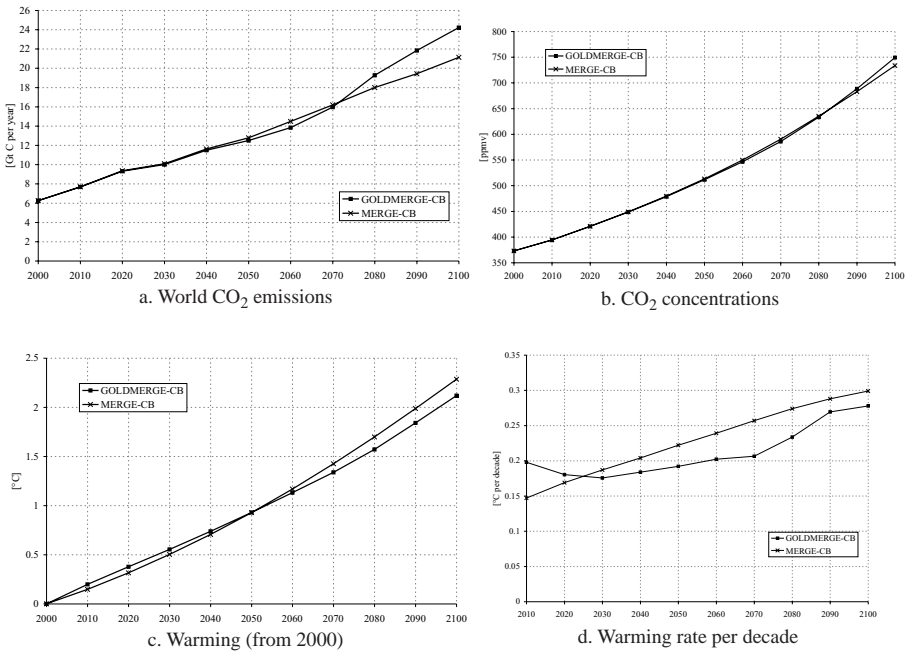
Fig. 5 World energy-related CO_2 emissions and atmospheric CO_2 concentrations trajectories and warming from 2000 for MERGE in cost-benefit mode (MERGE-CB) and GOLDMERGE-CB.
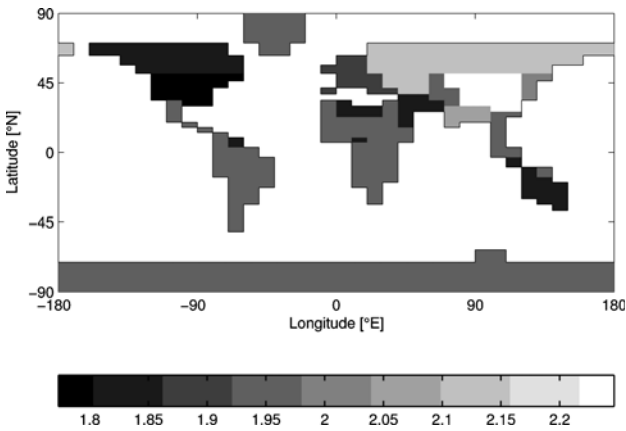
Fig. 6 Distribution of the temperature increase for the standard MERGE regions in 2100 for GOLDMERGE-CB.

Regionalized temperature increases lie within a range from $1.76\,^{\circ}C$ to $2.25\,^{\circ}C$. Another important remark concerns the compatibility of the approach with the use of TW constraints. Indeed, since the climate model is sufficiently detailed, the THC shutdown phenomenon is implicitly represented in it. By imposing regionalized "viability" constraints[8] on purely

---

[8] See (Aubin et al. 2005) for a discussion of viability methods in climate modeling.

climatic variables like precipitation, temperature, ice and snow cover etc. a tolerable windows approach to climate change policies could be defined based on relatively detailed economic and climate models, while still maintaining computational feasibility. The method could in principle be utilised for the coupling of any optimal economic growth model with any general circulation model. Limitations remain in computation time and model convexity. This kind of coupling is highly relevant for community based assessment because it effectively resolves the problem of the inclusion of complex simulation models inside an optimization framework. To conduct a similar exercise with a high-resolution climate model with a detailed and realistic regional temperature and precipitation response would require significant computational resources, but the knowledge which would be gained may well justify such an investment.

5 Conclusion

In this paper we have presented two different ways to establish a dialogue between a climate model and an economic model in order to obtain an integrated assessment of climate policies. First we have shown how a TW constraint can be introduced in the MERGE integrated assessment model in a cost-effectiveness fashion to attempt to prevent the occurrence of a drastic THC weakening. Our TW constraint was obtained from ensemble simulations performed with a spatially resolved climate model (the Bern 2.5-D model) to delineate the conditions that would prevent a THC shutdown. This approach has the advantage of using information coming from a reliable climate model to introduce a TW constraint in MERGE. The climate response to the GHG emissions coming from the economy is however derived from the simplified and schematic climate module that is included in MERGE. In the second example developed here we have described an approach to realize a hard link between an economic growth module and a 3-D climate model of reduced complexity. This approach yields interesting results when the economic growth, carbon cycle and damage modules of MERGE are coupled with the intermediate complexity 3D-model C-GOLDSTEIN. In a reasonable computing time (a few hours on a 2.4 GHz Intel machine) it has been possible to produce consistent simulations of economic growth and climate change paths in either cost-effectiveness or cost-benefit analysis frameworks (the GOLDMERGE-CE and -CB models). The tool that has been used to realize the coupling (OBOT) implements an optimization method using "oracles" that correspond to different models.

The results reported here pave the way to the building of more comprehensive and more detailed IAMs. Currently the method is being tested for a coupling between the economic part of MERGE and CBM-GOLDSTEIN (GENIE-1), a more advanced climate model including a description of the carbon cycle. It will also be possible to exploit the fact that the climate model gives a spatially distributed view of the evolution of climate variables. This should permit us to build regional damage functions or to link climate feedbacks with the economic activity (e.g. agriculture). The method could also be extended to realize a coupling between the macroeconomic growth module and a more detailed techno-economic model of the energy sector, in addition to the coupling with a moderate complexity climate model.

References

Aubin J-P, Bernardo T, Saint-Pierre P (2005) A viability approach to global climate change issues. In: Haurie A and Viguier L (eds.) The coupling of climate and economic dynamics. Kluwer, pp 113–140

Babonneau F, Beltran C, Haurie A, Tadonki C, Vial J-P (2005) Proximal-ACCPM: a versatile oracle based optimization method. Computational and Management Science. Submitted.

Bahn O, Edwards N, Knutti R, Stocker T (2004) Climate policy preserving an atlantic thermohaline circulation collapse. Climatic Change. Submitted. Available in Les Cahiers du GERAD, reference G-2004-72

Bruckner T, Zickfeld K (2004) Low risk emissions corridors for safeguarding the atlantic thermohaline circulation. In: paper presented at the Expert Workshop "Greenhouse Gas Emissions and Abrupt Climate Change", Paris.

Drouet L, Beltran C, Edwards N, Haurie A, Vial J-P, Zachary D (2005a) An oracle method to couple climate and economic dynamics. In: Haurie A and Viguier L (eds.) The coupling of climate and economic dynamics. Kluwer pp 69–94

Drouet L, Edwards N, Haurie (2005b) Coupling climate and economic models in a cost-benefit framework: a convex optimization approach. Environmental Modeling and Assessment. Submitted.

Edwards N, Marsh R (2005) Uncertainties due to transport-parameter sensitivity in an efficient 3-D ocean-climate model. Climate Dynamics 24:415–433

Goffin J-L, Haurie A, Vial J-P (1992) Decomposition and non-differentiable optimization with the projective algorithm. Management Science 38:284–302

Gordon C, Cooper C, Senior C, Banks H, Gregory J, Johns T, Mitchell J, Wood R (2000) The simulation of SST, sea-ice extents and ocean heat transports in a version of the Hadley Centre coupled model without flux adjustments. Climate Dynamics 16:147–168

Haarsma R, Goosse H, Selten F, Opsteegh JD (2001) Decadal variability in high northern latitudes as simulated by an intermediate-complexity climate model. Annals of Glaciology 33:525–532

Hargreaves J, Annan J, Edwards N, Marsh R (2005) Climate forecasting using an intermediate complexity earth system model and the ensemble kalman filter. Climate Dynamics 23(7–8):745–760

IPCC (2001a) Climate change 2001: mitigation, contribution of working group III to the third assessment report of the intergovernmental panel on climate change. Metz B et al. (eds) Cambridge University Press. Cambridge, U.K.

IPCC (2001b) Climate change 2001: the scientific basis, contribution of working group I to the third assessment report of the intergovernmental panel on climate change. Houghtom J et al. (eds) Cambridge University Press, Cambridge, U.K.

Jaeger CC, Leimbach M, Carraro C, Hasselmann K, Hourcade JC, Keeler A, Klein R (2002) Integrated assessment modeling: modules for cooperation. FEEM Working Paper No. 53

Keller K, Bolker B, Bradford D (2004) Uncertain climate thresholds and optimal economic growth. Journal of Environmental Economics and Management 48(1):723–741

Knutti R, Meehl G, Allen MR, Stain forth DA (2005) Constraining climate sensitivity from the seasonal cycle in surface temperature. J. Climate 19:4224–4233

Knutti R, Stocker T (2002) Limited predictability of the future thermohaline circulation close to an instability threshold. Journal of Climate 15:179–186

Knutti R, Stocker T, Joos F, Plattner G-K (2002) Constraints on radiative forcing and future climate change from observations and climate model ensembles. Nature 416:719–723

Knutti R, Stocker TF, Joos F, Plattner G-K (2003) Probabilistic climate change projections using neural networks. Climate Dynamics 21:257–272

Leimbach M, Jaeger C (2004) A modular approach to integrated assessment modeling. Environmental Modelling and Assessment 9(4):207–220

Lenton TM, Williamson MS, Edwards NR, Marsh R, Price AR, Ridgwell AJ, Shepherd JG, and the GENIE team (2005) Millennial timescale carbon cycle and climate change in an efficient Earth system model. Climate Dynamics. Submitted.

Manne A, Mendelsohn R, Richels R (1995) MERGE - a model for evaluating regional and global effects of GHG reduction policies. Energy Policy 23(1):17–34

Manne A, Richels R (2005) MERGE: an integrated assessment model for global climate change. In: Loulou R, Waaub J-P, Zaccour G, (eds) Energy and Environment. GERAD 25th Anniversary Series. Springer, pp 175–189

Moré J (1983) Recent developments in algorithms and software for trust region methods. In: Mathematical Programming: The State of the Art. Springer Verlag, Berlin, pp. 258–287

Negishi T (1972) General equilibrium theory and international trade. North-Holland.

Nordhaus W (1993) Rolling the 'DICE': an optimal transition path for controlling greenhouse gases. Resource and Energy Economics 15:27–50

Nordhaus W, Boyer J (2000) Warming the world: economic models of global warming. MIT Press

Péton O, Vial J-P (2001) A brief tutorial on ACCPM. Technical report. Logilab, University of Geneva

Prinn R, et al. (1999) Integrated global system model for climate policy assessment: feedbacks and sensitivity studies. Climatic Change 3/4(41):469–546

Schmittner A, Stocker T (1999) The stability of the thermohaline circulation in global warming experiments. Journal of Climate 12:1117–1133

Schramm H, Zowe J (1992) A version of the bundle idea for minimizing a non-smooth function: conceptual idea, convergence analysis, numerical results. SIAM Journal on Optimization 2:121–152

Stainforth D, et al (2005) Uncertainty in predictions of the climate response to rising levels of greenhouse gases. Nature 433:403–406

Stocker T, Schmittner A (1997) Influence of CO_2 emissions rates on the stability of the thermohaline circulation. Nature 388:862–865

Stocker T, Wright D, Mysak L (1992) A zonally averaged, coupled ocean-atmosphere model for paleoclimate studies. Journal of Climate 4:773–797

Stott P, Mitchell J, Gregory J, Santer B, Meehl G, Delworth T, Allen M (2005) Observational constraints on past attributable warming and predictions of future global warming. J. Climate 19:3055–3069

Toth F, Bruckner T, Fuessel H-M, Leimbach M, Petshel-Held G (2003) Integrated assessment of long-term climate policies: part 1 – model presentation. Climatic Change 56:37–56

WBGU (2003) Climate protection strategies for the 21st century. Earthscan, London.

Weaver A, Eby M, Wiebe E, Bitz C, Duffy P, Ewen T, Fanning A, Holland M, MacFadyen A, Matthews H, Meissner K, Saenko O, Schmittner A, Wang H, Yoshimori M (2001) The UVic earth system climate model: model description, climatology, and applications to past, present and future climates. Atmos-Ocean 39:361–428

Modeling endogenous learning and imperfect competition effects in climate change economics

**Laurent Viguier · Leonardo Barreto · Alain Haurie ·
Socrates Kypreos · Peter Rafaj**

Abstract In this two-part paper we evaluate the effect of "endogenizing" technological learning and strategic behavior of agents in economic models used to assess climate change policies. In the first part we show the potential impact of R&D policies or demonstration and deployment (D&D) programs in the context of stringent stabilization scenarios. In the second part we show how game-theoretic methods can be implemented in climate change economic models to take into account three types of strategic interactions: (i) the market power of the countries benefiting from very low abatement costs on international markets for CO_2 emissions, (ii) the strategic behavior of governments in the domestic allocation of CO_2 emissions quotas, and (iii) the non-cooperative behavior of countries and regions in the burden sharing of CO_2 concentration stabilization. The two topics of endogenous learning and game-theoretic approach to economic modeling are two manifestations of the need to take into account the strategic behavior of agents in the evaluation of climate change policies. In the first case an R&D policy or a demonstration and deployment (D&D) program are put in place in order to attain a cost reduction through the learning effect; in the second case the agents (countries) reply optimally to the actions decided by the other agents by exploiting their strategic advantages. Simulations based on integrated assessment models illustrate the approaches. These studies have been conducted under the Swiss NCCR-Climate program.

Keywords Endogenous technological learning · Strategic behavior · Climate policy ·
Emissions trading · Economic models · Dynamic games

L. Viguier (✉)
Ecole Polytechnique Fédérale de Lausanne (EPFL), Switzerland; MIT Joint Program on the Science and
Policy of Global Change, Cambridge, MA, USA
e-mail: laurent.viguier@epfl.ch

L. Barreto · S. Kypreos
Paul Scherrer Institute, Villigen, Switzerland

A. Haurie
HEC-Geneva, Switzerland

P. Rafaj
International Institute for Applied Systems Analysis, Laxenburg, Austria

⬣ Springer

1 Introduction

In this paper we propose different ways to introduce strategic decision making in the economic models used for the global assessment of climate policies. The paper summarizes several examples of models including strategically behaving agents that have been developed in the realm of the NCCR-Climate research program.[1]

In general, model-based assessments of climate policy assume a competitive framework, and emissions targets are supposed to be reached through cost-effective economic instruments (i.e. uniform carbon tax or economy-wide emission trading regime). However, many recent studies in environmental economics focused on strategic behaviors, incentive problems, and transaction costs associated with information, implementation, learning, administration, monitoring, and compliance (Hahn 1984; Stavins 1995; Goulder and Mathai 2000). A strategic behavior is obtained when the economic agents take into action the reaction of the system or of the other agents to their proposed policies. A first set of examples we present is related to the learning effect of new technologies introduction in the economy. A technology which is currently too costly to penetrate the market could become attractive if enough investment is done due to the learning effect. Therefore a planner should take into account this learning response in the design of an R&D policy or demonstration and deployment (D&D) programs. However due to the introduction of increasing returns to scale associated with the learning effect one cannot count on an "invisible hand" to guide the economy purely from market signals. The R&D and D&D efforts are strategic in the sense that it is done in the purpose of exploiting the learning curve and thus reaching lower costs levels.

Other studies in climate economics focused on market imperfections such as pre-existing taxation (Babiker et al. 2003, 2004; Goulder and Mathai 2000), and the role of strategic behaviors in policy implementations, i.e. exemptions and subsidies (Babiker et al. 2003). Game theoretic models in climate change policy assessment have been considered in very aggregated qualitative models (Carraro and Siniscalco 1996; Barrett 1997; Germain et al. 1998), with an emphasis on the stability and credibility of commitments. They have also been used recently to evaluate the possibility to establish a linkage between climate policies and other issues related to international negotiations (Carraro and Siniscalco 1996; Barrett 1999). The game-theoretic approach has also been applied to assess the effects of CO_2 market imperfections in the realm of current Kyoto Protocol implementation (Bernard et al. 2005, 2003; Haurie and Viguier 2003).

In this paper, we explore the representation of strategic behavior in three categories of models, namely an optimal economic growth models like MERGE (Manne and Richels 2001), a multi-region bottom-up process model like MARKAL (Fishbone and Abilock 1981; Loulou and Lavigne 1996), and a multi-region computable CGE model like GEMINI-E3 (Bernard and Vielle 1998, 2003). These three classes of models have been used by the economic analysis group of the NCCR-Climate to produce an integrated assessment of climate policies in conjunction with climate and climate-change impact models produced by other groups of the research network (see the companion paper on coupling). The paper is therefore organized in two parts. In the first part we show selected examples of endogenous technological learning (ETL) in the MERGE5 model and a multi-regional energy-system model (GMM) for assessing the impact of technological learning in atmospheric CO_2 stabilization scenarios. In the second part of the paper we address the problem of representing three types of strategic interactions in IAMs: (i) market power in international emission trading, (ii) strategic behavior

---

[1] A research network on climate supported by the Swiss NSF.

of government during the initial allocation of emission quotas across sectors, and (iii) strategic behavior of competing agents (nations) that are parties to the international negotiations on climate policies and have to share the burden of stabilizing CO_2 concentration in the long run.

2 Modeling endogenous learning in an IAM

In this first part we show how to endogenize technological learning in MERGE, an IAM that includes a "bottom-up" representation of the energy supply sector (Kypreos 2000, 2005; Kypreos and Bahn 2002; Manne and Barreto 2004) and also in GMM, a multi-regional energy system model (Barreto 2001; Rafaj et al. 2005). These studies evaluate the economic advantages of endogenous and induced learning via public and private RD&D spending in support of carbon-free generation technology. The method investigated herein prescribes early R&D support and learning investments in carbon-free systems to aid these technologies to follow learning curves. This dedicated RD&D spending influences developments during the demonstration and deployment phases and reduces the cost of new technologies. We assume that public RD&D spending of research institutes, together with the research investments of industries that act as global players, creates knowledge that can be compensated and appropriated via market diffusion and uptake of these new technological systems on the global level.

2.1 Technological learning in the MERGE model

As mentioned above, technological learning describes how the specific cost of a given technology is reduced through the accumulation of knowledge with respect to that technology. This learning process evolves either from manufacturing and operation of the technology (LBD) or research-and-development (LBS) expenditures allocated to that technology. A learning curve relates the specific cost incurred by a given technology to one or more factors describing the accumulation of knowledge in that technology. In MERGE, these factors are taken as the cumulative power generation in the one-factor learning curve, and the cumulative R&D expenditures in the two-factor learning curve. A number of ETL systems for electric and non-electric technologies have been introduced into MERGE (Bahn and Kypreos 2002; Kypreos 2000, 2005; Kypreos and Bahn 2002; Manne and Richels 2002). The first generic learning technology modeled in MERGE, corresponding to power generation and the second technology referring to a non-electric energy system. We have assumed for LBD that a 15% cost reduction is incurred for each doubling in production, and a 10% cost reduction for each doubling in the knowledge stock. Also, a barrier is introduced to represent a maximum possible reduction of generating cost of (e.g., 50 mills per kWh for electric backstop systems and 6 US$/GJ for the non-electric backstop). All technologies and the non-learning costs associated with these backstop systems, which represent the balance of plant, are assumed to be encompassed in an autonomous cost reduction at a rate of 0.5% per annum.

2.1.1 The Two Factor Learning Curve (TFLC)

The section describes the inclusion of endogenous technological learning in MERGE5, using the TFLC formula (e.g., with Learning-by-Doing and Learning -by- Searching components) (Criqui and Viguier 2000; Kouvaritakis et al. 2000). In the two-factor learning curve, the cumulative production (output) is used as a proxy for the accumulation of experience that

affects the specific investment cost of a given technology. Similarly, the knowledge stock, defined as the accumulation of a depreciated R&D spending, is used to determine cost reductions attendant to LBS processes. For example, the learning curve for the cost of electricity generation $GC_{k,t}$ (in US$ per MWh or US$ per GJ) of a technology k is defined as

$$GC_{k,t} = a \cdot CP_{k,t}^{-b} \cdot KS_{k,t}^{-c} \tag{1}$$

where $CP_{k,0}$ is the cumulative production, and $KS_{k,t}$ stands for the knowledge stock estimated as the depreciated sum of annual R&D

$$KS_{k,t} = KS_{k,t-1} \cdot (1 - s) + RD_{k,t} \cdot ypp_t \tag{2}$$

where $RD_{k,t}$ is the annualized research and development spending, s is the depreciation factor, and ypp_t the number of year per period.

The a parameter can be calibrated by applying equation 1 for the initial point of the learning curve ($GC_{k,0}, KS_{k,0}, CP_{k,0}$), and the b and c parameters are the learning indices. The latter define the speed of learning and are derived from the learning ratio. The learning ratio lr is the rate at which the generating cost declines each time the cumulative capacity doubles, while lrs is the rate at which the cost declines each time the knowledge stock doubles. The relation between b, c, lr and lrs can be expressed as follows:

$$1 - lr = 2^{-b} \tag{3}$$
$$1 - lrs = 2^{-c}.$$

For the introduction of LBD and LBS options and learning subsidies into the model, a few new variables and equations are defined. The cumulative production, $CP_{k,t}$, is based on the annual generation of unsubsidized, $PE_{k,t}$, and the amount of subsidized electricity production, $SPE_{k,t}$:

$$CP_{k,t} = CP_{k,t-1} + 0.5 \cdot (PE_{k,t} \cdot ypp_t + SPE_{k,t} \cdot ypp_t$$
$$+ PE_{k,t-1} \cdot ypp_{t-1} + SPE_{k,t-1} \cdot ypp_{t-1}). \tag{4}$$

The learning curve is represented as a non-linear and non-convex formulation in MERGE5 according to equation (5), which is based on cumulative production and the knowledge stock relative to the starting year[2]:

$$GC_{k,t} = \frac{GC_{k,0} \cdot CP_{k,t}^{-b} \cdot KS_{k,t}^{-c}}{CP_{k,0}^{-b} \cdot KS_{k,0}^{-c}} = GC_{k,0} \cdot \left(\frac{CP_{k,t}}{CP_{k,0}}\right)^{-b} \cdot \left(\frac{KS_{k,t}}{KS_{k,0}}\right)^{-c}. \tag{5}$$

The economic production variable Y_{rt} of MERGE must be reformulated to take into account the annualized R&D spending and the subsidies in learning investments:

$$Y_{rt} = C_{rt} + I_{rt} + EC_{rt} + DC_{rt} + NTX_{rt} + RD_{rt}$$
$$- \sum_k SPE_{rkt} \cdot sdy_{k,0} \left(\frac{CP_{k,t}}{CP_{k,0}}\right)^{-b} \cdot \left(\frac{KS_{k,t}}{KS_{k,0}}\right)^{-c}. \tag{6}$$

---

[2] The model is solved with the CONOPT3 optimizer using the procedure described in Manne and Barreto (2004).

We assume that in the periods 2010–2030, part of the costs for the two technologies (i.e. *sdy* in Equation (6) above) is either subsidized or is anyhow introduced in niche markets without charge. This cost consists of a maximum of 9 US$/GJ for the non-electric systems and 75 mills/kWh for the LBDE technology at the starting point of their introduction (e.g., in the year 2005), and diminishes strongly as the generation costs follow the autonomous reduction rate and the learning curves. Additionally, extra R&D spending is made available in the same periods to demonstrate technical feasibility, to reduce further the generation cost of carbon-free technology, and to accelerate their introduction.

2.1.2 The role of technological learning in CO_2 stabilization

Several scenarios related to CO_2 emission control are presented as illustrations of the results generated by this version of MERGE. Apart from the business-as-usual (BaU), cases where CO_2 emissions are not limited, we have considered the implications of stabilizing atmospheric CO_2 concentration to 450 ppmv and a case with 2 °C maximum temperature change. All three scenarios are assessed with and without ETL options. The baseline case is designated by BaU-N, where technological change is exogenous, whereas BaU-L denotes the baseline case where LBD applies, and BaU-S designates the case where the TFLC and learning subsidies apply. The database for the baseline cases reflects the original data of MERGE5, while the stabilization cases consider policies to abate all greenhouse gases (GHGs) and adopt carbon sinks.

In the BaU-N case, the world GDP grows more than 11 times (i.e., to US$365 trillion) between 2000 and 2100; but primary-energy supply and carbon emissions are strongly decoupled from economic growth and increase by only 3.8 times (i.e., to 1,430 EJ of primary energy per annum and 22.3 GtC/yr carbon emissions in 2100). In the BaU (-N, -L) cases, the global CO_2 concentration increases to 750 ppmv, while the global average temperature rise is 2.48 °C. Most of the economic growth occurs in economies (currently) in transition and in developing countries.

Policies that support technological learning result in a strong contribution of renewables in meeting non-electric-sector demands. This shift enhances the use of non-electric backstop technologies for which a learning rate of 15% cost reduction per doubling of production, and a 10% decrease per doubling of the knowledge stock has been assumed. For the BaU-S case, therefore, renewable-energy sources contribute 39%, coal 45%, nuclear 2% of the energy mix, with oil and gas contributing the remaining 14% compared to a 56% contribution for coal in the BaU-N scenario. Learning in the BaU-L case reduces emissions to 20.4 GtC/yr in the year 2100.

Properly applied R&D policies could result in a significant cost reduction of energy and carbon control costs. The scenarios where the atmospheric CO_2 concentration is held to 450 ppmv assume that efficient strategies will be adopted worldwide and a full-scope transfer of "know-how" will take place. Under these circumstances, the following conclusions can be made: First, the cumulative and undiscounted GDP losses because of the introduction of carbon-stabilization constraints at 450 ppmv, in relation to the cumulative baseline-GDP production, are low. For example, below 1.26% in the base case, while with LBD and LBS favorable policies the GDP losses[3] are less than 0.42% (Figure 1). Secondly, the marginal costs related to carbon stabilization are also reduced to a fraction of the marginal cost without learning (Figure 2), but remain significant for the case of the 450 ppmv atmospheric carbon limit.

---

[3] Cumulative GDP refers to the net present value (NPV). The discount rate is 5%.
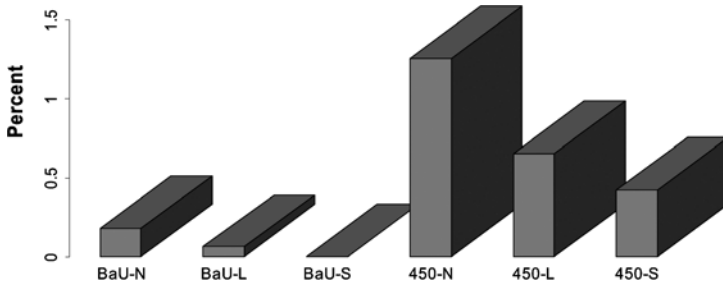
Fig. 1 Cumulative and discounted GDP losses for the stabilization cases of carbon concentration, relative to the GDP of BaU-S. The cumulative and undiscounted GDP losses are significantly reduced in the case of LBD and LBS. For the 450-ppmv cases, the cumulative loss of below 1.26% in the base case, while with LBD and LBS favorable policies the GDP losses are less than 0.42% (e.g., in LBD & LBS case)
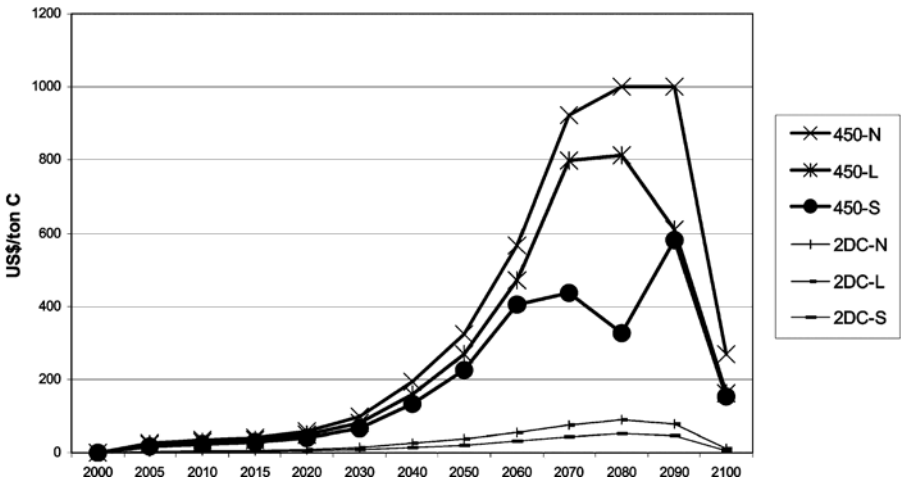
Fig. 2 The marginal costs of carbon control are significantly reduced in the case of RD&D policies

2.2 Technological learning in the energy-system GMM model

Technological learning is an important mechanism influencing the technology dynamics of the global energy system. Market experience is one of the main channels to accumulate technology learning, leading to cost reductions and performance improvements that could allow new technologies to become competitive in the long term. Demonstration and deployment (D&D) programs play an important role in enabling the accumulation of valuable market experience for cleaner and more efficient emerging energy technologies and are key policy instruments to stimulate their progress. Impact assessment of policy instruments is an important component of the policy-making process of, among others, the European Commission, in particular in the context of the implementation of sustainable development strategies (EC 2002). It represents a systematic effort to evaluate changes on sustainability indicators due to a policy measure (EC 2002). This section provides some insights into the effects of D&D programs in achieving diffusion of new technologies and their impact on indicators of sustainability of the global energy system in the areas of climate change and security of

energy supply. The analysis has been conducted with an extended version of the "bottom-up" energy-systems GMM model (Barreto and Kypreos 2004a,b; Rafaj et al. 2005). GMM is a global, multi-regional optimization model that allows a detailed representation of energy supply and end-use technologies. The GMM model endogenizes one-factor learning, or experience, curves (hereon referred to as 1FLC), where cumulative installed capacity is used as a proxy for accumulated experience.[4]

For this analysis, the energy-system GMM model has been substantially extended (Barreto and Kypreos 2004b). Marginal abatement curves for two main non-CO_2 gases (CH_4 and N_2O) have been incorporated. Among others, a clusters approach to technology learning, based on the "key technology" approach, where key learning components (e.g. a gas turbine) are shared by several technologies (e.g. gas combined-cycle, IGCC, etc), has been implemented. The model is calibrated to year-2000 international energy statistics and spans through the time horizon 2000–2050 with ten-year time steps. A discount rate of 5% is used in all calculations reported herein (see Barreto and Kypreos (2004b) for a more detailed description of the model).

2.2.1 Methodology

In order to assess the impact of a given policy instrument, we examine the incremental change in a number of sustainability indicators when the policy instrument, D&D programs in this case, is applied relative to the costs of application of the instrument. In what follows, this measure is referred to as the "impact" of the policy instrument and is defined as follows:

$$\text{Impact} = \frac{\Delta \text{ Indicator}}{\text{Instrument Cost}}. \tag{7}$$

In conducting this analysis, the methodology of D&D "shocks" has been applied. D&D shocks are one-time increments in the installed cumulative capacity, a proxy for the accumulated experience of a given key learning component, at the beginning of the time horizon. Essentially, a D&D shock will let the key component move down its learning curve, i.e. by increasing the installed cumulative capacity it will reduce the corresponding specific investment costs as illustrated in Figure 3.

2.2.2 Simulation results

In the illustrative results presented here, standard D&D shocks of US$ 10 billion size have been applied to the GMM model during the first time period when the technology is assumed to be available (equivalent to US$1 billion per year during a 10-year time period). A standard D&D shock size has been chosen in order to be able to compare the effects of D&D shocks for different technologies on a common basis. This gives a policy maker a clearer notion of what the impacts on sustainability indicators would be if a given sum of money is invested on a D&D program for a particular technology. The impact of D&D shocks on selected technologies on two sustainability indicators related to climate change and security of energy supply, namely global CO_2 emissions and global resource-to-production (Ru/P) ratio for oil (measured in years) is illustrated in Figures 4 and 5. Both indicators are reported for the

---

[4] For this 1FLC representation, a piece-wise linear approximation of the learning curve is implemented through Mixed Integer Programming (MIP) techniques in the GMM model. For a detailed description (see Barreto and Kypreos 2004a).
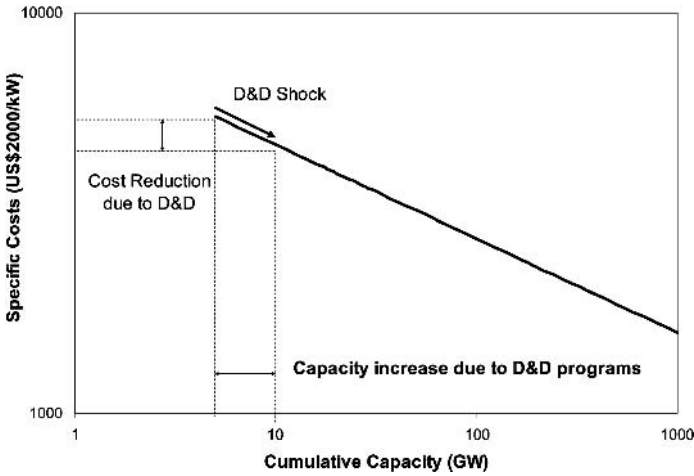
Fig. 3 Schematic illustration of the effect of demonstration and deployment (D&D) programs ("shock") on the learning curve of a key component

Fig. 4 Impact of selected D&D shocks on the global CO_2 emissions in the year 2050
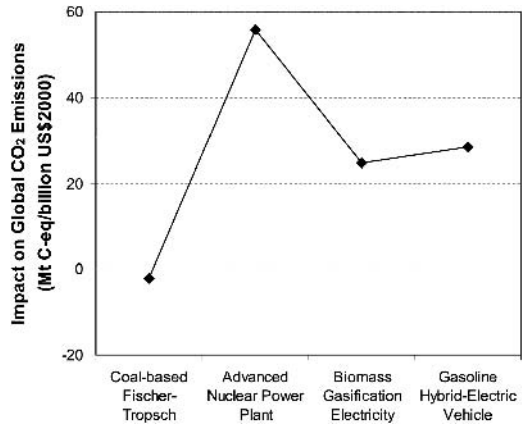
year 2050. For the estimation of the global oil Ru/P ratio only conventional resources were considered. The illustrative technologies chosen here for the D&D shocks are as follows: Coal-based Fischer-Tropsch liquids, advanced nuclear power plants, biomass gasification power plants and gasoline hybrid-electric cars.

Impacts are measured relative to the baseline case. That is, no other policy instruments (e.g. CO_2 taxes) have been assumed to be imposed on the global energy system. Notice that, by convention, positive impacts are associated with an improvement of the sustainability indicator (e.g. a reduction in CO_2 emissions). As expected, positive impacts on CO_2 emissions are higher for low-carbon technologies (see Figure 4). Specifically, under our assumptions, advanced nuclear power plants achieve the highest positive impact on CO_2 emissions. Coal-based Fischer-Tropsch liquids, on the other hand, have a negative impact on CO_2 emissions. The set of illustrative technologies chosen here shows positive impacts on the global petroleum resource-to-production ratio (see Figure 5).

Among other factors, the clusters approach to technology learning may have a significant impact on the results, because of the interactions it creates between technologies. When a given technology receives a D&D shock, this implies a stimulus for the installations of its learning and non-learning components. Through the action of clusters, the D&D "shock" is a stimulus to deploy other technologies sharing the key learning components as well. Demonstration and deployment (D&D) programs constitute an important policy measure for accumulating valuable market experience that could stimulate technology learning of emerging, cleaner and more efficient energy technologies. Specifically, a strategic management of niche markets, where a technology may be attractive due to specific advantages or particular applications, may stimulate its diffusion process.

3 Modeling strategic competition

The second part of this paper addresses another strand of problems where strategic behavior of the agents should be taken into account. They concern the implementation of international emissions trading systems either in the Kyoto or post-Kyoto frameworks.

Under the Kyoto agreement, the states of the former Soviet Union (FSU) have received emissions quotas based on their 1990 performances. After the collapse of Soviet Union these quotas have yield large levels of almost zero-cost abatement opportunities that have been called "hot air" in the negotiators jargon. This gives to Russia in particular a potential domination of the emissions trading market. However another source of low cost abatement opportunities exists in developing countries, in particular China. The stage is therefore set for a sort of oligopolistic competition between between these two potential large sellers of emissions rights. In the first subsection below we shall briefly review a two-level dynamic game model that has been developed to evaluate the possible effects of this competitive structure on the evolution of carbon price in the Kyoto emissions permit market scheme Bernard et al. (2005); Haurie and Viguier (2003).

Another possibility of strategic behavior appears in the implementation of the emissions trading scheme in the European Union (EU) when each country has to decide how to allocate the quotas to different sectors of the economy. Due to market imperfections associated with the fiscal systems and also with the fact that the whole economy is not allowed to take part

in the trading system, the way countries allocate the quotas is not indifferent. Furthermore, because of trade effects the welfare gains obtained from the allocations decided by the different countries are interdependent. This defines a gaming situation, described in the second subsection, that has been addressed by Viguier et al. (2006) in a two-level m-matrix game model for which correlated equilibrium solutions can be computed to evaluate the actions of the dominating countries in EU.[5]

In the third subsection below we present the extension of this game theoretic framework to the possible post-Kyoto negotiations that should take place once one knows the real extent of the global climate change process and hence the limits to impose on global GHG emissions over the rest of the century. An international agreement should be "self-enforcing" and this calls for a set of national policies that constitute a Nash equilibrium for a strategic game. We present below a dynamic game model where a set of nations bound to satisfy collectively a constraint on global emissions play a noncooperative game on the definition of their relative emission quotas.

These three game theoretic models share the same two-level structure. At the lower level one represents the world economy in the form of a computable general economic equilibrium (CGE) model. Emissions rights or quotas are the strategic variables whereas emissions trading is the result of a market equilibrium. These two-level games represent a step in the direction of a better representation of the strategic opportunities that are inherent to the implementation of an international emissions trading system.

3.1 A two-level dynamic game of "hot-air" competition

3.1.1 The model

Bernard et al. (2005) have proposed a deterministic dynamic game model to show the possible competition between Russia and entrant developing countries on the emissions market. They formalized the "hot-air" competition problem as a dynamic multistage game for which they computed an open-loop Nash equilibrium solution (Başar and Olsder 1989; Dockner et al. 2000; Rosen 1965).[6] The model has the structure of a Cournot duopoly model with depletable resource stocks representing the banked emission permits. These stocks can be replenished via an abatement activity. The discrete time model has periods $t = 0, 1, \ldots, T$. Each player controls a dynamical system described as follows:

– **Player 1**: It represents Russia which benefits from "hot air". The following variables and parameters enter into the description of Player 1:

β_1: discount factor for player 1
$x_1(t)$: stock of permits that are banked by player 1 at time t
$u_1(t)$: permits that are supplied by player 1 at time t
$h(t)$: "hot air" input for player 1 at time t
$q(t)$: emissions abatement for player 1 at time t
$c_1(q_1)$: cost function for emissions abatement
π_1: terminal value of the stock of permits

In the above list of parameters and variables, the time function $h(t)$, which is exogenously given, represents the amount of credited "hot air" emissions abatement at each

---

time t. We assume $h(t) \geq 0$ if $t < T$ and $h(T) = 0$. The dynamical system representing Player 1 is defined as follows:

$$\max \quad \sum_{t=0}^{T-1} \beta_1^t [p(t)u_1(t) - c_1(q_1(t))] + \beta_1^T \pi_1 x_1(T) \tag{8}$$

$$\text{s.t.} \quad x_1(t+1) = x_1(t) - u_1(t) + h(t) + q_1(t) \tag{9}$$

$$x_1(0) = 0 \tag{10}$$

$$u_1(t) \geq 0 \tag{11}$$

$$x_1(t) \geq 0. \tag{12}$$

– **Player 2**: It represents a large developing country (typically China) which may develop its own market of emission rights instead of the CDM scheme. The following variables and parameters enter into the description of Player 2:

β_2: discount factor for player 2
$x_2(t)$: stock of permits that are banked by player 2 at time t
$u_2(t)$: permits that are supplied by player 2 at time t
$q_2(t)$: emissions decrease due to Player 2 abatement activities
$c_2(q_2)$: cost function for emissions abatement
π_2: terminal value of the stock of permits
θ: period at which China may join the market

The dynamical system representing Player 2 is defined as follows:

$$\max \quad \sum_{t=0}^{T-1} \beta_2^t [p(t)u_1(t) - c_2(q_2(t))] + \beta_2^T \pi_2 x_2(T) \tag{13}$$

$$\text{s.t.} \quad x_2(t+1) = x_2(t) - u_2(t) + q_2(t) \tag{14}$$

$$x_2(0) = 0 \tag{15}$$

$$u_2(t) \geq 0 \tag{16}$$

$$u_2(t) \equiv 0 \quad \forall t \in [0, \theta] \text{ where } \theta < T \tag{17}$$

$$x_2(t) \geq 0. \tag{18}$$

– **Price of permits**: An inverse demand law describes the market clearing price for permits in Annex B countries.

$$p(t) = D(u_1(t) + u_2(t)). \tag{19}$$

This demand function is derived from the competitive equilibrium conditions for the Annex B countries in each period.

We look for a Nash equilibrium solution, assuming an open-loop information structure (the reader is referred to Başar and Olsder (1989) for a presentation of the information structures in dynamic games). It means that the competing agents select an open-loop control, that is a time schedule for their supply of emission permits over the planning horizon $0, 1, \ldots, T-1$. The optimality conditions are obtained by formulating the first order Nash equilibrium conditions.

The search for an equilibrium solution is then formulated as a nonlinear complementarity problem for which efficient algorithms exist.

3.1.2 Simulation results

For the numerical experiments, we use simulation results of a CGE model, GEMINI-E3, and a partial equilibrium model of the world energy system, POLES, (Criqui 1996). In order to investigate the impact of strategic behaviors on the markets for tradable permits, we compare a case where Russia is the only supplier in the market, and thus acts as a monopoly with a case where Russia and China play the emission permits game described in the previous section.

In the two cases, the demand of emission permits is assessed under a "Kyoto Forever" scenario, implying that Annex B countries (except the US) are committed to a constant level of emissions over time - the one sets in the Protocol – while non-Annex B countries remain free of any commitment. We suppose that emission permits are freely tradable in the international market. It is also assumed that Russia can freely trade its hot air, and that emission permits can be banked without constraint. The terminal value of the stock of permits is supposed to be equal to zero. We apply a 5% discount rate. Finally, we assume no transaction costs in the two base cases. The impacts of China's participation in the post-Kyoto regime, and transaction costs on the emission markets, will be assessed further.

Russia banks a large portion of "hot air" (88% in 2010) in the monopoly case in order to maximize its trading gains. Since the permits demand is relatively inelastic to prices in GEMINI-E3, there is a rather high incentive for Russia to act as a monopolist, and to let prices go up by restricting its supply of permits. In the monopoly case, the permit price rises from 140$/tC in 2010 to 213$/tC in 2030 (Figure 6). As expected, the amount of permits banked by Russia decreases when it has to compete with China in CO_2 emission markets. When revenues from permits sales depend on its own supply and the other country's supply (duopoly scenario), the Nash-Cournot equilibrium price is much lower than the monopoly price. Set at 90$/tC in 2010, the permit price rises slowly to 128$/tC in 2030.

3.2 A correlated equilibrium solution to the EU emission quotas allocation game

In this section we analyze another risk of strategic behavior of the countries involved in the implementation of CO_2 markets: a manipulation of the initial allocation of emission quotas

Fig. 6 Price of CO_2 permits (Monopoly & Duopoly cases)
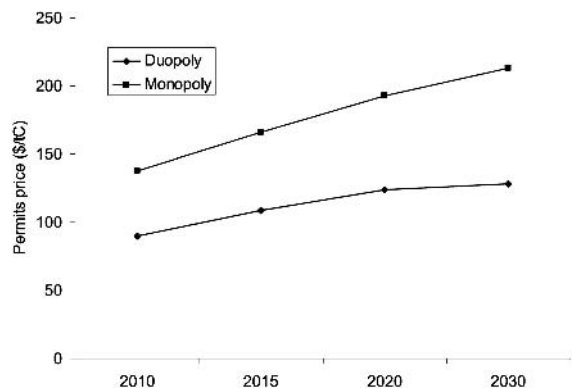
in order to subsidize their energy-intensive industries. One should represent the problem as a non-cooperative game and look for some equilibrium solution. As explained in Viguier et al. (2006), this game has a two-level structure since the strategies selected by the players have consequences that are calculated from a computable general equilibrium model. The upper-level game is represented as an M-matrix game, where M is the set of active countries and where the payoffs are obtained by running a CGE model (i.e. GEMINI-E3) under the configurations associated with the different possible strategy choices. The upper-level game will be solved for the characterization of the set of *correlated equilibria* (see Aumann 1974).

3.2.1 The model

The games is played by countries or groups of countries that may manipulate the initial allocation of emission quotas. The strategies are the different (contrasted) allocation schemes that could result from individual decisions over quotas allocation. The payoffs of the game are the welfare gains (-losses) for each player resulting from Kyoto emission targets under the EU-wide trading regime. Again, we say that these games have a two-level structure since the strategies selected by the players have consequences that are calculated from a computable general equilibrium model. The upper-level game is represented as an M-matrix game, where M is the set of active countries and where the payoffs are obtained by running GEMINI-E3 under the configurations associated with the different possible strategy choices. The upper-level game is solved for the characterization of the set of *correlated equilibria*. The game in strategic form is defined by $\Gamma = (M, (S_j)_{j \in M}, (u_j)_{j \in M})$ where M is the set of players, S_j is the set of our strategies of player j and $u_j : \Pi_{i \in M} S_i \to \mathbf{R}$ is the payoff function for player j. Let us denote $\mathcal{S} = \Pi_{i \in M} S_i$ and $\mathbf{s} = (s_j)_{j \in M} \in \mathcal{S}$. A correlated equilibrium is defined by a probability distribution on $\mathcal{S}$, $\pi(\mathbf{s}) \geq 0$, $\sum_{\mathbf{s} \in \mathcal{S}} \pi(\mathbf{s}) = 1$ such that the following inequalities hold

$$\sum_{\mathbf{s} \in \mathcal{S}} \pi(\mathbf{s}) u_j(\mathbf{s}) \geq \sum_{\mathbf{s} \in \mathbf{S}} \pi(\mathbf{s}) u_j(\mathbf{s}_{-j}, \sigma_j), \quad \forall j \in M, \forall \sigma_j \in S_j. \tag{20}$$

where

$$(\mathbf{s}_{-j}, \sigma_j) = (s_i, \ldots, s_{j-1}, \sigma_j, s_{j+1}, \ldots, s_m) \tag{21}$$

and $M = 1, \ldots, m$.

The interpretation can be the following: through a preplay communication scheme the agents may exchange signals that sum up to each player receiving a recommendation to play a given strategy. The probability $\pi(\mathbf{s})$ is affected to the event: *the vector* $\mathbf{s}$ *is recommended as a way to play the game*. We have to realize that, in this interpretation, each player knows only the recommendation to play that concerns him. The inequalities (20) express the fact that a player has no incentive to play other than as recommended.

In brief we could view a correlated equilibrium either as the result of playing a game where a *mediator* sends private information to each player, in the form of a recommendation to play a given strategy, or as the result of the use of communication strategies by the players, where each player would send reports to the other players (and receive reports from the others) before deciding what to do. We can see the relevance of this scheme in the context of EU-wide negotiation for the implementation of a tradable emission permit scheme.

It is well known that the set of correlated equilibria in an M-matrix game is closed and compact and can be characterized through the solution of linear programs. The set of

correlated equilibria contains the set of Nash equilibria. Therefore, if this set of correlated equilibria reduces to a singleton, it is the unique Nash equilibria for the game.

3.2.2 Simulation results

The allocation of CO_2 emission quotas in the implementation of the EU-wide emission trading market can be viewed as an example of a "permits allocation game". Viguier et al. (2006) represent this situation as an M-matrix game, where the strategic players are Germany (DEU), the United Kingdom (UK), Italy (ITA), and the rest of the European Union (REU). We assume that these regions may choose among four different rules to allocate emission allowances across economic sectors:

1. Grandfathering (GF): Emission allowances are allocated among sectors according to their historical emissions taking into account a global target of emissions reduction at the national level;
2. Historical emissions (HE): The total number of allowances allocated to a given trading sector is determined by its share in each Member Stateís emissions from economic sectors included in the trading scheme emitted in a particular year (e.g. 2001), multiplied by total allowable emissions for the economy;
3. Domestic Tax-based (DT): Sectoral allowances correspond to the ones that would occur if a uniform carbon tax were to be implemented at the domestic level;
4. European Tax-based (ET): Sectoral allowances correspond to the ones that would occur if a uniform carbon tax were to be implemented at the European level.

We simulate three different games with four players and three strategies. In Game 1, one assumes that the reference rule for quotas allocation corresponds to the one equalizing marginal abatement costs across sectors at the domestic level (DT). We assess the incentive for EU countries to deviate from the DT allocation by giving 10 percent more (or less) quotas to the trading sector. In Game 2, the players can choose among more contrasted strategies. We allow EU countries to deviate a little bit more from the DT approach by giving more (GF) or less (e.g. ET in Germany) quotas to the trading sector. In Game 3, the only way for EU countries to strategize on the allocation of quotas is to give more quotas to the trading sector; the GF approach corresponds to a lower deviation from the ET rule than the HE approach.

In our numerical experiments it turns out that the games have a unique correlated equilibrium which then corresponds to a unique Nash equilibrium in pure (instead of mixed) strategies (see Table 1). The equilibria are always different from the competitive equilibrium solutions, where the different regions would play the same DT strategy. Germany, which is the main supplier of emission allowances, tends to rely on the domestic tax-based approach (DT) but the other regions, which are permits buyers, have an incentive to depart from this approach to maximize their own payoffs. The outcomes of the non-cooperative equilibria

Table 1 Unique correlated equilibria

	Game 1	Game 2	Game 3
Germany	DT	DT	DT
UK	DT−10	GF	GF
Italy	DT+10	DT	HE
Rest of EU-15	DT+10	GF	GF

Table 2 Payoffs in correlated equilibria versus cooperative equilibria (in million dollars)

	Cooperative equilibria			Correlated equilibria		
	Game 1	*Game 2*	*Game 3*	*Game 1*	*Game 2*	*Game 3*
Germany	1254	1308	953	599	808	526
UK	−1646	−1807	−1526	−1880	−2090	−1933
Italy	−2665	−2854	−2726	−2614	−2844	−2709
Rest of EU−15	−4384	−4578	−4482	−4072	−4117	−4095
Total	−7442	−7931	−7781	−7967	−8244	−8211

are globally lower than what the players would obtain by playing the cooperative solution (see Table 2). There is no strict dominance of the correlated equilibria by the cooperative solutions with equal weight. Germany and the United Kingdom are always worse off with the non-cooperative solution but Italy and the rest of Europe are better off. Italy and the other EU countries have thus an incentive to depart from the cooperative solution. But this incentive to act strategically is relatively weak since strategic behaviors have a limited impact on the payoffs of the players.

3.3 A normalized equilibrium solution to a Post-Kyoto game of quota negotiations

Haurie et al. (2005a, 2005b) propose a dynamic game model for the international negotiations that will take place to share the burden of stabilizing in the long run the global CO_2 concentration in the atmosphere. The model assumes a non-cooperative behavior of the parties except for the fact that they will be collectively committed to reach a target on total cumulative emissions by the year 2050. Indeed, we assume that countries have thus to agree on the long term CO_2 concentration target that should be reached collectively. Given this common target each (group of) nation's respective contribution to the international effort will be guided by its own interest, if the agreement has to be self-enforcing. In that context, international emission trading might be used as a mean to reduce the economic costs of the emission constraint, and to create incentives for participation through financial transfers. Once the global goal is defined the degrees of freedom left to the players reside in the level and timing of their abatement commitments. The concept of normalized equilibrium is used to characterize a family of dynamic equilibrium solutions in an m-player game where the agents are (groups of) countries and the payoffs are the welfare gains obtained from economic activities, including trading of goods and emission permits. A coupled constraint is introduced to represent the needed global emissions abatement.

3.3.1 The model

The game is played over T periods. M is a set of m groups of countries hereafter called *players* which must decide on the caps they impose on their respective global emissions of CO_2 in each period. We denote $\bar{e}_j(t)$ the cap decided by player j for period $t = 1, \ldots, T$. A global limit $\bar{E}$ will be imposed on the cumulative emissions over the time horizon T.

Therefore the following constraints are imposed on all players together

$$\sum_{j \in M} \sum_{t=1}^{T} \bar{e}_j(t) \leq \bar{E}. \tag{22}$$

Let $\bar{\mathbf{e}}(t) = \{\bar{e}_j(t)\}_{j \in M}$ denote the vector of caps decided for all players in period t. The result of a global economic m-country equilibrium defines a welfare gain for each player, hereafter called its payoff at t and denoted $W_j(\bar{\mathbf{e}}(t))$. Given a choice of moves $\bar{\mathbf{e}} = \{\bar{\mathbf{e}}(t)| : t = 1, \ldots, T\}$ also called an *emissions program* the total payoff to player j is given by

$$J_j(\bar{\mathbf{e}}) = \sum_{t=1}^{T} \beta^{t-1} W_j(\bar{\mathbf{e}}(t)) \quad j \in M. \tag{23}$$

where β is a common discount factor.

3.3.2 Normalized equilibrium solutions

We assume that the players behave in a noncooperative way but are bound to satisfy the global cumulative emissions constraints (22) that are consistent with a long term CO_2 concentration target. We therefore use the *normalized equilibrium* solution concept as proposed by Rosen (1965) to deal with concave m-player games when coupled constraints are linking the decisions of all players. We call $\mathcal{E}$ the set of emissions $\bar{\mathbf{e}}$ that satisfy the constraints (22). We denote $[\bar{\mathbf{e}}^{*-j}, \bar{e}_j]$ the emissions program obtained from $\bar{\mathbf{e}}^*$ by replacing only the emissions program $\bar{e}_j^*$ of player j by $\bar{e}_j$.

Definition. The emissions program $\bar{\mathbf{e}}^*$ is an equilibrium under the coupled constraints (22) if the following holds for each player $j \in M$

$$\bar{\mathbf{e}}^* \in \mathcal{E} \tag{24}$$

$$J_j(\bar{\mathbf{e}}^*) \geq J_j([\bar{\mathbf{e}}^{*-j}, \bar{e}_j]) \quad \forall \bar{e}_j \text{ s.t. } [\bar{\mathbf{e}}^{*-j}, \bar{e}_j] \in \mathcal{E}. \tag{25}$$

Therefore, in this equilibrium, each player replies optimally to the emissions programs chosen by the other players, under the constraint that the global cumulative emission limits must be respected.

It has been shown by Rosen that a class of equilibria under coupled constraints, called *normalized equilibria*, could be obtained in the following way. Let $\mathbf{r} = (r_j)_{j \in M}$ with $r_j > 0$ and $\sum_{j \in M} r_j = 1$ be a given weighting of the different players. Assuming the required regularity we can introduce a Kuhn-Tucker (K-T) multiplier λ^o for the constraint $\sum_{t=1}^{T} \bar{e}_j(t) \leq \bar{E}$ and form the Lagrangians

$$J_j(\bar{\mathbf{e}}) + \lambda^j \left(\bar{E} - \sum_{j \in M} \sum_{t=1}^{T} \bar{e}_j(t) \right), \tag{26}$$

where

$$\lambda^j = \frac{1}{r_j} \lambda^o. \tag{27}$$

The *normalized equilibrium* associated with the weighting **r** is the Nash equilibrium solution for the auxiliary game with a payoff function defined for each player j by (26), where the common K-T multiplier λ^o is such that

$$0 \leq \lambda^o$$

$$0 = \lambda^o \left(\bar{E} - \sum_{j \in M} \sum_{t=1}^{T} \bar{e}_j(t) \right).$$

This characterization has an interesting interpretation in terms of negotiation for a climate change policy. A common "tax" λ^o is defined and applied to each player with an intensity $\frac{1}{r_j}$ that depends on the weight given to this player in the global response function. Rosen has also given conditions, called diagonal strict concavity, on the function $\sum_{j \in M} r_j J_j(\bar{\mathbf{e}})$ which ensure existence and uniqueness of the normalized equilibrium associated with the weighting **r**. Therefore, under these conditions, we can define a manifold of equilibria outcomes indexed over the set of possible weights **r**. In general, when its relative weight r_j increases the burden of Player j in satisfying the coupled constraint diminishes and its payoff increases at equilibrium.

3.3.3 Simulation results

The policy scenario is built on the assumption that we are collectively committed to stabilize global CO_2 concentration at no more than 550 parts per million (ppm) in order to limit global temperature rise to 2 degrees Celsius above pre-industrial levels (see Haurie et al., 2005a). The CO_2 concentration target is translated into a global target on total cumulative emissions by 2050. It is thus assumed that the countries and regions decide unilaterally on their own abatement targets under this coupled emission constraint. In this first experiment, we only consider two periods of commitment of 25 years each (2000–2025 and 2025–2050). It means that countries and regions have to take decisions on their own abatement reduction level in 2000 and 2025.[7] The payoffs are based on households surplus (payoffs) computed by GEMINI-E3 are discounted at 3% per year, and the target is supposed to be reached through a global emissions trading system. The problem is solved by implementing an oracle based method where at each iteration the CGE, hereafter called the "oracle" is queried and returns an information consisting of (i) the evaluation of the payoff values and, (ii) the evaluation of the pseudogradient at the query point (Haurie et al. 2005a).

As explained by Rosen (1965), the unique normalized equilibrium should change with the weighting **r** of the different players. This weighting might be defined in consistency with distributive justice precludes. It could be based on population, macro-economic indicators (i.e. GDP, consumption) and/or environmental indicators (i.e. history of GHG emissions). The weighting could also reflect the negotiating power of the players. In order to explore how equilibria might change with different weights, one can assess the effect of increasing the weight of developing countries compared to a "balanced" policy case where the same weight is put on the different players. As expected, this has the effect of reducing the cost of the climate policy for developing countries (DCs) (Figure 7).

As shown on the graph, one can define a weighting that would lead to an equilibrium where DCs do not support any welfare cost. This equilibrium does not correspond to the

---

[7] Since GEMINI-E3 computes an equilibrium every year, we assume a linear emissions reduction rate for each period of 25 years.
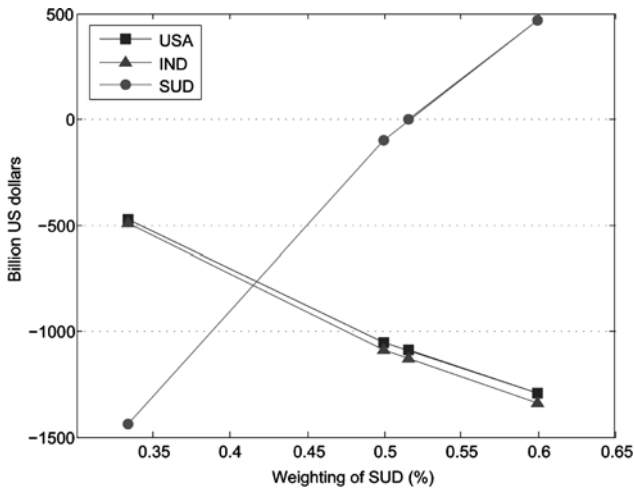
Fig. 7 The impact of changing the relative weight of SUD on discounted welfare costs for USA, other industrialized countries (IND) and developing countries (SUD), 2000–2050 (in billion USD).

burden sharing option, advocated by IEA (2002) and Philibert and Pershing (2001), where the baseline emissions are given to the DCs (also called the "non-constraining target" option). It is a situation where the costs of meeting the domestic reduction targets are balanced by the gains associated with the selling of emission permits. Based on GEMINI-E3 estimates, we find that DCs might preserve their welfare growth while accepting a 20% reduction target (compared to their baseline). As shown in Figure 7, DCs are better off when their weight increases above 53%. They might voluntarily accept to reduce their GHG emissions in order to participate in international emission trading. This result tend to show that market-based environmental instruments might be used as a good incentive for future global climate policy.

4 Conclusion

This paper has presented selected examples of attempts to represent endogenous technological learning and imperfect competition effects in different modelling frameworks. In the examples developed in this paper, we have shown the potential effects of strategic investments on R&D activities and demonstration and deployment (D&D) programs in climate-change mitigation policies quantified with perfect-foresight models. In addition, we have used game-theoretic models of Kyoto protocol implementation to illustrate the decrease in cost-effectiveness due to the possible strategic behaviour of powerful agents. Specifically, we highlight the fact that the conclusions obtained from models based on the pure competition paradigm can be far from those that could result from strategic behavior of governments in the concerned countries. Although these issues have been dealt with separately in our studies, in reality both represent important elements affecting the architecture and success of international climate-policy agreements. Moreover, strategic decisions by important global players in one area could affect the other as well. Examining the two topics in a common framework could be a promising avenue for further work. For instance, the interplay between R&D activities and climate change cooperation can be considered together in a game-theoretic approach (e.g. Buchner et al. 2005; Kemfert 2005).

The main results of our analysis can be summarized as follows:

– The endogenization of experience curves represents an advance in the modeling of tech-
nological change in energy-system models, capturing the early investments required for
a technology to progress and achieve long-term cost competitiveness in the marketplace
(Messner 1997). Our analysis illustrates the role that early investments on R&D activities
and demonstration and deployment (D&D) programs could play in supporting the devel-
opment and diffusion of cleaner technologies in the long term. Public-private partnerships
and international co-operation on these topics could be useful to share the risks and costs of
clean technology development and diffusion. Our results highlight the importance of these
two policy instruments as key strategic elements in climate-change mitigation strategies,
which must be designed such that they encourage technological innovation and progress
and enable a transition in the long run towards a cleaner, more efficient, and supply secure
technological path.
– As a consequence of the U.S. withdrawal of the Kyoto Protocol, low-cost countries (i.e.
Russia) may have a strong incentive for strategic behavior on the CO_2 market; however, our
simulations show that this market power will ultimately depend on developing countries'
strategies in future commitment periods.
– High-cost countries might be tempted to act strategically in climate policy implementation,
and to favor their domestic industry through the initial allocation of emissions quotas; when
the emissions markets are imperfect (i.e. some sectors are excluded from the EU emissions
trading system), these non-cooperative behaviors increase the global cost of the carbon
constraint.
– The Post-Kyoto negotiation should focus on the global GHG concentration target to be met
collectively and the implementation of a world emission trading regime; Once countries and
regions agree on the coupled long term constraint, developing countries might voluntary
accept emissions caps that would result from a non-cooperative equilibria in order to sell
emission permits.

References

Aumann RJ (1974) Subjectivity and correlation in randomized strategies. Journal of Mathematical Economics
1:67–96
Babiker M, Criqui P, Ellerman D, Reilly J, Viguier L (2003) Assessing the impact of carbon tax differentiation
in the European Union. Environmental Modeling & Assessment 8(3):187–197
Babiker M, Reilly J, Viguier L (2004) Is international emission trading always beneficial? The Energy Journal
25(2):33–56
Başar T, Olsder G (1989) Dynamic noncooperative game theory. Academic Press, London
Bahn O, Kypreos S (2002) MERGE-ETL: An optimisation equilibrium model with two different endogenous
technological learning formulations. PSI Report 02-16, Paul Scherrer Institute, Villigen
Barreto L (2001) Technological learning in energy optimisation models and the deployment of emerging
technologies. Thesis no. 14151, Swiss Federal Institute of Technology Zurich (ETHZ)
Barreto L, Kypreos S (2004a) Emissions trading and technology deployment in an energy-systems "Bottom-
Up" model with technology learning. European Journal of Operational Research 158:243–261
Barreto L, Kypreos S (2004b) Extensions to the Energy-System GMM Model for SAPIENTIA. Report to the
EC-sponsored SAPIENTIA Project ENK6-CT-2002-00614, Paul Scherrer Institute, Energy Economics
Group, Paul Scherrer Institute, Villigen, Switzerland
Barrett S (1997) The strategy of trade sanctions in international environmental agreements. Resource and
Energy Economics 19:345–561

Barrett S (1999) A theory of full international cooperation. Journal of Theoretical Politics 11(4):519–41

Bernard A, Haurie A, Vielle M, Viguier L (2005) A two-level dynamic game of carbon emissions trading between Russia, China, and Annex B Countries. Journal of Economic Dynamic & Control. Preliminary Accepted for Publication

Bernard A, Paltsev S, Reilly J, Vielle M, Viguier L (2003) Russia's role in the Kyoto Protocol. Report 98, MIT Joint Program on the Science and Policy of Global Change, Cambridge MA

Bernard A, Vielle M (1998) La structure du modèle GEMINI-E3. Economie & Prévision 5(136)

Bernard A, Vielle M (2003) Measuring the welfare cost of climate change policies: A comparative assessment based on the computable general equilibrium model GEMINI-E3. Environmental Modeling & Assessment 8(3):199–217

Buchner B, Carraro C, Cersosimo I, Marchiori C (2005) Back to Kyoto? US participation and the linkage between R&D and climate cooperation. In: Haurie A, Viguier L (eds) Cloupling climate and economic dynamics. Kluwer Academic Publishers, Chapt. 5

Carraro C, Siniscalco D (1996) R&D cooperation and the stability of international environmental agreements, In: Carraro C (ed) International environmental negotiations. Kluwer Academic Publishers

Ciscar J, Soria A (2004) Kyoto and beyond Kyoto climate policy: comparison of open-loop and feedback game outcomes. In: Carraro C, Fragnelli V (eds) Game practice and the environment. Cheltenham, UK -Northampton, MA: Edward Elgar

Criqui P (1996) POLES 2.2, Technical Report, JOULE II Programme, European Commission DG XVII - Science Research Development, Bruxelles, Belgium

Criqui P, Viguier L (2000) Kyoto and technology at world level: Costs of CO_2 reduction under flexibility mechanisms and technical progress. International Journal of Global Energy Issues 14:155–168

Dockner E, Jorgensen S, Long N, Sorger G (2000) Differential games in economics and management sciences. Cambridge, UK: Cambridge University Press

EC (2002) Communication from the commission on impact assessment. Technical Report COM(2002) 276 Final, European Commission, Brussels, Belgium

Fishbone L, Abilock H (1981) MARKAL, a linear programming model for energy systems analysis: technical description of the BNL version. International Journal of Energy Research 5:353–375

Forgo F, Fulop J, Prill M (2005) Game theoretic models for climate change negotiations. European Journal of Operational Research 160:252–267

Germain M, Toint P, Tulkens H, de Zeew A (1998) Transfers to sustain core-theoretic cooperation in international stock pollutant control. Discussion Paper 9832, CORE

Goulder L, Mathai K (2000) Optimal CO_2 abatement in the presence of induced technological change. Journal of Environmental Economics and Management 39:1–38

Hahn R (1984) Market power and transferable property rights. Quarterly Journal of Economics 99(4):753–765

Haurie A, Moresino F, Vielle M, Viguier L (2005a) A coupled equilibrium model of international climate policy. Mimeo

Haurie A, Moresino F, Viguier L (2005b) A two-level differential game of international emissions trading. Annals of the International Society of Dynamic Games. To appear

Haurie A, Viguier L (2003) A stochastic dynamic game of carbon emissions trading. Environmental Modeling and Assessment 8:239–248

IEA (2002) Beyond Kyoto. Energy dynamics and climate stabilisation. Paris, France: International Energy Agency

Kemfert C (2005) Climate policy cooperation games between developed and developing nations: a quantitative, applied analysis. In: Haurie A, Viguier L (eds) Cloupling climate and economic dynamics. Kluwer Academic Publishers, Chapt. 5

Kouvaritakis N, Soria A, Isoard S (2000) Modelling energy technology dynamics: methodology for adaptive expectations models with learning by doing and learning by searching. Int. J. of Global Energy Issues 14(1/2/3/4):104–115

Kypreos S (2000) The MERGE model with endogenous technological change. In: Proceedings of the economic modeling of environmental policy and endogenous technological change workshop. Amsterdam, The Netherlands, pp. 16–17

Kypreos S (2005) Modeling experience curves in MERGE. Energy 30(14):2721–2737

Kypreos S, Bahn O (2002) A MERGE model with endogenous technological change. Environmental Modeling and Assessment 8:249–259

Loulou R, Lavigne D (1996) MARKAL model with elastic demands: application to GHG emission control, In: Carraro C, Haurie A (eds) Operations research and environmental management. Vol. 5 of The FEEM/KLUWER International series on economics, energy and environment. Kluwer Academic Publishers, pp. 201–220

Manne A, Barreto L (2004) Learn-by-doing and carbon dioxide abatement. Energy Economics 26:621–633
Manne A, Richels R (2001) An alternative approach to establishing trade-offs among greenhouse gases. Nature 401:675–677
Manne A, Richels R (2002) The impact of learning-by-doing on the timing and costs of CO_2 abatement. In: International Energy Workshop. Stanford, USA, pp. 18–20
Messner S (1997) Endogenised technological learning in an energy systems model. Journal of Evolutionary Economics 7:291–313
Philibert C, Pershing J (2001) Considering the options: Climate targets for all countries. Climate Policy 1:211–227
Rafaj P, Kypreos S, Barreto L (2005) Flexible carbon mitigation policies: analysis with a global multi-regional MARKAL model. In: Haurie A Viguier L (eds) Cloupling climate and economic dynamics. Kluwer Academic Publishers, Chapt. 5
Rosen JB (1965) Existence and uniqueness of equilibrium points for concave N-person games. Econometrica 33(3):520–534
Stavins R (1995) Transaction costs and tradable permits. Journal of Environmental Economics and Management 29:133–48
Viguier L, Vielle M, Haurie A, Bernard A (2006) A two-level computable equilibrium model to assess the strategic allocation of emission allowances within the european union. Computers & Operations Research 33(2):369–385

Economics of climate policy and collective decision making

Beat Bürgenmeier · Andrea Baranzini ·
Catherine Ferrier · Céline Germond-Duret ·
Karin Ingold · Sylvain Perret · Peter Rafaj ·
Socrates Kypreos · Alexander Wokaun

Abstract This paper explores the reasons why economic instruments of climate change are reluctantly applied and stresses the need for interdisciplinary research linking economic theory and empirical testing to deliberative political procedures. It is divided in three parts. The first one recalls the main issues in implementing Cost-Benefit Analysis such as information problems, uncertainties, discounting the future and irreversibilities. The second part shows how these issues can be treated in integrated assessment and techno-economic models and presents a case study, which shows that

- The chosen scenario tends to stabilize atmospheric CO_2 concentration at around 550 ppm in the long run.
- Exclusion of possibility to trade CO_2 emission permits under a cap regime would increase the cost of emission abatement for OECD countries.
- Combining different flexibility instruments might lead to significant gains in the overall cost of climate policy.

The third part presents results of a survey conducted among the main economic and environmental associations in Switzerland. The survey reveals conflicting views on economic

B. Bürgenmeier (✉) · C. Ferrier · K. Ingold · S. Perret
Centre of Human Ecology and Environmental Sciences, University of Geneva, 40 Bd du Pont-d'Arve,
CH-1211, Geneva, Switzerland
e-mail: Beat.Burgenmeier@ses.unige.ch

A. Baranzini
Geneva School of Business Administration, University of Applied Sciences of Western Switzerland

C. Germond-Duret
Graduate Institute of International Relations, University of Geneva

S. Kypreos · A. Wokaun
Paul Scherrer Institute

P. Rafaj
International Institute for Applied Systems Analysis, Austria

instruments. It shows how the social acceptability of these instruments can be improved in taking explicitly into account these opposing views of special interest groups. Therefore, policy scenarios should be selected in combining techno-economic models with empirical studies about their political and normative context.

1 Introduction

Climate change calls for a policy response. The Kyoto Protocol explicitly refers to economic instruments and delegates their application to the ratifying States. However as the OECD noted, these instruments are theoretically well founded, but badly applied (Barde 1997). This chapter examines the reasons for this limited success of economic instruments and explores some conceptual problems and in implementing Cost-Benefit Analysis in a political decision making process. Different policy recommendations face a social acceptance problem indeed (cf. Spash and Carter 2002).

This contribution is divided into three parts. The first one recalls some theoretical aspects of economic instruments based on cost-benefit analysis (CBA). The second one presents case studies for greenhouse gas emission control using models of the NCCR project to overcome the weaknesses related to CBA or the precautionary principle. Based on neoclassical economic theory and the use of techno-economic models some policy responses are evaluated. Finally, the third part, discusses the social acceptance problem in presenting the result of a survey conducted among 240 Swiss economic and the nine main environmental associations that form the main special interest groups in the implementation process of climate change policies. As a way of conclusion, some fundamental issues of economic instruments for climate change policy are discussed as controversies on their implementation are at the root of their social acceptance.

2 Issues in implementing cost-benefit and cost effectiveness analysis

The global warming problem can be addressed through five interrelated questions:

 i By *how much* should greenhouse gases (GHGs) emissions be reduced? Answers to this question would help, for instance to assess the reduction targets actually discussed at the international level, e.g. in the Kyoto Protocol.
 ii *When* should GHGs emissions be reduced? This issue is related to the timing of emissions abatement, e.g. is it better to reach a predetermined target relatively fast or is it preferred to wait and benefit from new information and technological advances?
 iii *How* should emissions be reduced? This question is closely associated with the choice of policy instruments (e.g. regulations, economic instruments, voluntary agreements, and public investments) that could be implemented to achieve the required targets.
 iv *Who* should reduce emissions? Responses to this interrogation involve equity considerations on, in particular, who has to bear the burden of the costs of climate policies and impacts.
 v At which level should the decision intervene? Though climate change is a global phenomenon, actions are needed on all levels of intervention; the link between the international, national and local levels raises a coordination problem, as different jurisdictions intervene.

The answers to these questions are particularly challenging, because of the peculiar features of the global warming problem, such as large uncertainties, non-linearities and irreversibilities, possible catastrophes with small probabilities, asymmetric distribution of impacts, very long planning horizon, changing social perception, and the global and public good characteristics of the problem (IPCC 1996).

CBA plays a prominent part in modelling economic decision-making procedures (cf. Nordhaus (1993), Falk and Mendelsohn (1993), and Maddison (1995)). CBA is a decision support technique, which was initially developed for project evaluation. The aim of CBA is to maximise economic efficiency or, in other words, to determine (economically) optimal policies. To achieve this, the CBA approach expresses widely different impacts in monetary terms, usually using market prices (or adjusted market prices, when markets are distorted or when the policy implies non-marginal changes). CBA applies a discounting procedure, to account for the fact that benefits and costs occur in different points in time.

To evaluate climate policies in a CBA framework, it is then necessary to calculate the ratio of the sum of expected discounted benefits (V) and costs (F) of reducing global warming, $Y_0 = V_0/F_0$. Where

$$V_0 = \sum_{t=0}^{T} \frac{B_t}{(1+r)^t} \quad \text{and} \quad F_0 = \sum_{t=0}^{T} \frac{C_t}{(1+r)^t},$$

with B_t and C_t the expected benefits and costs at time t, r the appropriate discount rate, and T the time horizon.

The discounted costs are the monetary costs of abatement policies, while discounted benefits are the level of damage avoidance–the difference between the cost of global warming in the absence of intervention and the unavoidable costs of global warming associated with a given abatement policy (which cannot be avoided because greenhouse gases are long-lived).

Following the CBA approach, a policy improves economic efficiency if discounted benefits are greater than discounted costs (i.e., when $Y_t = V_t / F_t > 1$). When there are alternative climate policies, the optimal is the one with the greatest difference among the sum of discounted benefits and cost.

2.1 Information problems

To implement the CBA approach, it is thus necessary to know and quantify all the previous parameters, i.e. costs, benefits and the discount rate, as well as their evolution through time. Of course, in the context of global warming, this is an incredibly complex task and it has to overcome an extraordinary information problem. Moreover, if global warming in the very long term will banish life on Earth, then only the costs to avoid this outcome have to be accounted for Benefits derived from human activities will disappear too.

The evaluation of costs of climate policies is illustrated in the GMM model, which will be presented in the second part of this chapter. The evaluation of the benefits of climate policies, especially in monetary terms, is much more subject to debate and dispute. Indeed, fundamental impacts of climate change are not subject to trading in markets, or are traded in very imperfect and limited markets. For instance, climate change may have impacts on human health and increase mortality and morbidity; may oblige people to migrate from an exposed area; or may modify ecosystems and reduce biodiversity. The most serious consequences of those impacts are of course outside the realm of the markets. In the past decade, a large body of the environmental economics literature developed and applied several techniques

to value non-market assets in monetary terms, ranging from human capital techniques and defensive expenditures approaches to hedonic techniques and contingent valuation methods (e.g. see Cropper 2000). Those techniques are different in their application, but they are all fundamentally based on the same principle: simulate the existence of a market, for an asset, which is not marketed. Those techniques are thus inferring the willingness to pay (willingness to accept a compensation) of individuals for an improvement in environmental quality (decrease in environmental impacts). This implies that the monetary assessments of climate change are strongly conditioned by income and income distribution, which means that the value of similar impacts, such as the risks to human life, turns out to be very different in different countries (see Anaheim 2002).

However, economic valuation techniques are but one step in the complex process for the monetary valuation of the benefits of climate change policies. As E. J. Mishan pointed out: ". . . benefits aggregates, of course, no longer carry any independent economic recommendation. They are value only insofar as they are made use of by the political authority as an input into the decision making process, an input to which any weight/including a zero weight) can be attached" (Mishan 1980, p. 157). Therefore, valuation of the benefits of climate change policies is an interdisciplinary endeavour, involving sciences like climatology, epidemiology and ecology, while economic techniques are then used to express the impacts in monetary terms, and other social sciences can be implicated to assess their social pertinence. But expressing costs and benefits of climate change policies in monetary terms is challenged by the view that the main aspects of environment evaluation fundamentally escape quantification and involves beliefs and finally symbolic social representations of nature, which cannot be expressed in monetary terms (cf. Funtowicz and Rawetz 1994).

2.2 Uncertainties

Monetary valuation will inevitably be faced with fundamental uncertainties. Those uncertainties will never be solved, since valuation has to be carried out not only for the present, but also for the future. Indeed, in the future we will not only have different economies, but different individuals and societies, with different preferences and attitudes. According to Arrow et al. (1996), those uncertainties may be classified in three areas:

- Scientific uncertainties, which relate e.g. to the relationships between ghg emissions and concentrations, climate feedbacks, and effects of climate change on temperature and on bio-geo-chemical cycles. The understanding of global climate change and its inter-connexions with microclimate change is only at its beginnings. This link may be of crucial importance for implementing climate change on national or regional levels.
- Socio-ecologic uncertainties, concerning the relationships between human societies and nature, e.g. agriculture production and diseases, water use and air pollution.
- Socio-economic uncertainties, which are connected to the effects of climate change on human welfare.

2.3 Discounting the future

The final parameter that has to be quantified to apply the CBA approach is the discount rate. The issue of the correct discount rate to be used in CBA is an endless debate in economics, which can be traced back to Ramsey (1928). Ramsey contended that at the public level it is not ethically defendable to actualise future generations' welfare (i.e. the discount rate should be nil). In the climate change context, the role of the discount rate is amplified, given the

very long planning horizon. Indeed, using a real discount rate of 5 to 10 percent (as used in many public projects) corresponds to artificially shortening the time horizon. In other words, a relatively high discount rate implies that some of the impacts of climate policies will not be considered, when they will occur relatively far into the future (e.g. 50 to 100 years from now). For instance, 1 million damages in 100 years resulting from climate change is worth in present value about 70 if discounted at 10%, about 7'600 discounted at 5% and 370'000 at 1%.

The choice of the discount rate will thus have a decisive impact on the optimality of a given climate policy. In fact, given the very long time horizon, climate change strengthens the trade-off concerning the ambivalent role of the discount rate as a mean to reach simultaneously the efficiency in the inter-temporal allocation of resources and inter-generation equity. How can efficiency be separated analytically from equity in order to recommend economic policies to climate change though in the implementation process both are interrelated? The discount rate, which also refers to the inter-temporal efficiency and equity, can only be analysed with reference to the social objective function (cf. Burgenmeier 2003). For the latter, it means that it is necessary to consider the ethical foundations of maximising the sum of discounted net benefits as the social objective (of climate change policies). Indeed, maximising the sum of discounted net benefits (which corresponds to the CBA Social objective) does not prevent decreasing net benefits for some generations, which may be in contrast with the concept of sustainable development where the common denominator is an ethical claim of intergenerational equity.

For the inter-temporal efficiency aspects, the discount rate should reflect the opportunity costs of future social net benefits (benefits minus costs) resulting from a given policy. At the *individual* level, the discount rate is likely to be greater than zero, if capital is productive and if individuals have a preference for the present vs. the future. It can be shown that the individual discount rate of consumption (r_c) is equal to (cf. Hanley 1992): $r_c = \rho + \varepsilon(c)\frac{\dot{c}}{c}$, with ρ the individual "pure" time preference (due to impatience, the limited duration of life and uncertainty) and $\varepsilon(c)$ the elasticity of the utility of consumption. Thus, even if the pure time preference is nil, the individual discount rate can be positive, if consumption is growing.

If capital markets are perfectly competitive, the interest rate is a good measure of the individual discount rate. However, in reality capital markets are often distorted. In addition, and more fundamentally, the individual discount rate may be different from the one that *society* would use to express preferences through time. There are several reasons, which may justify that the social discount rate is lower than the individual one. In particular, contrary to individuals, society has a planning horizon that is infinite, since its expected life is (hopefully) not finite. Moreover, some risks may be spread at the collective level, whereas it is not possible at the individual level. In their seminal paper Arrow and Lind (1970) have even demonstrated that if the risk may be perfectly spread, then the community may be considered as risk neutral, even if it composed of risk-averse individuals. In that case, the discount rate should not be corrected (increased) to account for uncertainty.

However, the risks associated with climate change are relatively difficult to spread, in particular those related to catastrophic events. Indeed, those risks may be very high and thus different from zero, even when divided among a (finite) number of individuals. In addition, these kinds of risks possess public good characteristics and thus it cannot be divided between individuals, since uncertainty will nevertheless remain the same for each individual (non-rivalry).

2.4 Uncertainty, irreversibilities and climate catastrophes

As detailed above, uncertainty is an inherent feature of climate change. Moreover, the effects of uncertainty on optimal abatement policies are amplified by irreversibility. In the literature,

irreversibility possesses two forms (see Goldemberg et al. 1996). A decision may be considered as irreversible when it reduces future possibilities of choice for a long period of time (Henry 1974).

The first is the irreversibility of climate change: once GHG emissions go into the atmosphere, they can only be removed naturally, but the rate of decay is extremely low, in particular for CO_2. The second is capital irreversibility: to control ghg emissions, significant investments could be involved, and once made, they cannot be undone quickly.

The possibility of catastrophic events is also a main feature of global warming. Indeed, climate change could be a gradual and slow process, but some of its impacts may occur abruptly or over a short period of time, as some climatological parameters cross threshold values (National Research Council 2002). Examples of sudden global warming catastrophes are:

  (i) The "runaway" greenhouse effect (climate change is much greater and occurs much faster than the common consensus indicates);
 (ii) Disintegration of the West Antarctic Ice Sheet;
(iii) Structural changes in ocean currents (which may lead to a sharp drop in European mean temperatures).

The first studies applying CBA to determine optimal climate policies did not address these important features, but there is now a substantial literature, which extends traditional CBA to account for uncertainty and irreversibility in the global warming context. However, only a few authors have attempted to include the possibility of catastrophic events (c.g. Baranzini et al. (2003), who show that (i) gradual, continuous uncertainty in the global warming process is likely to delay the adoption of optimal abatement policies, with respect to the standard CBA; but (ii) the possibility of climate catastrophes accelerates the implementation of these policies as their net discounted benefits increase significantly).

3 CBA in integrated assessment and techno-economic models

Having in mind the fundamental critique of CBA for setting climate-change policies described before, we operate two models of the NCCR project to address these questions.

First the Integrated Assessment Model (IAM) MERGE is applied in a CBA framework or under the precautionary principle to describe scenarios that stabilise the carbon concentration or the maximum temperature change to low levels. MERGE is able to address issues of uncertainties for key parameters like the climate sensitivity and the ocean diffusivity in a stochastic framework where uncertainties will be resolved in the future (Manne and Richels 2005).

This IA model can be also extended to address problems of non-linearity and irreversibility or climate catastrophes. For example, the MERGE-E version (Bahn et al. 2006b) specifies time constraints on temperature changes and rates of temperature changes such that the thermohaline circulation (THC) of the North Atlantic will never be interrupted. Temperature constraints are estimated with the help of specific climate models (Knutti et al. 2002) concerning the THC. Examples applying MERGE are given in the same special issue (Bahn et al. 2006a). The report of Bahn et al. describes how a neoclassical economic model like MERGE can be linked with a climate model of intermediate complexity to perform analyses in a CBA or in a cost effectiveness framework.

The second model applied in the NCCR project is the energy systems model GMM (a partial equilibrium bottom-up model) where following the precautionary principle we evaluate different policies and targets that stabilize carbon emissions to 10 GtC/yr by the year 2050. These case studies are imposed as a set of policy overlays on a Baseline sce-

nario to define the responses to climate change. The case studies are described in some details here and explain how the "what", "where", "when" and the "technological" flexibility can be realized. The model is also used to perform sensitivity analyses on the discount rate.

The GMM model is a technology oriented "bottom-up" model that obtains the least-cost configuration of the global energy system for a given time horizon (50 years) under a set of climate-response policy settings (Rafaj et al. 2005). At the same time, GMM endogenises the technological learning (ETL) for emerging technologies, as is described in detail in Viguier et al. (2006) also in this volume. The economic feedback of climate-response policies is captured in GMM by the partial equilibrium procedure, in which the model calculates its objective function as a sum of (a) the energy/technology production cost and (b) the loss of consumer welfare associated with demand reduction.

In the case of climate policies, the change in the objective function, i.e., an increase or decrease in the total cumulative discounted system cost over the reference development indicates the cost impacts of a specific policy instrument applied (Loulou et al. 2004).

Another economic indicator that is frequently used for the evaluation of climate policies is the marginal abatement cost, which defines the cost of reduction of the last unit of GHG emission in order to reach the prescribed emission level. Both indicators, i.e., the change in the total system cost, as well as marginal abatement cost of GHG reduction are used below for the evaluation of different setups of climate policies.

The way, in which questions of cost effectiveness or CBA with respect to climate polices can be translated into the formalised GMM modelling framework, is exemplified using an illustrative policy scenario GHG-Cap&Trade and its modalities that reflect different climate policy setups and flexibility mechanisms as being imposed on the Baseline development.

Section 3.1 refers to cost effectiveness analyses with GMM while Section 3.2 to CBA.

3.1 Illustrative policy scenarios

The selection of the reference case is crucial for the modelling-based policy analysis, therefore a short description of the Baseline scenario and its assumption is provided here. The Baseline scenario that underlines all policy cases is closely related to the B2 scenario reported by the IPCC (2000). The baseline storyline assumes a given degree of increased concern for environmental and social aspects and is consistent with current institutional frameworks and current technology dynamics. Although not calibrated to match exactly the results of the original B2 scenario, the Baseline scenario reported herein may represent a plausible development of the global energy system. The allocation of resources is based on an optimisation performed under conditions of perfect foresight with ETL considerations included. In addition, global spillovers of experience and knowledge transfer (including from North to South) are assumed to take place. Time evolution of global energy related CO_2 and other GHG emissions in the reference development are summarised in Figure 1. Total global energy-related carbon emission rates in the Baseline scenario increase continuously from the present level of 6.3 GtC/yr throughout the time horizon modelled, giving an annual rate of 1.97%/yr and reaching a level of 16.8 GtC/yr by the year 2050. Inclusion of non-CO_2 gases in the Baseline increases the total carbon-equivalent (C-eq) emissions to 19 GtC-eq/yr in the year 2050.

3.1.1 "How much and what?"

The total level of CO_2 reduction in the GHG-Cap&Trade scenario follows in our example a precautionary principle that imposes a stabilising cap on the global energy-related CO_2
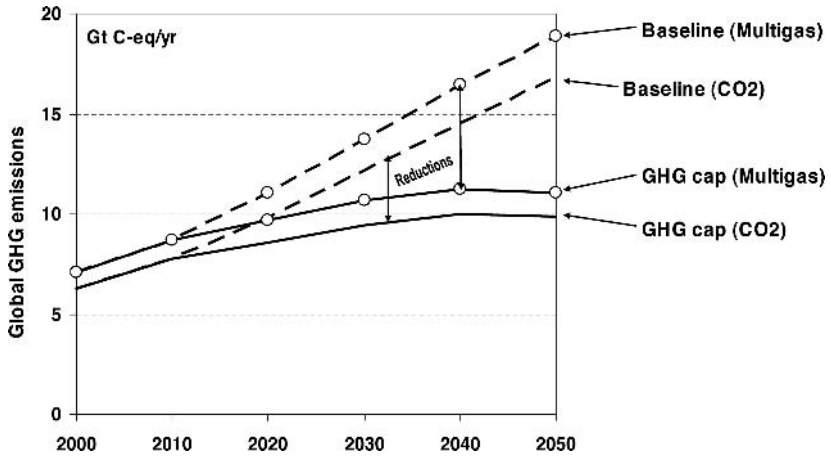
Fig. 1 Global GHG emissions (CO_2, CH_4, N_2O) in the Baseline scenario and the reduction target in the CO_2-
and Multigas-mitigation scenarios

emissions to 10 GtC/yr by the year 2050. The global emission trajectory considered in this
exercise might in a long run lead to a stabilisation of the atmospheric CO_2 concentration
at around 550 ppm. Inclusion of non-CO_2 GHGs (i.e., the multigas abatement strategy)
increases the reduction target in 2050 to 11 GtC-eq/yr proportionally to the higher level of
GHG emissions in the Baseline, as is illustrated in Figure 1.

Consideration of non-CO_2 GHGs involves the first type of flexibility in the climate policy-
making and refers to the "what" flexibility, i.e., the possibility to abate the most cost-efficient
mix of GHGs in a given time period. The Kyoto protocol identifies six substances that can
contribute to reaching the overall GHG mitigation goal (UNFCCC 1999). In addition to
CO_2, the GMM considers emissions of methane (CH_4) and nitrous oxide (N_2O). Although
the CO_2 emissions associated with the fossil-fuel combustion represent the far largest con-
tribution to the total GHG-emission levels, ignoring other Kyoto-gases would lead to the
abandonment of a range of cost-efficient abatement options and potential gains because of
substitution among gases. The impact of "what" flexibility on the overall cost of GHG miti-
gation policy is depicted in Figure 2, showing the cost-reducing effect of multigas abatement
strategies.

3.1.2 "Who and where?"

The allocation of emission entitlements across world regions in the GHG-Cap&Trade sce-
nario is based on an assumption of extending the Kyoto protocol targets beyond the first
commitment period of 2008–2012 to the global level such that a smooth global CO_2 emis-
sion trajectory to 10 GtC/yr will be obtained while taking into consideration the aspiration
of developing countries for economic growth. The allocation principles for the distribution
of entitlements are described in Rafaj et al. (2005). The Kyoto protocol suggests a number
of international mechanisms, with which the reduction commitments can be achieved more
efficiently at a minimum cost. These mechanisms take advantage of the "where" flexibility
of mitigation. The case study presented herein introduces the "where" flexibility through
a generic GHG-emission trading scheme without distinguishing between the specifics of
Kyoto-instruments, i.e., IET, JI, or CDM. As is shown in Figure 3, exclusion of possi-
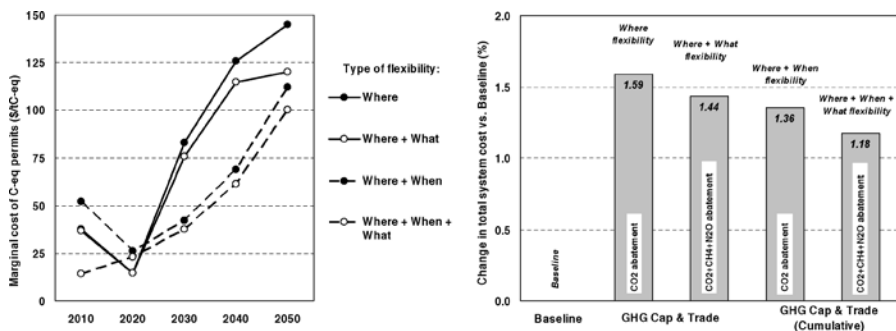
Fig. 2 Cost impacts of the flexibility mechanisms for the GHG-abatement strategies. Under the "when" flexibility case a cumulative emission constraint for the period 2010–2050 is imposed instead of annual emission targets
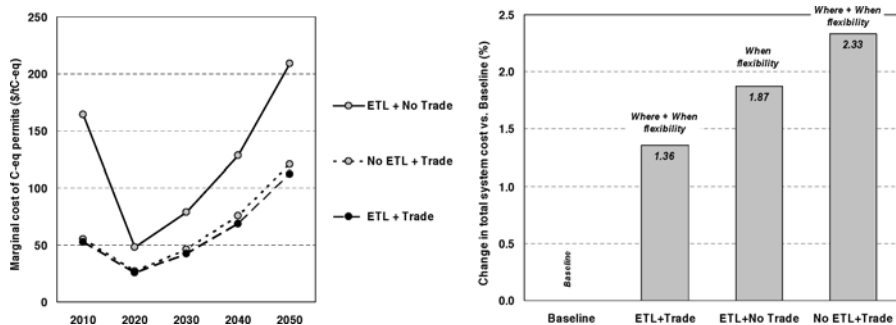

Fig. 3 Cost impacts of the "technological" flexibility and international trading with C-eq emission permits

bility to trade CO_2 emission permits under a carbon cap regime would increase the cost of emission abatement for regions with expensive mitigation possibilities, such as OECD region.

3.1.3 "When?"

The timing of imposition of stringent climate policies is particularly important for the policy acceptability. Considering the climate change as a global problem with long-term consequences, the question is how to allocate the global carbon budget over time to achieve cost optimality in achieving a given policy goal. In GMM, this question is addressed by using a "cumulative" GHG constraint for the whole commitment period, i.e., 2010–2050. This constraint is equal the integral of the regionalised annual targets introduced above, and involves the "when" flexibility in GHG mitigation. Optimal timing in GHG reductions is associated with important cost impacts. Marginal cost reduction due to "when" flexibility is quantified in 2050 at about 35\$ /tC-eq as compared to the GHG-Cap&Trade case with annualised emission bounds. As shown in Figure 2, combining the different flexibility instruments, i.e., "where", "when" and/or "what", might lead to significant gains in the overall cost of climate policy.

3.1.4 "How and at which level?"

Successful achievement of prescribed GHG-reduction targets requires the implementation of appropriate policy instruments. The Kyoto protocol and subsequent international agreements are less specific in the choice of methods to be used for domestic reduction efforts. Nevertheless, adoption of proper domestic policy instruments will be essential if the GHG-reduction targets are to be met. Such policies could vary from application of "command & control" regulatory options to a carbon tax or voluntary measures. Due to the level of regional aggregation, specific domestic policy instruments are not modelled individually in this case study, but they are assumed to be implicit to the emission cap imposed on the regional energy systems. A detailed analysis of the acceptance of a group of selected domestic policy instruments for Switzerland is provided in Section 4.

The question of "how" the emission reduction shall be realised is closely related also to the last type of flexibility addressed in this paper. The so called "technological" flexibility would refer to the ability of the energy system to adopt for a "carbon-constrained" world. Decarbonisation of the global energy system implies the substantial structural changes in the energy sector and deployment of advanced technology options. In this context it is interesting to evaluate the impacts of technological progress under the climate-policy regime. An example of this phenomenon is provided in Figure 3, where the costs of the GHG-Cap&Trade policy-scenario with ETL are compared with scenario that does not consider cost-reducing effects of technological learning.

3.2 Information problems

As discussed in Section 2.1., economic valuation of costs and benefits that could be linked to the adoption of climate policies is a complex task surrounded with a broad range of uncertainties. An example of valuation of potential benefits of the illustrative policy scenario GHG-Cap&Trade is provided here based on avoided damages due to air pollution.

It is well recognised that climate policies could indirectly lead to a significant reduction in air polluting substances. This effect is considered as a secondary benefit of a climate policy. Reduction in air pollution might be substantial especially in the developing regions with relatively low air quality standards. The question that arises in the CBA context is how to monetize the avoided damage that would occur because of the implementation of climate policies with GMM.

An approach used in this exercise is to scale first the damages per unit of kWh of a specific power plant based on the results of the ExternE project (EC 1999). The information problem to be overcome is the adjustment of ExternE values of damage costs valid for typical conditions in Western Europe (based on specific willingness-to-pay (WTP) measures) to the regions with unknown WTP. The scaling method can be based simply on the population density of the affected region, or the welfare of affected population using expected projections of GDP. Then, based on the electricity generated by region and power stations in a scenario, one could estimate the avoided damages due to the climate policy adopted. As is illustrated in Figure 4, the selection of a specific scaling approach leads to a significant difference in the value of avoided damage. The lower range of avoided damages in the figure represents the damage cost adjusted to the population density, and the upper range reflects the damage cost scaled to GDP in market exchange rates. The middle value reflects the scaling to the per capita GDP in purchase power parity (Rafaj 2005). Notice that in the same reference, the GMM model is
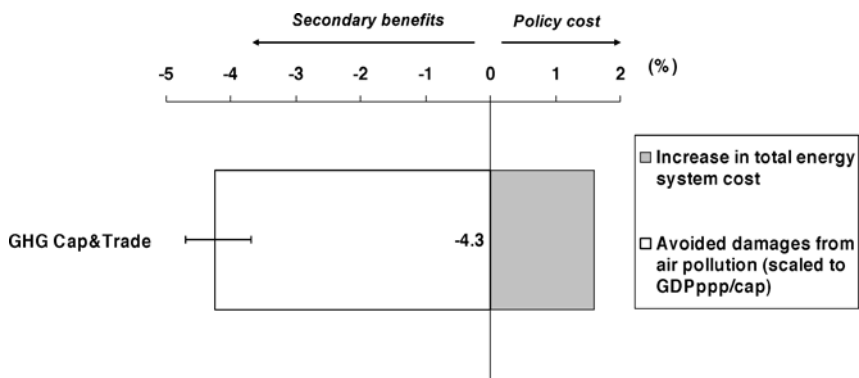
Fig. 4 Comparison of cost and secondary benefits for the GHG-Cap&Trade policy scenario expressed as a change in the cumulative discounted energy system cost relative to the Baseline scenario. (Note: d$r = 5\%$)

used in a more formal CBA framework addressing simultaneously climate policies and the external costs associated with electricity generation.

Implications of the modelling results presented in Figure 4 can be highly relevant for policy-making efforts in the area of climate change, particularly for the developing countries, since they suggest that the secondary benefits of the CO_2-abatement might offset the direct costs of mitigation.

3.3 Discounting issue in the GMM modelling framework

Given the controversy in the proper selection of the discount rate (dr) for climate policies outlined in Section 2.3., it is advisable to evaluate the cost impacts using different dr values. A 5% per annum discount rate has been used in the Baseline and policy scenarios reported above. Two sensitivity cases are analysed herein for the GHG-Cap&Trade scenario, using the values of 3% and 7%. The rate of 3% is indicated by IPCC (2001) as a rate based on "ethical" considerations. The latter value of 7% reflects more the present energy-market situation and the dr value is used to approximate the cost of capital invested in more risky projects (see, e.g., AEN-NEA 2005).

Figure 5 shows the change in objective function over the Baseline for the GHG-Cap&Trade scenario applying different discount rates of 3, 5, and 7%. For consistency, the cumulative system cost in the policy scenarios is compared to the Baseline scenario, calculated by using the same discount rates as in the policy cases. Variations in the total discounted cumulative cost relative to the Baseline disclose a decreasing trend in the total cost for the sensitivity scenarios with an increasing dr. The 3%-discounting results in a total cost that is higher than in the scenarios with dr of 5 and 7%. On the other hand, marginal costs (undiscounted) of C-eq permits globally traded across world regions are the highest in the case of $dr = 7\%$, which reflects the increase in the cost of investments in the abatement options needed for reaching the GHG-reduction target. This trend is pronounced in the second half of the computational period, where the carbon constraint is the most stringent.

3.4 Final thoughts on the policy recommendations based on a modelling exercise

The purpose of the modelling exercise presented in this section was to provide an example of how to handle the critical issues raised by CBA as pointed out in Section 2. Clearly, the
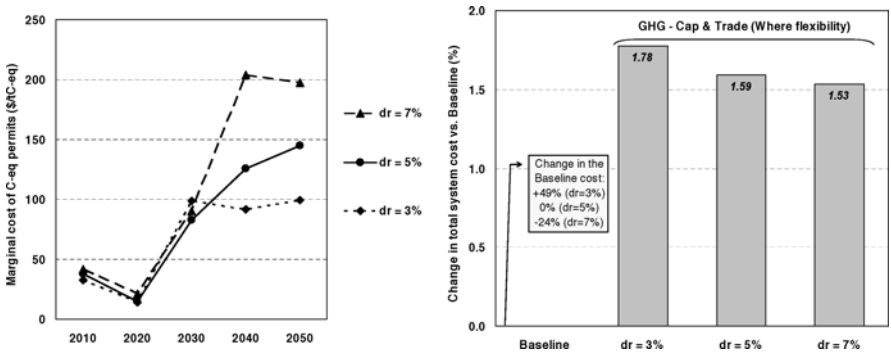
Fig. 5 Changes in the climate policy cost in relation to different discount rates

case study performed with the "bottom-up" GMM model suggests that a number of the key questions related to the climate policy-making can be addressed and the quantitative results provided might be used to support policy decisions.

The modelling results indicate that at the regional and global level the flexibility mechanisms for climate policies constitute powerful instruments to moderate the cost penalty invoked by the policy adoption. The analysis also shows that the combination of elements within a cost-efficient portfolio of climate policy instruments might provide significant gains and could potentially improve the acceptability of the policy implementation. At the same time, the successful implementation of climate policy tools is unthinkable without policy actions in favour of technology progress.

Overcoming the information problems associated with uncertainties (in, e.g., valuation of damages, the choice of discount rates, or irreversibility) represents a challenging task for any formalised modelling analysis. The results reported here illustrate that the choice of these key parameters influence the overall outcomes of a given policy-scenario. In this context it is highly relevant to explore, how the policy responses evaluated and proposed on the basis of neoclassical economic theory and the use of techno-economic models could be accepted by all relevant actors needed to reach a consensus in the debate on climate change policy specification.

4 Social acceptance of policy recommendations

When it comes to translate policy recommendations derived from modelling into the implementation process, considerable resistance can be observed. One of the main obstacles is linked to the distributional aspects of such policy recommendations. In order to overcome this obstacle, income redistribution proposes the recycling of tax revenues. However, using regional and individual data, Thalmann showed that for most voters the mode of revenue recycling did not matter during the Swiss vote on energy taxes in September 2000 (Thalmann 2001). Therefore, a more detailed study is needed in order to understand why there is such a resistance to climate change policy. Wallart identified the main factors for environmental tax opposition (Wallart 2000) and our own findings on the dilemma between theory and practice of economic instruments for environmental protection are based on an inquiry which we have conducted among the 300 most important Swiss corporations (Bürgenmeier et al. 1997).

The firms have been asked about the importance of the major objections raised in the public debate about the introduction of ecological taxes. Though the majority of the answers are

overwhelmingly positive (66.7%), a first proposal to implement a CO_2 tax at the beginning of the '90s has been rejected in the preliminary consulting process which precedes any new legislation in Switzerland. The majority of firms agree on an environmental tax, but reply through their professional organisations negatively in the consultation. It may be that these organisations have to protect the weakest member and reflect, therefore, the firms, which replied negatively. These responses may also illustrate the paradox of collective action, where in the decision-making process the collective outcome is in opposition to individual beliefs (Olson 1971).

Finally, another explanation is linked to the conditions in which ecological taxes are introduced. If these taxes are accepted as a principle only, they raise many objections as far as concrete and very much differentiated individual situations are concerned.

4.1 Special interest groups and policy implementation

In order to further explore the issue of social acceptability of economic instruments in the field of climate change, we have carried out another survey among 240 economic and 9 ecological associations in Switzerland during 2003. This research is part of a larger project, which deals more generally with the socio-economic aspects of climate research within the Swiss National Centre of Competence and Research on climate (Bürgenmeier et al. 2006).

Figure 6 shows that the Swiss economic associations are more favourable to the introduction of voluntary agreements and incentive measures, such as taxes and tradable emissions certificates, comparing with direct controls (i.e. regulation or standards). For each of the
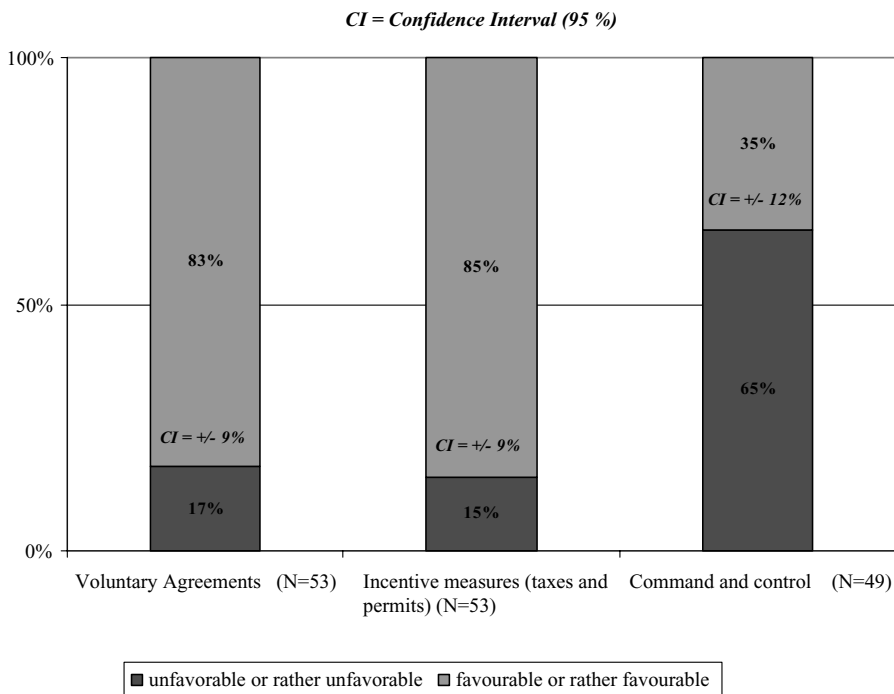

Fig. 6 Introduction of climate policy instruments: Opinions of the Swiss economic associations

	Voluntary Agreements	Information Education	Certificates international	Certificates national	Taxes	Command and control
Economic Associations	1	2	3	4	5	6

Fig. 7 Ranking of preferences of forty-nine Swiss economic associations for economic instruments

three measure, we directly asked the associations if they were favorable (or not) to their introduction in the field of climate policy.

Indeed, a significant majority (85% +/−9%) of Swiss economic associations state they are in favour of incentive measures (i.e. taxes and permits). Figures 7 and 8 give more detailed results about this type of instruments and clearly show that Swiss economic stakeholders favour tradable certificates rather than taxes.

According to Figure 7, our survey shows that the favourite instruments to these economic associations are in this order: voluntary agreements are ranked first, information and education programmes second, international certificates third, national certificates fourth, taxes fifth, and command and control instruments were ranked the last.

According to the N-Persons Game Theory, this ranking was established based on the Condorcet Winner (CW) method (i.e. the alternate which beats all the others if on compares them even per pair), which is considered the best one so the result of a game (i.e. collective choice) reflects the structure of individual preferences.

This ranking clearly reflects the previous results regarding voluntary agreements (first position) and direct controls (last position). It also makes a difference between two types of incentive measures: taxes and tradable emissions permits or certificates. In fact, we can guess that taxes obtained a high score in Figure 6 because they were combined with permits under the "incentive measures" label. But taxes are probably perceived as a more stringent instrument compared to tradable certificates, both national and international as with the former measure the price is set by the government, whereas in the latter the price is set by the market. In addition, taxes imply a different structure of property rights, compared to freely distributed tradable certificates (cf. Baranzini et al. 2000). Indeed, with the former the polluter has to pay for each ton emitted, while with the latter, it receives an amount of emission rights free of charge. Of course, at the emitter's level, this implies that the tax is costlier than freely distributed tradable certificates. In addition, as pointed out by Vatter (2002), another reason for the weak success of taxes is that stronger redistributive measures (like an emission tax) create more identified winners and losers. In the political decision process, those who have to pay have often a strong lobby to combat such an amendment bill. The cost factors as well as every change of the status quo represent a threat to the introduction of ecological taxes (Vatter 2002).

Swiss economic associations were then asked what was their position on votes on four different kinds of energy taxes that were already submitted to the Swiss population (all the proposals were refused):

1. The "Solar initiative", which aimed to introduce a tax of Sfr. 0.05/kWh on non renewable energy,

2. The "Energy conservation package" to introduce a Sfr. 0.03/kWh incentive tax on energy to promote renewable forms of energy,
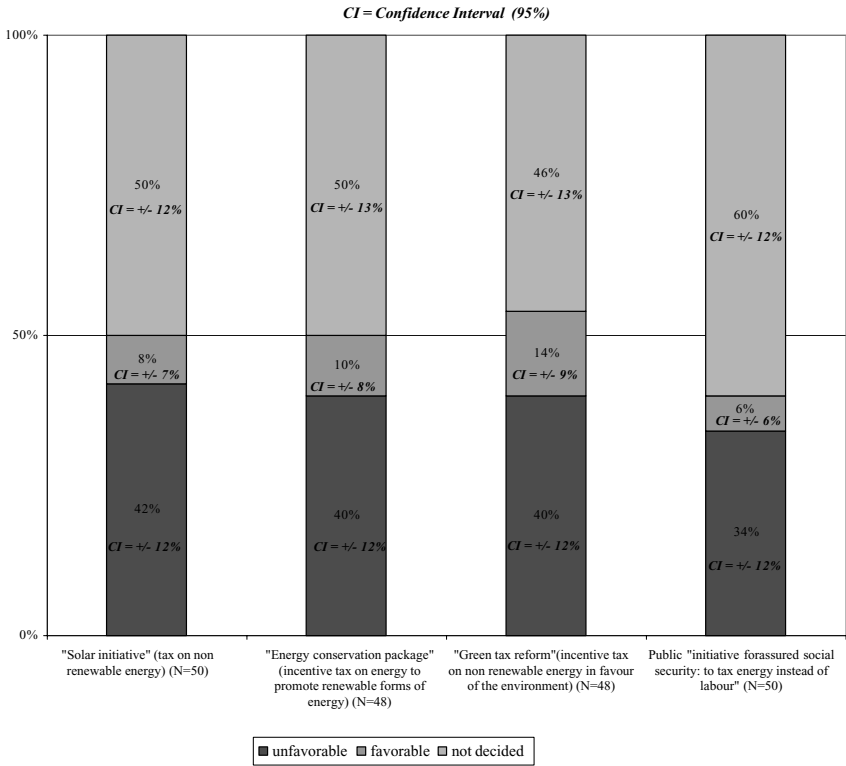
Fig. 8 Federal popular ballots on energy taxes: position of the Swiss economic associations

3. The "Green tax reform", an incentive tax on non-renewable energy of Sfr. 0.20 as a maximum; and finally

4. The "initiative for assured social security: to tax energy instead of labour".

   The first three ballots took place on September 24, 2000 and the last one on December 2, 2001.

   Figure 8 shows that half of the economic associations stated that they did not take position on these issues. However, one can wonder about the reasons for this: it may be possible that these associations did not want to show their opposition to the measure. The other half overwhelmingly took position against these green taxes and only a minority of the economic association were favourable to green taxes, which thus are less better accepted by economic associations that Figure 6 does let it show.

   It appears that economic associations are more favourable to less stringent measures that leaves them a greater room for manoeuvre; the example of the efforts of some of them in favour of a "climate centime" instead of a tax on CO_2 shows how reluctant they are to the implementation of a tax.

   If we compare the results of both surveys – the 1997 one on 300 Swiss corporations and the 2003 one among 240 Swiss economic associations–we can raise a paradox in the behaviour of the Swiss economic associations concerning their acceptance of incentive measures, and

🍋 Springer

	Voluntary Agreements	Information Education	Certificates international	Certificates national	Taxes	Command and control
Economic Associations	1	2	3	4	5	6
Environmental Associations	5	4	6	3	2	1

Fig. 9 Ranking of preferences of forty-nine Swiss economic associations and four Swiss environmental associations for economic instruments. This ranking was established based on the Condorcet Winner (Cw) method

in particular of an ecological tax, and more generally between measures accepted in theory and rejected in practice.

In order to go deeper into the analysis, we compared the answers from the economic associations with the ones obtained from four environmental associations. These results are not statistically representative due to the small number of answers from green associations and serve only to give a broad idea of their preferences, as all these four associations established the same classification.

The results summarized in Figure 9 show a clear opposition between economic lobbies and ecological interest groups. The former prefer voluntary agreements and market incentives. The latter are for command and control. These opposing views show the potential for paralysing the policy debate and express the mutual lack of trust of these pressure groups. The lack of consensus makes CBA difficult to apply, as the valuation of cost and benefits are discussed in a very controversial way when it comes to apply policy of climate change.

We suggest that a difference in the perception of economic instruments policy can be found in conceptual problems raised by an economic approach to climate change and not so much in technical difficulties related to CBA.

4.2 Conceptual problems of economic approaches to the environment

Neoclassical theory considers the natural environment as a free good, having no monetary value until its over exploitation makes it scarce and converts it into an economic good. The theory that tries to model this transformation considers the environment as an externality to the economic sphere. This surprises most researchers in the social sciences. Robert Hettlage expresses this astonishment as follows: "Externalities are built, whose exploration can be delegated to other sciences as they contaminate the model (this would at once clean the theory), if this explanation effort were necessary" (Hettlage 1993, p. 84).

The conceptual aspects arising in the economics environment relationship concern the notion of externality, the determination of non market values and the social learning process, which has to legitimate any policy in environment protection (cf. Söderbaum 2000).

4.2.1 The environment: An externality?

When it treats the environment as an externality, the concept of social cost is at the hearth of the debate. The externality argument states that market failures arise, when private benefits from some economic activity impose an uncompensated cost to someone else. Such a case directly pertains to pollution, but has a more general scope. Every time there is an immediate

benefit from an economic activity whose marginal cost is less than the expected marginal revenue because a third party bears part of the total costs, we are confronted with market failure. No incentive to reduce or to stop such an activity exists. The total cost to society is greater than the cost borne by the one who receives the private benefit. This situation calls for government intervention. The recommended policy is to ask the government to invoice the individual for the social cost created, for example through a CO_2 tax. This method of justifying government intervention consistent with market rules raises a daunting question: to what degree can the private marginal cost be compared to the social one? Such a comparison would only be conceptually acceptable if the costs could be measured objectively (Buchanan 1969).

If pollution reduces this value and requires a tax to be introduced, it is followed by income transfers, which ultimately cannot be evaluated without value judgements.

4.2.2 Non-market values

The value of the natural environment as determined by a market refers to an economic use of it. Yet the value of the environment is also determined outside the market and independently of any economic use. Because the natural environment has an intrinsic value, the market cannot exclusively determine its worth. Likewise, failure to subject the natural environment to economic use–albeit possible on both a technological and a normative plane–can give the environment a "non-use" value that economists readily associate with an opportunity cost. This cost is part of every economic choice, and is defined by the fact that any economic decision related to managing scarce productive resources necessarily implies giving something up (cf. Fankhauser 1995).

Climate change policy essentially finds its legitimacy in the change of non-market values determined by its social perception. This change takes place over a long time, and is codified in laws, regulations, morals and customs, which reflect the fact that people are increasingly aware of problems related to the protection of the environment, despite the fact that the intensity of this awareness can vary. Social concern about an undamaged environment can be supplanted by other, temporarily more worrying problems such as unemployment.

It is therefore illusory to think that changing social perceptions of the natural environment will only change the institutions of a society and leave its perceptions of the economy untouched. Accordingly, we cannot observe constant and inalterable economic behaviour, but rather a permanent interaction between social values and human behaviour. The origin of changing motivations in individual as well as collective behaviour thus becomes crucial to the building of an operational climate change policy.

However, there is no scientific criterion that enables us to move from an individual to a collective level. Society's economic welfare cannot be defined by simply adding up individual behaviours, and then treated as a simple problem of factor allocation. A change in the social utility function does not take into account of the factors, which induced it (Feldman 1983).

4.2.3 Environment protection: A social learning process

In practice, cost-benefit analysis assumes away those factors and relies on engineering expertise. Even if, due to the complexity of the criteria used, impact assessments are made by teams, which also include social scientists, most analyses use a multi-criteria approach, where the weighting of the different explanatory factors becomes essential. Engineers apparently prefer the weighted sum approach, which does not differentiate between explanatory factors on a qualitative level. Thus, if one variable is considered less important, the low weighting

assigned to it cannot do justice to cases where this variable – for example above a certain emission level and sometimes only in relation to another variable – can, during the valuation procedure, take on a totally different meaning.

A learning aspect not only makes it likely that the value function of the criteria will be changed, but also increases the information of the actors concerned by the project and their knowledge of possible interactions between different variables. Consequently, we encounter a problem that has become familiar by now, namely the estimation of the social values and costs submitted to normative judgements, which varies according to the changing social perception of climate change over time. In other words, taking the related costs into account is a normative process, dependent on a politico-legal context, which is also supposed to reflect these changes. This conclusion thus rules out any allegedly objective valuation method.

Recent developments try to weight the different criteria by a normalize approach involving non-scientists in the assessment effort (for a survey of the issues and methods used in this field, see Rotmans and van Asselt 2002). Therefore, the actors' information improve during the negotiation. The normative dimension of policy recommendations becomes part of the analysis. As our survey has shown, economic actors such as special interest groups stress that any assessment must be combined with a negotiation process. They expect increased transparency in applying valuation criteria, as well as a learning effect for all the partners concerned by a policy recommendation, in order to improve the instruments that are to be introduced with a view to enhancing climate change.

5 Conclusion: Towards a socially accepted policy mix

The debate about values, the internalisation of social costs and the explicit recognition of ethical aspects make a single minded, exclusive economic approach to climate change policy obsolete. Such an approach contributes to the problems of the social acceptance of economic instruments. In order to overcome this obstacle the following two interrelated research strategies are followed:

- The first research strategy consists of conventional models, that take the environment into account, either through public goods theory or through property rights theory. These two theories cover the main issues in environmental economics.
- The second strategy refers to more global models, which try to feature relationships between economics and the biosphere. In the same way, models, which add a social dimension in order to come closer to the concept of sustainable development (where these three levels: economic, environmental, social are included) also belong to this group, and cover the field of ecological economics.

Finally, the crucial point is the integration of the ethical dimension in the traditional theoretical representations of the economy that society has adopted (Bürgenmeier 1993). The trend is to delegate ethical questions to the human sciences and thereby to "clean" the economic model, which then constitutes the main reference. Ethics, as well as the environment, are then being treated as an externality to the market. This distinction makes it possible to work on a "scientific" level and root criteria in a positive sense. Theology and moral philosophy are assigned the task of maintaining the social representation of the workings of the economy as intact as possible, treating these aspects outside the economic sphere. The intellectual challenge lies not only in preventing such a development (which is already well under way if one is to judge by the many institutes specialised in economical ethics), but also in integrating ethical considerations in economic reasoning itself (Harsani 1955). The

promotion of economic policies of climate change has to be completed by social policies in order to catch such ethical aspects (Spash 2002). Such social policies not only include transfers of income, but also basic values of the institutional setting of the market, such as legal regulation of "fairness" and non-discriminatory practices. This extension inevitably exposes economics to a dilemma.

- Economic reasoning tries to reduce pollution at the lowest possible cost. It proposes an optimisation calculus that equalises the marginal cost with the marginal benefit of any economic activity. If many actors on a market are responsible for a given polluting emission, it recommends a policy reducing these where the marginal costs of doing so are smallest. Following the efficiency criterion, economic reasoning therefore allows for a differentiated treatment of actors on a market according to their cost or utility functions.
- On the contrary, moral reasoning, often legally codified, is concerned with equality of treatment, which originates in a normative judgement (for example, through the collective memory of a community). This normative judgement may also come out of a political process. If this process is democratic, it is supposed to express the opinion of a majority. Once economic theory recognises that there may be as many normative judgements as actors on the markets (and as many individual actions), legal reasoning only refers to collective preferences. Therefore, implementation of climate change policies is normative by nature. Economic modelling has to be extended to the understanding of a political process.

References

AEN-NEA (Nuclear Energy Agency) (2005) Projected costs of generating electricity – 2005 update. OECD-Nuclear Energy Agency, OECD/IEA. Paris, France

Anaheim HA (2002), Impacts of climate change in monetary terms? Issues for Developing Countries. In Baranzini A, Buergenmeier B (Guest Editors) Climate change: issues and opportunities for developing countries. Special Issue of the Int J Global Env Issues, November 2002, 2(3/4):223–239

Arrow KJ (1951) Social choice and individual values. Wiley, New York

Arrow KJ, Lind RC (1970) Uncertainty and the evaluation of public investment decisions. Am Econ Rev 60(3):364–378

Arrow KJ, Parikh, J, Pillet G (1996) Decision-Making Frameworks for addressing climate change, in IPCC, cit. below, pp 52–77

Bahn O, Drouet L, Edwards N, Haurie A, Kypreos S, Stocker T, Vial J-P (2006a) Optimal economic growth under climate change threats. Climatic Change, DOI 10.1007/s10584-006-9108-4, this issue

Bahn O, Edwards N, Knutti R, Stocker TF (2006b) Climate policy preventing an Atlantic thermohaline collapse. Climatic Change (submitted)

Baranzini A, Goldemberg J, Speck S (2000) A future for carbon taxes. Ecol Econ 32(3):395–412

Baranzini A, Chesney M, Morisset J (2003) The impact of possible climate catastrophes on global warming policy. Energy Policy 31(8):691–701

Barde JP (1997) Economic instruments for environmental protection: experience in OECD countries. in applying market-based instruments to environmental policies in China and OECD countries, Paris, OECD, pp 31–58

Buchanan J (1969) Cost and choice, an inquiry in economic theory. Chicago University Press, Chicago

Bürgenmeier B (1993) Ethical aspects of environmental protection. In: Vernet JP (ed), Environmental contamination, studies in environmental sciences, no. 55. Amsterdam, Londres, New York, Tokyo: Elsevier

Bürgenmeier B, Harayama Y, Wallart N (1997), Théorie et pratique des taxes environmentales, Economica, Paris

Bürgenmeier B (2003) Modelling equity: a debate about values, in Environment Modelling and Assessment, No 8, pp. 165–174

Bürgenmeier B, Ferrier C, Germond-Duret C, Ingold K, Perret S (2006) Acceptation des instruments de marché dans la politique climatique suisse: enquête auprès des principaux acteurs économiques suisses, forthcoming (see also Perret S (2004) "L'acceptabilité des instruments économiques dans le domaine de la politique climatique en Suisse: résultats préliminaires", Working Paper, No WP4–25)

Cropper M (2000) Has economic research answered the needs of environmental policy?. J Environ Econ Manag 39:328–350

Falk I, Mendelsohn R (1993) The economics of controlling stock pollutants: an efficient strategy for greenhouse gases. J Environ Econ Manag 25:76–88

Fankhauser S (1995) Valuing climate change. the economics of the greenhouse. Earthscan, London

Funtowicz SO, Ravetz JR (1994) The worth of a songbird: ecological economics as a post-normal science. Ecol Econ 10:197–207

Henry C (1974) Investment decisions under uncertainty: the irreversibility effect. Am Econ Rev 64(6):1006–1012

Hettlage R (1993) Ökonomie auf dem Weg zur Sozialwissenschaft? Revue Suisse de Sociologie 19(1)

Intergovernmental Panel on Climate Change (IPCC) (1996) climate change 1995. economic and social dimensions of climate change. contribution of working group iii to the 2nd assessment report of the IPCC. WMO and UNEP, New York, Cambridge (U.K.): Cambridge University Press

Intergovernmental Panel on Climate Change (IPCC) (2000) special report on emission scenarios, a special report of the working group iii. of intergovernmental panel on climate change, Cambridge University Press, Cambridge (U.K.)

Intergovernmental Panel on Climate Change (IPCC) (2001) climate change 2001: mitigation. contribution of working group iii to the third assessment report of the intergovernmental panel on climate change, Cambridge University Press

Knutti R, Stocker TF, Joos F, Plattner G-K (2002) Constraints on radiative forcing and future climate change from observations and climate model ensembles. Nature 416:719–723

Loulou R, Goldstein G, Noble K (2004). Documentation for the MARKAL family of models. Energy Technology Systems Analysis Programme (ETSAP), October 2004

Maddison D (1995) A cost-benefit analysis of slowing climate change. Energy Policy 23(4/5):337–346

Manne AS, Richels RG (2005) Global climate decisions under uncertainty. a paper presented at annual meeting of the international energy workshop 2005, 5–7 July 2005 at the Pa-lu-lu Plaza Kyoto, Kyoto, Japan

Mishan EJ (1980) How valid are economic evaluations of allocative changes? J Econ Issues XIV(1):143–161

National Research Council (2002), Abrupt climate change: inevitable surprises. The National Academics Press, Washington, DC

Nordhaus, WD (1993) Rolling the DICE: an optimal transition path for controlling greenhouse gases. Resou Energy Econ 15:27–50

Olson M (1971) Logic of collective action: public goods and the theory of groups. Harvard Universty Press, revised edition, Cambridge (Mass.)

Rafaj P (2005): Analysis of policies contributing to sustainability of the global energy system using the global multi-regional MARKAL model (GMM), Ph.D. Thesis, Nr. 16122, ETH Zürich 2005

Rafaj P, Kypreos S, Barreto L (2005) Flexible carbon mitigation policies: Analysis with a global multi-regional MARKAL model. In: Haurie A, Viguier L (eds), Coupling climate and economic dynamics. Kluwer Academic Publishers, Dordrecht, The Netherlands, pp 237–66

Rotmans J, van Asselt MBA (2002) Integrated assessment: current practices and challenges for the future. in Abaza H, Baranzini A (eds) implementing sustainable development. integrated assessment and participatory decision-making processes. Edward Elgar, Cheltenham, UK, pp 78–116

Söderbaum P (2000) Ecological economics. Earthcan, London

Spash CL, Carter C (2001) Environmental valuation in Europe: findings from the concerted action, policy research brief, No 11, European Commission DG-XII, Cambridge Research for Environment (CRE)

Spash CL (2002) Greenhouse economics, value and ethics, Routledge, London

Thalmann, Ph (2001) The public acceptance of green taxes: two million voters express their opinion. NCCR – WP4 Working Paper 1

United Nations Framework Convention on Climate Change (UNFCCC): 1999, The Kyoto protocol to the convention on climate change, UNFCCC Climate Change Secretariat and UNEP, UNEP/IUC/99/10, Geneva, Switzerland

Vatter A (2002), Erfolgsfaktoren klimapolitischer Abstimmungsvorlagen, Büro Vatter

Viguier L, Barreto L, Haurie A, Kypreos S, Rafaj P (2006) Modelling endogenous learning and imperfect competition effects in climate change economics. Climatic Change, DOI 10.1007/s10584-006-9070-1, this issue

Wallart N (2000), The political economy of environmental taxes. Edgar Elgar, Cheltenham